Doctoral Dissertation
Doctoral Program in Chemical Engineering (30th Cycle)

A multifunctional approach to the reduction of I.C.E. emissions

- a *chemical* point of view -

By

Paolo Miceli

******

Supervisor:
Prof. Debora Fino

Prof. Samir Bensaid, Co-Supervisor

Doctoral Examination Committee:
Prof. Andrzej Kotarba, Referee, Jagiellonian University, Krakow
Prof. Fabrizio Scala, Referee, University "Federico II", Naples
Prof. Maria Cristina Paganini , Examiner, University of Turin
Prof. Isabella Nova, Examiner, Polytechnic University of Milan
Prof. Raffaele Pirone, Examiner, Polytechnic University of Turin

Politecnico di Torino
2018

Declaration

I hereby declare that, the contents and organization of this dissertation constitute my own original work and does not compromise in any way the rights of third parties, including those relating to the security of personal data.

Paolo Miceli

2018

* This dissertation is presented in partial fulfillment of the requirements for **Ph.D. degree** in the Graduate School of Politecnico di Torino (ScuDo), checked with anti-plagiarism systems and then approved by supervisors.

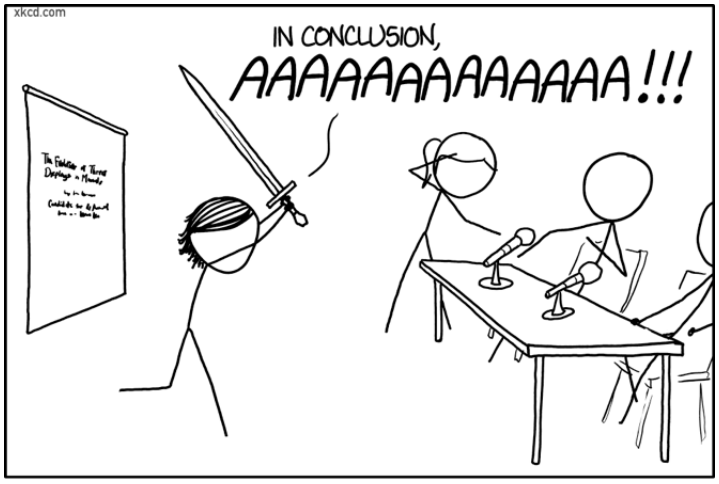

THE BEST THESIS DEFENSE IS A GOOD THESIS OFFENSE.

Credits

DIRECTOR
Debora Fino
DIRECTOR ASSISTANTS
Marco Chiodi
Samir Bensaid
Pietro Salino
Giovanni Cipolla
Andy Holmes

CASTING
Debora Fino
Pietro Salino
Giovanni Cipolla

PRODUCERS
Debora Fino
Paolo Miceli
PRODUCERS ASSISTANTS
Margherita Cerrina
Fabio Deorsola
Giorgia Mangiullo

MACHINE OPERATORS
Clara Fabre
Francesco Laviano
Mauro Raimondo
Micaela Castellino

SPECIAL EFFECTS
Giorgia Mangiullo

STUNTS
Pilar Orihuela
Luca Gesiot
Gianluca Patrone
Andrea Polito
Alessandro Martino
Carmine Costantino
Luca Barbero

STARRING
Paolo Miceli
CAST *(no special order)*
Silvia A., Sergio C., Federico B., Simone R., Sorani M., Beatrice M., Melodj D., Viviana N., Giuseppe P., Annalisa A., Enrico C., Giulio C., Elahe D., Amin F., Siavash F., Simone A., Emanuele G., Mouli T., Camilo F., "MaVi", Marco P., Camilla G., Simelys H., Tahrizi A., Marco D., Stefano C., the DISAT crew, Prof. Russo, Dung, Marianna C., Piotr L., Francesco M., Prof. Pirone, Francesca C., Corrado D., Luigi C., Alexandru M., Prof. Bargende, Francesco C., Antonino V., Andreas K., Marlene W., Oliver M., Lisa K., Antonina S., Lukas U., Sebastian H., Hubert F., Prof. Wachtmeister, Mahsa R., Prof. Millo, Giuseppe F., the Petronas Italy Crew, Federica L., Paolo M., and many others…

ANIMATION
Giorgia M., Erica G., Alessandro C., Lorenzo C., Alessandro D., Natalino D.

LOCATION
Politecnico di Torino – Turin (ITA)
Petronas Italy – Villastellone (ITA)
FKFS – Stuttgart (GER)

Special thanks to my lovely family:
Thy firmness makes my circle just.

Credits also to all the people around me who motivated me, supporting or even setting blocks: we did it!

Abstract

Since its birth, in the late 19th century, the thermal engine has contributed to drive Society towards a continuous development, which finally led everybody to live in the so called Global Village. In this new modern World, the keyword is *mobility*.

Mobility for money, for goods, for people. Nowadays of course, not all these things actually move by car but we all have a new mindset, for which everything is on hand and everywhere is right behind the corner. Worldwide, according to the economic development of each country, more and more families are getting a slice of this freedom, as example by affording a new car, so that we can now count, on the planet, about one billion vehicles running every day, and this is just about the private fleet.

But this last kind of freedom comes at a price. All these vehicles work burning fossil fuels and so producing emissions, made of a large variety of polluting substances, plus CO_2. This is now affecting cities, human health and global climate to such a level that governments of the World started imposing compelling limitations to these emissions. Consequently, Automotive OEMs began to develop their cars from a new point of view: nowadays a car, in order to catch customers, has to ensure the same freedom as always while also being *greener*.

From the engineering point of view, this has been the starting point from where the development of new internal combustion engines (I.C.E.) and vehicles in

general began to be a business not just for automotive engineers, but also for new ranges of professionals, such as IT, Electric, Materials Science and Chemical engineers. The development of a greener car is now so complex that it became a sort of multidisciplinary job, now more than ever. At the beginning, the different approaches were barely connected to each other but, as the complexity was increasing, the need of much dialogue arose.

The challenge for the Automotive Industry of today is to provide technologies that still grant freedom of mobility for everyone but making its products environmentally sustainable. About this subject, the most interesting proposals are gradually swapping the fleet towards electric-like vehicles but current technologies about batteries and fuel cells are not fully developed and ready for this revolution as they need more time for their wide spreading on the market, which appears indeed to be pushed far in the future. In the meanwhile, a prompt solution to the quest for a sustainable mobility can be found in the development of greener thermal engines (beside the change of the traditional mobility paradigm, topic of this research).

From the chemical engineer's point of view, these new greener I.C.E. offer several challenges, such as the development of better after-treatment systems, new solid and liquid lubricants tailored on non-ferrous surfaces and cleaner and more sustainable fuels. These three macro-subjects, coupled with new thermo-mechanical designs and better IT technologies integration, are crucial to make an engine greener, also offering the opportunity to be applied as retrofit, enhancing the speed of their spreading.

One of the first successful approaches to cost and emissions reduction, maybe the one which really found its way in most transport applications (from motorsport to motorbikes), has been the so-called downsizing. Smaller but more efficient engines units can squeeze more power off a single drop of fuel than their predecessors, with

consequent reduction of fuel consumption and emissions. Turbocharging, variable valve timings, lighter alloys are technologies examples but above all friction reduction allowed this outstanding result. Light alloys in particular, can be sources of high gain and high pain at the same time. To let light alloys work as engine components, they must be protected by proper coatings in those zones which are more severe for friction and wear, and this may cause some issues to lubricants. Lubricants in fact, have been developed for decades with a chemistry based on ferrous surfaces: are these recipes still effective on non-ferrous, coated surfaces? A study of the effects of a modern lubricant's recipe on bare steel and DLC coated steel is presented in this work, with interesting outcomes and some suggestions about how to achieve an effective, universal lubricant for automotive applications without using Sulphur and Phosphorous based compounds, considered to be responsible of catalysts poisoning and, consequently, of emissions increasing.

Since particulate matter emissions now concern also gasoline engines, the abatement of this pollutant is more than ever a trend topic in catalysis research environments. For the particular solid/solid reaction between the catalyst and the soot particle is proven to be highly dependent from the contact, a study of new morphologies and their effects on catalysts reactivity is presented in this thesis. Three different morphologies of ceria-based catalysts have been compared: amorphous nitrate-decomposition ceria to structured ceria nanofibers, self-assembled ceria microstars and ceria nanocubes. The investigations on materials characterization and particular soot oxidation tests will show if and how the morphology plays a relevant role in solid/solid catalytic reactions.

Finally, since efficiency and cleanliness of engines cannot be treated only considering external agents like lubricants, coatings or exhaust after-treatment, but it is above all a matter of better design, the role of the so-called Virtual Engines has become more and more relevant throughout years, for their speed, cheapness and

reliability, compared to traditional test benches, nowadays relegated to a mere validation role. The rush for the zero-emission vehicle sets on the table the old chimaera of automotive engineers: the HCCI engine. This particular engine has high efficiency and produces neither PM nor NO_x but, however, for its development, it cannot be simulated trustfully with virtual tools (because of the complexity of that kind of combustion) nor tested on real benches (because of the dangerousness of that kind of combustion). In partnership with a virtual engine developer, a better description of the combustion characteristics of gasoline and ethanol-blended gasoline surrogates has been developed, as far as flame speed and ignition point is concerned, and the results are presented in this work.

These three topics are individual subjects, all of them worthy of consideration from a chemical engineering point of view, but nevertheless they are linked to each other. Since exhaust aftertreatment is considered to be an essential device of modern vehicles, it does deserve to be improved more and more, but its catalysts suffer very much of S and P poisoning originated by lubricants (and fuels), which now need to be tailored on non-ferrous surfaces - brought in by downsizing approach - and, however, aimed towards ultra-low friction performances without using S and P based compounds. Finally, the comprehension of combustion by developing better gasoline surrogates for simulation tools it's not just helpful for the achievement of the aforementioned HCCI engine, but also opens research opportunities towards alternative, cleaner and sustainable fuels in a faster and cheaper way.

Three little steps towards the *zero-emission vehicle*.

Contents

List of Figures

List of Tables

List of acronyms

AFM	Atomic Force Microscope
AKI	Anti-Knock Index
ATS	After-Treatment System
BET	Brunauer–Emmett–Teller (analysis)
CAE	Computer Aided Engineering
CFD	Computed Fluid Dynamics
CN	Cetane Number
COF	Coefficient Of Friction
CPC	Condensation Particle Counter
DLC	Diamond-Like Carbon
DOC	Diesel Oxidative Catalyst
DPF	Diesel Particulate Filter
DVPE	Dry Vapor Pressure Equivalent
ECU	Engine Control Unit
EDS	Energy Dispersive X-ray Spectroscopy
EGR	Exhaust Gas Recirculation
FAE	Fatty Acid Esters
FBC	Fuel-Born Catalyst

FESEM	Field Effect Scanning Electron Microscope
FWHM	Full-Widht Half-Maximum
GMO	Glycol Mono-Oleate
GPF	Gasoline Particulate Filter
HCCI	Homogeneous Charge Combustion Ignition
HCSI	Homogeneous Charge Spark Ignition
HRTEM	High Resolution Transmission Electron Microscope
ICE	Internal Combustion Engine
LPM	Liters Per Minute
LUT	Look-Up Table
MoDTC	Molybdenum Dialkyl-dihioarbamate
MON	Motor Octane Number
MTM	Mini Traction Machine
NC	NanoCube
ND	Nitrate Decomposition
NTC	Negative Temperature Coefficient
OEM	Original Equipment Manufacturer
OI	Octane Index
PAO	Poly-Alpha Olephine
PM	Particulate Matter
PRF	Primary Reference Fuel
PTFE	Polytetrafluoroethylene
RON	Research Octane Number

SACI	Spark Assisted Compression Ignition
SAS	Self-Assembled Star
SCCI	Stratified Charge Compression Ignition
SCR	Selective Catalytic Reduction
SCRoF	SCR on Filter
SCS	Solution Combustion Synthesis
SEM	Scanning Electron Microscope
SI	Spark Ignition
SMPS	Scanning Mobility Particle Sizer
SOC	Start Of Combustion
SOI	Start Of Injection
SRR	Slide-to-Roll Ratio
SSA	Specific Surface Area
TPC	Temperature Programmed Combustion
TPD	Temperature Programmed Desorption
TPE	Temperature Programmed Experiment
TPO	Temperature Programmed Oxidation
TRF	Toluene Reference Number
TWC	Three-Ways Catalyst
XPS	X-ray Photoelectron Spectroscopy
XRD	X-Ray Diffraction
ZDDP	Zinc dialkyl-dithiophosphates

Chapter 1

Lubrication on coated surfaces

1.1 Lubrication: background

The overall efficiency of I.C.E. has different contributions, such as the design itself, the pumping losses, the thermal and fluids management, eddy vibrations and internal friction. Friction saps about 30% of fuel energy so the importance of keeping it under control and making every effort aimed to reduce its negative effects it's very clear. Despite the design and materials selections evolution throughout years of development, there are components of a I.C.E. for which their working will be always afflicted by some kind of friction, as examples the piston-ring sliding against the liner, the crankshaft rolling onto the journal bearings or the cams spinning on the tappets. An uncontrolled friction leads not just to a low efficiency (high fuel consumption, high emissions) engine but also to heavy wear and, therefore, to premature and unpredictable failures.

A proper lubrication of the engine is essential to ensure a certain level of reliability and overall performances and this has been historically achieved by using oils, with origins and formulations that may vary depending on the applications, the type of engine and, of course, the technology level of the epoch. Basically, a liquid engine lubricant is made of a base oil, mineral or synthetic, plus a certain type and amount of additives, together able to grip the ferrous surfaces of moving components, by separating and protecting them.

In our particular era, the need of developing a greener and more efficient engine is greater than ever, and several approaches have been explored to achieve this goal. One of the most impressive solutions, with great effects on the market, is the application of the so-called *downsizing* philosophy, according to which a smaller engine would be better than the traditional big motors, especially for light-duty vehicles and family cars (which is the greatest share of the market). A smaller engine, compared to a classic size one, would work likely with a more open throttle (less pumping losses), it would have less cylinders (low mechanical friction), it would have a lower displacement (low fuel consumption), it would need to be turbocharged to grant good performances (high combustion efficiency) and, for the sake of weight reduction, it should be built with light alloys.

Often, these light alloys are also softer than steel and they wouldn't bear the operative conditions in an engine that good without a proper "shield"; that's why coating surfaces has been being widely used in these last generations of downsized engines[1]. Coating surfaces means that the metal surface of a component is now covered by a thin layer of another material, with a different chemistry and different behavior in friction and wear, as example graphite, polymers or hard ceramics.

However, these new technologies deliver a question: are traditional lubricants, tailored on ferrous surfaces, able to perform well also with these new surfaces? In case, do we need to develop new base oils or new additives?

If lowering friction is so crucial to the efficiency of I.C.E. then, the behavior of these new tribo-couples is worth of investigations and, coherently with the initial aim of achieving a low emission engine, the chance of develop a greener lubrication, eventually by tuning these couples, should be taken into account.

Friction first and wear consequently are among the first reasons of sudden failure and, even when the situation is monitored, keeping them under control represents a huge cost each year in Industry. Introducing better tribological practices is helpful in saving time and money but it needs at least a certain amount of initial investments in research and development.

[1] Actually, in particular applications like heavy-duty, hard and soft coatings are used also on ferrous surfaces, with the same purposes.

Since polluting became a cost (as example, considering fines and penalties from Governments to OEMs which are not compliant with current emissions limits), carmakers are implementing more technologies aimed to lower friction, that is lower fuel consumption and emissions, and wear, that is longer mileages and less maintenance.

The first successful approach to new I.C.E. designs for lower emissions vehicles developed the so-called *downsized* power unit. A smaller, lighter, turbocharged engine works in a range of higher efficiency, due to higher volumetric efficiency (turbocharger and open throttle). A lighter construction, with lighter alloys, such as aluminium, decreases the mass of the unit itself, enhancing the power-to-weight ratio. These solutions allow to equip vehicles with smaller engines but way more efficient (and with the same or even higher performances as before), that means improvements for lower fuel consumptions.

Lower fuel consumption means lower emissions. (1) (2)

However, the enlightment of the engine units made with the introduction of aluminium alloys placed softer metals into I.C.E. designs, that needed to be shielded with tough and harder surfaces. So, the quest for lower frictional forces, aimed to increase the mechanical efficiency, set new needs for these units: the lubrication of innovative surfaces (3) (4). The subject of this work.

1.2 Foundations of tribology

This section is not meant to discuss extensively about the principles of tribology (5) *but it is just a brief introduction to the subject with the needed references to the topics of this chapter.*

…

Tribology is a term originated from Greek words τριβος (tribos) "rubbing" and λόγος (logos) “word”, and it currently refers to the name of the science which studies friction, wear and lubrication. Actually, these disciplines have been studied since the times of Leonardo da Vinci but a better understanding and extensive discussion has been done in modern ages by Hertz, Reynolds and Sommerfeld.

A simplistic definition of friction is “the resistance to motion due to the interaction between surfaces asperities (mechanical constraint) and/or surfaces affinities (chemical constraint)”. Similarly, wear can be defined as “the loss of weight over time”; there is no connection to motion in wear definition. One last definition is for lubricant, “a substance which is able to reduce friction and wear when placed between two surfaces”; again, no indications if the phase must be solid or liquid. Understanding the phenomena of friction and wear has been recognized as a crucial factor in enhancing performances and lifetime of mechanical components.

Among several types of friction and of wear, some of them are particularly worth in I.C.E. applications and therefore listed as follows.

FRICTION

1. Dry Friction

- Static: between non-moving counterparts.

The force needed to start moving is related to a coefficient of friction (COF) which considers physical and chemical affinities between the surfaces:

$$F_{stat} = \mu_{stat} \cdot F_N$$

- Kinetic (sliding or rolling): between moving counterparts.

In this case, the force needed to motion is lower, because the coefficient of friction itself is lower, due to minor effects of adhesive forces

$$\mu_{stat} > \mu_{kin}$$

2. Fluid friction
   Internal forces which block layers of fluid to flow against each other. Also called "viscosity". So, it is the inertia of fluid to flow within itself. In an engine oil, it is important to consider its kinematic viscosity, which is related to the Reynolds number of the system, since the working conditions of the fluid lean on the operating conditions of the engine itself.

3. Lubricated friction
   When there is a lubricant, solid or liquid, separating the counterparts. Despite it depends on the lubricating conditions (later discussed in this section), the coefficient of friction is generally lower than in the dry case, because the pressure in the lubricant layer, generate by its viscosity, tends to separate surfaces, reducing asperities and affinities interactions.

WEAR

1. Adhesive
   When a certain amount of the softer surface moves onto the harder counterpart's surface. It's a regular and smooth type of wear, with low friction.

2. Abrasive
   When the differences in hardness and/or in roughness between the counterparts is very high, the softer surface can be dramatically removed. It's an irregular and aggressive kind of wear, with very high friction.

3. Erosive
   It's a kind of abrasive wear but the counterpart is a fluid or a fluid transporting hard particles. When the surface is grinded by air bubbles exploding, it's called *cavitation wear*. It can be however avoided or reduced with a better component design.

4. Corrosion
   When there are forms of chemical corrosion enhanced, promoted or caused by wear. In most case, corrosion is coupled with other types of wear

5. Surface Fatigue
   A form of failure caused by a cyclic loading applied by long reciprocating movement or continuous rolling. For this reason, when a component fails because of surface fatigue, there can be tragic consequences and, therefore, understanding this type of wear is nowadays a trend topic in tribology.

6. Fretting
   When the failure of the surface is due to the contact with the counterpart, even if the relative movement is very limited (i.e. in the space of vibrations amplitude). In this case, the critical wearing agent is the prolonged contact pressure. It's a particular case of fatigue.

In most cases, all these forms of wear act simultaneously, that is: the final component failure is caused by different but synergic effects.

LUBRICATION REGIMES

One of the most explicative way to teach and understand tribology is the reading of a "Stribeck curve". Stribeck evaluated the behavior of COF with respect of a non-dimensional parameter which consider kinematic viscosity, speed and contact load

$$\eta \cdot N/p$$

With this particular plot, one can distinguish between four regimes of lubrication:

1. Boundary (BL)
   Surfaces are in direct contact and their asperities are nestled within each other blocking tangential motion. In this regime, pure liquid lubricants do not have any kind of effect but additive packages do have a positive role. The tribocouple shows the highest value of COF.
2. Mixed (ML)
   It is a transition zone where the liquid lubricant starts applying pressure and, therefore, slightly separating the asperities. There is a dramatic decrease of COF.
3. Elasto-hydrodynamic (EHL)
   The hydrodynamic behavior is enhanced by the elastic deformation of solid bodies due to increasing viscosity of fluid film. Now the system shows the lowest COF.
4. Hydrodynamic (HDL)
   The liquid lubricant applies enough pressure to separate completely the surfaces. The COF in this regime depends merely on the viscosity of the oil, which may increase as the speed and load increase, due to oil thinning and viscoelastic phenomena.

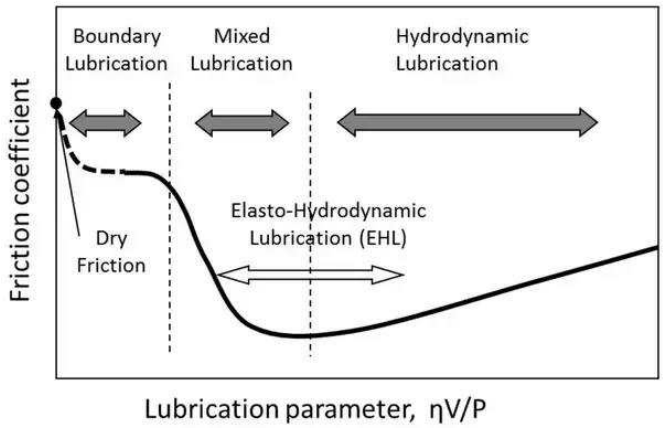

Figure 1 Stribeck curve explained (6)

In Hydrodynamic Lubrication regime, the oil is in pressure and so able to keep asperities separated. This pressure can be external-sourced (*hydrostatic*, with a pump) or internal-sourced (*hydrodynamic*, by oil viscosity). A hydrostatic pressure can be maintained even when the bodies are stand still while a hydrodynamic pressure cannot, and this is important for the lubrication of modern *Start&Stop* equipped engines, since they often are switched off during urban cycles and work mostly in BL/ML conditions.

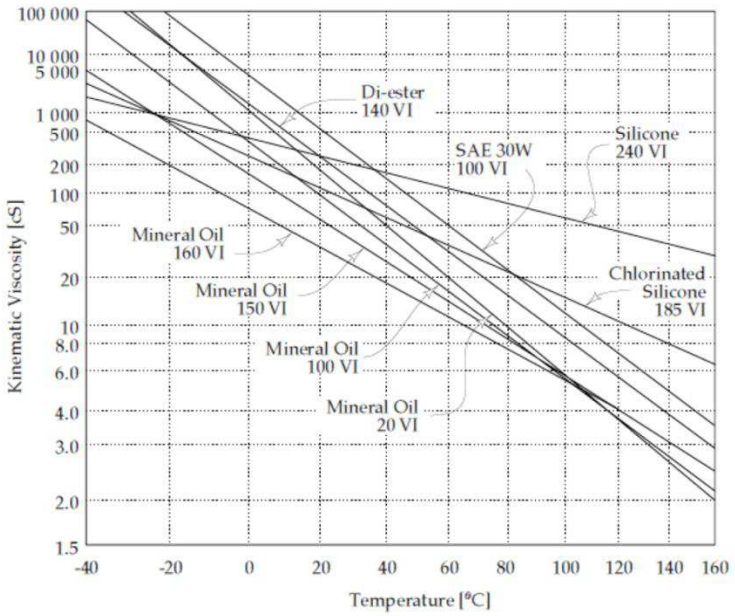

Figure 2 Viscosity/Temperature relationship of some automotive lubricants (7)

Viscosity and Temperature are correlated, since the viscosity of an oil decreases with increasing temperature (thinning) and, doing so, it reduces its ability to separate the asperities. Viscosity is also dependent on shear and, in the case of I.C.E. lubricants, they can be considered as dilatant fluids.

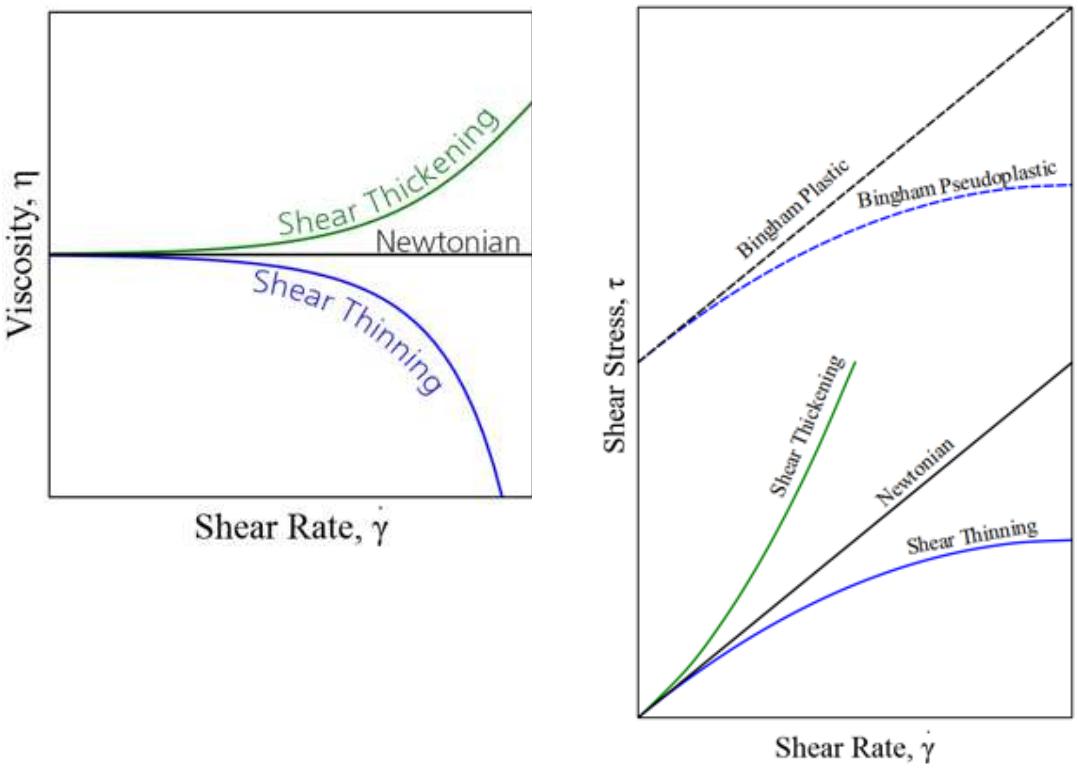

Figure 3 Fluids behaviors in Rheology

CONTACT MECHANICS

In the previous paragraphs, words like *contact load* and *normal force* have been used to explain basic concepts in tribology, even if the evaluation of forces and loads in mechanical contacts was solved only in 1882 by Hertz and lately completed in the 1970s by the DMT and JKR models, with the implementation of adhesive forces and elastoplastic behavior and deformation of surfaces.

Basically, these theories describe how the tension in two bodies does evolve when these are in contact, considering their elastic behavior, the consequent deformation and how this afflicts the size of contact area.

When a load is applied through a body to another, the elastic deformation does change the contact area. And even the contact area itself, is not the overall macroscopic area between the bodies, but only the area generated by the asperities in touch. These two discoveries were helpful to get a better comprehension not only of friction, but also of wear, since the load can involve the body at a deepness which depends on the conditions of the contact, provoking deep strains and, eventually, cracks (that is, surface fatigue wear).

So finally, contact can be divided into two kinds:

- Conform
  The surfaces are in touch through multiple points, with no strains. Contact pressure is distributed with maximum shear stresses below the surface.
- Not conform
  The surfaces are in touch through a single point (or a line). Contact pressure is concentrated on the point (or the line) with main effects at the borders.

Finally, conform and not conform contact can be elastoplastic, plastic or brittle.

At this point, several types of different tribological systems can be recognized into an I.C.E.

1.2.1 I.C.E. subsections by tribology

Most of all internal combustion engines have pistons, linked to a rotating crankshaft by a conrod and a pin, and sliding into a liner capped with a complex head which hosts the combustion chamber, the manifolds and the whole valvetrain.

All the components moving into this mechanical system generate friction losses but not all these frictions are equal. So, one can distinguish different tribological systems just considering these different kinds of friction and, therefore, the different kinds of lubrication needed:

1. The so-called *piston assembly* consists, from a tribological point of view, in a piston skirt shaking against the liner, the piston rings roto-sliding against the liner and the conrod end oscillating around the piston pin.
2. The *crankshaft system* is made of the conrod heads and the crankshaft itself, both rolling on the journal bearings. The crankcase is also the oil sump, where the shaft masses are plunged it and rotate, so it can be considered as an additional small friction generator. Furthermore, this regular diving into the oil sump, help the engine to dissipate heat (modern engine oils are specifically designed also to dissipate heat).
3. The *valvetrain system* is made of the camshaft rotating on the journal bearings, the cams pushing on tappets or on roller followers. There are actually several kinds of valvetrain systems, which differ in the position of the camshaft and the way the cam/follower couple work.

There are also other sources of frictional losses in a I.C.E., like pumps, chains and gears but they work in less aggressive conditions and have a smaller effect compared to the aforementioned systems and so they have not been considered in this study.

1.2.2 Lubrication in I.C.E. applications

Early lubrication for I.C.E. was a business for pure mineral oils and certain types of metal alloys with self-lubricating properties, but as engines technologies got finer and finer, so did the lubrication materials and methods, now including special coatings, polymeric components, synthetic oil recipes, friction modifiers and anti-wear agents and multi-grade low viscosity oils (8)

Table 1. Base oil categories

		Sulfur %	Saturates %	Viscosity Index
from refinery	**Group I** (solvent refined)	>0.03	<90	80 to 120
	Group II (hydrotreated)	>0.03	<90	80 to 120
	Group III (hydrocracked)	>0.03	<90	≥120
	Group IV	PAO Synthetic Lubricants (VI>120)		
	Group V	All other base oils (esters, POE, PAG…)		

Nowadays, mineral oils of Group I and II are not used in passenger cars application anymore, yet Group III and IV and their blends are preferred.

Oils blends are useful to achieve a proper viscosity, a multi-grade recipe, a good polarity (it decreases from Group I to Group IV) and the right dispersion of the additives packages.

Base oils are however useless in modern applications without proper additives packages, which include:

- Anti-wear agents
- Friction modifiers
- Viscosity modifiers
- Dispersants, detergents and antifoam agents

It is worth focusing on two of the items listed above.

Antiwear agents

Antiwear agents are those which are able, provoked by rubbing, to form a layer (so called *tribofilm*) resistant, hard and adherent to the underneath surface, protecting it. Generally, they are likely to be compounds with S and P in their formulation. *Zinc dialkyl-dithiophosphates* (ZDDP), since 1940s, are the most common anti-wear agents in engine oils' Industry (9) (10). The reason for this success is due to their *intimate affinity with iron* and their ability to form a glassy tribofilm upon it, with a good adhesion and hardness, able to cover and protect surfaces beneath. These compounds can be separated into two families: *primary ZDDP* and *secondary ZDDP*, with the primary alkylate compounds more stable at high temperatures (11). Unfortunately, they contain Sulphur, Phosphor and, of course, the Zinc itself which are likely to generate ashes, poisoning and fouling catalysts in the after-treatment system (ATS) and thus lowering the capability to abate pollutants. For this reason, Industry is searching for a substitute that is able to provide at least the same performances but also having affinity with both ferrous and non-ferrous surfaces and with no ATS poisoning species in its formulation.

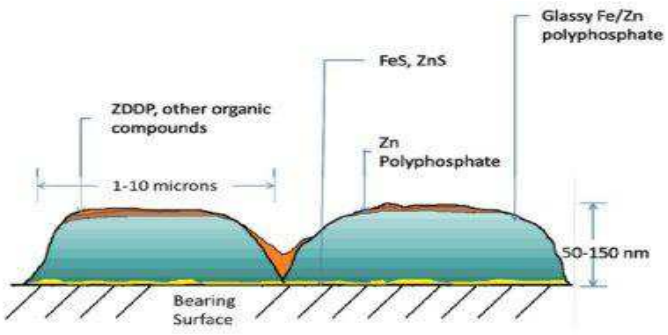

Figure 4 ZDDP derived protecting tribofilm (12)

I.C.E. working conditions range from low loads to high loads even in very short periods (fast transients) and so do the lubrication regimes, varying from BL to HL very quickly. In BL regimes, liquid lubricant is not very effective in separating surfaces and lowering COF, for this reason there are additives called *friction modifiers* which purpose is to help the system to bear the severe boundary conditions. These oil additives are usually able to provide - directly or as precursors - solid particles with a layered structure able to slide and absorb shear stresses, lowering COF.

Among all the materials with layered structure, molybdenum disulphide MoS_2 is the best representative in engine oils technology[2] since it is the most used in engine oils, mostly because of its precursor MoDTC, *molybdenum dialkyl-dithiocarbamate*, a salt which can be easily dispersed within the oil blend. However, MoS_2 can be hardly found as pre-dispersed solid particles as well: its solid particles are spherical (fullerene-like), so the layers are concentric indeed, and before being exfoliated by shear stresses, they are able to roll between the surfaces; the COF lowering power of rolling spheres is actually enhanced in comparison, as example, with two-dimensional graphite sliding platelets (13) (14).

MoS_2 of course contains metal and sulphur, that's why it suffers of the same issue of ZDDP: incompatibility with modern ATS, especially if generated by MoDTC (15). For this, it is desirable to find a greener alternative as universal friction modifier.

This time the difficulty does not consist in the affinity with the surface but in the oil itself, which is aimed to keep particles homogeneously dispersed in the liquid phase. Of course, it is not mandatory to use a solid friction modifier as it is not mandatory to couple it with the oil and not with the surface.

[2] WS_2, tungsten disulphide, and Graphene have the same structure and working mechanism as described for MoS_2. The differences between these layered materials are the following: COF, maximum load, stability, operating conditions and quality of the tribofilm generated on the surface after rubbing. Among these, graphene can be considered a greener alternative, for being metal and sulphur free but, up to date, it is the most expensive lubricous layered material.

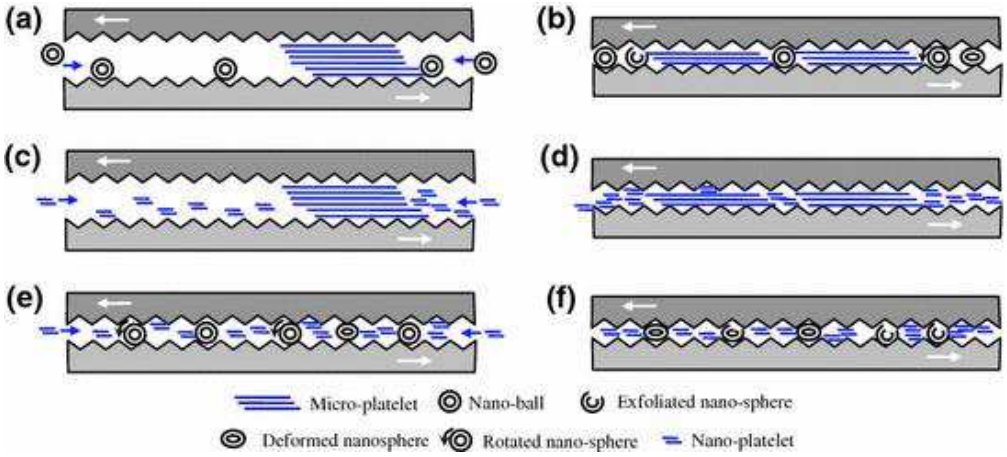

Figure 5 MoS_2 exfoliating mechanism (16)

1.3 Lubrication: state of the art

1.3.1 Components: friction & wear

For an average passenger car (17), 33% of fuel energy is spent to overcome friction in the car.

The part of the fuel energy devoted to mechanical power to overcome friction can be subdivided into groups,

- 35% (12–45%) to overcome the rolling friction in the tire–road contact
- 35% (30–35%) to overcome friction in the engine system
- 15% (7–18%) to overcome friction in the transmission system
- 15% (10–18%) to overcome friction in the brake contact

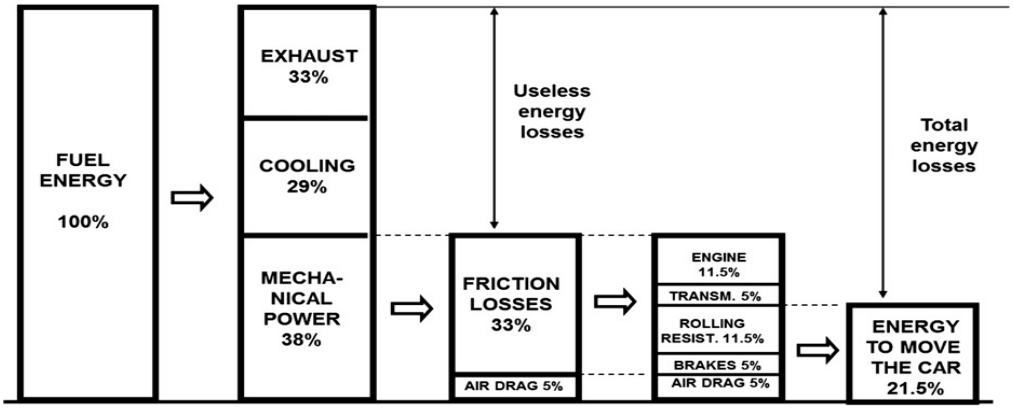

Figure 6 Breakdown of passenger car energy consumption (17)

Engine systems in passenger cars have many designs but can be divided into three basic subgroups, namely, the piston assembly, the valvetrain, and the bearings and seals.

One can subdivide engine friction losses as follows (average values):

- 45% is consumed in the piston assembly (pure sliding)
- 30% is consumed in bearings, mainly of crankshaft
- 15% is consumed in the valvetrain
- 10% is consumed by pumping and hydraulic viscous losses

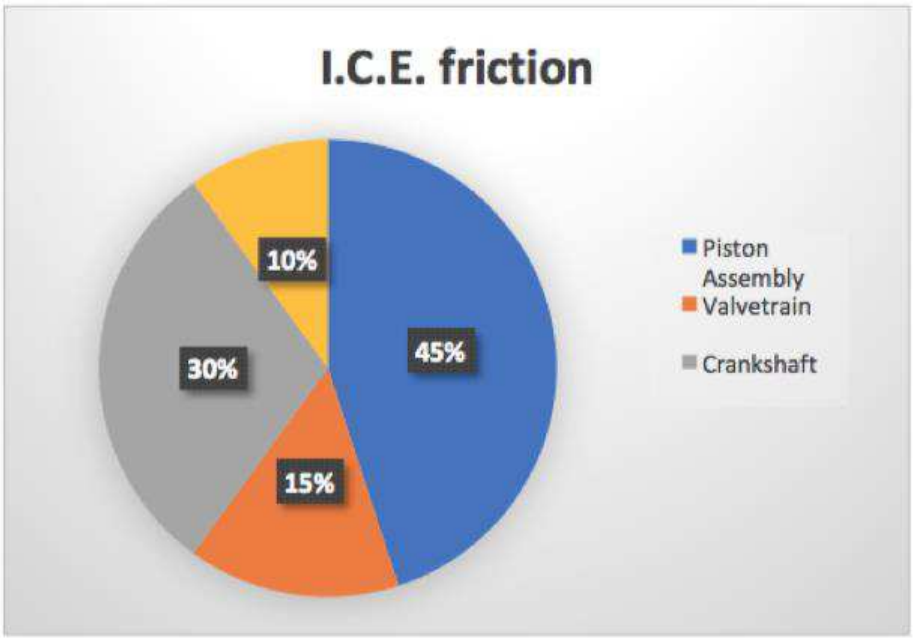

Figure 7 I.C.E. friction cake plot: 85% of total friction is due to components' sliding and can be controlled by accurate design, materials selection and lubricants development.

Lubrication regimes of I.C.E. components

For engine bearings and seals hydrodynamic lubrication (HD) dominates, while in the valvetrain mixed lubrication (ML) dominates. Mixed lubrication includes effects from hydrodynamic or elasto-hydrodynamic lubrication (EHD) and boundary lubrication (BL). Boundary lubrication is normally regarded as a mechanism of nominal fluid film lubrication with frequent solid-to-solid asperity contact incidents. The EHD contacts can be divided into three groups: EHD in sliding contacts (EHDS), such as in piston/cylinder contacts and cam-follower contacts, with possible interfacial ‘‘Stribeck-type’’ dry-friction; EHD in rolling contacts (EHDR), such as in ball-and-roller bearings, where friction originates from lubricant flow and elastic hysteresis; and EHD in sliding-rolling contacts (EHDSR), such as in gears, with a combination of sliding and rolling (18).

Coatings in I.C.E. applications

Compelling regulations about pollutant emissions have led to engines rich of technology in every detail, especially about the private cars fleet, as example, the introduction of low viscosity engine oils and coated surfaces components with improved tribological performances.

Engine parts with coated surfaces are not new but they have been being largely used in I.C.E. since the introduction of downsized units, mainly made of Al alloys, because of their poor wear resistance in specific operating conditions. At first, coated components were only piston rings (hard coatings) and piston skirts (soft coatings), but now it's quite common also to find Nikasil coated liners, DLC coated valvetrain components and piston pins and PTFE-like soaked journal bearings[3].

Of course, the chemistry of these coatings is the first characteristic of relevance in these applications. A good coating must show not just good tribological performances but also good affinity with the substrate at the interface and with the liquid lubricant: with substrate, because the adhesion must be enough to bear all the forces acting on the component during its work and with lubricant because the fluid layer must stay on the solid surfaces to provide lubrication in BL conditions, and the generated tribofilm must stay firmly on the surface meant to be protected, as it were another temporary coating.

Development of coating technologies like physical vapour deposition (PVD) (19), chemical vapour deposition (CVD) (20), and Plasma Spray (PS) techniques like High Velocity Oxy-fuel Spray (HVOF) (21) has been crucial for a massive industrial production of coated components. Since an additional suprafacial coating would mean a change in designed clearances of components, the coating thickness is an important design factor and the possibility to control thickness is desirable from a reliable coating technique, especially in case of retrofit (that is coating components already designed, with no worries about clearances issues).

[3] *Nikasil* is an electrophoretic hard coating made of a nickel matrix with silicon carbide particles. DLC is the acronym for *diamond-like carbon*, a matrix of sp_2 carbon with isles of metastable sp_3, that is a variable hard-to-soft coating aimed to work in touch with another DLC counterpart. *PTFE polymers* are used for their low friction properties in those areas of the engine where the temperatures are quite low; they also work like an oil reservoir, holding lubricant like a sponge and suppling it in oil starving conditions.

So, by choosing the right technique, one can obtain coatings with thickness ranging from micrometres to several millimetres, applicable to existing or completely re-examined components designs.

Historically, friction of coated components has been reduced by more than 90% for dry contacts and up to 50% for BL conditions. Usually, the highest values of friction reduction are related to severe rubbing conditions like in BL, since in ML and HDL contacts have few asperities engaging each other and shear takes place within the lubricant. In this sense, the main role of a coating is as safety layer (22).

Engine components can be coated for several reasons. Meaningful techniques in tribology involve anti-scuff and anti-friction coatings aimed to protect solid surfaces below and to provide a low friction counterpart in BL operating conditions.

These protective layers can be *hard coatings*, if the hardness is higher than the bulk, or *soft coatings*, if the hardness is lower than the bulk. Of course, soft coatings will serve as anti-friction layer while hard coatings can fulfill both roles of anti-scuff and friction modifier. Examples of *hard coatings* are DLC, nitrides (mainly of Ti and Cr) and anodized (made of oxides) surfaces; *soft coatings* are represented by graphite and oil-shedding fluorinated-polymers thick coatings and of very thin layers of MoS_2, WS_2, PTFE.

A good designer will always prevent to couple bulks and coatings with excessive difference in hardness and Young modulus, to avoid the so-called *thin ice effect* (a sort of provoked notch effect), where the bulk below the coatings is so softer that cannot bear the same contact force, ceasing and so denying support to the coating itself, which will be easily wrecked as consequence (an issue for Al components with nitrides coatings, as example).

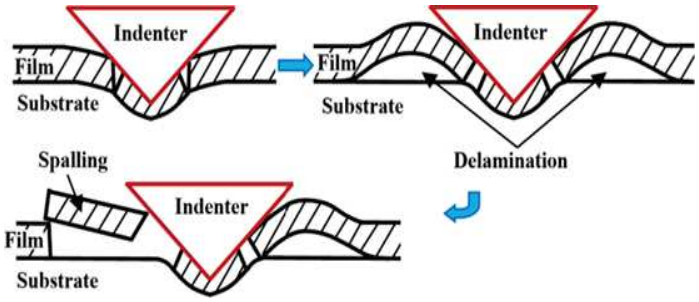

Figure 8 Failures of DLC thin films: buckle formation and consequent delamination due to excessive elastoplastic bulk deformation (23)

For Al-alloys, materials largely used in downsizing approaches of I.C.E., these effects have been strongly reduced by hardening the surfaces by shot peening with fine W particles. The resulting DLC coated Al-pistons show better scuffing wear resistance than the non-coated piston, proving that coating and native surface should be carefully selected (24).

However, DLC is not commonly used for aluminium I.C.E. components; in series application it is rather preferred coating hard steel surfaces, such as valvetrain or particular piston assemblies, in order to avoid the aforementioned thin-ice effect on softer aluminium. Coupling the smooth surfaces of DLC coatings with hardened aluminium, is still able to reduce friction and wear and help reducing engine mass without afflicting its reliability and lifespan.

Surface texturing

Another way to improve lubrication of solid surfaces is to implement surface patterns. Topography of surfaces in sliding contact has been considered as influencing only on the macroscale, that is just as surface roughness and waviness of the component. Nowadays, the comprehension of pressure profiles led to fine-tuned surfaces at micro and nanoscale. An example of these new techniques is *Laser Surface Texturing* (LST) (25), which has become a common way to create patterns on engine components' surfaces. A usual pattern adopted, especially for piston rings and liners (26), consists in a succession of equally spaced circular hollows, *fully* or *partially* distributed all across the surface.

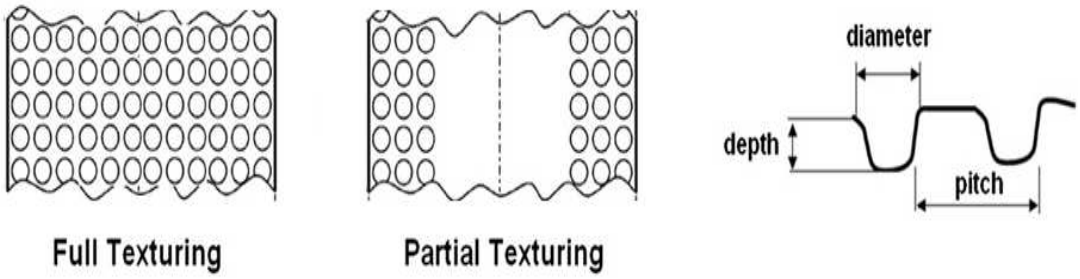

Figure 9 Characteristics, distribution and dimensions of dimple texturing (27). LST can be regulated to obtain a more complex partial texturing, i.e. 100-50-150 pattern (diameter-depth-pitch in µm), and partial surface texturing.

Such improvements are related to the following effects:

- Micro-bearing: textures generate hydrodynamic pressures even between flat profiled surfaces.
- Oil reservoir: textures act like lubricant micro-reservoirs dampening critical lubrication conditions.
- Debris trap: deep hollows can work as micro-traps storing and avoiding the presence of abrasive and debris at the contact interface
- Scratches stopper: An eventual hard particle or an asperity in contact will, at least momentarily, reduce contact when passing through the micro-dimple.

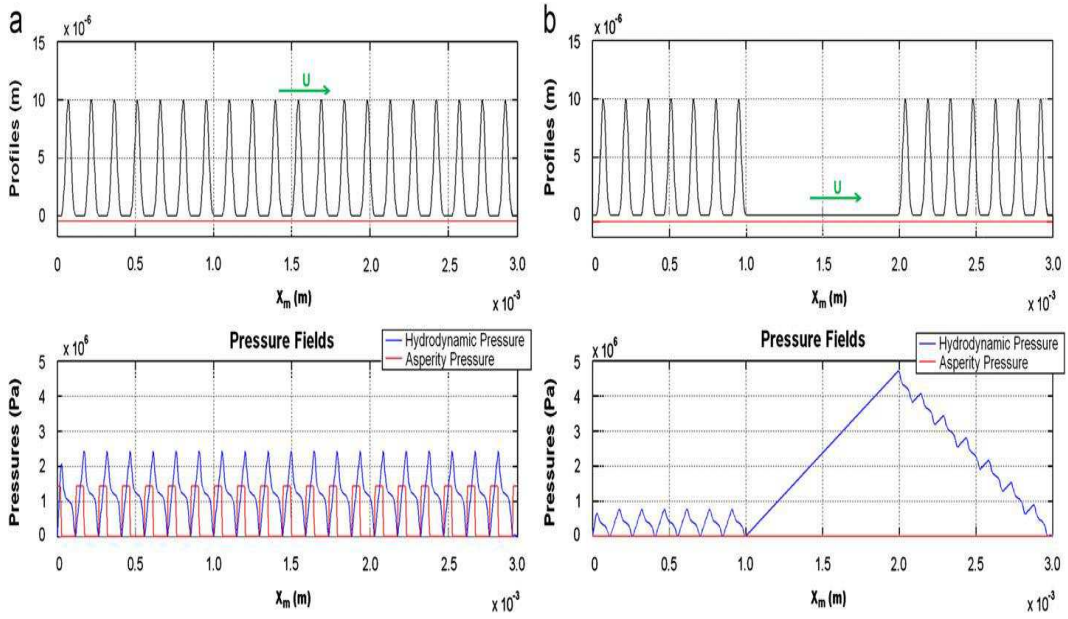

Figure 10 Texturing geometry (on top) and hydrodynamic and asperity contact pressures for the texturing variant 100-10-150. (a) full texturing (b) partial texturing (28).

Nitrides and other Coatings

On traditional iron-based components, hard coatings have been used since decades mainly to prevent wear without a great advantage about friction, which explains the need of new technologies for Fe-based components.

For Al-based parts, hard coatings are practically mandatory, especially in high performances applications or when two aluminium-made components are coupled together. A lowering of COF by using these materials is not granted, except in case of improved topography and morphology of the new surfaces; alumina coatings, as example, are known to have a worst COF compared to bare metal (29).

However, the possibility to fill the characteristic pores of anodized Al with friction modifiers opens new opportunities for Al-oriented coatings to improve both friction and wear performances (30).

Table 2. Example of traditional hard coatings for I.C.E. components. All the layers on ferrous alloys are applied by PVD/ Rotating-PVD, while Nikasil/anodizing are applied by electrophoretic processes. (31) (32)

Application	Substrate	Layer applied	COF (vs Steel)	Hardness (HV)
Stem valve	Steel	CrN, ZrN, ZrCN	0.3, 0.4, 0.5	1500, 2800,3100
Piston ring	Nitrided Steel	CrN, ZrN, ZrCN	0.3, 0.4, 0.5	1500, 2800,3100
Camshaft	Cast Iron, medium C-steel	CrN, (carburized)	0.3, (0.4)	1500 (1000)
Piston skirt, Liner	Cast Iron // Al-Cu/Al-Si alloys	Cr, Nikasil // Nikasil, Al_2O_3	0.5, 0.3 // 0.3, 0.7	800 // 2000, 700

Carbon coatings

Among the most common materials used for coatings in automotive applications, there are those based on amorphous carbon, which combine friction and wear properties with tuneable hardness and chemical stability and which mechanical properties, function of composition, can be tailored on the component surface material.

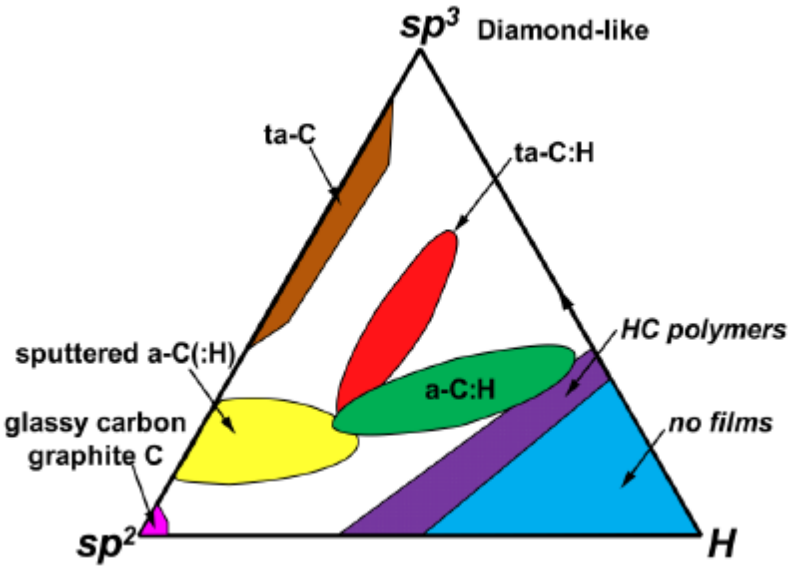

Figure 11 Ternary phase diagram of carbon films (33)

Graphite

Soft carbon coatings consist of amorphous sp_2 carbon (graphite), which may be hydrogenated (a-C:H) and contain metals (a-C:H:Me) or other non-metal elements (a-C:H:X). Hardness of those coatings depends mostly on hydrogen content, as well as affinity with substrate. Other elements can be used to influence ductility, fatigue resistance, and wettability. Hydrogen-containing carbon coatings are state of the art and are deposited by PE-CVD processes. As already said, they are already commercially used for many automotive applications like fuel injection system (valve needles, plungers, and pumping pistons), valve train (cam followers, tappets, and valves) and piston group (piston rings, piston head, and piston pin). Often, a-C:H, a-C:H:W coatings, and multilayer structures thereof are used (34).

Soft carbon coatings are mainly used in I.C.E applications as sacrificial layer with low-friction properties, achieved generating a graphitic layer transferred on the counterpart and thus dampening frictional forces of sliding (i.e. piston skirts and piston pins).

Diamond-like Carbon

Hard carbon coatings are represented by DLC (diamond-like carbon) which arises as the most promising material because of its versatile performances; the structure is a hybrid between graphite and diamond, where the graphitic region is considered the matrix and the diamond one is the reinforcement, thus achieving a tetragonal configuration (for this reason DLC is often referred as *ta-C*). DLC can be tuned in hardness by regulating the ratio sp_2:sp_3, can be doped to improve hardness and affinity with oil (usually with H, W, WC, Si, Ta) , and can be applied by PE-CVD (a low-temperature plasma-assisted CVD process which prevents issues with components metallurgical state) (35). Mechanical properties, like hardness, tensile strength and elastic modulus, largely depends on the relative amount of these two types bonding. Higher amount of sp_3 bondings results in better mechanical property (36) (37). A peculiarity of DLC is that it works better when also the counterpart is coated with DLC. That's because, during rubbing, the metastable sp_3 regions transform into sp_2, transferred to the counterpart's surface (coating's adhesive wear) and creating an interface made by two graphitic layers sliding each other. If both the components are coated with DLC, the loss of graphite by transfer is smaller, leading to higher sliding wear resistance.

As already said, the components responsible for the highest friction losses in I.C.E. are especially in piston and valvetrain assemblies, which operate at relatively high temperatures, pressures and sliding velocities, ranging as function of speed and load, with a variety of fuels and lubricants. Therefore, usage of DLC coatings in those engine systems parts is quite challenging.

Tribological properties of DLC coatings is mainly influenced by several parameters such as temperature, relative humidity, etc. (38) (39); a correct implementation of DLC coatings in I.C.E. is critical because engine parts often work at high temperatures, fast low-high-low loads, partial or starving lubrication regimes and in an environment favourable for oxidation. For these reasons, variations of DLC films by doping with hydrogen, different kinds of metals, nitrides

and carbides have been developed to improve the mechanical and tribological performances and to enhance adhesion strength to substrates of these coatings (40).

From a mixed phase, in dry sliding conditions and with the increase of temperatures and loads, a graphitic transfer layer is formed by a sp_3-to-sp_2 phase transformation of the DLC thin film (41). The steady-state low friction of DLC in dry lubrication is due to the temperature increasing at contact asperities facilitating the decay of diamond carbon to graphite and the formation of a graphitized tribo-layer (42). Thus, DLC is capable to perform self-lubrication in dry air or in inert atmospheric conditions. But degradation of DLC increases with temperature: friction and wear performances deteriorate because of the damage of DLC coating at elevated temperature (43). It has been reported that the tribological behaviour of DLC starts turning at about 100°C (44) and delaminating above 300°C (45).

High temperatures also facilitate the release of hydrogen from the DLC graphitic matrix, resulting in a shift in the ternary phase diagram towards soft coatings zones. Moreover, increasing of humidity does reduce the rate of graphitization (38) and thereby increasing friction and wear, where the friction coefficient may go tenfold higher in very high humidity conditions. Thus, the temperature and environmental parameters, plus the chemistry of lubricants and fuels, greatly influence the stability of friction and wear of DLC films.

DLC and lubricants

If the tribological performances of DLC coated I.C.E. components are influenced by the operating environment conditions, then it's very important to evaluate them under lubricated conditions to find the right additives for a significant reduction of friction and wear. Because automotive engine oils contain many kinds of complex additives, such as ZDDP and MoS_2, interactions between these additives and DLC coatings are still under investigation (46) (47).

Today however, most commercially available lubricants are optimized on ferrous surfaces, as to scale up their production and be suitable for modern (coated) and legacy (not coated) I.C.E., these last being the majority, of course. Recently, many researches are focused to understand the interactions between current lubricant additives and different types of modern coatings, such as DLC, and non-ferrous bare surfaces (48) (49) (50) (51).

Some questions - in particular tribofilm formation, decomposition of additives rubbing, chemical and physical adsorption and coatings wear mechanism - have been the subject of extensive debates (52) (53) (54) (55) (56) (57).

Kano et al. conducted several test using a *pin-on-disc* tribometer for a basic evaluation of the effects of basic oil recipes on the friction properties of some DLC coated discs (58) (59) (60).

Typical DLC coatings selected for those studies included hydrogenated amorphous carbon (a-C:H) and hydrogen-free tetrahedral amorphous carbon (ta-C). The aim of those studies was to compare the COF of these two DLC coatings and SCM415 bare steel - against steel - and coupled with fully formulated engine oil, pure PAO and PAO blended with ester (GMO - Glycerol Mono-Oleate). It was found that a ta-C coating/steel pair lubricated with a PAO oil containing $1\%_{mass}$ of ester (PAO+GMO) showed an ultra-low friction coefficient of 0,02, whereas an a-C:H coating/steel pair displayed a much higher friction coefficient of 0,09 and that of a steel/steel pair was as high as 0,100.

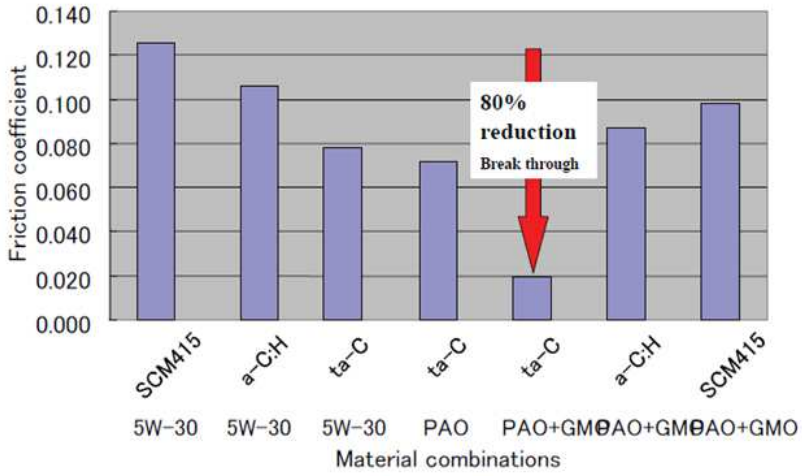

Figure 12 Ultra-low friction property of ta-C under GMO containing oil lubrication (SCM415 is DIN 15CrMo5 carburable steel). Data obtained with pin-on-disc tribometer (59)

Amazing results have been achieved by the ta-C/ta-C couple. COFs of the ta-C pairs are lower than those of the a-C:H ones. These outcomes suggest that *ultra-low friction* may be obtained thank to the interaction between the ta-C coating and the ester-containing oil (60).

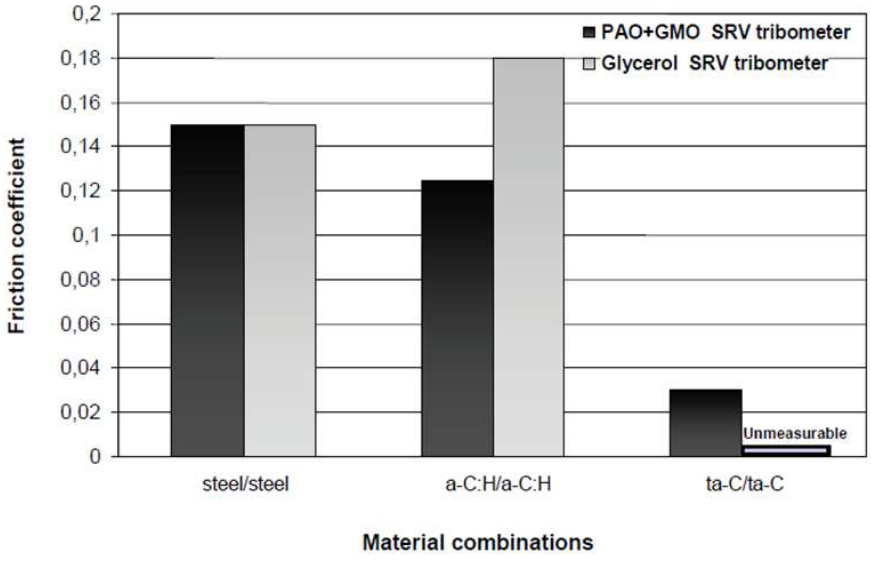

Figure 13 COF obtained for different kinds of material combinations lubricated with PAO+GMO and pure glycerin (60)

Ultra-low friction behaviour was notably obtained for the ta-C/ta-C coating combination when lubricated with glycerol at 353K. As shown in the figure above, the friction coefficient was below 0.01 and actually not well measurable by the equipment. Moreover, even the wear scar was not visible under the optical microscope. This result suggests that *superlubricity* is related to an alcohol chemical function (OH), which is common to both GMO and glycerol molecules, a conclusion shared with Simik et al., who studied tribofilm mechanism of DLC coatings with AFM technique. (61)

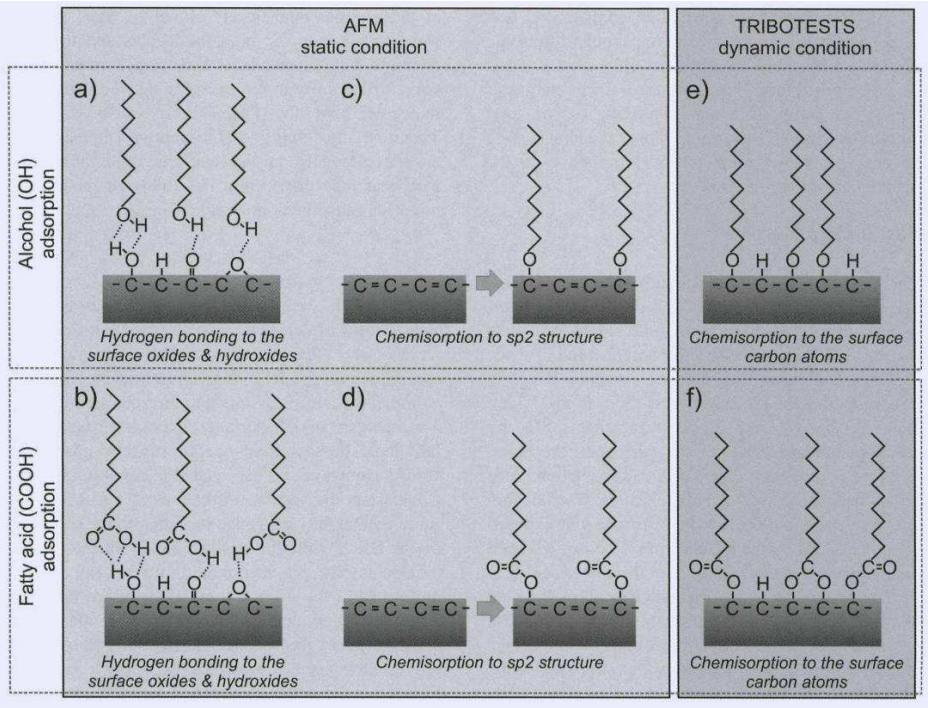

Figure 14 How alcohol and glycerol could enhance tribological performances of DLC thin films. "Tentative adsorption mechanisms for alcohol and fatty acid molecules onto DLC; alcohol a) and fatty acid b) molecules physisorb by the hydrogen bonding to the surface of DLC

Similar results also from Yang et al., who proposed a full comparison of the behaviour of an a-C:H/W coating (DLC doped with W) with several kinds of basic formulation oils (62).

Yang built an experiment where six model oils, namely from Oil A to Oil F, have been chosen, using steel/steel and steel/DLC pin-on-disc tribometer, in order to assess the individual effect of some oil additives. In particular, the oil additives were friction modifiers (GMO and MoDTC) and an anti-wear additive (secondary

ZDDP). These simplified recipes allow the study of single additive roles compared to fully formulated oils which contain a more complex package of additives.

Oil[a]	Additive type	Treat rate (wt%)	Viscosity at 100° C (Pa s)[a]
Oil A	–	Base oil	0.0026
Oil B	ZDDP	0.08% P	0.0032
Oil C	GMO	0.2%	0.0031
Oil D	GMO+ZDDP	0.08% P	0.0028
Oil E	MoDTC	100 ppm Mo	0.0029
Oil F	MoDTC+ZDDP	0.08% P, 100 ppm Mo	0.0028

[a] Base oil of the model oils are all poly-alpha olefin Group IV base stock (PAO 4).

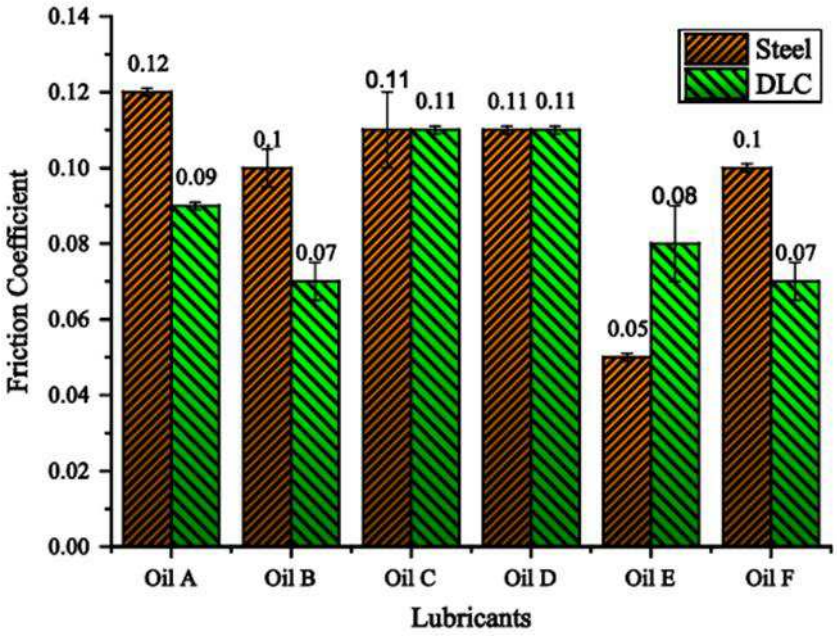

Figure 15 Description of the oils used by Yang and bar graph about friction coefficients comparisons between W-DLC coating and steel in model oils (62)

Clearly, from Figure 15, COF of DLC is lower in case of pure base oil, with just ZDDP and with both ZDDP/MoDTC while the oils with GMO or with pure MoDTC resulted in odd performances. In the case with MoDTC alone in particular, steel performed better, because a severe wear of the thin DLC film occurred. It seemed that ZDDP does have some protecting properties towards those coatings. A probable explanation to this behaviour is that the presence of sulphur-donors, as

ZDDP, may help the formation of WS_2, lowering the COF and retarding wear failures. The glassy tribofilm resulted by ZDDP is able to protect the hard but brittle DLC thin film from the MoO_3 hard particles derived from MoS_2 decay, which have been proved to wreck the coating, shortening the working life and increasing COF (63).

Sulphur and Phosphor seem to play an essential role in the formation of a good tribofilm, for sure in relation with ferrous surfaces. But a greener lubricant formulation, able also to not generate poisoning ashes for the ATS, should include components sulphur and phosphor free (despite Fino et al. proved that MoS_2 nanoparticles added to the liquid phase have no influence on the performances of ATS, compared to MoS_2 generated from MoDTC (64).

Finally, it seems that those engine oils formulated with esters (or with a certain amount of esters) as friction modifiers, somehow allow to easily achieve ultra-low COF when coupled with innovative coatings, like DLC films. Consequently, oils designed for performance engines or even for light-duty downsized engine units (with coated components) should be designed with high amounts of esters.

Unfortunately, these kinds of lubricants are often shelved by producers and, in general, FAE (*fatty acid esters)* are used in low amount in commercial recipes. A reason for this could be that, despite esters are extremely biodegradable, thus more sustainable (65), and more effective in COF reduction than traditional oil additives, their costs (additive production and lubricant engineering) is still too high and, despite their overall performances allow further costs savings, the final products may be perceived as too expensive in the short term by the final customers.

A more feasible solution would be to simply swap traditional additives, such as MoS_2 and ZDDP, with other anti-wear and friction modifying agents without - or with minor- other changes in the lubricant formulation.

For this, a better comprehension of lubrication of coated surfaces and of the formation of good tribofilms is crucial to design modern lubricant recipes. Oil and tribofilm affinity of DLC coatings are the current issue of these application, which investigation is the main object of this thesis.

Final considerations

Finally, here are some conclusions and forecasts from an analysis of friction in passenger cars as proposed by Holmberg in 2012 (17), literally:

- *Considering the whole vehicle, about one-third of the fuel energy is used to overcome mechanical friction (split as in engine, transmission, brakes and tires). In total, about 20% of the fuel energy is used to move the car, the remaining part is wasted in friction and heat.*

- *Considering this value, one can calculate that, worldwide, more than 200 billion litres of fuel (gasoline and Diesel) was used in 2009 to overcome friction in passenger cars. Reductions in frictional losses will have a big improvement in fuel economy, as it will reduce both the exhaust and cooling losses also at the same ratio.*

- *By taking advantage of new technologies for friction reduction in passenger cars, friction losses could be reduced by 20% in the short term (5–10 years) and by 60% in the long term (15–25 years). This would equal worldwide economic savings of billions of euros, billions of litres of fuels, and emission reduction of million tonnes of CO_2.*

- *Potential mechanisms to reduce friction in passenger cars include the use of advanced coatings and surface texturing on engine and transmission components, beside low-viscosity and low-shear lubricants and novel additives.*

1.3.2 Oil technology

In the previous paragraphs, the current qualities of base oils and additives currently used by Lubricants Makers and how these recipes should be modified to fit new technologies like non-ferrous alloys or coated surfaces has been discussed. Some studies suggest the introduction of GMO or, in general, a higher amount of esters in modern lubricants formulations; other studies show different working mechanisms for classic oil additives when coupled with innovative surfaces. In general, what is asked to Oil Makers is to provide new formulations able to protect these new surfaces and allow lower friction as well.

Nowadays, few research groups are focused on developing commercial cheap formulations; more often synthetic base oils, like PAO, are used to investigate the behaviour of coated surfaces and friction modifiers/anti-wear agents. Eventually, very expensive solutions are proposed, like ionic liquids or graphene-based recipes.

Final customers however are interested in cheap solutions while, as example, fully synthetic formulations or ester additivated lubricants are far from being cheap (still being way less expensive than graphene!).

Waiting for a larger availability of new generation of refinery products called *Group III+* oils (extremely highly refined mineral oils, ranked between group III and IV but not synthetic[4]), which should allow thinner lubricants, high purity and low costs, a nice achievement should be to develop modern lubricants, able to work in these modern engines, or at least to understand the basic tribological needs of these new I.C.E. technologies.

[4] NEXBASE® from Neste and YUBASE® from SK are some first commercial examples of group III+ base oils. Their particular processes in the oil refinery, involve hydrocracking and isomerization in order to achieve higher purity grades with respect to traditional group III base oils.

1.4 Mini Traction Machine (MTM)

All the test campaigns have been conducted by using the same tribometer, a MTM2 by PCS (Mini Traction Machine, mk II) (66).

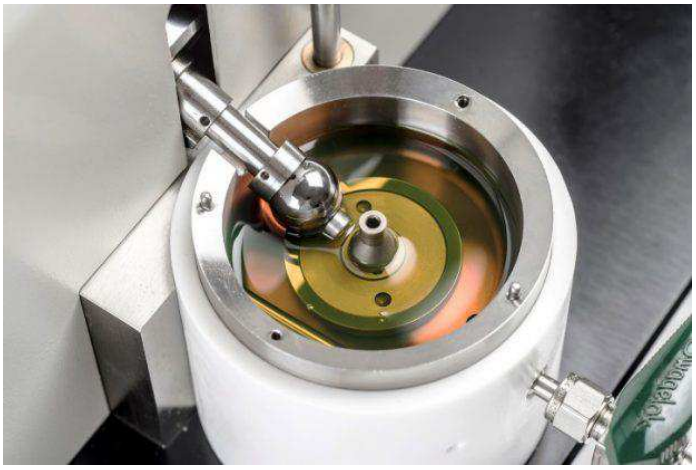

Figure 16 View of MTM pot, already filled with lubricant and with mounted specimens, in open position.

The MTM is a very versatile tribometer, capable of rapid COF assessments and to investigate on mild lubricated wear. It is possible, in the basic setup (the same setup used within this work), to regulate the temperature of the oil, the contact load and, thanks to two independent rotors, absolute and relative speed of the specimens (Figure 17). The MTM is also able to work in contra-rotation, to enhance sliding speed while still controlling the entrainment[5] speed.

The sliding speed is the difference between the speed of the ball u_1 and the speed of the disc u_2, while the entrainment speed (or rolling speed) is the average of the two values. The ratio between these two speeds represents an important value, in tribology and in every MTM test: the *Slide-to-Roll Ratio* (SRR).

[5] Entrainment is the transport of fluid across an interface by a shear induced turbulent flux (69). For lubricated tests in a two-rollers machine, where the axes of rotation are fixed, the Rolling Velocity is the same as the lubricant Entrainment Velocity.

$$SRR = \frac{\text{sliding speed}}{\text{entrainment speed}} = \frac{|u_1 - u_2|}{(u_1 + u_2)/2}$$

Equation 1 Slide-to-roll Ratio definition

Because the properties of the lubricating film may vary according to entrainment speed and sliding speed (that is, SRR), the resulting friction and wear performances of the system would change as well (67).

The asperities contact type obtained with a specific SRR is able to influence the formation and growth of the tribofilm, thus showing different COF and wear rate for a given test setup (68). The highest value of SRR with the MTM basic settings is 2, that is that when the sliding speed is twice the entrainment speed. For higher SRR, contra-rotation settings are needed.

The MTM specimens are a disc and a ball, made with a specific geometry but supplied in a variety of materials, coatings and surface finishing, on customer demand (Figure 16).

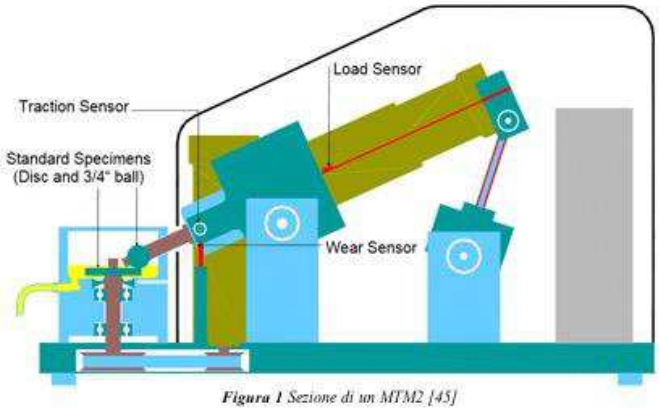

Figura 1 Sezione di un MTM2 [45]

Figure 17 Schematic of MTM working principles (66)

From the MTM official website: *"In the standard configuration the test specimens are a 19.05mm (3/4") steel ball and a 46mm diameter steel disc. The ball is loaded against the face of the disc and the ball and disc are driven independently to create a mixed rolling/sliding contact. The frictional force between the ball and*

disc is measured by a force transducer. Additional sensors measure the applied load, the lubricant temperature […] and the relative wear between the specimens."

To perform the tests of this work, a particular program has been conceived in order to assess the performances of the lubricants, additives and surfaces of interest. Basically, there are two kinds of test:

- Method #1: SRR set to 200%, rubbing time up to 2 hours. Aimed to provoke wear.
- Method #2: SRR set to 50%, rubbing time up to 1 hour. Aimed to assess tribofilm formation and growth.

Contact load is always set to 31 N, resulting in a contact pressure of 1 GPa with the given geometry of the specimens. Every endurance test is programmed in ten steps, as listed below (rubbing time is *method #2/method #1*):

1. Step 1: Stribeck curve at T = 40 °C (*cold start*)
2. Step 2: Stribeck curve at T = 100 °C
3. Step 3: Rubbing, t = 5/10 minutes, T = 100 ° C
4. Step 4: Stribeck curve at T = 100 °C
5. Step 5: Rubbing, t = 10/20 minutes, T = 100 ° C
6. Step 6: Stribeck curve at T = 100 °C
7. Step 7: Rubbing, t = 15/30 minutes, T = 100 ° C
8. Step 8: Stribeck curve at T = 100 °C
9. Step 9: Rubbing, t = 30/60 minutes, T = 100 ° C
10. Step 10: Stribeck curve at T = 100 °C

Hardened AISI52100, bare and coated with DLC, is the material selected for these tests. DLC has a ratio of 1:1 of sp_2:sp_3 bondings, with a hydrogen surface coverage of about 40%. Endurance tests of 1 and 2 hours consist of 20 steps of alternate *Stribeck curve mode*, running from 3000 to 10 mm/s, and rubbing periods, at 1000 mm/s of constant mean speed.

The tests have been executed several times to achieve reliable results. The outputs from method #1 are fuzzy Stribeck curves, which are not very meaningful, while the outcomes from method #2 clearly depict the evolution of the tribofilm and the resulting COF.

In particular, in the following pictures some explaining example of method #2 outputs are reported.

The plot is logarithmic and for very low speeds there is the Boundary Lubrication zone, for very high speeds there is the Hydrodynamic Lubrication zone. In the middle, of course, Mixed Lubrication occurs. The first plot regards an endurance test of steel/steel (always consider this code as ball/disc) with pure base oil (fig16).

This system is not able, without specific additives, to generate a good tribofilm, able to lower COF so, step by step, the friction is increasing in every area of the plot. Of course, the HL zone for the 40°C curve shows lower COF, because the thickness of the oil film is not afflicted by temperature yet.

Table 3 Materials specifications of the specimens

Specimen Surface	Hardness	Specific Wear Rate	Roughness
Steel **AISI52100**	800 HV	10^{-15} m^3/Nm	Ra<0,01um
DLC **ta-C:H**	1600 HV	10^{-17} m^3/Nm	½ steel

Finally, the outputs from method #2 are meant to be interpreted immediately while method #1 is used just to generate worn specimens, to be later analyzed with other investigating instruments (like microscopes, profilometers, etc.).

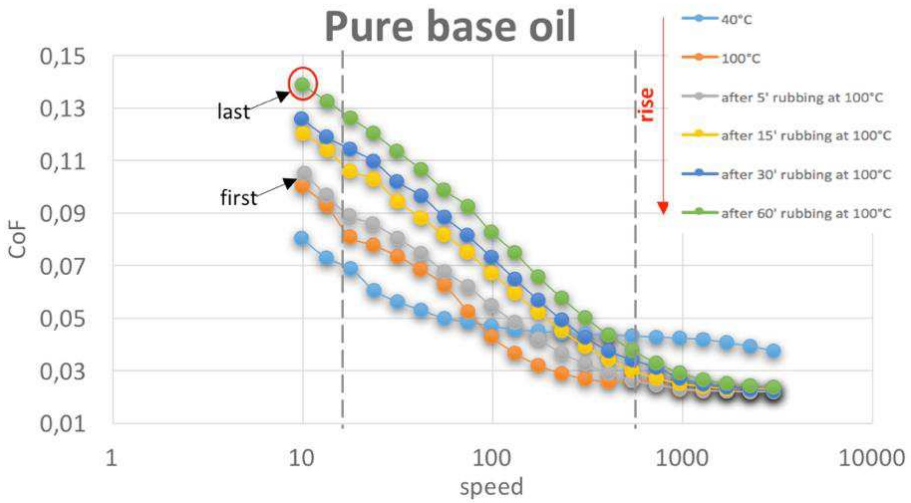

Figure 18 Endurance friction test output example with pure base oil

A very different behaviour is shown in the following picture (Figure 19), where a steel/steel tribocouple has been tested with the same base oil, this time blended with a friction modifier. Here one can notice that the formation of the tribofilm slows down the rise of the COF and, at a certain point, overall performances of the grown tribofilm are so good that COF starts decreasing, till COF values even lower than the starting conditions.

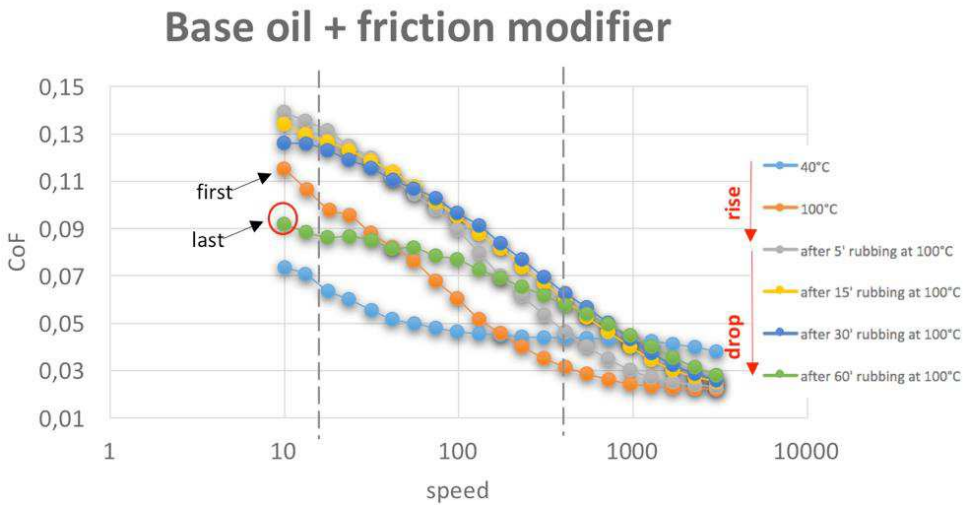

Figure 19 Endurance friction test output example with additivated base oil

1.5 Experimental activities on MTM

In order to evaluate the behaviour of DLC coated surfaces at the tribometer, a full test campaign has been set up (using DoE methodology), involving a secondary ZDDP as anti-wear agent and MoDTC as friction modifier[6].

At first, some base oils have been compared in steel/steel tests to assess the differences between each quality of lubricant and their behaviour at different MTM setup. This first approach had the aim to choose a unique base oil for the next full test campaign.

The base oils selected for this very first screening have the same kinematic viscosity (6 cSt at 100°C); later also 4 cSt at 100°C oils have been added to the campaign. They are:

- Group I, a mineral oil (>C20)
- Group III, a mineral hydrocracked oil (C15)
- Group IV, a PAO (C10)
- Group V, a glycol ester (C18)

Before each run, the specimens have been sonicated in petrol ether for 30 minutes, in order to rinse them from their protective oil layer. The same procedure, but with a mixture of hexane, petrol ether and isopropanol, has been executed before further instrumental analysis, such as XPS, AFM, Raman Spectroscopy and FESEM.

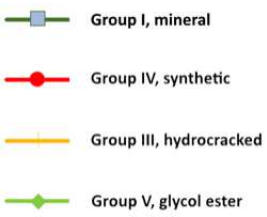

Figure 20 Legend for all the endurance tests of this work

[6] Instruments and most of the materials used in this experimental activity, including base oils, ZDDP, MoDTC, the MTM and its specimens, have been kindly provided by Petronas Lubricants Italy (Villastellone, IT). The activities at the tribometer have been entirely ran in the laboratories of Petronas Lubricant Italy.

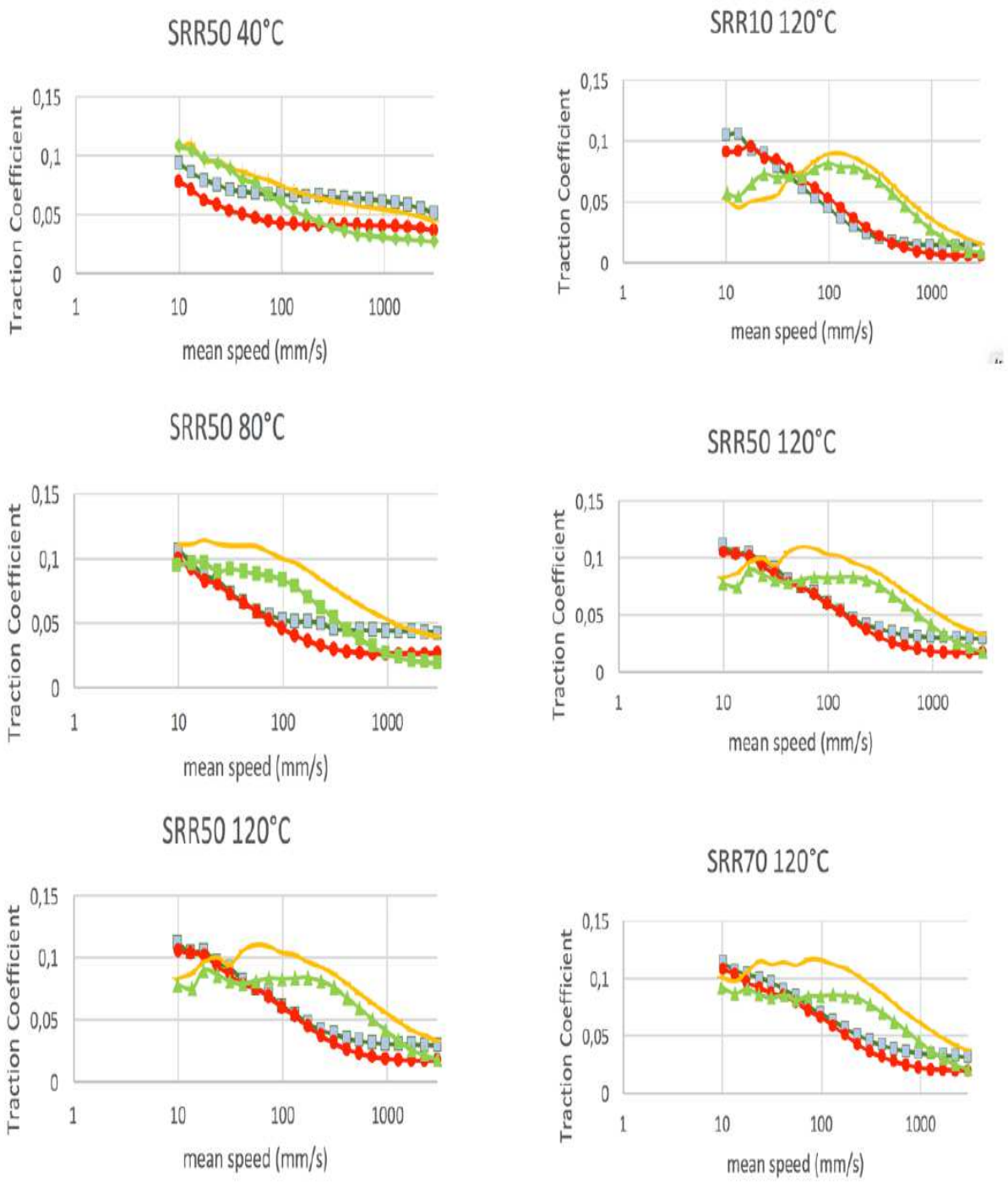

Figure 21 Screening of a suitable base oil for the test campaign, varying temperature and SRR.

Group I base oil was, of course, the less performing and put into the bunch only for comparison, with no will of success. Group III and Group V show some negative friction modifying capabilities, as one can see from the flattened curve in ML areas of the plots (in particular, COF is always the worst of the comparison) (Figure 21).

For this reason, they both have been rejected as *baseline oil*s for further tests for they could cover the effects of tribofilms and other friction modifying agents.

Group IV, for its good performances, its constant behaviour at different temperatures and SRR, its "transparency" towards friction and its intrinsic purity (that means, no chemical reactions may occur with oil additives and solid surfaces) has been chosen as reference for all future tests at the MTM tribometer.

Furthermore, using a group IV base oil as baseline could project this work and its results further in the future, as only synthetic base oils are able (up to date) to achieve the viscosity, the thickness and the ageing resistance required by current and future SAE regulation.

All the MTM test in the next sections, have been made with lubricants formulated with Group IV base oils, running at 100°C and with SRR varying from 50% (method #2, friction) and 200% (method #1, wear).

1.5.1 Base oils and Formulated Lubricants

After the selection of the base oil, some experiments have been conducted to determinate the correct amount and ratio of anti-wear and friction modifier, necessary to determinate the right recipe for what in this work is referred as a *fully formulated oil*.

The first issue has been the difficulty of merging MoDTC into pure PAO base oil; the very low polarity and high purity of this oil cannot sustain the friction modifier in a stable solution.

A prompt answer could have been to add up to 20% of ester, to compensate the low polarity of PAO.But esters are friction modifiers themselves and they may somehow affect the correct assessment of external agents. Finally, a blend of PAO and 20% Group III oil has been chosen as reference.

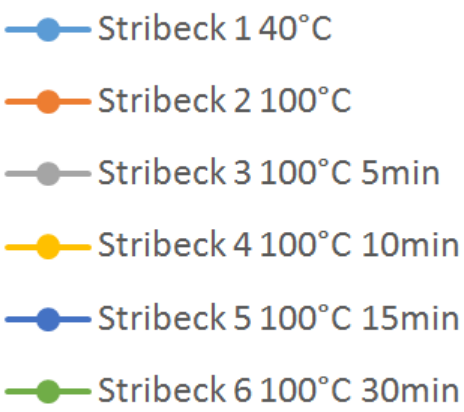

Figure 22 Legend for all the endurance tests presented in this section

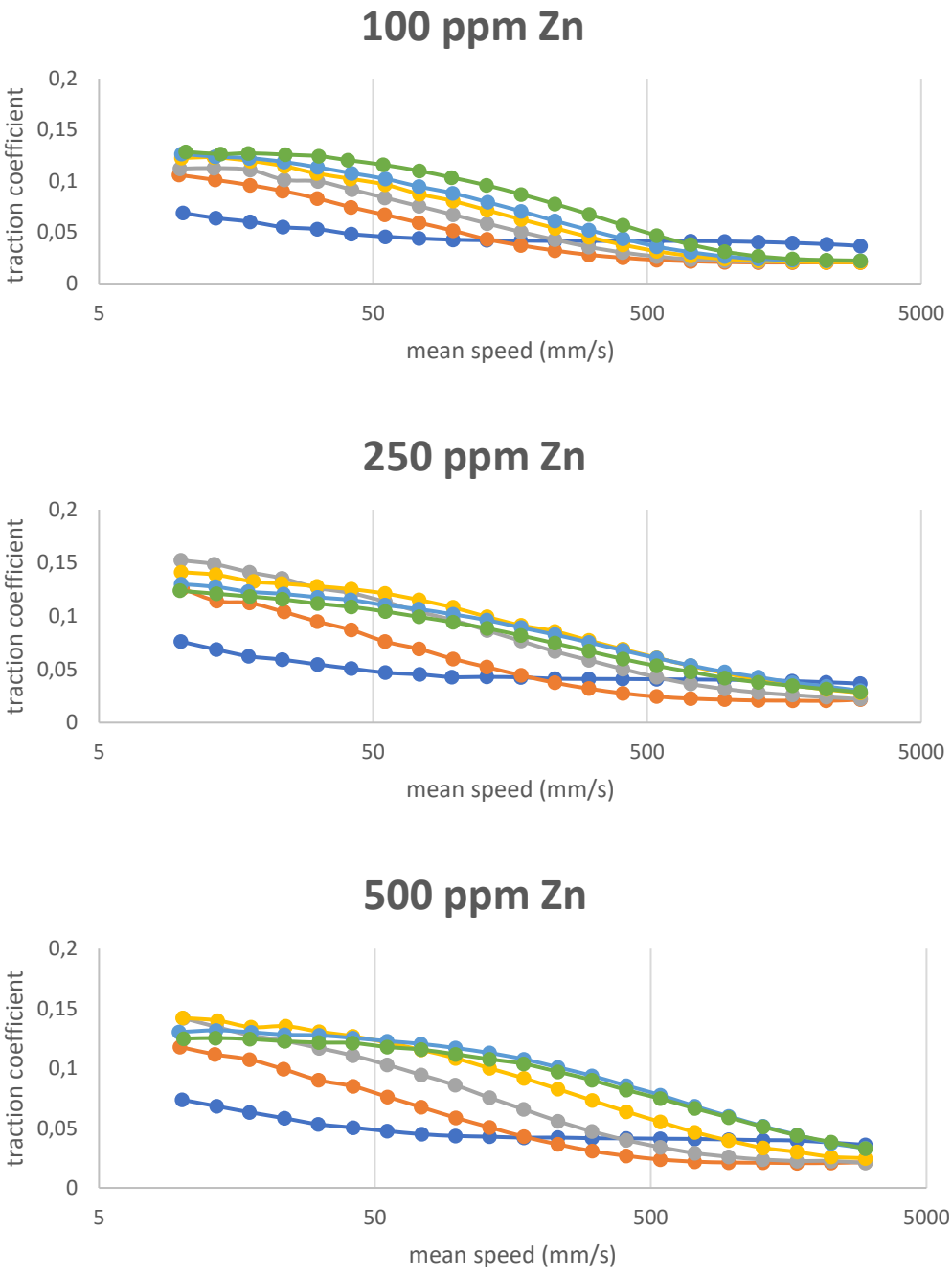

Figure 23 Effects of ZDDP to PAO6 blend (legend above)

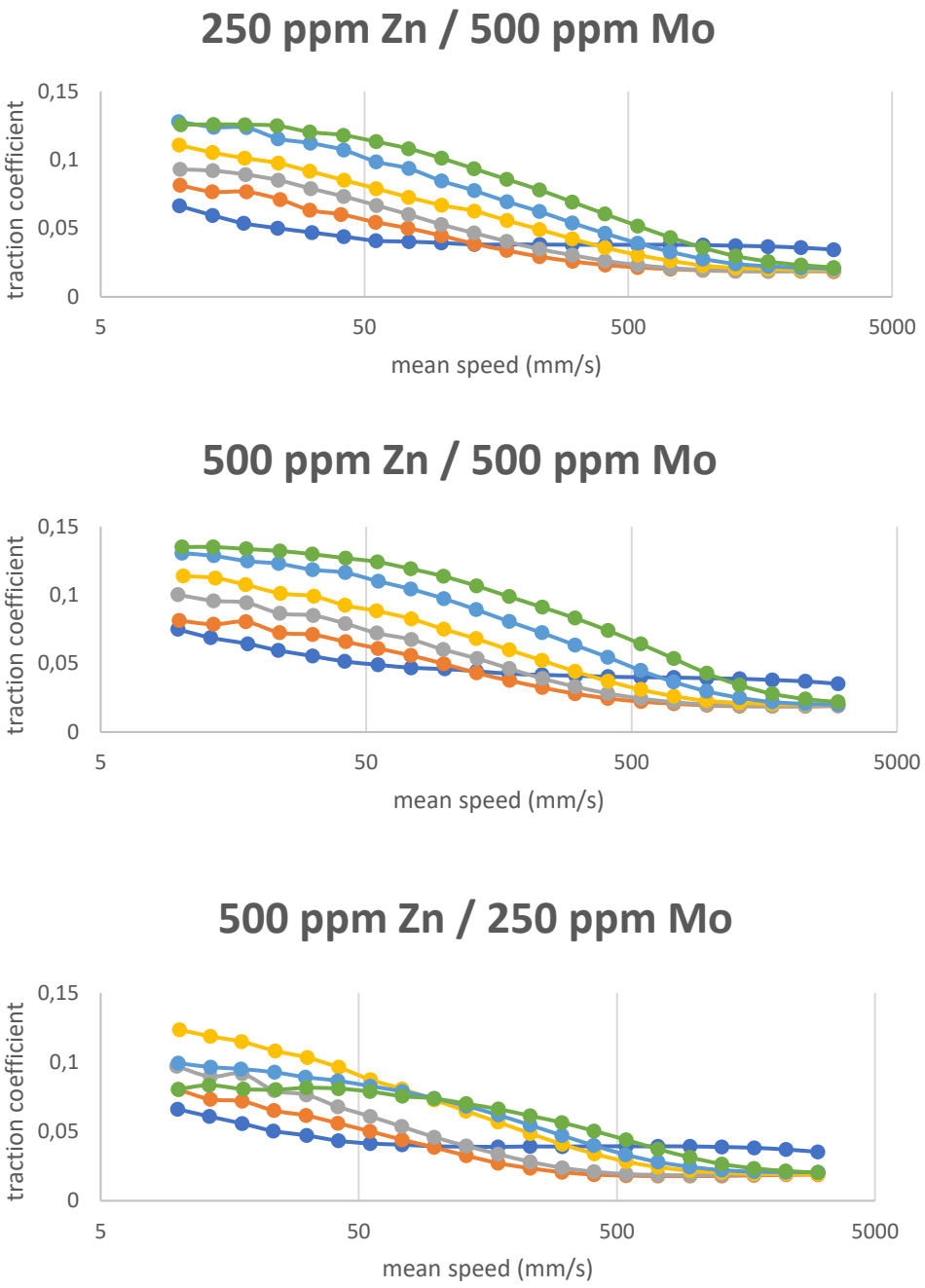

Figure 24 Different ratios of ZDDP and MoDTC in PAO6 blends (legend above)

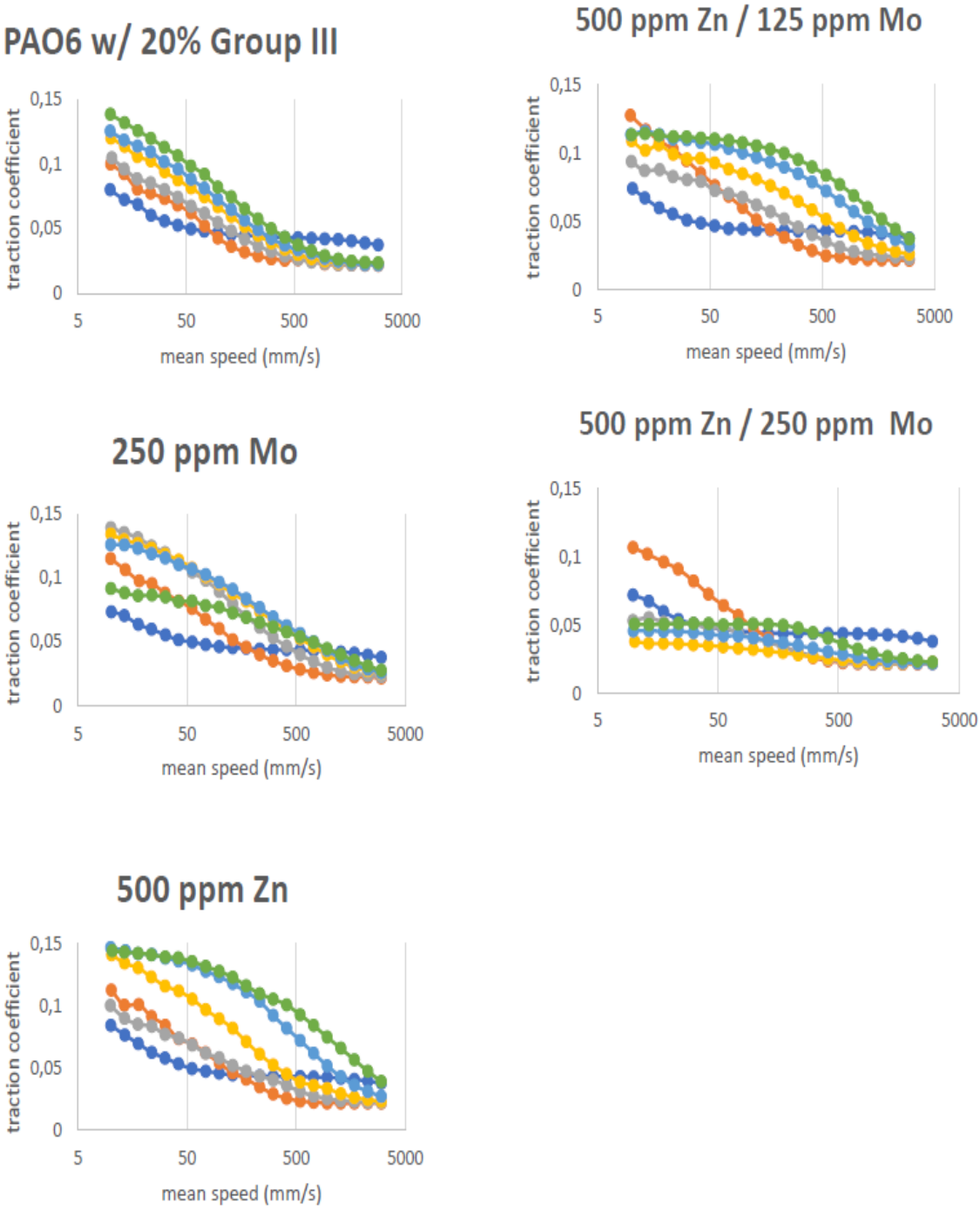

Figure 25 Assessment at MTM of the ratio and amount of ZDDP/MoDTC. Steel/Steel tribopair (legend above)

A ratio Zn:Mo of 2:1 has been found to be the most effective in friction reduction, with a minimum amount of 250 ppm Mo (Figure 25). The total amount of Mo influences only the duration of the low friction period. As rubbing time rises, more MoDTC decays into oxides, and when the lubricant is completely depleted of friction modifier, overall performances start decreasing as well.

A ghost tests campaign has been conducted with an amount of Zn and Mo of 200 and 100 ppm, respectively, to investigate the opportunity of a lower S content in the lubricant. The results of those runs are not showed, since the COF are generally higher the Zn/Mo:500/250, as predicted by the preliminary screening.

Kinematic viscosity effects have been investigated comparing a PAO6 and a PAO4 (Figure 26). Moving towards thinner oils, like from 6 cSt to 4 cSt at 100°C, resulted in no convenience at all or even in higher COF in BL. This means that lubrication with thin oils in critical operating conditions (like BL, or cold start) is not reliable if leaning only on the lubricants alone. Surfaces able to self-lubricate are essential for these purposes.

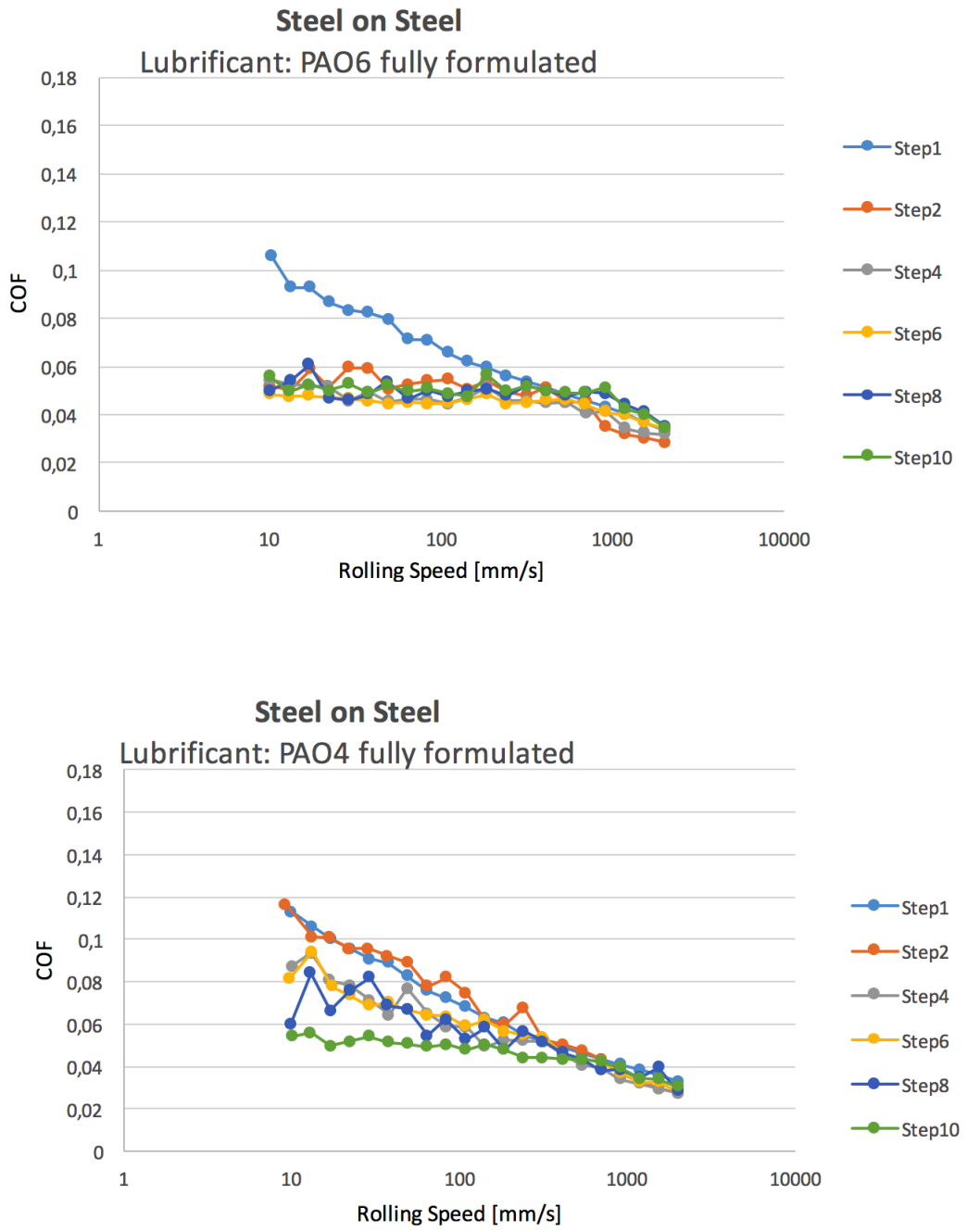

Figure 26 Viscosity comparison at MTM for PAO4 and PAO6 formulated oils

The same comments also for the formulated version of the two base oils: PAO4 shows worst performances compared to PAO6 in this test campaign (see Figure 27).

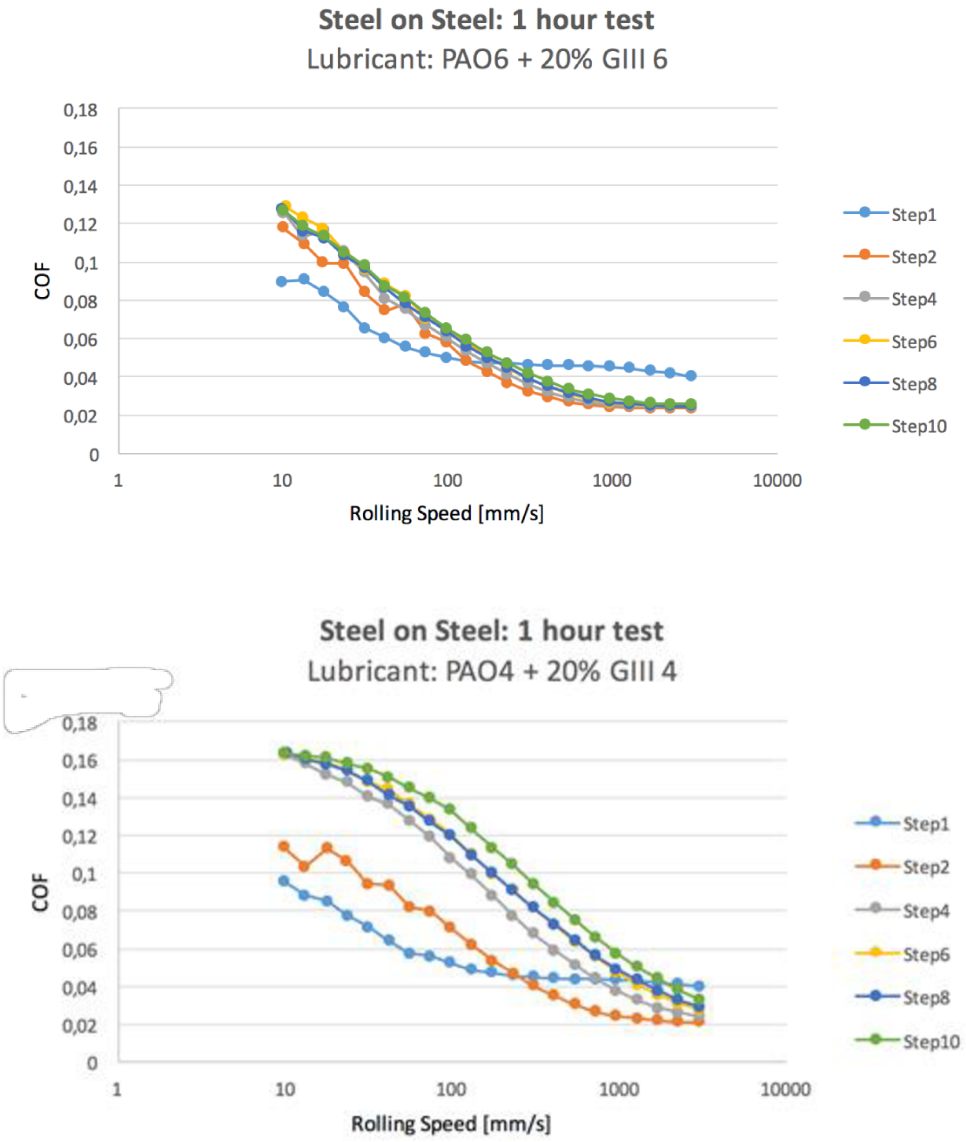

Figure 27 Viscosity comparison at MTM for pure PAO4 and PAO6

A quick comparison has been done between G III and G IV oils. G III oils show always lower friction compared to G IV. This may be due to impurities, such as Sulphur and Phosphor compounds, which are in general friction modifiers themselves and, furthermore, they enhance the wettability of the ferrous surface, acting like bridges between solid and liquid phases.

1.5.2 Friction assessment

As already mentioned in the previous paragraphs, method #2 has been used not just to select a common base oil and its formulation for all the campaign, but also to assess the performances of the systems Steel/Steel and DLC/DLC.

Tests with DLC/Steel and Steel/DLC have been done, but the difference in hardness and wear resistance between the two surfaces always has led to premature failure of each run. There is no hint about the use of such couples in automotive applications however.

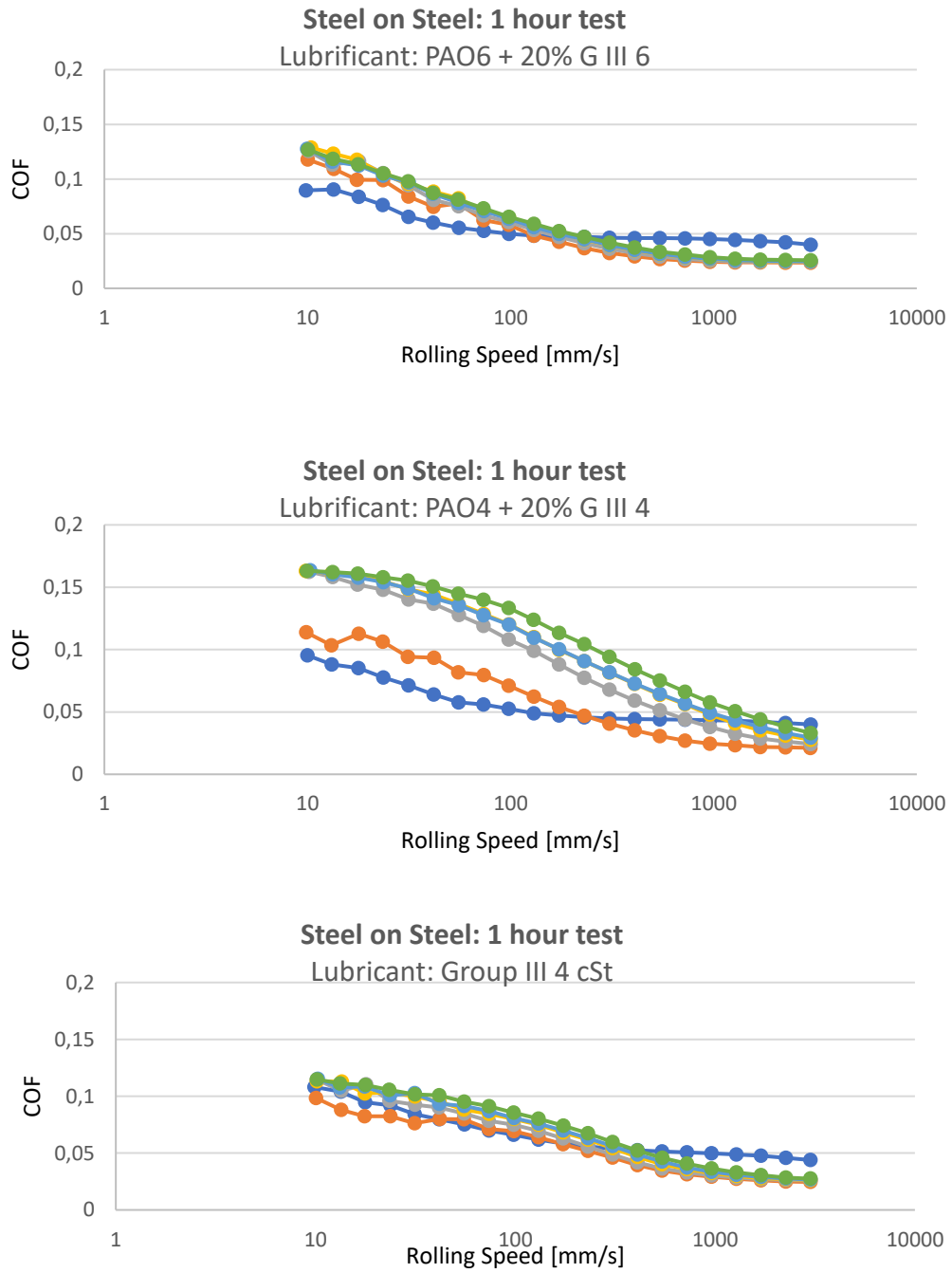

Figure 28 Comparison between pure Group III, PAO6 and PAO4 blends. Steel/Steel on MTM (legend above).

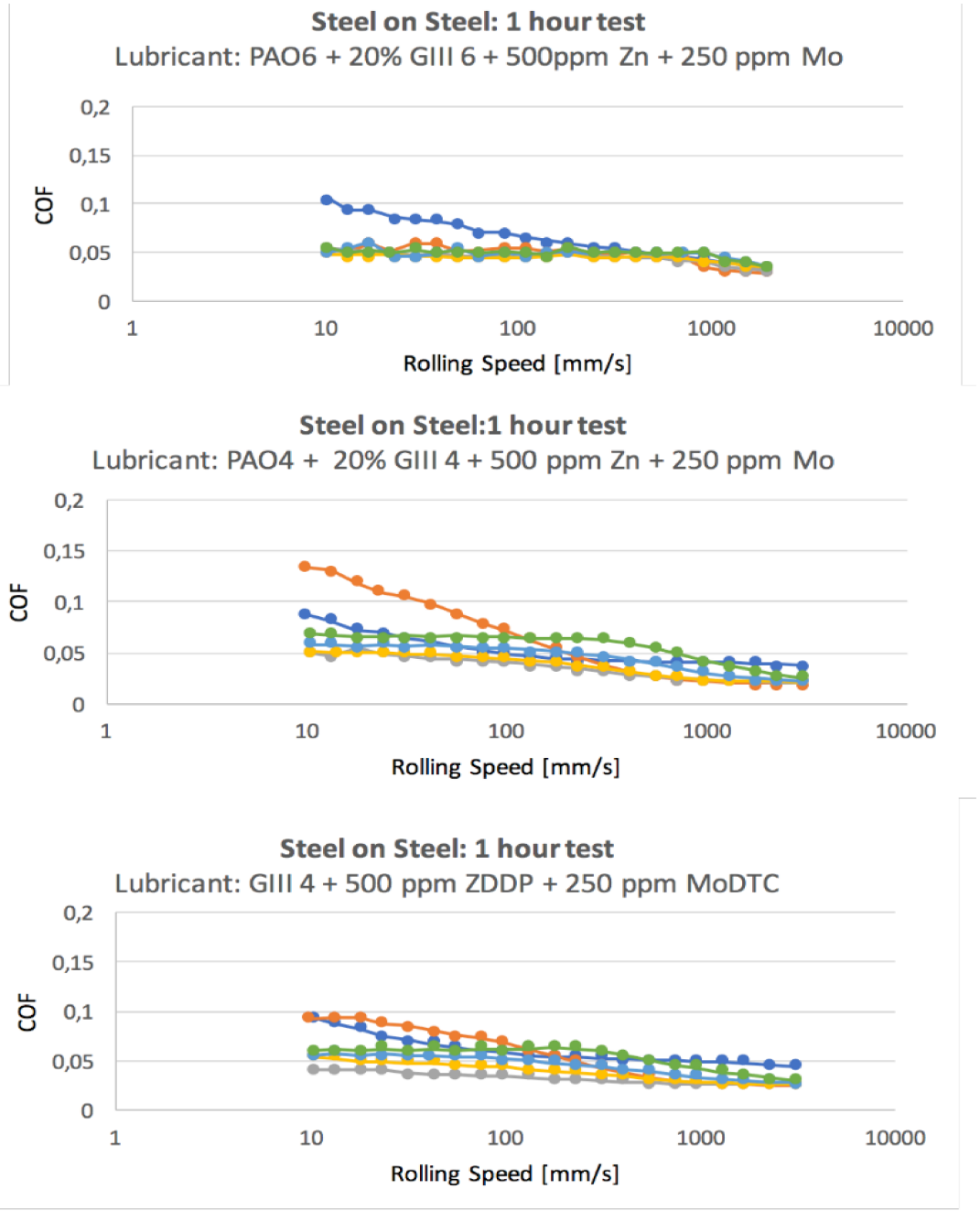

Figure 29 Comparison between fully formulated Group III, PAO6 and PAO4 blends. Steel/Steel on MTM (legend above).

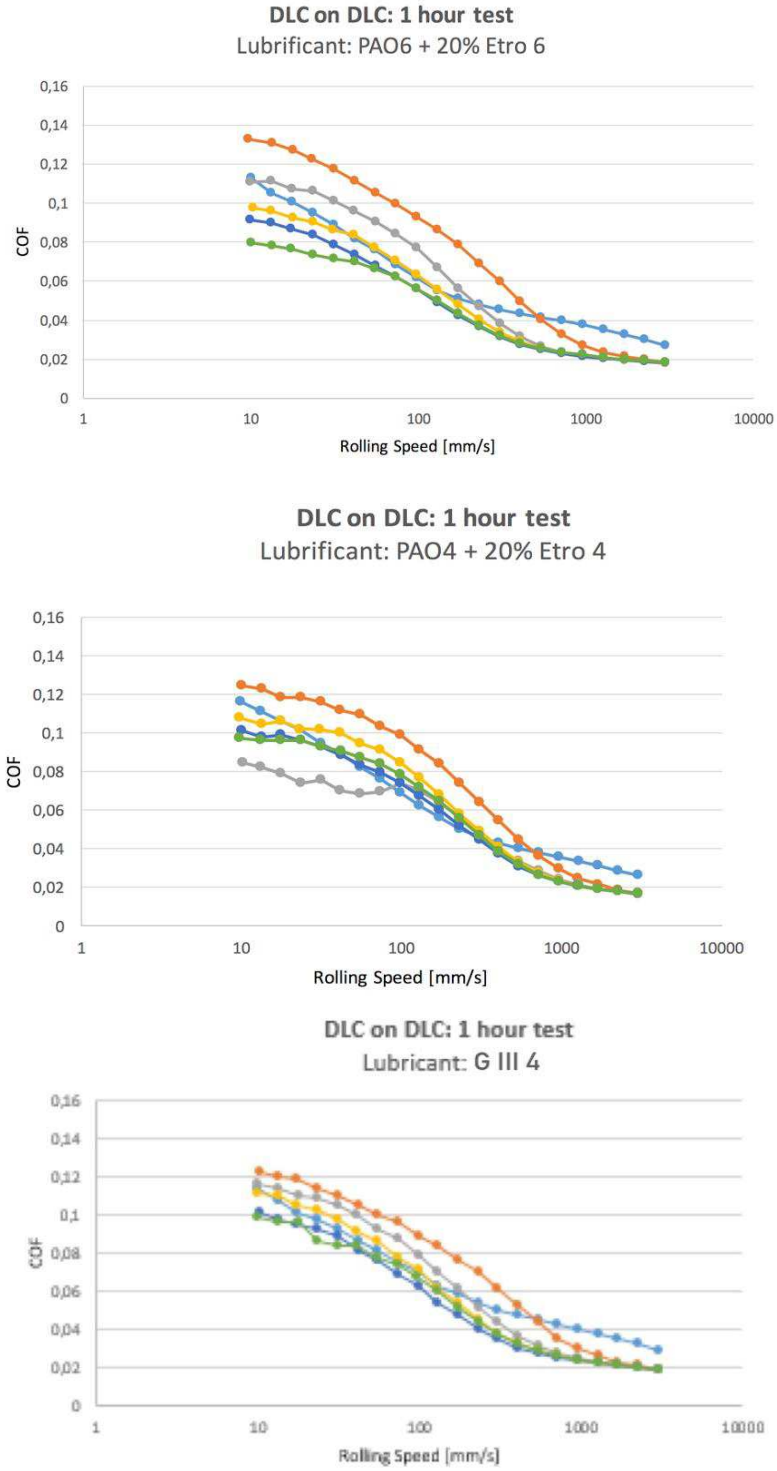

Figure 30 DLC/DLC with pure base oils, tested on MTM with method #2

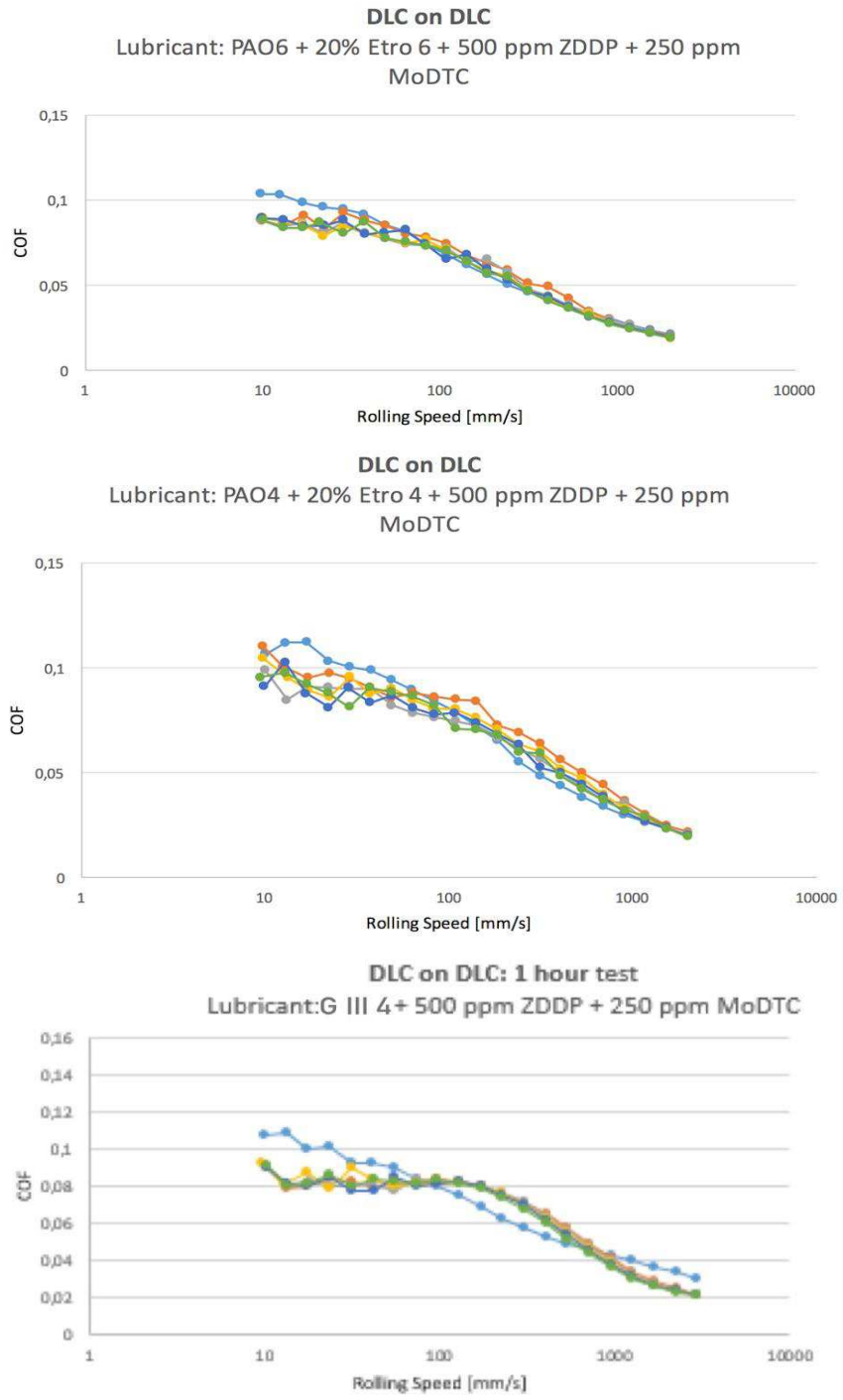

Figure 31 DLC/DLC with fully formulated oils, tested on MTM with method #2

Table 4 COF comparison between Steel/Steel and DLC/DLC with pure and fully formulated oils (only 4 cSt at 100°C), taken at step 1 and step 10 of the endurance tests, that is before and after the formation of the tribofilm.

COF	Step 1		Step 10	
	steel	DLC	steel	DLC
PAO4 full formulation	0,0879	0,1049	0,0686	0,0866
G III 4 full formulation	0,0943	0,1069	0,0597	0,0909
PAO 4	0,0954	0,1164	0,1632	0,0976
G III 4	0,1081	0,1135	0,1148	0,0984

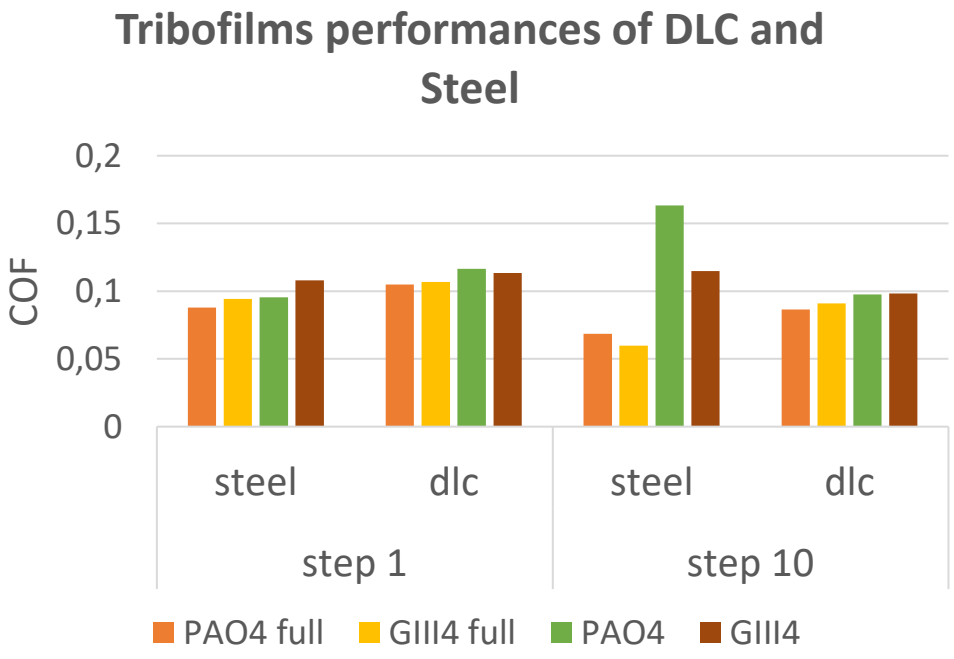

Figure 32 A quick view of the behaviors of steel/steel and DLC/DLC tests with pure and formulated lubricants

DLC/DLC with GIII4 oil always showed a sort of plateau in their Stribeck curves, flattened from BL to ML. This extension of the higher BL's COF up to ML has credit in the quality of the tribofilm formed on the surface.

The increased roughness leads to higher COF even in areas of the plot where usually COF start decreasing.

In general, ferrous surfaces work extremely good with fully formulated lubricants both when the surface is bare and new (step 1, cold start simulation) and when the tribofilm is formed (step 10).

DLC coated specimens seem to be not influenced by the presence or the absence of additives into the oil formulation, despite the COF are generally higher than steel, probably because of a better affinity of oils with iron.

The big difference occurs when the specimens work with pure non additivated oils. In step 10, the tribofilm formed on steel appears to have worst performances, leading COF to increase.

This could be due to excessive wear or corrosive wear which may cause damages to the ferrous surface, in these conditions literally naked and without any protection.

Some quick conclusions of this friction investigations are as follows:

- **DLC has higher resistance to surface corruption than bare steel**
  With pure oils, DLC specimens keep about the same COF all along the whole endurance test, from step 1 to step 10; Bare steel surfaces don't, and it may be due to a mix of thermal, mechanical and chemical stresses.
- **Base oils do not afflict DLC performances like they do with steel**
  DLC specimens seem to perform about the same with pure and fully formulated lubricants made both with G III and G IV oils.
- **ZDDP and MoDTC do not improve DLC performances**
  These additives show not the same effectiveness in COF reduction when coupled with DLC coatings, compared to with steel surfaces.
- **A good base oil could be more effective than additives with DLC coatings**

Maybe, a better lubricant for DLC coatings has less or no additives at all and be made of one or more pure base oils (so being cheaper and greener).

There is indeed a lack of base oils and additives able to lower the COF of coated surfaces, by promoting the formation of a good tribofilm (or preventing the formation of the tribofilm at all, good in case of DLC). As far as friction is concerned, automotive applications that involve DLC coated surfaces are, if lubricated with traditional oils formulations, not performing as good as they can. The road to friction reduction is still on going. However, friction is just one side of the story…

1.5.3 Wear assessment

Friction tests had a duration of 1 hour and a SRR set to 50%; these settings were not enough severe to provoke measurable wear on the specimens. For this reason, wear investigations had different settings: SRR to 200% and 2 hours of total duration, always with intermediate Stribeck curves harvesting, to follow the evolution of the tribofilm.

Contra-rotation and longer durations have been tested but always resulting in failures (severe scuffing on the disc and extreme torques on the motors shaft, blocking the tribometer). In this session, the MTM has been used just to wear the discs, so its graphic output is almost meaningless for this work's purposes.

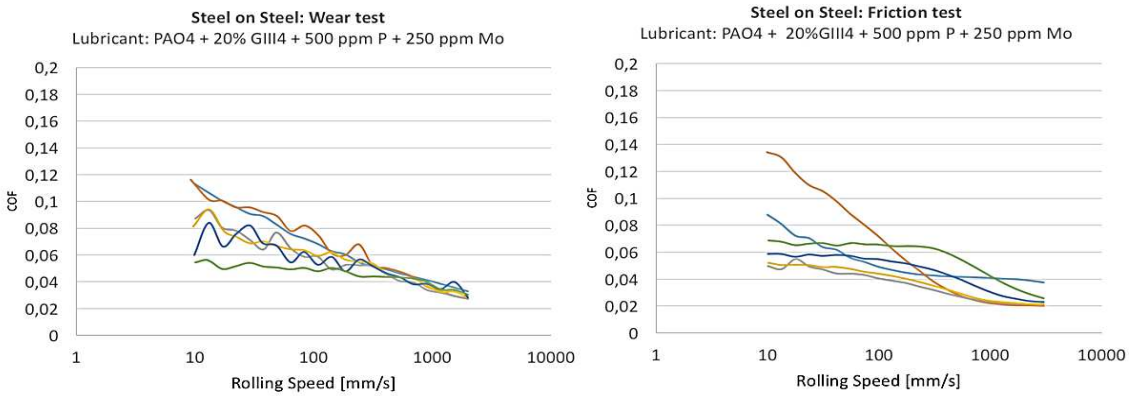

Figure 33 MTM output of a wear test (left) and a friction test (right). The wear curves are to fuzzy to be reliable of fine interpretations.

The real output from the tribometer were the discs, which have been submitted to several instrumental investigations.

The specimens used in this section are:

- Discs from DLC/DLC tests (DD)
- Discs from Steel/Steel tests (SS)

The lubricants of the tests were:

- PAO4 plus 20% GIII4
- GIII4
- PAO4 plus 20% GIII4, with 500 ppm Zn (ZDDP) and 250 ppm Mo (MoDTC)
- GIII4 with 500 ppm Zn (ZDDP) and 250 ppm Mo (MoDTC)

Optical microscope

At the optical microscope, the wear track of the DLC discs is barely visible. Especially for those discs which worked with pure oils, like GIII4 and PAO4. Wear track becomes more visible with DLC specimens which have worked with oils with additives.

With this basic analysis however, it is not possible to state if the different topology of the surface is due to chemical reactions between liquid and solid phases (a chemisorbed tribofilm) or if the stains are just persistent "halos" (that is, a physisorbed tribofilm).

In the second option, it is worth noting the strength of the tribofilm, survived to intense and severe rinsing with solvents and sonication.

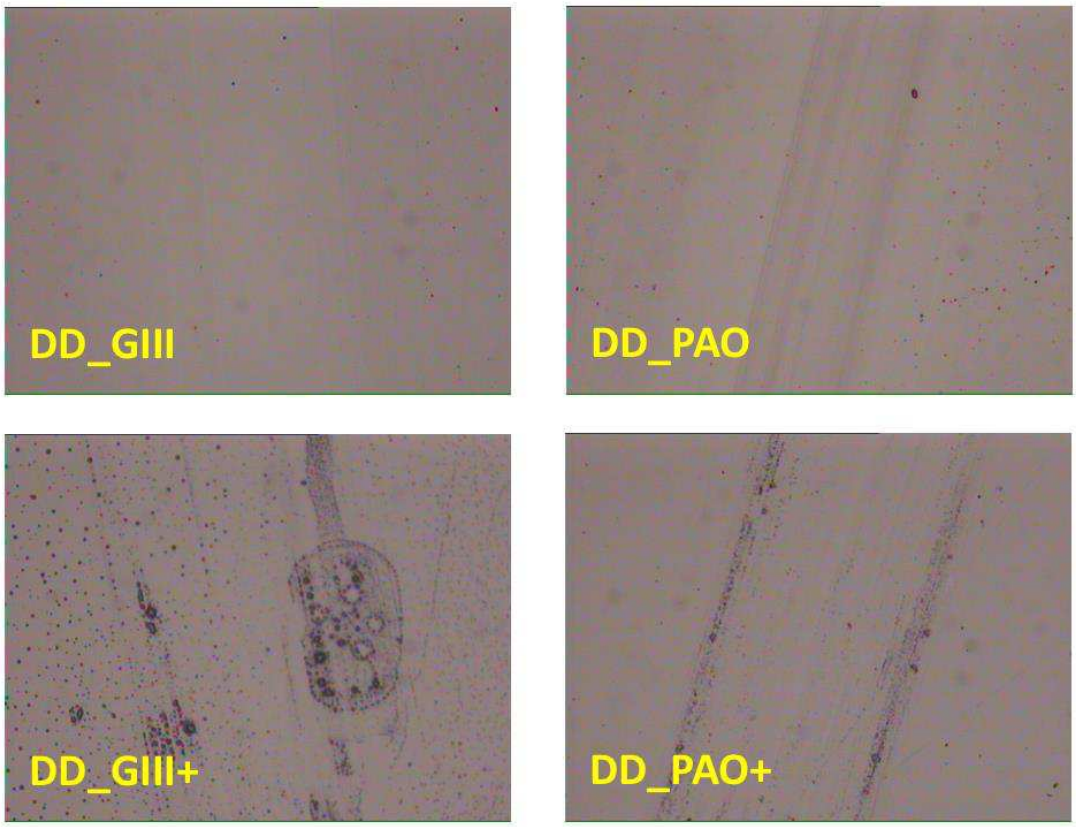

Figure 34 Images from optical microscope of DLC discs. "+" indicates fully formulated oils. Magnification 100x.

On the contrary, steel discs show their wear tracks pretty well. The typical grooves are clearly visible and some comments can be done. First, about the chemical aggressivity of a mineral oil compared to a fully synthetic one: pure GIII4 provoked an intense corrosion of the surface, while pure PAO4 does not. Despite this, the mineral oil still has a higher affinity with the ferrous surface, presenting a better wettability. In fact, the wear track of the pure PAO4 is brilliant and lapped track center, probably due to a higher asperities work in that area, that means that PAO4 has a fewer wettability than GIII4.

The additivated oils present almost the same topology at microscope: a moderate scuffing (*mild wear*). This behavior was expected since both the base oils and the additives are designed to work with iron-based alloys.

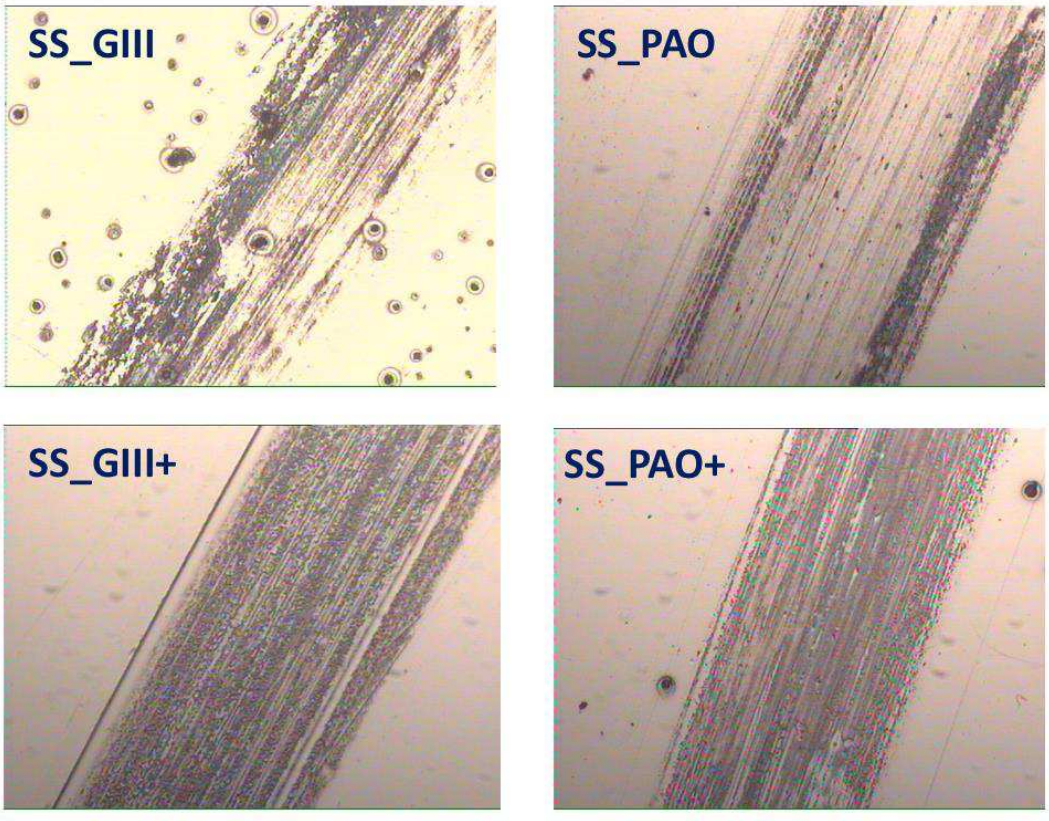

Figure 35 Images from optical microscope of steel discs. "+" indicates fully formulated oils. Magnification 100x.

Scanning Electron Microscope

With a SEM analysis it is possible to investigate topology and morphology of the wear tracks. Indeed, with a SEM add-on like EDS (Energy Dispersive X-ray Spectrometry) it is also possible to create elements maps butthe signal generated from a tribofilm (few nanometers of size in deepness) is way weaker than the one generated from the bulk;that's why this third kind of SEM analysis has been impossible.

In Figure 36, SEM pictures of steel discs are depicted. The white over-exposed area represents the external plastic-deformed part of the wear track (which is,indeed, shot halved).

Fully formulated oils work almost the same way, well protecting the surface. A certain amount of deposits is present on the border of the pure mineral oil specimen, maybe impurities agglomerates. Pure synthetic oil provoked more scuffing, of course, than the formulated recipe.

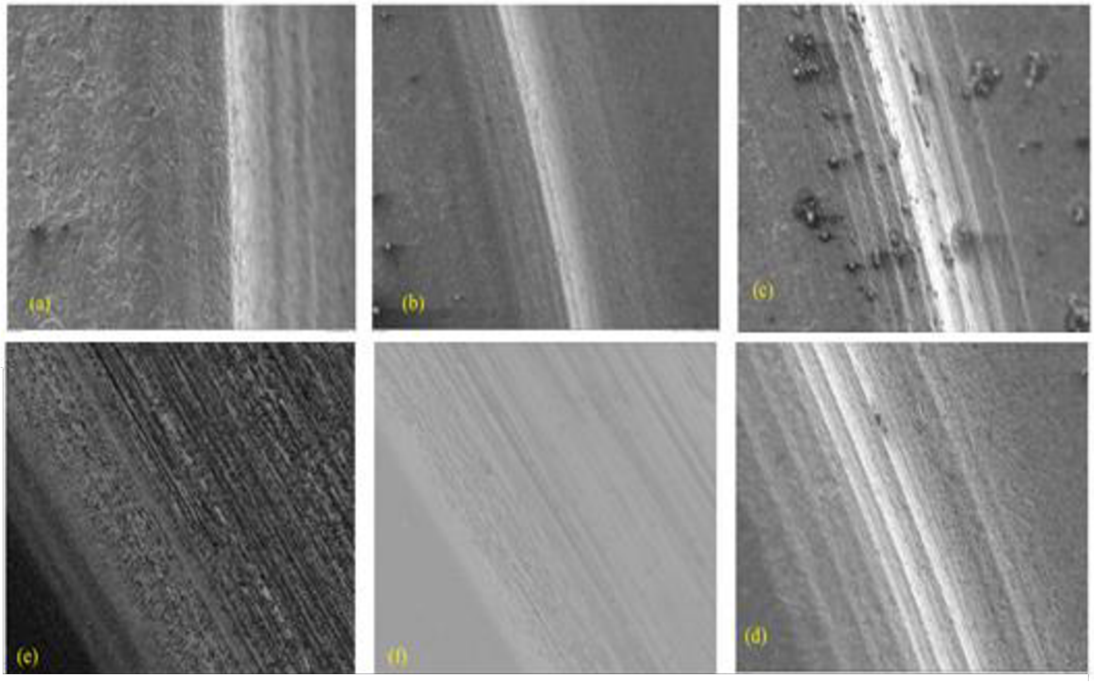

Figure 36 Steel discs wear track borders at SEM. A) GIII4 formul. B) PAO4 formul. C) GIII4 blank D) PAO4 blank E) GIII4 formul. wide view F) PAO4 formul. wide view

Centering the external border of the wear track of DLC discs has been challenging also with the SEM (Figure 37). For these coated specimens, it cannot be observed any sort of scuffing nor coating delamination. The wear track seems to be like a slight hollow, probably due to a plastic deformation of the ferrous bulk. The minor difference in hardness between ceramic coating and metallic bulk, prevented the coating to delaminate.

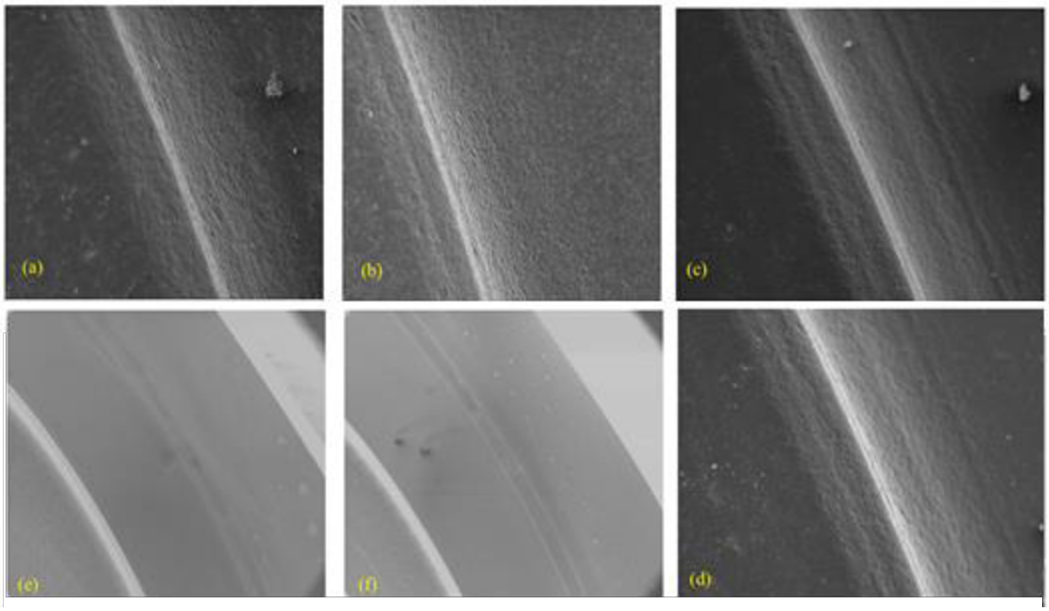

Figure 37 DLC discs wear track borders at SEM. A) PAO4 formul. 200x B) GIII4 formul. 200x C) GIII4 blank 200x D) PAO4 blank 200x E) PAO4 formul. wide view 50x F) GIII4 formul. wide view 50x

In general, the final comments of these two microscopy sessions are that:

- Fully formulated oils worked good with steel specimens, limiting wear to mild scuffing
- There is no clue about the adherence of tribofilms on DLC surfaces which have worked with formulated oils
- Wear track on DLC discs seems to be just a little breakage of the bulk, with no delamination.
- DLC discs showed practically no wear, while steel discs suffered if the lubricant is not additivated.

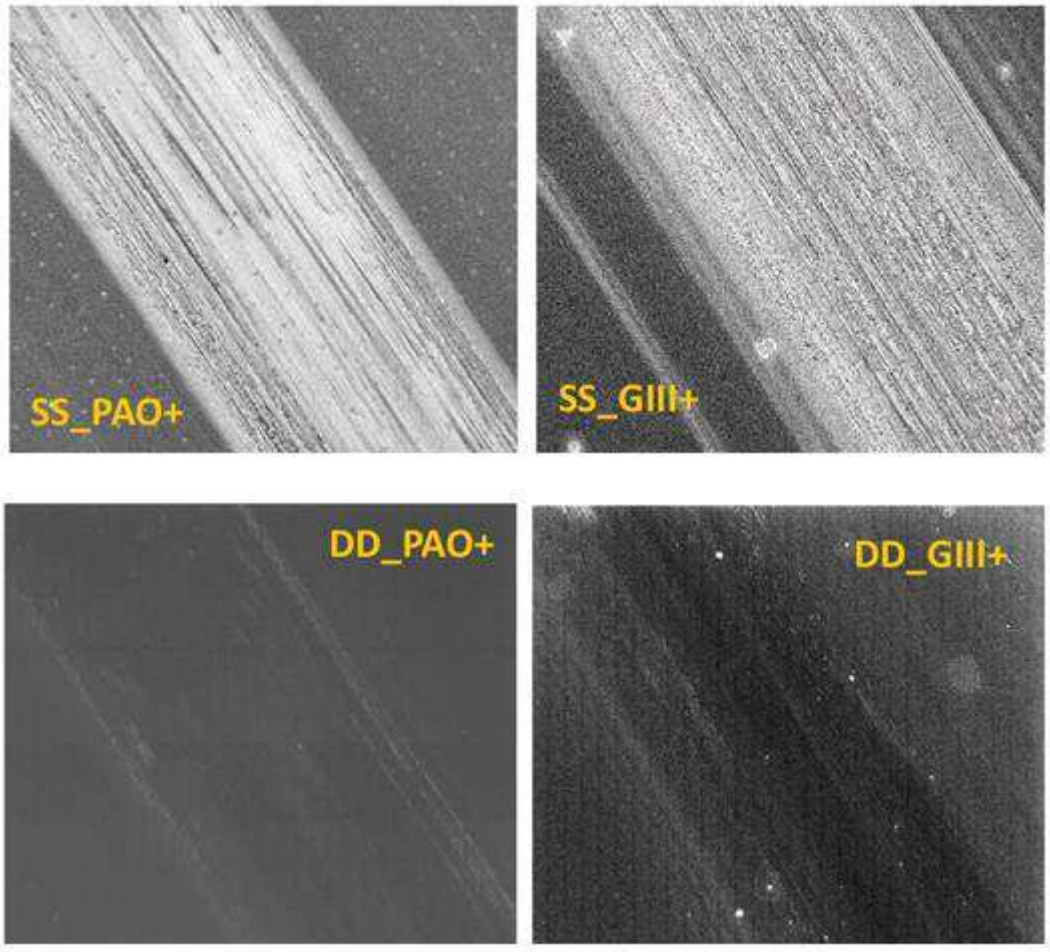

Figure 38 SEM in high contrast. "+" indicates a fully formulated oil. SS and DD stands for: discs from Steel/Steel and DLC/DLC tests, respectively. Magnification 500x.

Profilometer

With a self-made optical profilometer, some measurement of the aforementioned discs have been done. To avoid misinterpretations, each measure of the wear tracks was taken at the opposite sides of the discs but only the most significative has been taken into account. Probe speed was 0,005 mm/s (total length of the path was 0,5 mm) with an acquisition clock of 200 Hz.

The raw results from the profilometer were often fuzzy curves, which absolutely needed data treatment for a complete understanding, but in general, even at this stage, they represent pretty good the generic trend. As one can see in Figure 39, typical surface profiles are extremely fuzzy for steel specimens and incredibly smooth for DLC coated specimens. The fuzz is due to the low resolution of the optical probe coupled with the fine sizes of the wear grooves. The final data have been obtained using a post-processing software like Origin.

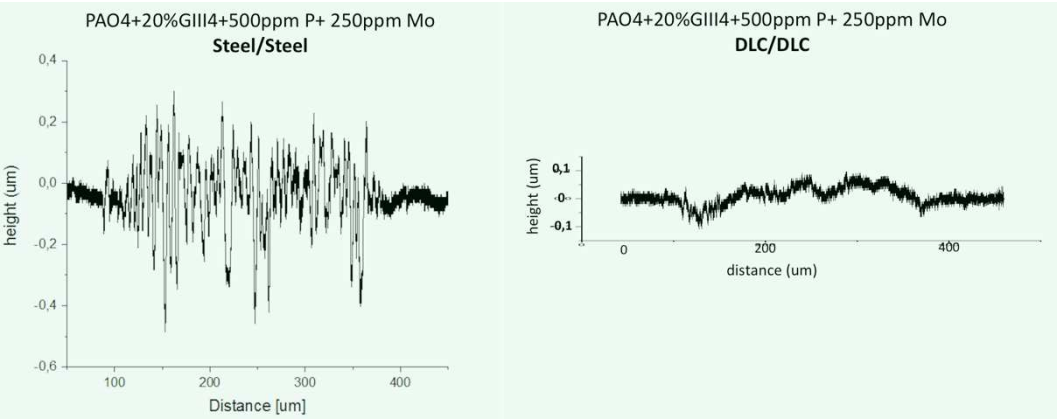

Figure 39 Example of raw output from the profilometer

In Figure 40, the final overview of this profilometer sessions. Also, with this analysis, it turned up the higher wear resistance of DLC coated specimens compared to bare metal ones. The kind of wear is also different, steel's wear is abrasive, resulting in an irregular surface, marked by a lots of fine grooves. DLC's wear, on the contrary, seems lighter and this can be due both to the lack of material transferred to the counterpart surface or lost in the liquid phase and to the plastic failure of the metallic bulk.

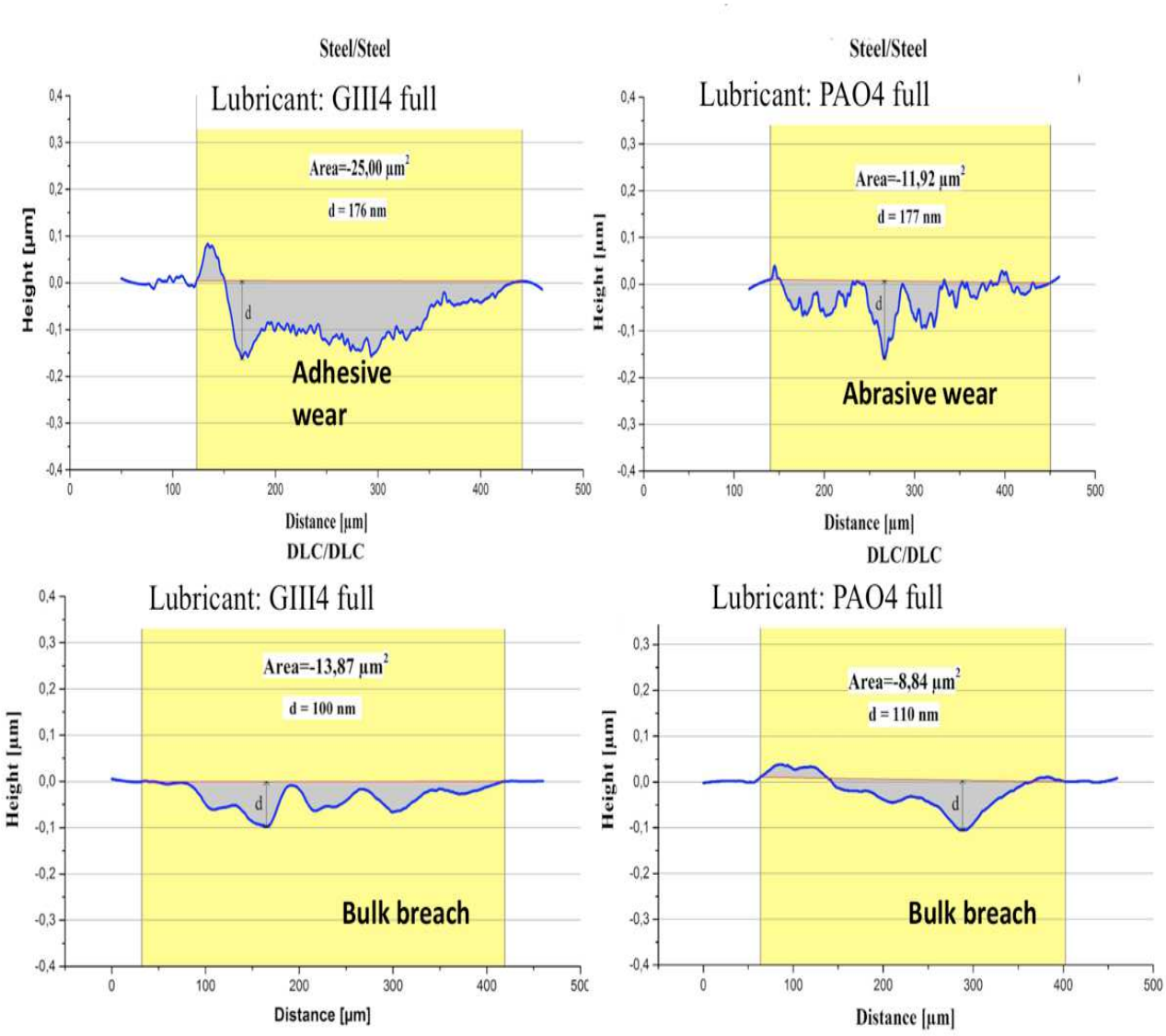

Figure 40 Profilometer analysis after data treatment with Origin, with integrals

X-Ray Photoelectron Spectroscopy

To investigate the presence and the quality of the tribofilms, XPS is a perfect technique. It is a surface analysis and its output is not afflicted by bulk signals like it is for EDS on SEM; that's why it is possible to study the quality of a tribofilm by qualifying and quantifying the atomic species which it's made of.

The elements (and their orbitals[7]) of interest are C1s, O1s, S2p, P2p, Zn2p, Mo3d and Fe3p, that are all those elements characteristic of the bulks and the possible tribofilms generated from ZDDP, MoDTC and the bulks themselves. In the end, only Zn, Mo, C and O will be considered for final comments. All the spectra have been shifted considering C1s' peak at 284,5 eV.

Despite the severe rinsing of the specimens, XPS is so sensitive that its probe can be afflicted even by a nanometrical layer of residual oil film. For this reason, each spot chosen for the analysis is previously sputtered for 1 minute with Argon at 2kV, to get rid of fake signals from the surface.

Of course, the specimens undergone in XPS analysis are those which formed an interesting tribofilm during MTM run, that are those worked with fully formulated lubricants. However, an example of blank runs analyzed at XPS is reported, as survey scan, in Figure 41. DLC coating is micrometrical-thick so the XPS probe cannot reach the metallic bulk beneath the ceramic coating. In case of coating thinning, breakage or delamination, Fe3p signal could be detected, thus measuring wear of the coating.

A survey is a very quick scan of the surface within a large domain of energies, only aimed to be sure of being on a suitable spot of the sample. The real analysis start collecting HR spectra (High Resolution) of specific energy ranges, and lately to execute a deconvolution of the spectra to obtain the exact position and area of the peaks, usually merged because of overlapping energy domains between different atomic species or orbitals.

[7] XPS recognizes the presence of specific atomic bonds. For this reason, it is necessary to list *a priori* (or even after a brief survey) a certain number and types of atomic orbitals which will be finally investigated in High Resolution. Each application, however, has a group of characteristic atom/orbital couples, recognizable by literature survey.

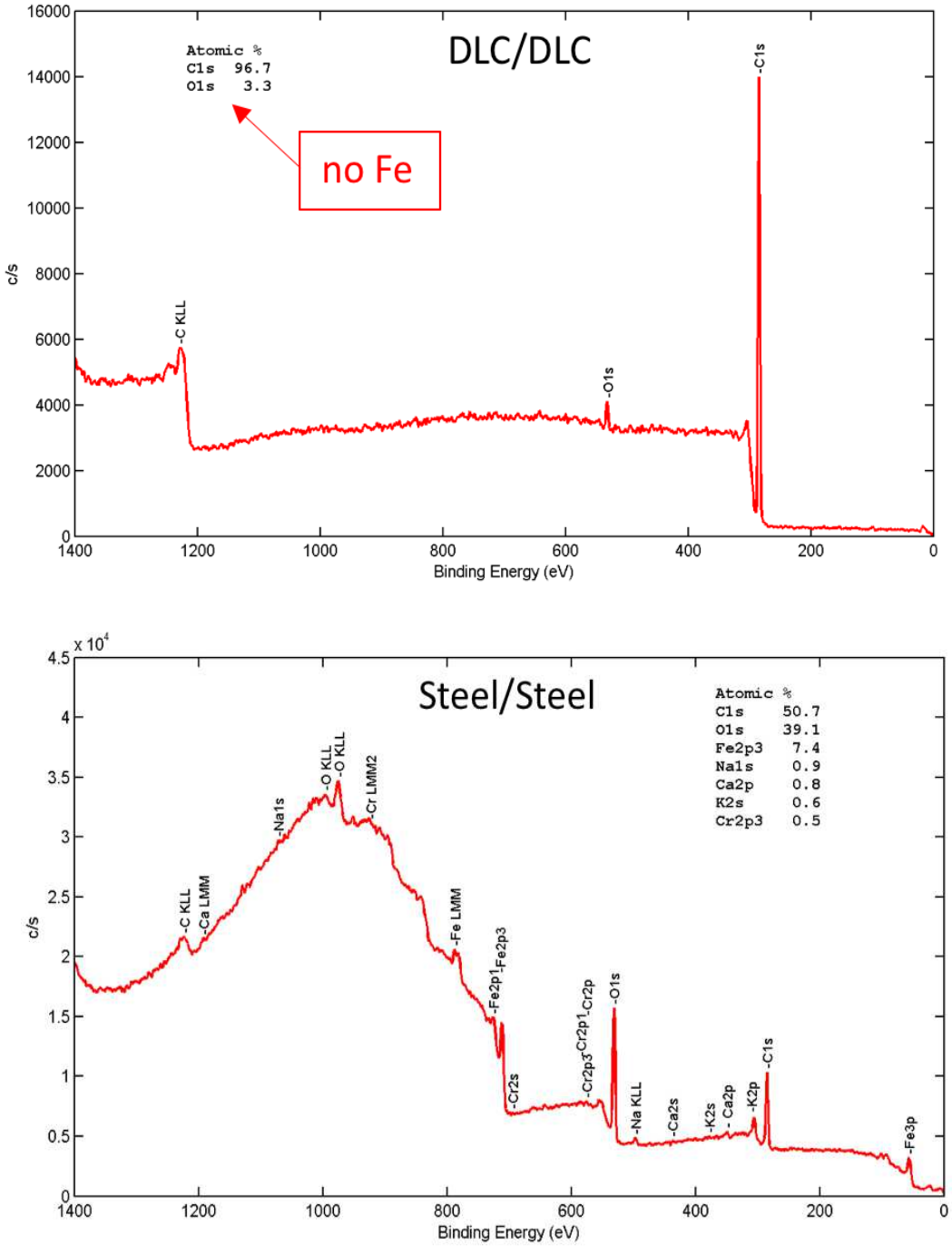

Figure 41 XPS survey of wear tracks of DLC and bare steel specimens after MTM run with PAO4 plus 20% GIII4 lubricant (no additives).

In Figure 42 HR spectra of Zn from DLC and Steel discs with PAO4 and GIII4 formulated oils are depicted. ZDDP has been proven to have a specific path of decomposition heading to a final stage of zinc oxide, passing through intermediate species like phosphates and sulphates. A large amount of oxide in the wear track means that the protecting effect of ZDDP is going to vanish (or it's vanished already). In a real automotive application, this would mean that the engine needs an oil refill.

At first sight, specimens which have worked with GIII4 oil show only the oxide signal, while the ones coupled with PAO4 oil also show a certain amount of Sulphur, more for steel than DLC. Probably, being ZDDP an extreme pressure additive (which gives help in high pressures conditions because it activates at high pressures), a less clean and thicker oil[8] or a less deformable surface, like a mineral oil or a ceramic oil respectively, accelerate the decomposition process leading to zinc oxide. If this could be confirmed, there it is another reason to develop appropriate lubricants for ceramic coated engine components.

In Figure 43, the same analysis but for Mo3d, indicating the evolution on MoDTC with different oil/surface couples. Right like ZDDP, also MoDTC has its own path of decomposition. It is worth to remember that MoDTC is just a precursor for MoS_2 solid nanoparticles; these particles, after exfoliating and doing their job of friction modifiers, start decomposing heading to the state of oxide, in particular MoO_3.

In the XPS language, which only talk about specific atomic orbitals, those two species can be identified as Mo^{4+} (for MoS_2) and Mo^{6+} (for MoO_3), always displayed as doublets spacing about 3 eV each other. So, the purpose of this specific analysis is to detect the amount of residual Mo^{4+} in the wear track, meaning that there still is a certain quantity of working friction modifier available. (69) (70) (71)

XPS analysis of DLC surfaces generally show a higher amount of Mo6+ bonds, with respect of the steel specimen. Mo6+ is related to MoO3, so this could be the proof of a higher consumption of MoDTC/MoS2 in those conditions.

[8] In terms of Viscosity Index (VI, the change of viscosity as function of temperature: the lower VI is, the greater the variation of viscosity), a GIII oil is less performant than a GIV. In the running in phase or during the first stage of the tests at low temperature, even if the two oils considered have the same kinematic viscosity at 100°C, they may have worked differently, generating different conditions for the growing tribofilm.

Perhaps, the higher purity of the PAO base oil, compared to mineral Group III lubricant, cannot cover the surface as good as the other oil, and its protection just leans on the additives, leading to fast depletion.

Table 5 Quantitative analysis of Mo4+ (MoS2) and Mo6+ (MoO3) bonds presence on specimens' surfaces (rounded values).

state	DLC/DLC		Steel/Steel	
	PAO+	GIII+	PAO+	GIII+
Mo^{4+}	34%	32%	68%	67%
Mo^{6+}	42%	64%	13%	10%

Generally, all the specimens show, at XPS, almost the same behavior of MoDTC. Probably, these additives do activate when temperatures and pressures are fine for their chemistry, despite the chemical characteristic of the working surface. This could mean that one should not put in connection the presence of a tribofilm with its adhesion to the substrate and its ability to work properly.

In Figure 44, there is an example of residual oil film. The C1s spectrum spotted outside the wear track (pristine surface) only shows one kind of peak, C-C. After the sputtering, always in external position from the wear track, also C-O/C-H peaks appear (72). Knowing that the pristine material has a surface functionalized with H (it is a *ta-C:H*), a first conclusion could be that the first spectrum was just about long carbon chains, like an oil, and that sputtering is needed to reach the real surface of the specimen. Lately, the same conclusions have been achieved also for steel made specimens. However, DLC discs show the same spectra for both PAO and GIII oil with just one little exception for GIII lubricant, which XPS spectrum depicts the small presence of C=O bonding. This oxidation of DLC could be due to chemical aggressivity of mineral oil.

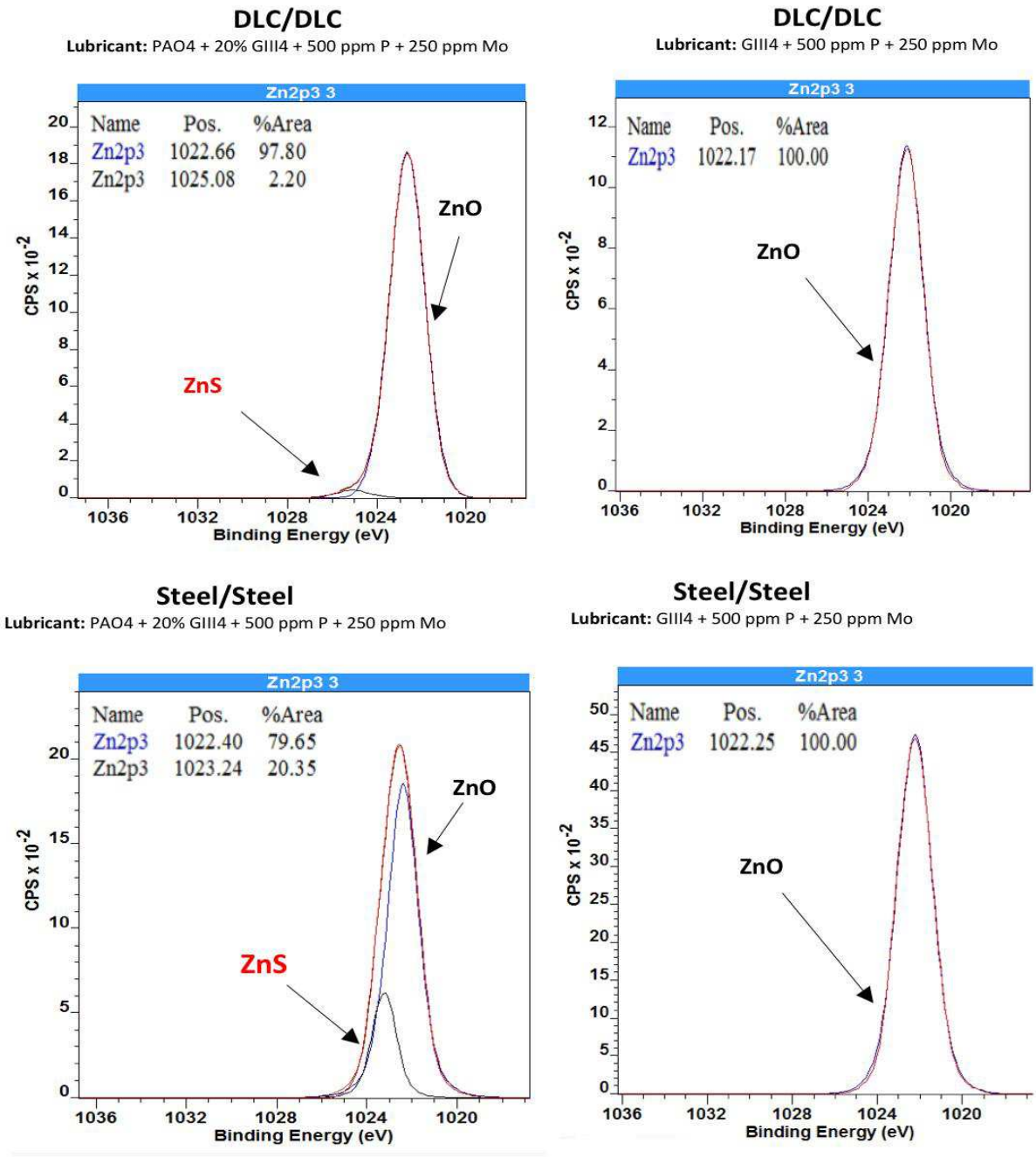

Figure 42 HR spectra at XPS of Zn: DLC and Steel discs with PAO and GIII fully formulated lubricant

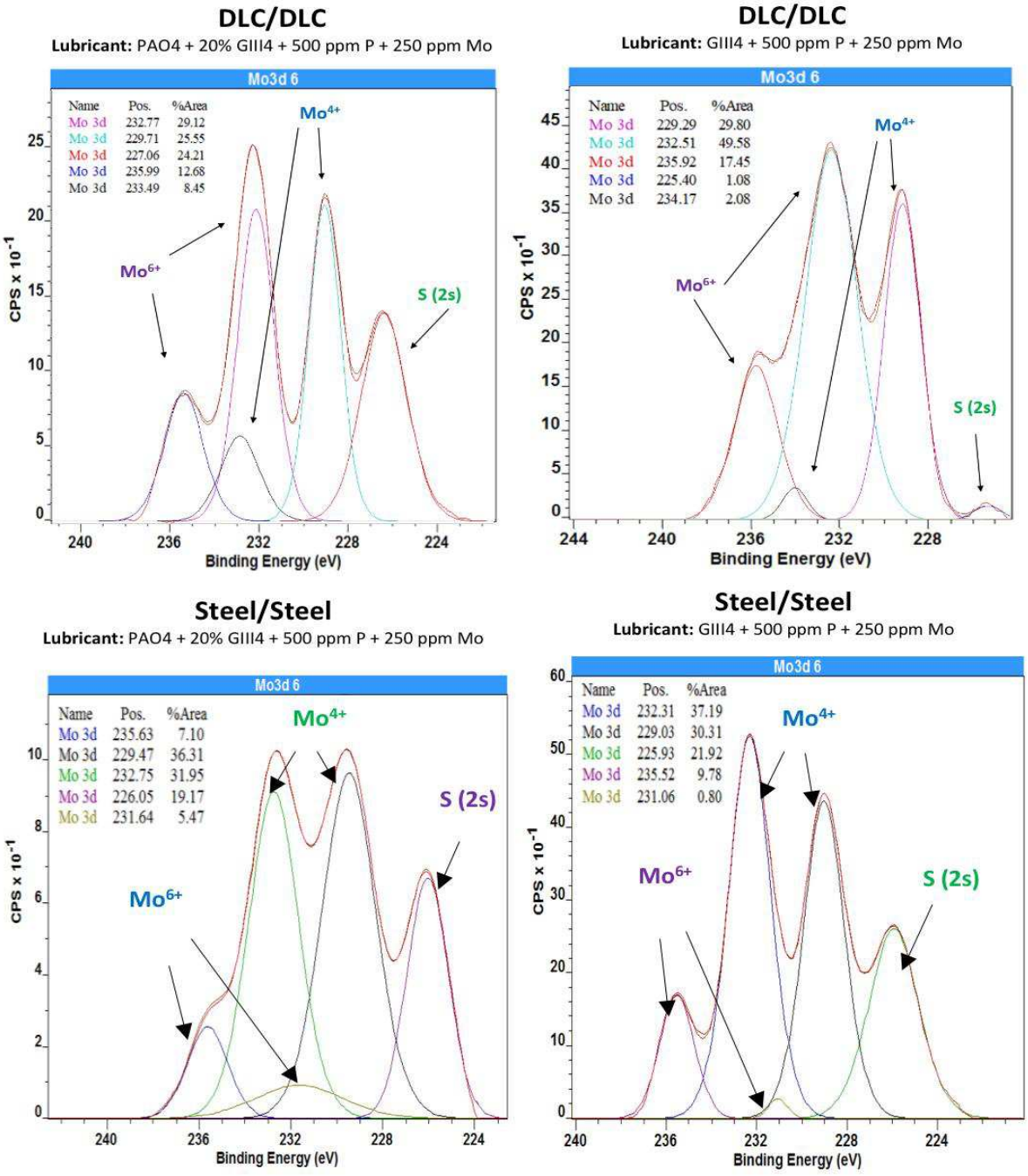

Figure 43 HR spectra at XPS of Mo: DLC and Steel discs with PAO and GIII fully formulated lubricant

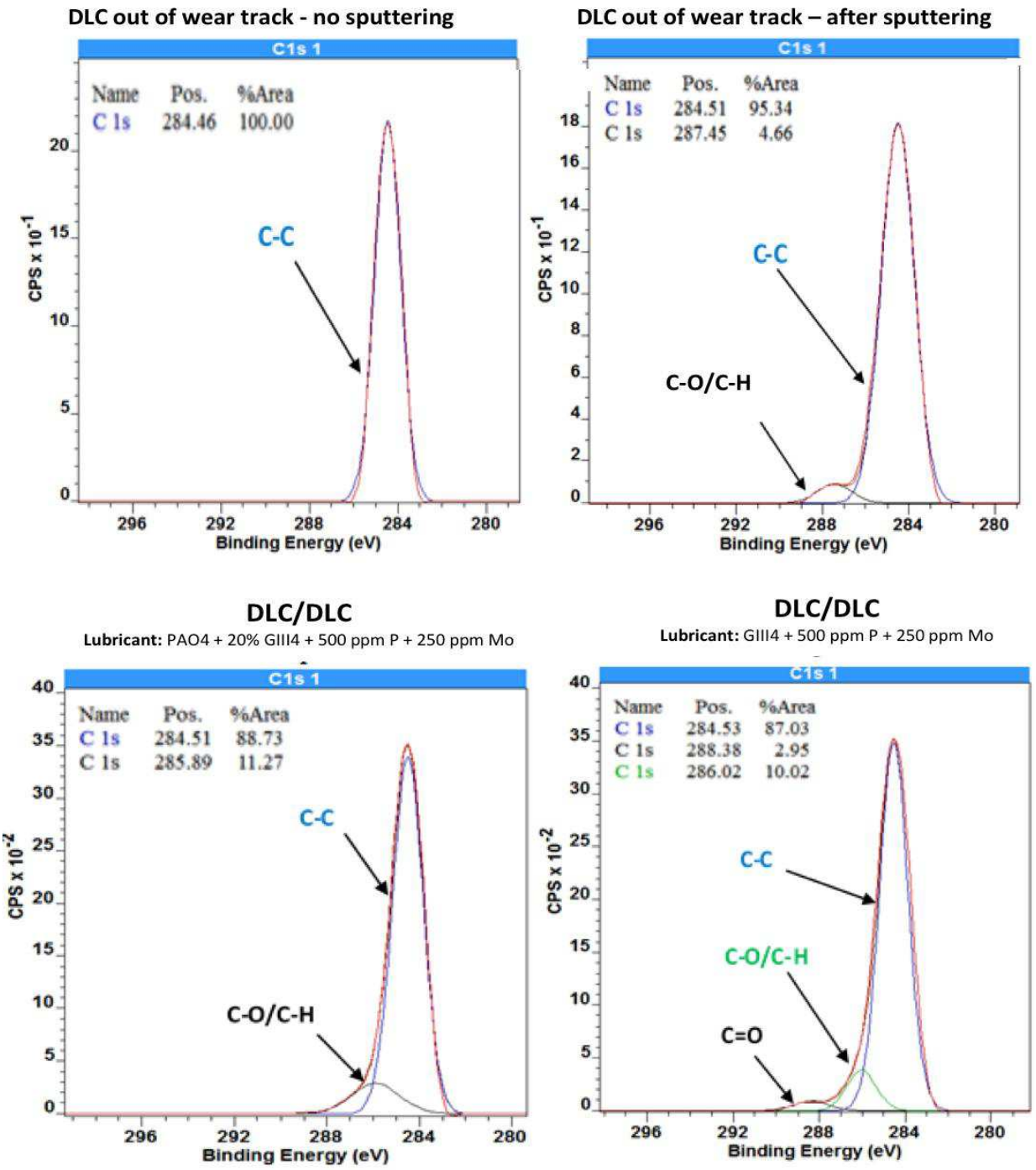

Figure 44 HR spectra at XPS of C for DLC discs. Above, outside the wear track. Below in the center of the wear track. Each column has the same lubricant.

Raman Spectroscopy

From the previous analysis, it seems that measuring DLC wear is a hard task, harder if one tries to use the same approach for traditional steel surfaces.

A good type of investigation able to detect the transition from sp3 to sp2, that is measuring the wear of a DLC coating, is the Raman Spectroscopy. For comparison, Raman spectra have been collected also for steel discs (73).

In Figure 45, Raman signal from the wear tracks of steel discs. It is remarkable how clean GIV-synthetic oils are, compared to GIII-mineral ones. The signal referred to carbon residuals is way bigger for GIII (both blank and fully formulated). Probably, the impurities form a strong bond between iron and the oil, resulting in a persistent thin oil film. This idea is somehow in agreement with the results from XPS.

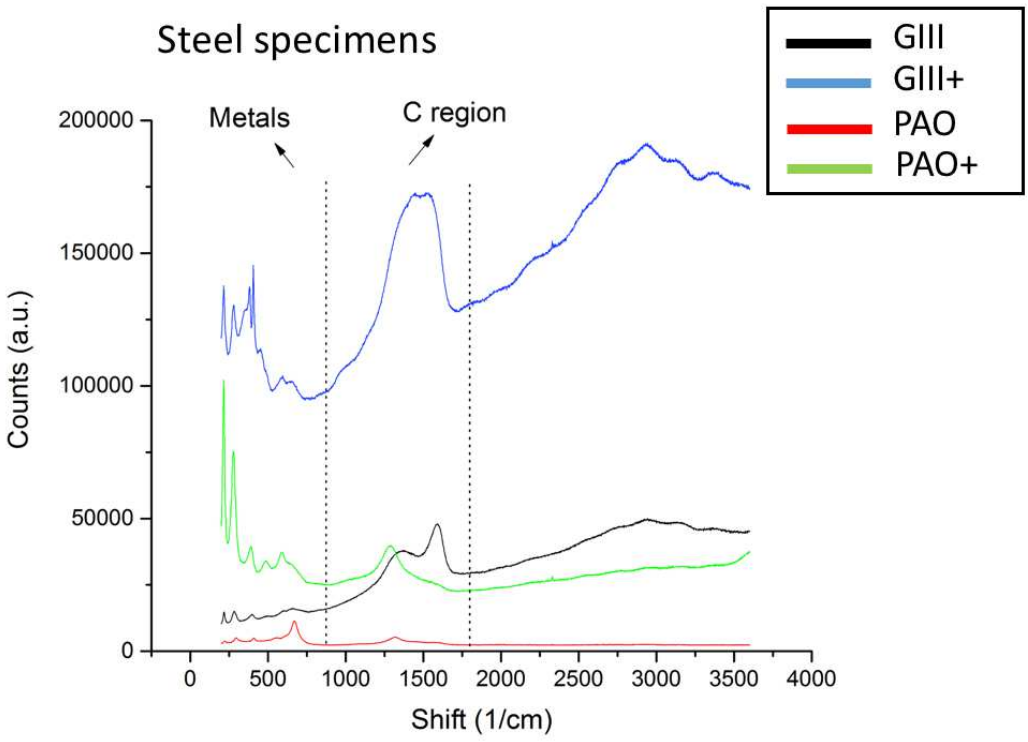

Figure 45 Raman spectra of steel discs for wear investigations

Raman spectroscopy of carbon is useful to investigate the order/disorder of a material. In this application, one can consider order as the diamond crystalline form (sp_3) and disorder the amorphous graphite phase (sp_2).

So, it should be possible to compare a pristine surface spectrum (out of track) and the surface of the wear track, in order to determine the shift towards sp_2, that is finally the wear of DLC coating. The first step has been to collect signals from a pristine DLC surface.

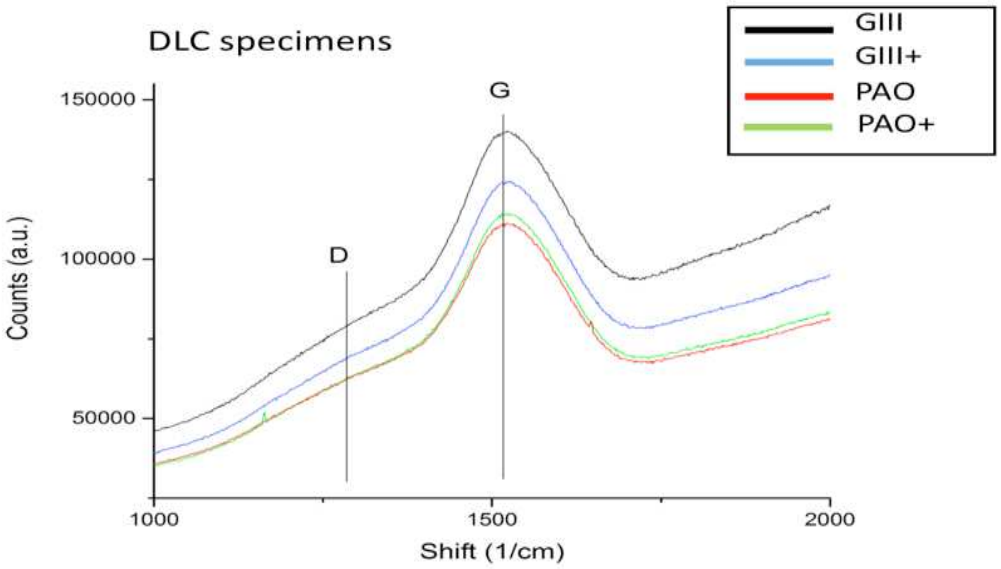

Figure 46 Raman spectra of DLC discs for wear investigations

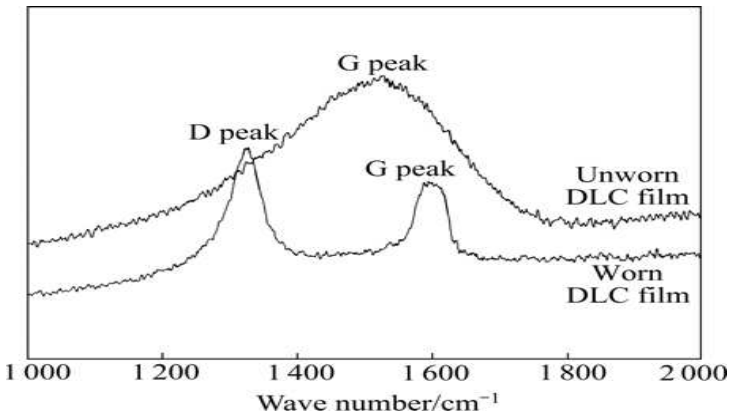

Figure 47 How a DLC Raman spectra should be before and after working (74)

As it turns out from the deconvolution of the peaks in the carbon region, the FWHM of the peaks, generally related to order/disorder of the structure, is lower in tracks; also, the ratio or the areas I_D/I_G, indicating of course the order/disorder level, appears to be, in the wear track, slightly lower than outside. These conclusions suggest that in the wear track of these DLC coatings, there could be entrapment-oriented graphite of even a very small quantity of graphite generated from diamond decay; it is not possible, however, to notice a proper wear of the coatings.

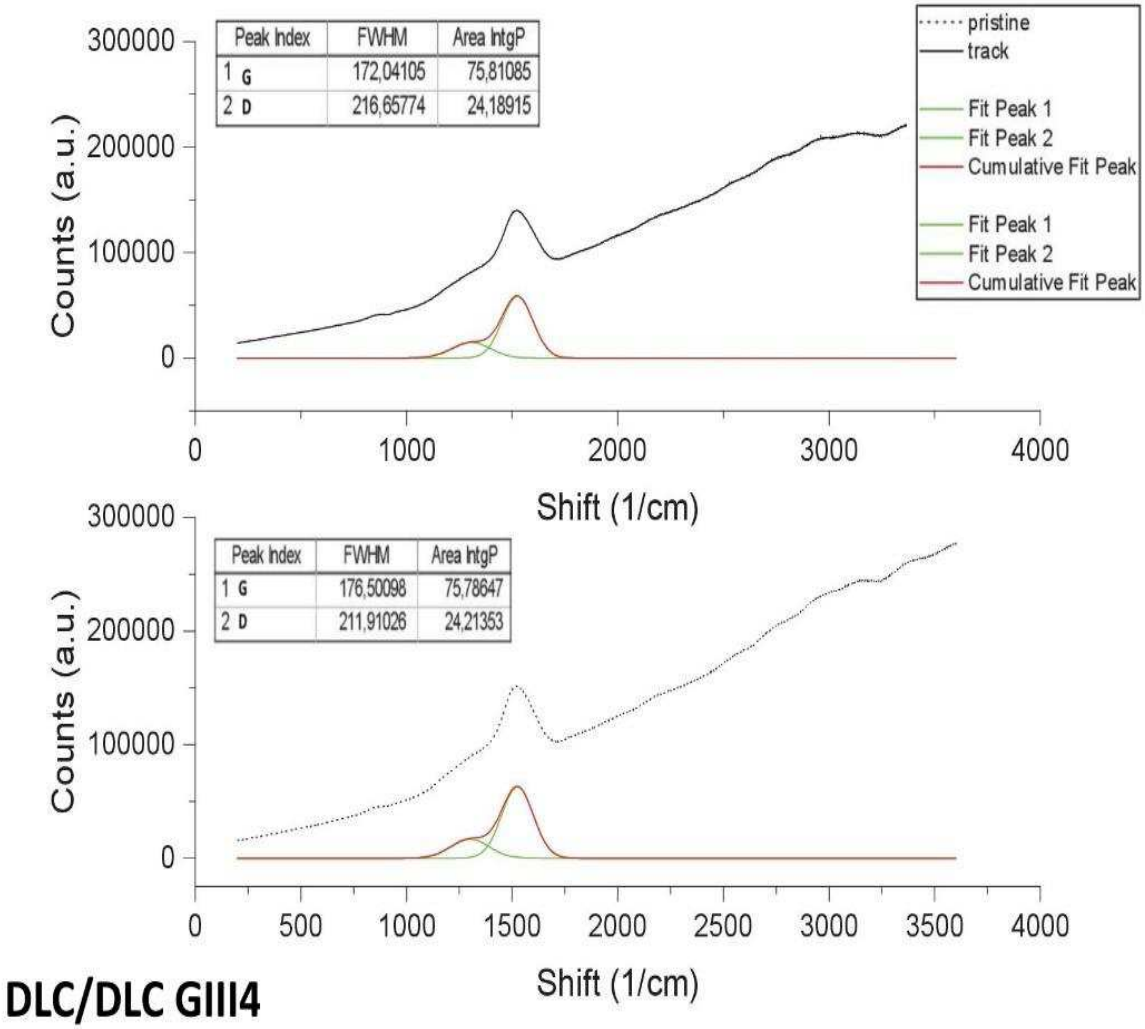

Figure 48 DLC with GIII4 blank oil

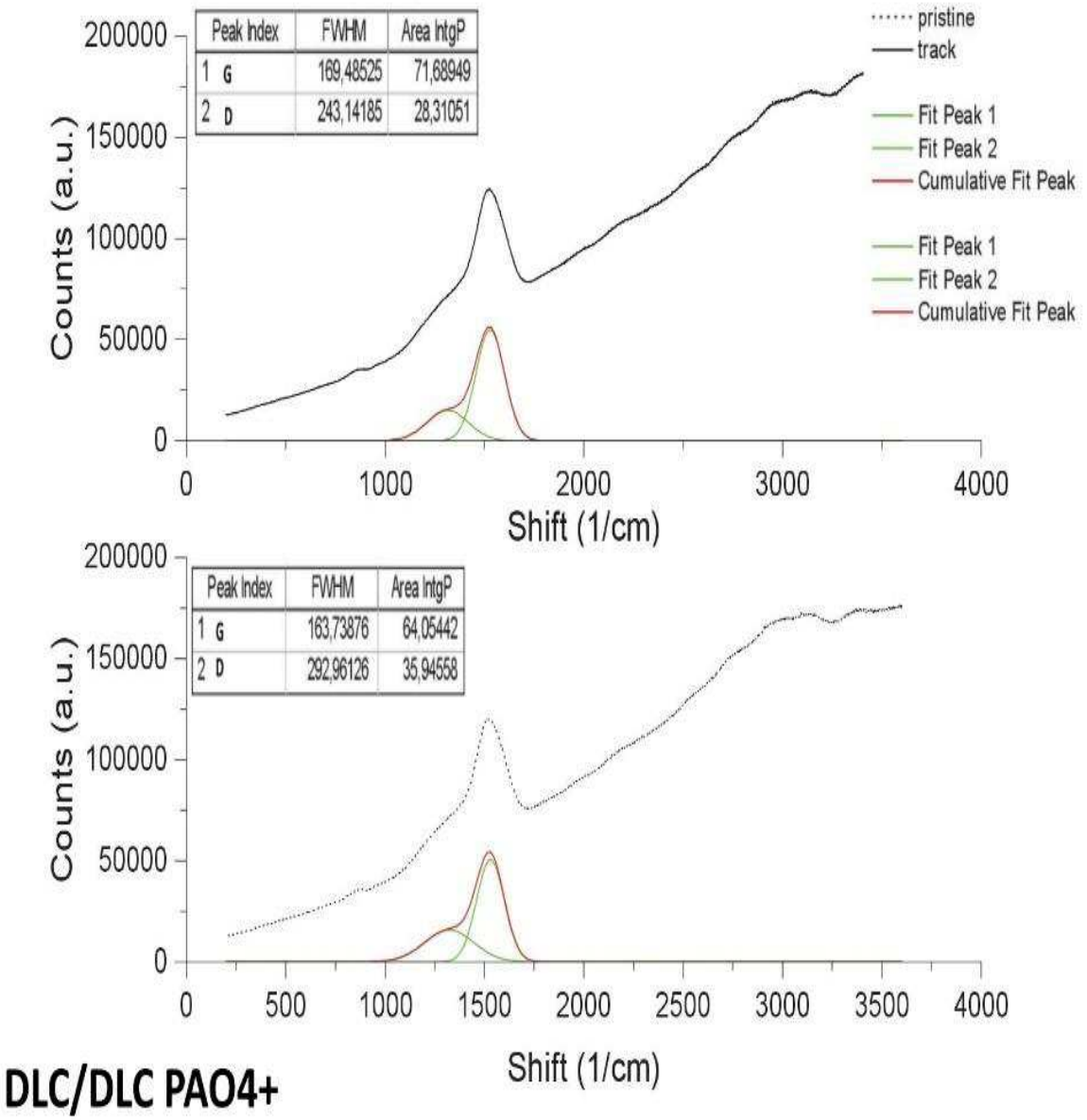

Figure 49 DLC with PAO4 fully formulated oil

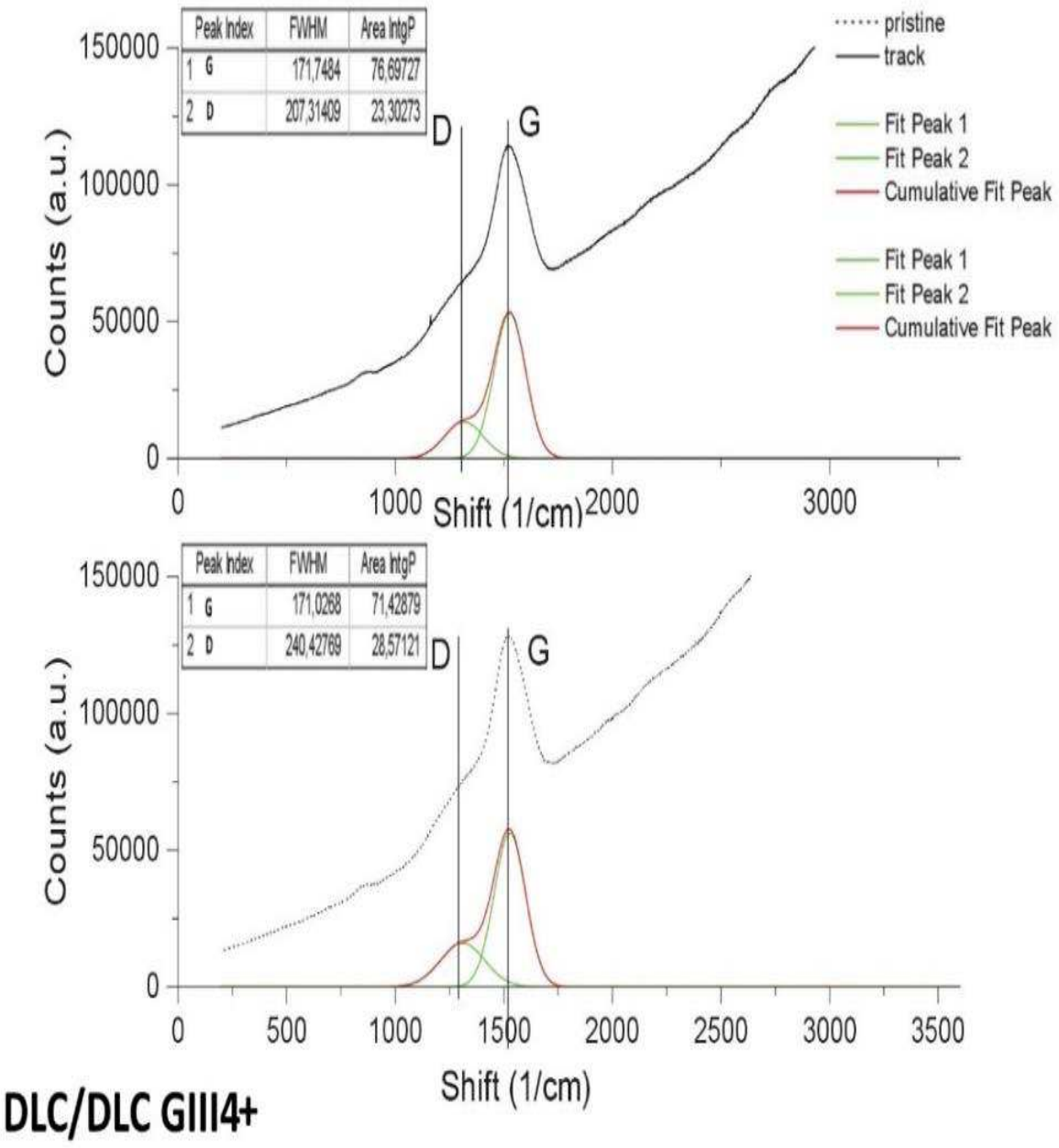

Figure 50 DLC with GIII4 fully formulated oil. Here peaks of diamond and graphite phases are indicated.

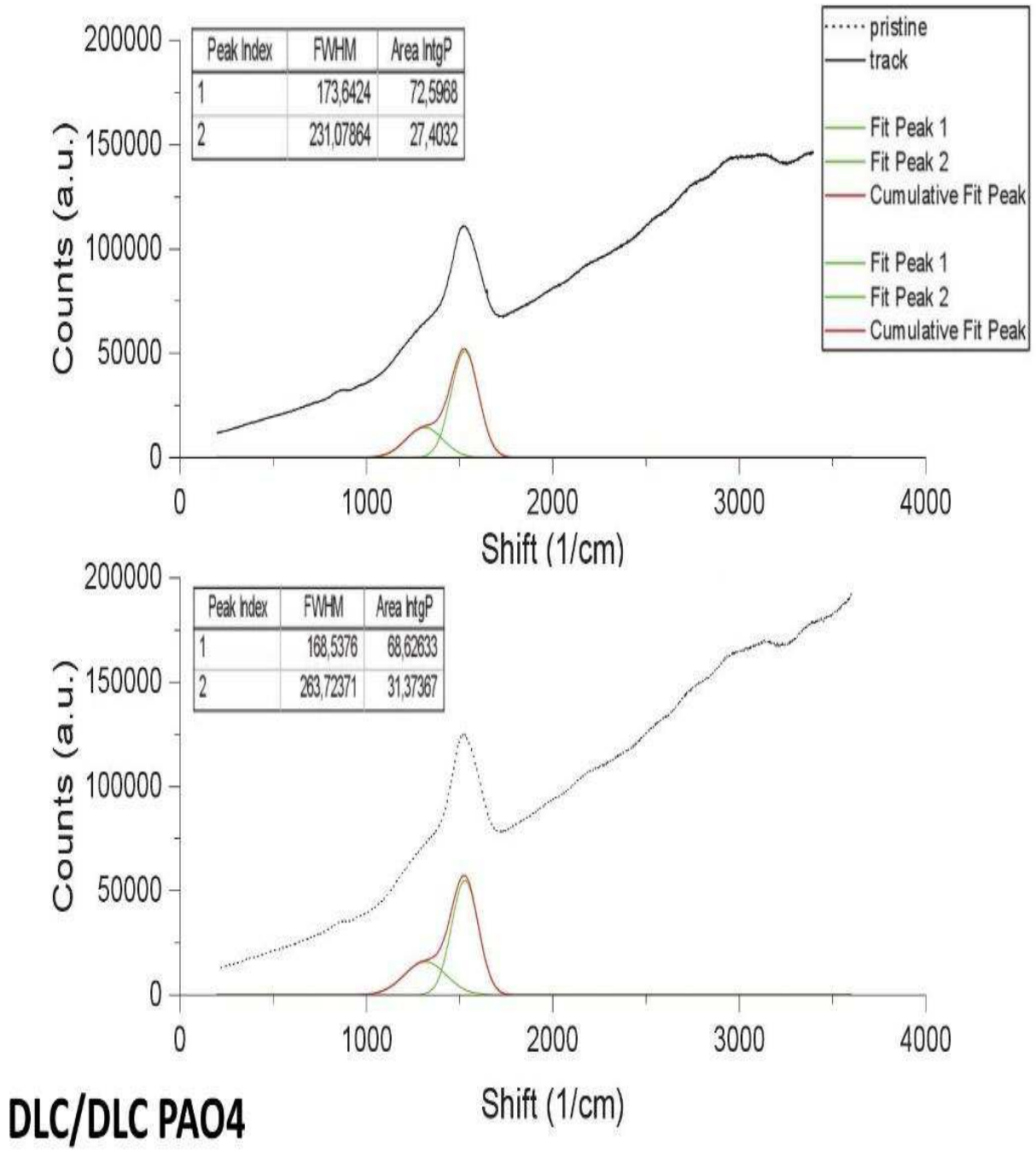

Figure 51 DLC with PAO4 blank oil

Atomic Force Microscope

An Atomic-Force Microscope (AFM) has been used to investigate topography and morphology of surfaces with tridimensional view capabilities. The instrument has been assembled within the DISAT laboratories at Politecnico di Torino.

The scan amplitude of the AFM tip is less than 150 μm, so this AFM characterization was not meant to provide a better profile of all the wear track, but a set of selected images which, once put together, are able to describe the morphology and topography of significant regions onto the surface of the discs, such as the center of the track and the borders between worn and untouched surface. Thus, one could be able to perceive the differences, if any, between different kinds of surfaces, lubricants and couples of them.

The raw pictures have been post-treated with *Gwyddion* software - which helps the interpretation – in order and to give back meaningful 2D and 3D representations of the scan.

Steel Specimens

Steel discs with pure PAO4 show a regular pattern of pits randomly spread everywhere (Figure 52). This peculiarity can be seen much better with SEM, however. It seems anyway that this condition was existing already before the test with oil (pristine specimens are kept in envelops wetted with a veil of protective oil, which has to be removed by a 60 minutes sonication in petroleum ether prior of the test). Beside this annotation, the image below shows that the border between worn and untouched regions is somehow smooth and this may be explained by the high polarity of group III oils, which are able to grip strongly to the metal surface and to form a resistant film in the contact area.

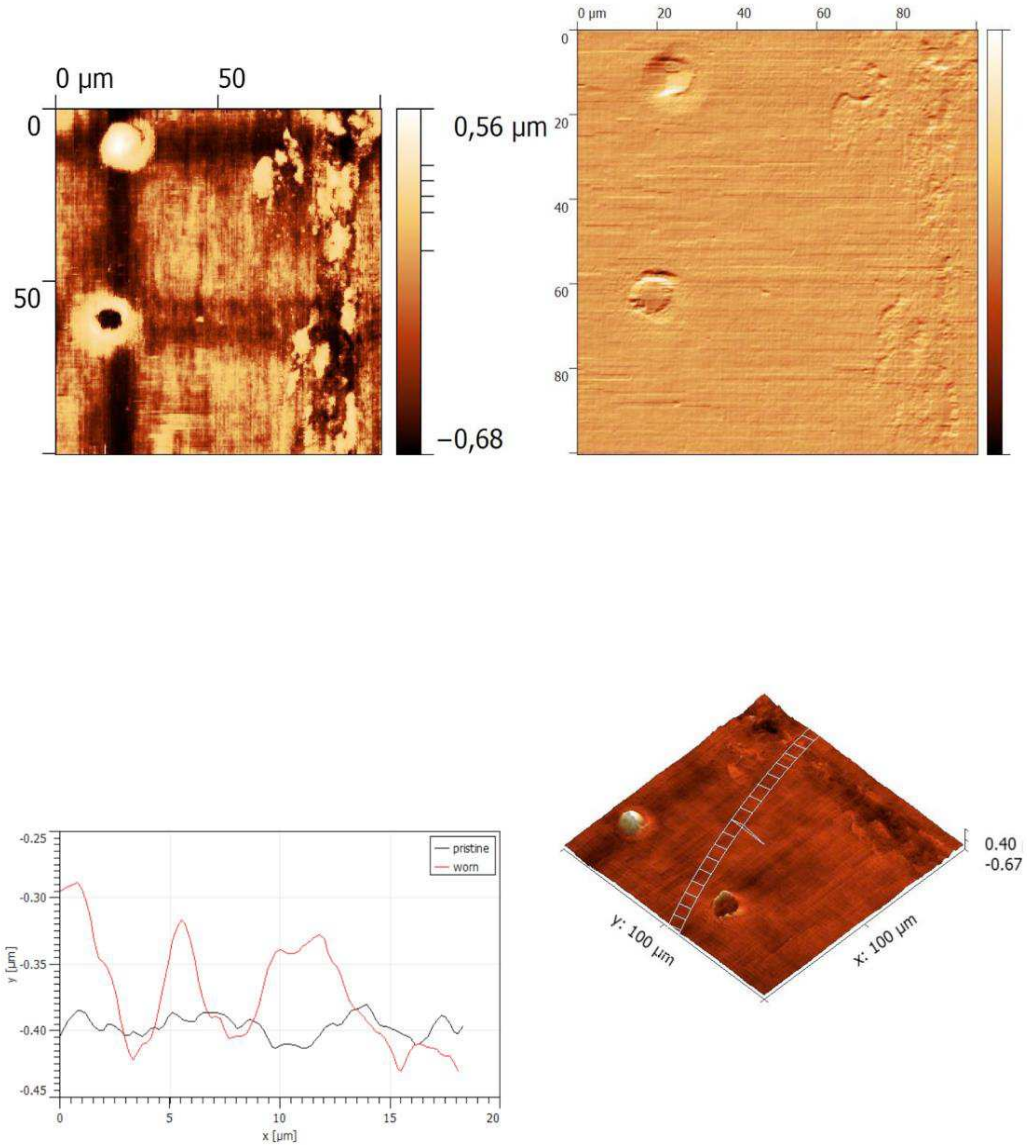

Figure 52 AFM raw, 2D, 3D and profilometry of Steel disc with pure PAO4 oil

Compared to pure Etro4, the PAO4-based base oil shows less protective capability towards bare metal surface (Figure 53). Here, surface roughness seems more afflicted by rubbing. Again, it seems that pure group IV's viscosity index is too low, compared to mineral base oils.

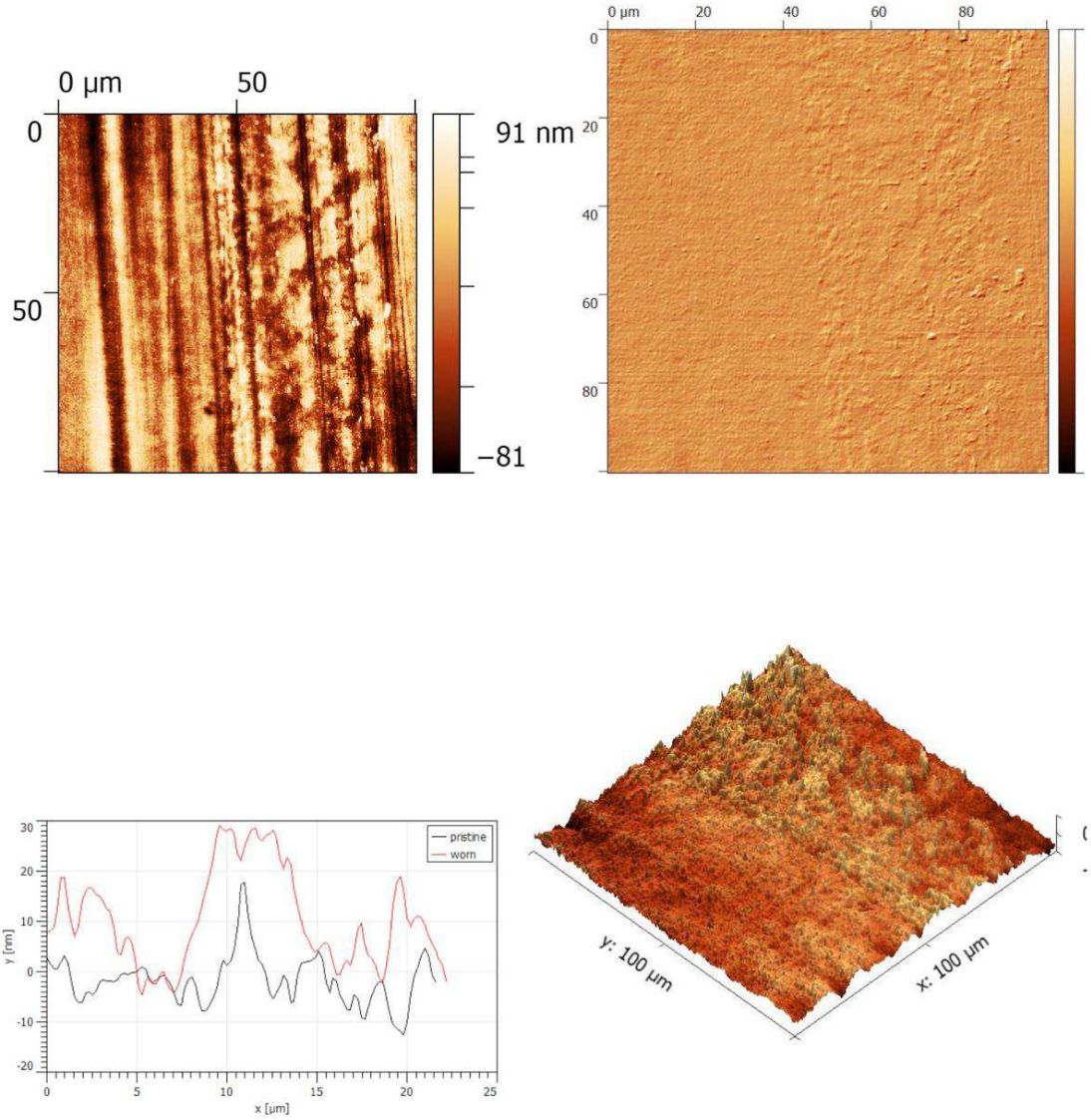

Figure 53 AFM raw, 2D, 3D and profilometry of Steel disc with pure GIII4 oil

In tests like GIII4 formulated oil with steel surfaces, a tribofilm always formed (Figure 54). Obviously, it can be visible with AFM. The shape of the tribofilm is like dried-up liquid stains, which lay along the wear track.

The wear track itself is clearly visible and definitely splits the surfaces into two regions with very different surface roughnesses.

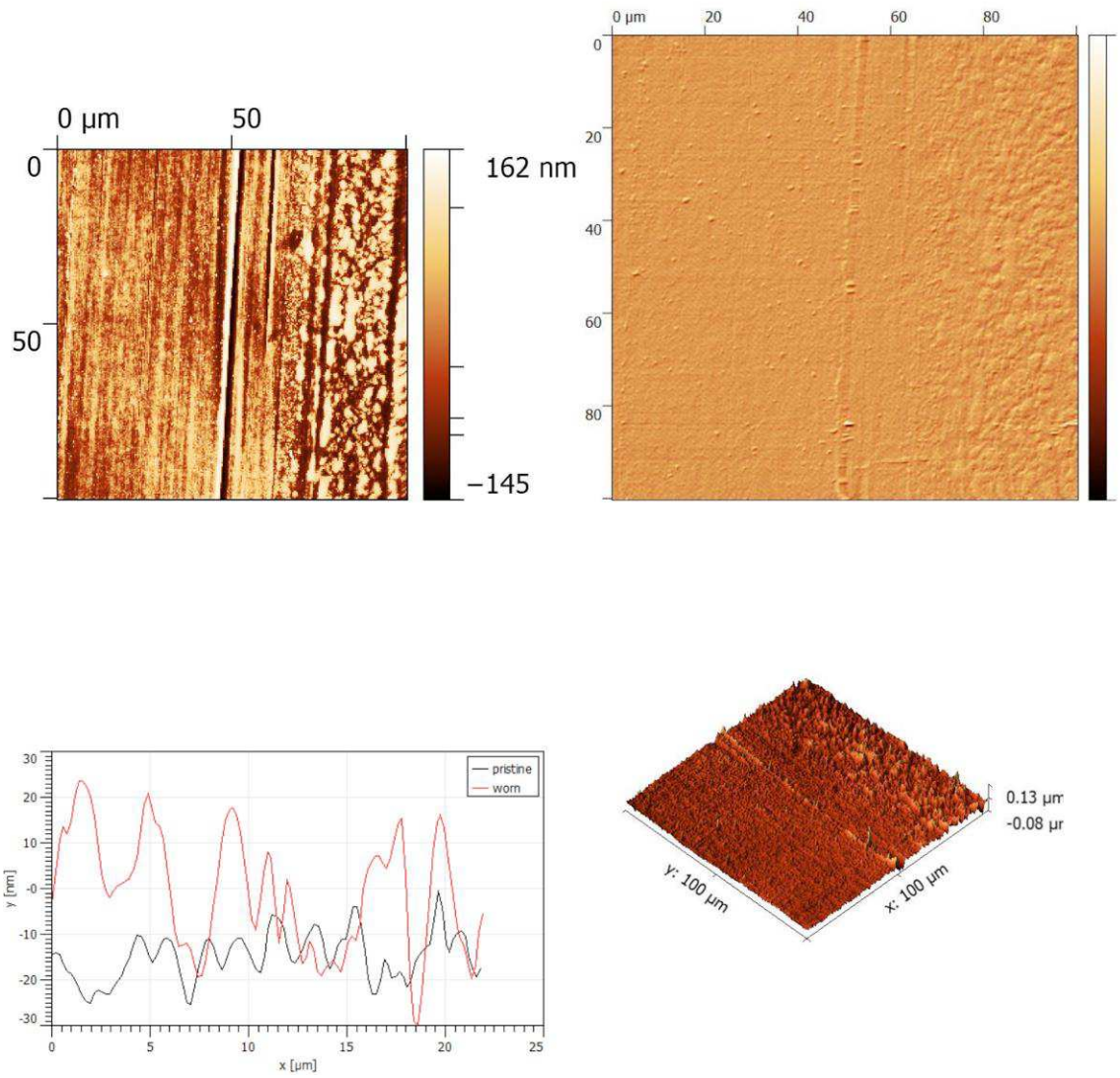

Figure 54 AFM raw, 2D, 3D and profilometry of Steel disc with formulated GIII4 oil

Finally, images from the test involving steel and group IV formulated lubricant (Figure 55). Tribofilm is clearly visible an so are the deep wear scares which form the wear track. Overall wear, in all the test with PAO-based oils, is the highest of the entire tests campaign.

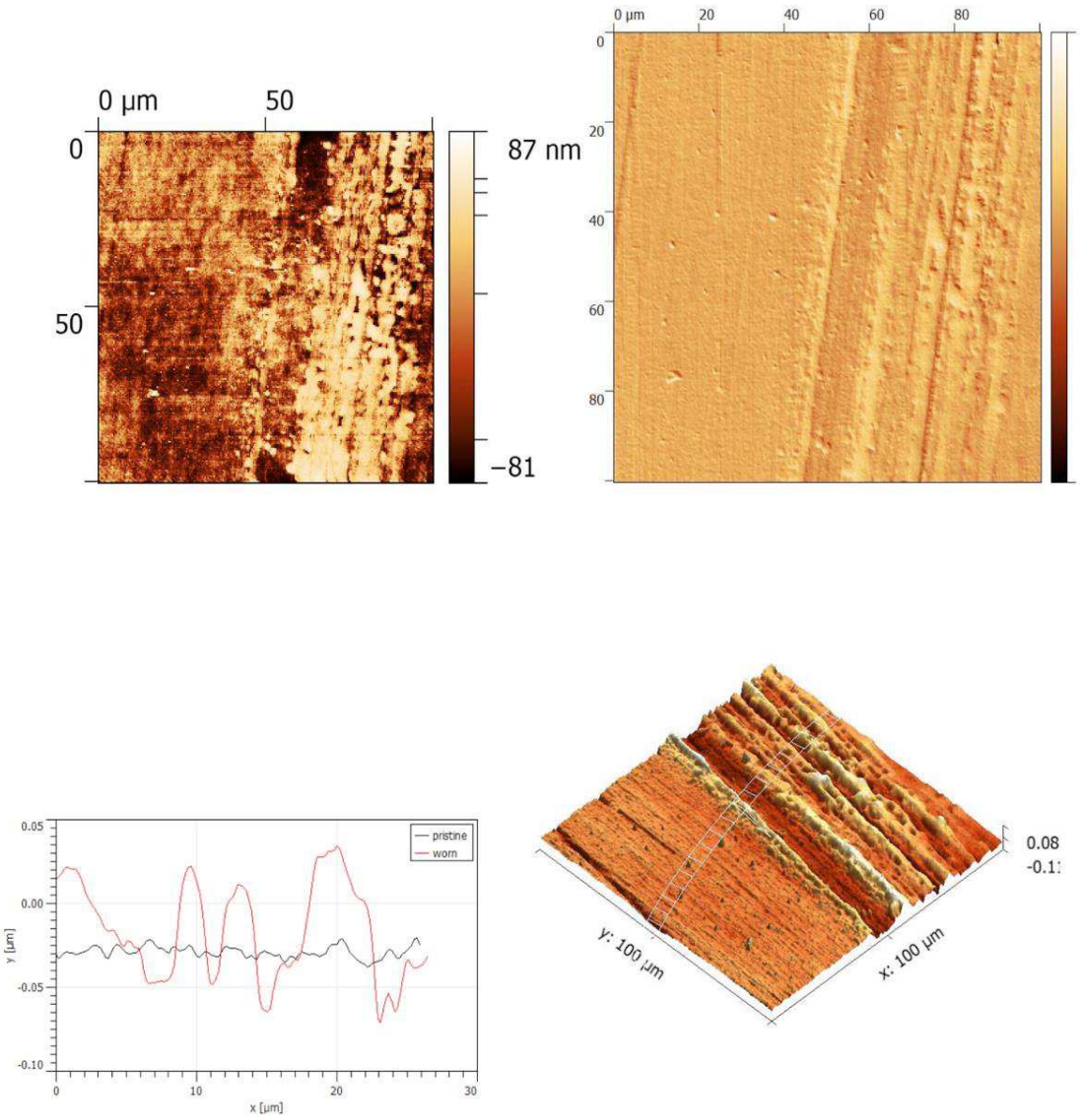

Figure 55 AFM raw, 2D, 3D and profilometry of Steel disc with formulated PAO4 oil

DLC specimens

Coupling a pure group III base oil, with a DLC/DLC setup results in a barely signed wear track on the disc's surface (Figure 56). GIII4, being a mineral based oil, it has impurities which keep the overall polarity of the lubricant quite high (especially if compared with synthetic oils, like group IV).

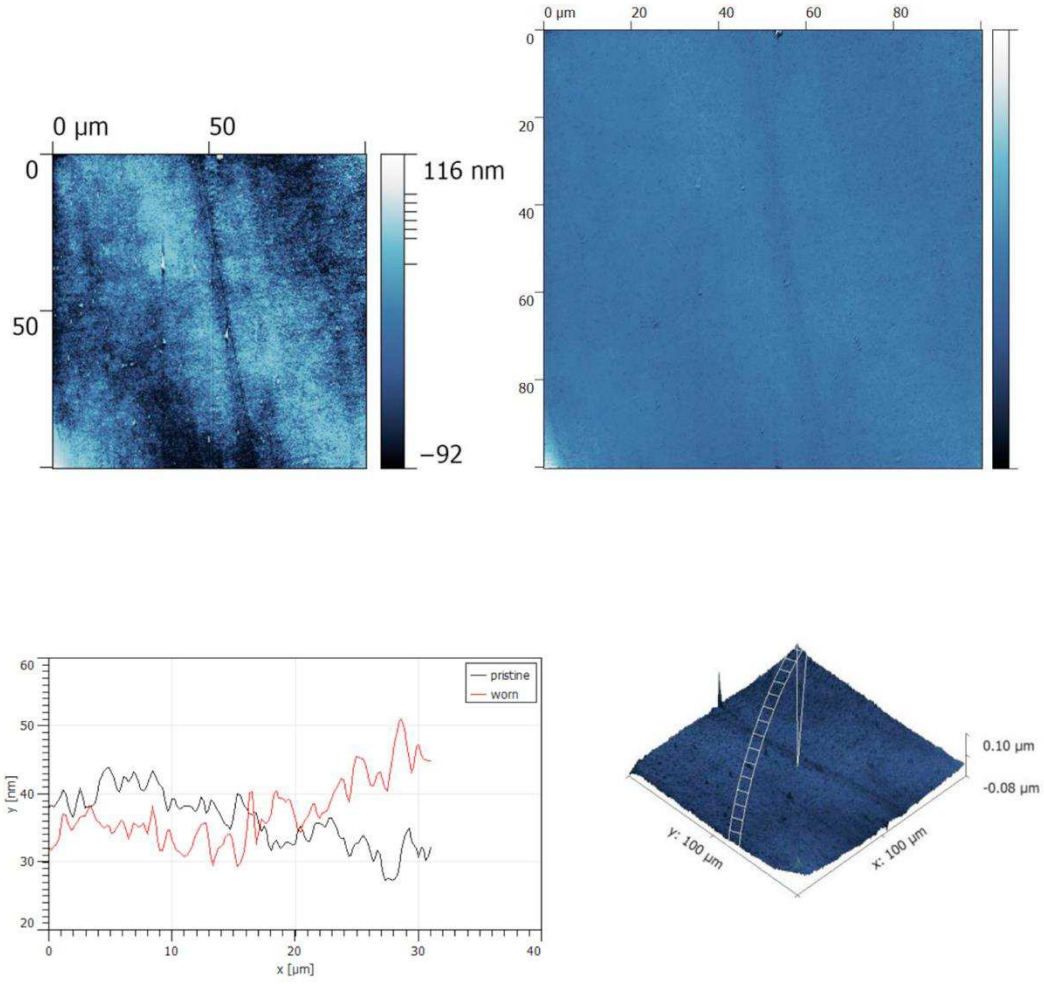

Figure 56 AFM raw, 2D, 3D and profilometry of DLC disc with pure PAO4 oil

However, DLC keeps the same aforementioned behavior with group IV oils (Figure 57). PAO4 has a very low polarity and a lower viscosity index compared to GIII4 so, for this specimen, the wear track is indeed visible because the oil film should have been not protective as the GIII4's one.

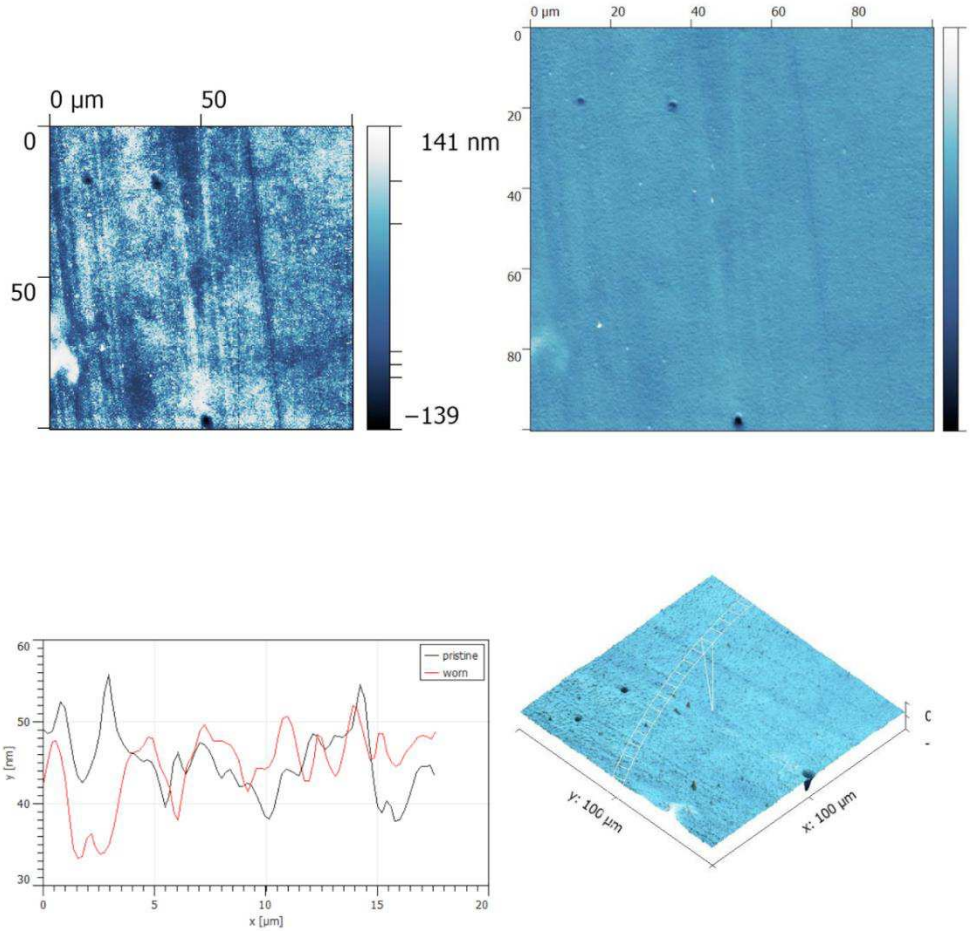

Figure 57 AFM raw, 2D, 3D and profilometry of DLC disc with pure GIII4 oil

Wear track originated by using a formulated GIII4 lubricant (Figure 58) is again visible on the surface of the disc but the difference in roughness is really low. So, the track in the picture may be related only to chemical reactions between hydrogenated surface and oil additives. There are no signs of a tribofilm formed onto the surface.

There can be some possible explanations to this: maybe the high polarity of the base oil keeps the solid fraction suspended, preventing the formation of solid coatings on DLC; maybe, the reactivity of surface is too low to form a strong tribofilm; maybe, the oil film thickness is so big that it's able to drag enough contact energy to inhibit the transformations mechanisms of the additives.

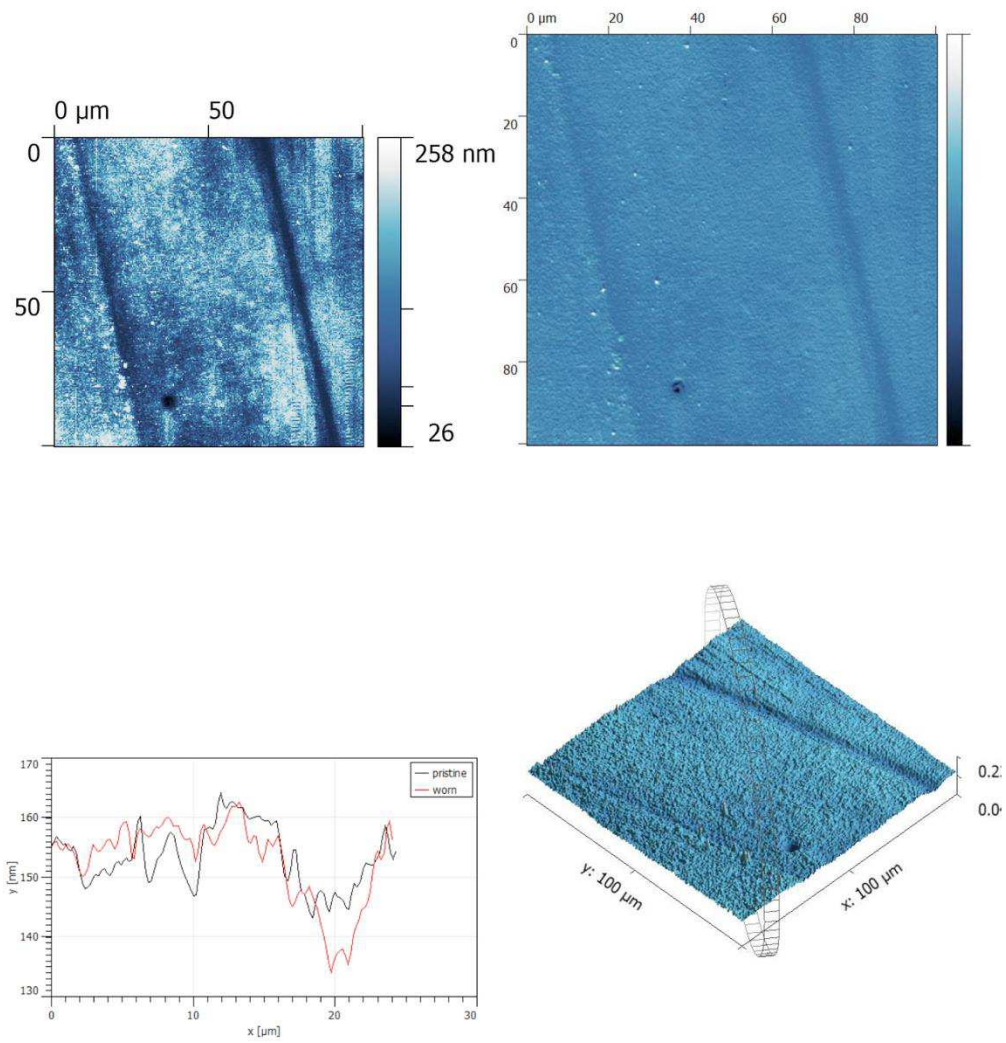

Figure 58 AFM raw, 2D, 3D and profilometry of DLC disc with formulated GIII4 oil

Finally, DLC specimen which has worked with formulated group IV oil (Figure 59) shows a different surface, compared to the other formulated oil. This time the tribofilm is very well visible as it forms a rough coating of solid spots onto the wear track. At this point, one cannot say that DLC surface has no reactivity: it has one indeed. The difference is the base oil. Group IV oils show lower capability of dispersing additives and of forming a thick film able to sap contact energy, "saving" additives.

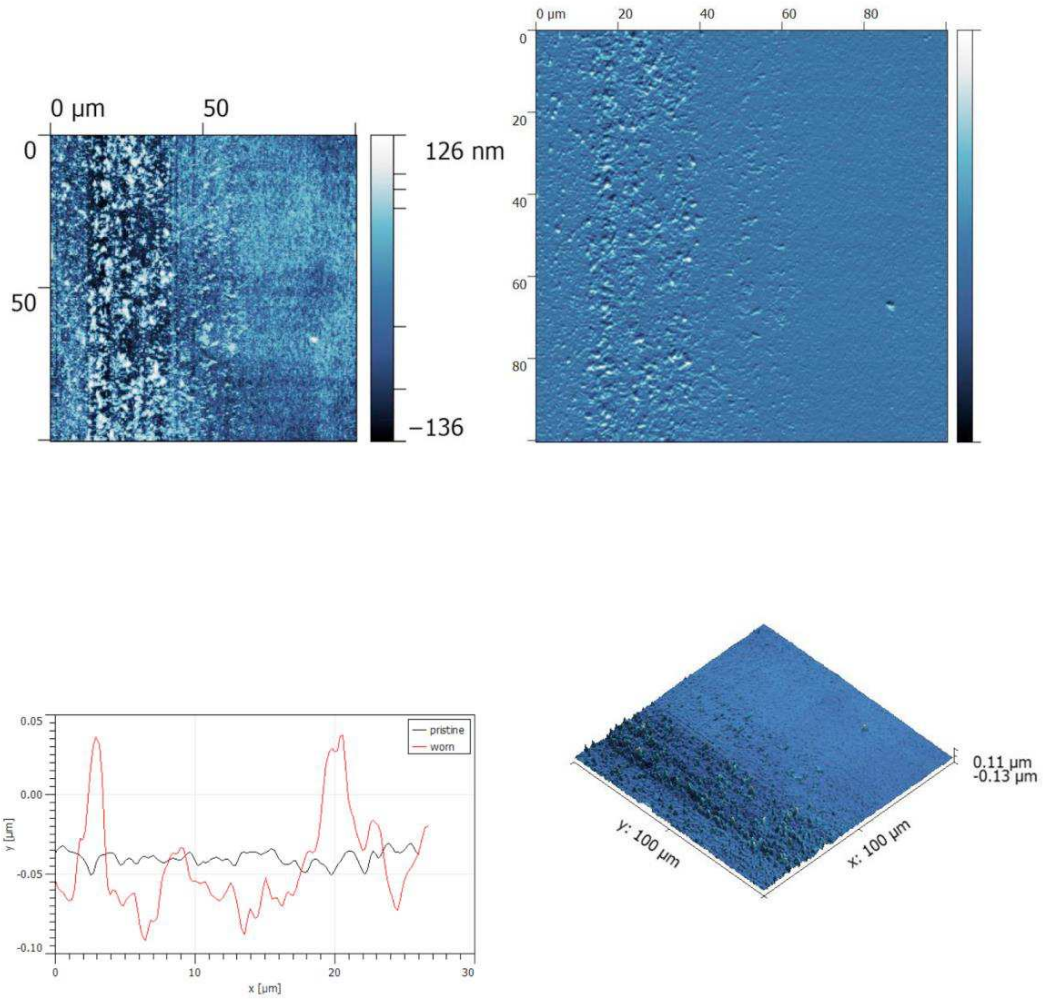

Figure 59 AFM raw, 2D, 3D and profilometry of DLC disc with formulated PAO4 oil

1.6 A better lubricant for coated surfaces

From the two previous friction and wear assessments, some final quick comments can be done on lubrication of modern coated surfaces:

- Formulation of I.C.E. lubricants has been developed through decades of experience and tailored on iron chemistry; the same improvements cannot be seen when these lubricants work with non-ferrous DLC coated components.
- DLC has worse, but still comparable, friction performances as steel when tested with formulated oils, containing ZDDP and MoDTC as anti-wear and friction modifier agents, respectively. Steel cannot bare running without these additives, while DLC can without any significant issue about, which opens opportunities for developing lubricants S and P free.
- In the conditions of the tests proposed, DLC coatings showed no signs of relevant wear. This means that, despite the slightly worse COF, DLC coatings can be competitive in green economy thank to their longer working life. DLC's importance in green economy is also given by its great performances with blank oils. For sure, ZDDP is not needed anymore. DLC however, has higher costs and accurate life-cycle assessment should be done to evaluate its effective convenience on I.C.E. applications (see Table 6).
- Considering the wear resistance of DLC coatings valid, there is still room to improve their friction performances.

Table 6 Cost comparison between bare steel and DLC coated steel (by PCS)

Surface	Cost (%)
Steel **AISI52100**	100
DLC **ta-C:H**	150

Despite all the possible explanations about the presence, the surface affinity and the quality of tribofilms on DLC coatings, it remains the doubt about how can a "protective tribofilm", like they are on steel surfaces, help to reduce COF also with

DLC surfaces, which are designed to keep lower friction by generating slipping layers of graphite between the sliding bodies: how can there be a lower COF if the graphite is covered by the additive's tribofilm?

Probably, a better lubricant for DLC surface should be free of ZDDP and MoDTC, additives that have been proved to generate covering layers of new chemical compounds onto the component's surface (DLC work great with blank oils) or it may be that proper additives should enhance, substitute or retard to the graphite generation mechanism, responsible of lowering COF. Such additives can be just made of another layered material, like graphite itself (or MoS_2/WS_2) and possibly free of chemical species able to pollute environment or damage the engine.

A good candidate seems to be hexagonal Boron Nitride (h-BN).

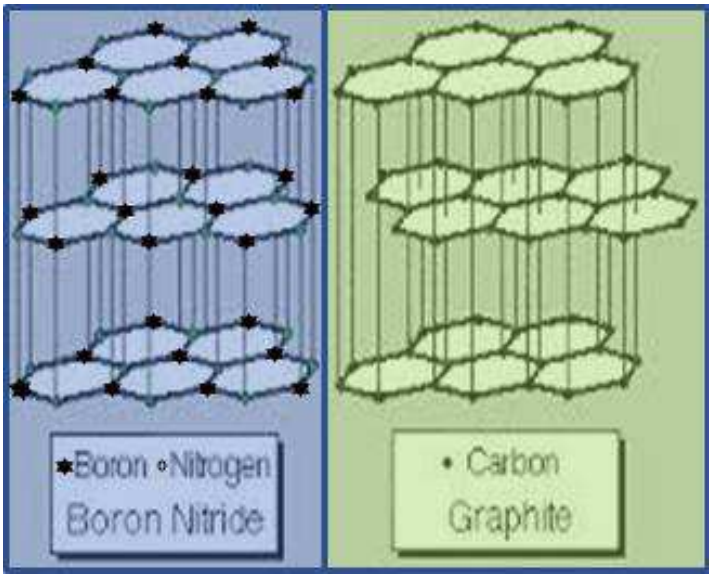

Figure 60 h-BN and Graphite are both layered materials (notes from class lecture)

Many studies have proposed graphene nanoparticles (or graphene oxide, for a better affinity with surfaces) as candidate for generic friction modifier in lubricants, meant as direct additive (75) (76) (77) or as borate precursors (78) (79).

Its performances are impressive in this sense, but its cost is really prohibitive, at least today (see Table 7). A MTM test campaign, like the one proposed in this thesis but using graphene additivated oil, could have reached incredible costs; h-BN is

way cheaper than graphene and, a nice to have, it has a good thermal conductivity (400 W/mK at 300 K), which does help in dissipating heat.

Table 7 Example of cost comparison between traditional oil additives and new proposals (by PCS)

Additive	Cost (€/g)	Common $\%_w$ in oil	€/L
ZDDP	0,003	0,5	0,0135
MoDTC	0,02	1	0,18
h-BN	1,50	5	67,50
Graphene	500	10	45000

The only stumbling block to solid particles additives in lubricants is *dispersion*. It is crucial to achieve a good homogeneity of formulation in the tank, during engine operations and in cold start situations, and preparing dispersant for lubricants is a sort of art, of which few companies worldwide are mastering. During the preparation of h-BN oils for this study (with Sigma Aldrich powders, CAS 10043-11-5), a black-box additive package has been used, suggested by our partner to be good for boron-based compounds.

Three recipes have been tested, 0,5, 1 and 5 $\%_w$ in h-BN (Figure 61). Of course, the higher the amount of h-BN is, the lower the Stribeck curves and COF (but also the final costs)are. At high amounts of h-BN particles (1 and 5%) steel/steel system seems to be clogged, since the COF of BL zone is prolonged also in ML zone, a sign that the asperities have not started to be separated by lube yet; the smoother surface of DLC coating contained this behavior, still well visible in the plots. Beside the ultra-low COF obtained with 1 and 5% of h-BN and DLC, what is worth noting is how - even with the lowest amount of boron nitride (0,5%) - the performances of both steel and DLC were comparable to the ones with traditional formulations with S and P compounds (Figure 64). At the end of each test, rinsing of steel surface has been a hard task, probably due to the groovy surface of the bare metal, enhancing the grip with the solid h-BN flakes (Figure 62). This could mean that, taking for granted the technologies for dispersing solid particles and implementing such kind

of lubricants into real engines, there is *already* the opportunity to run with S and P free oils. Greener lubricants are already here and there is still room for improvements.

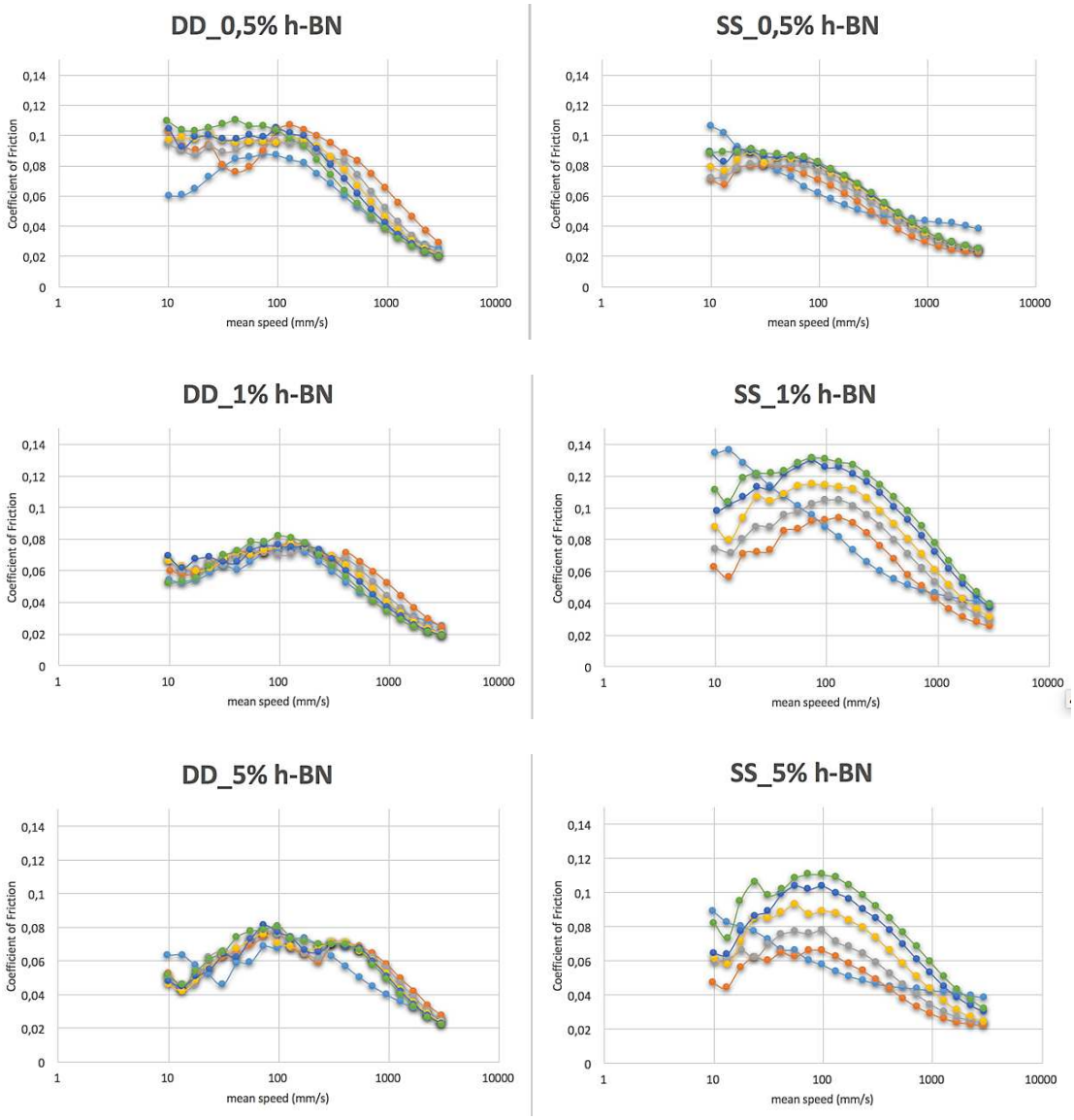

Figure 61 Comparison between bare steel and DLC coated steel with oil at different level of h-BN content

Figure 62 MTM pot, with mounted specimens, charged with 0,5%$_w$ h-BN PAO4, at the end of a test. It can be noticed the good wettability of the lubricant of the steel surface, maybe due to a less smooth surface than DLC.

The next step of this study should investigate on better solid particles dispersant - as the secret package proposed by the partner has not been enough to stabilize the formulated lubricant for more than few hours (Figure 63) - and liquid friction modifiers, like esters or ionic liquid, which do not interfere with the chemistry of both bare metals and coated components, offering better tribological properties than the lubricants of today.

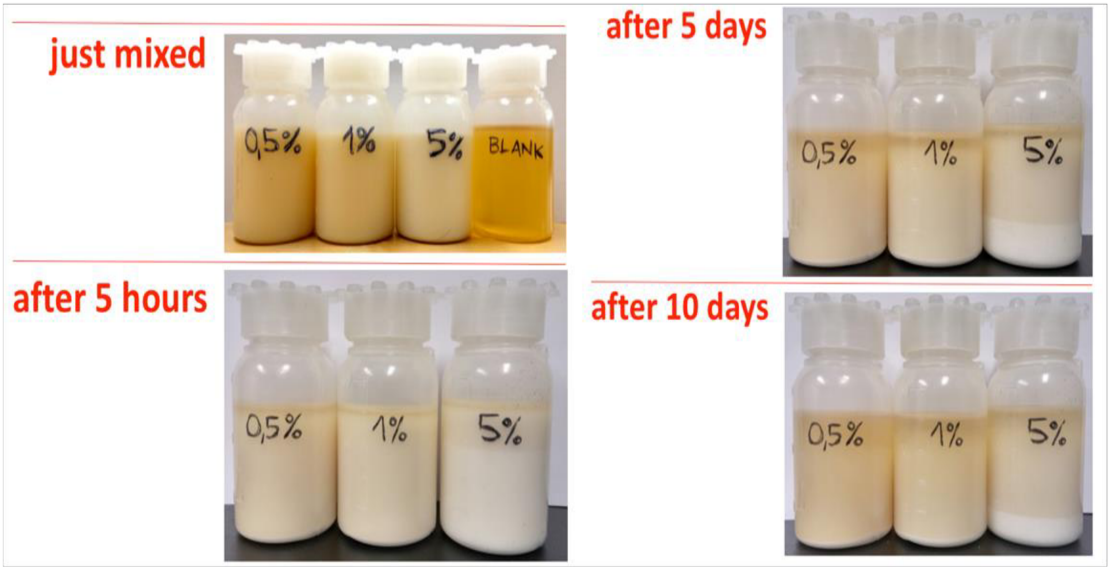

Figure 63 The secret package had the power of stabilize the h-BN dispersion only for few hours. A better dispersant should be investigated for these applications.

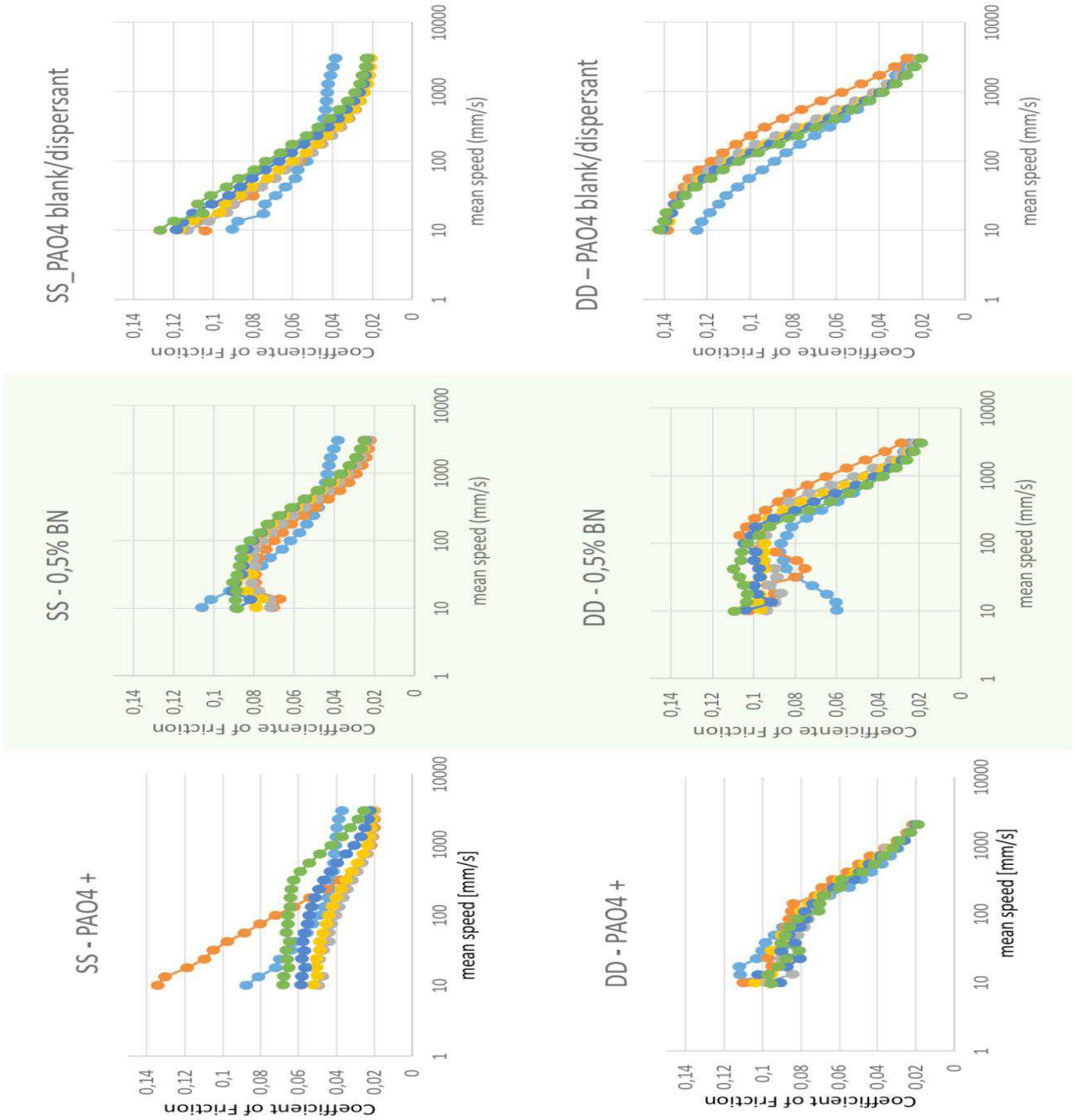

Figure 64 Comparison between traditional formulation (PAO4+), blank oils with secret dispersant (PAO4) and new formulation, like PAO4+secret dispersant and h-BN solid particles (legend in Figure 22).

Chapter 2

Improving After-treatment Systems

Part of the work presented in this chapter has been already published in:

(99) Miceli et al., Effect of the morphological and surface properties of CeO2-based catalysts on the soot oxidation activity, Chemical Engineering Journal 278 190–198, 2015.

(114) Miceli et al.: CeO2-based catalysts with engineered morphologies for soot oxidation to enhance soot-catalyst contact. Nanoscale Research Letters 9:254, 2014.

(123) Piumetti, Miceli et al., Contact dynamics for a solid–solid reaction mediated by gas-phase oxygen: Study on the soot oxidation over ceria-based catalysts, Applied Catalysis B: Environmental 199 96–107, 2016.

(128) Orihuela, Miceli et al., Experimental measurement of the filtration efficiency and pressure drop of wall-flow Diesel Particulate Filters (DPF) made of biomorphic Silicon Carbide using laboratory generated particles, Applied Thermal Engineering 131, 41-53, 2018

2.1 After-treatment: brief background

Nowadays, private transportation is led by I.C.E. equipped vehicles, mainly Diesel, then gasoline and finally LPG (Liquid Petroleum Gas) and methane as fuels, in order of share quota (80). By burning fossil fuels, these engines produce a large variety of pollutants, such as CO_2, NO_x, VOC (Volatile Organic Compounds) and PM[9]. Each of these classes of compounds has its own optimal conditions to born (and to be avoid as well) (81) (82):

- CO_2 emission is related to fuel consumption, that represents engine efficiency. It is a greenhouse gas.
- NO_x mainly derives from high temperatures and lean conditions. Responsible of water acidification and photochemical smog.
- PM (Particulate Matter) forms with low temperatures and lean mixtures. PM is the solid fraction of *soot*. It causes pulmonary diseases (83).
- VOC are generated by the incomplete combustion of fuel. Bringer of environment pollution and human health problems.

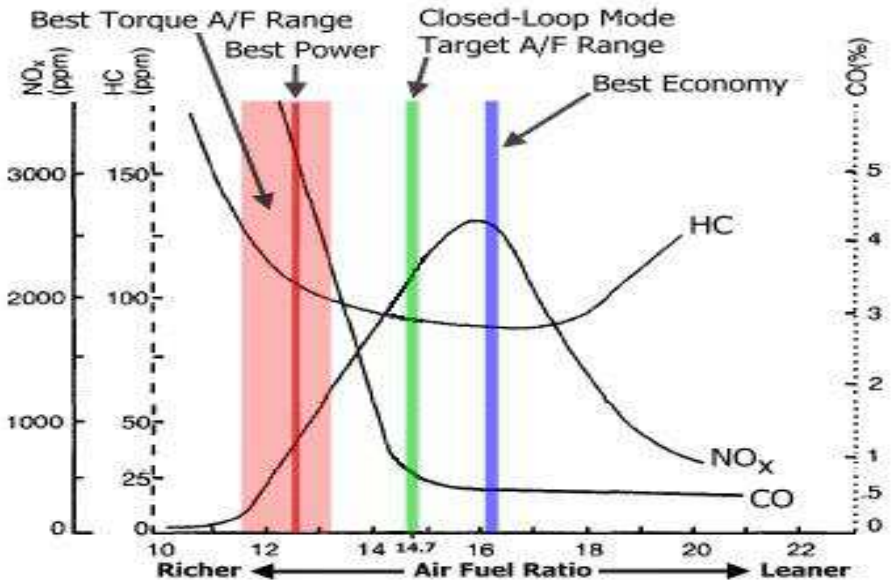

Figure 65 I.C.E. emissions range (notes from class lecture)

[9] Carbon dioxide (CO_2) is not officially recognized as a real pollutant since its effect on human health and environment is void. But being a greenhouse gas, and having been recognized its effect on climate change, in this work CO_2 is ranked among pollutants as well.

On 18th September 2015, the United States Environmental Protection Agency (EPA) issued a notice of violation, to Volkswagen Group, of the Clean Air Act (CAA, a US federal law to control air pollution at national level). VW was accused of installing special functionality in the ECU able to detect whenever the car is on testing or on real roads. In the first case, the so-called "defeat device" was able to change the calibration of the engine to stay compliant with the CAA limits, at the cost of lower performances. The engine was compliant to the law on testing benches but, to give the end user more performances, it was not in real life. In a sort of general misunderstanding, people in USA, and later in UE too, started losing faith in the claimed cleanliness of Diesel engine and a consistent number of majors and government started applying a Diesel ban on their roads. It was the beginning of the so-called *Diesel-gate* or *Volkswagen fraud* and also the start of a witch hunt, with Diesel engines as victim. Later on, other OEM were accused of installing defeat devices on some Diesel equipped models, but up to date, only VW declared itself guilty. (84).

Are Diesel engines *dirty*?

Actually, considering the latest version of a Diesel engine, a EURO6 compliant unit fully equipped of DOC, DPF and SCR, it seems to be the cleanest internal combustion engine on the market (Figure 66).

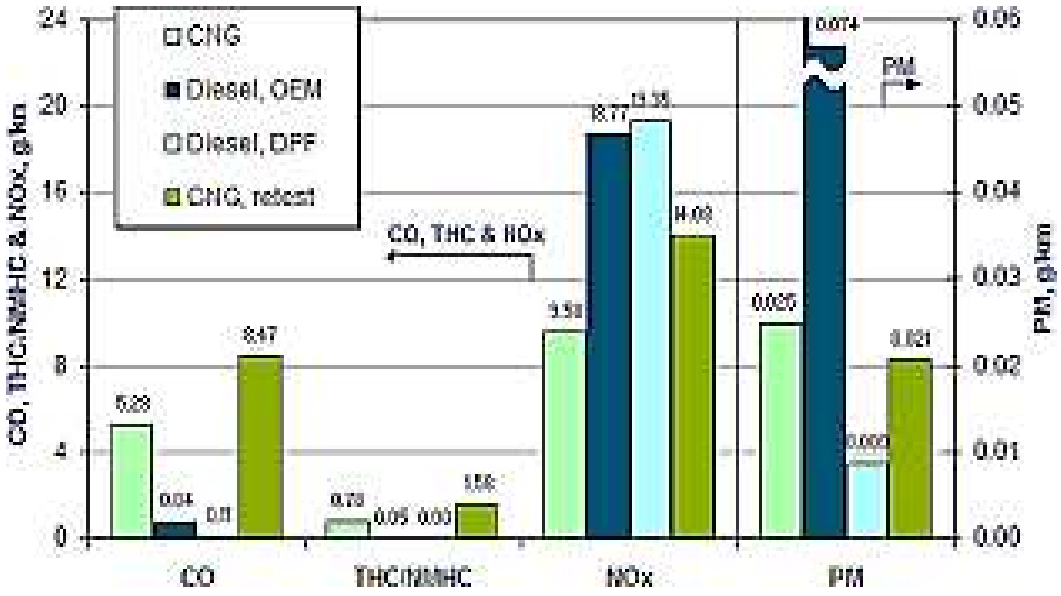

Figure 66 Comparison of overall emissions of Diesel, gasoline and CNG fuelled engines (85)

Diesel thermal cycle has a higher efficiency in comparison with Otto's cycle; this means that Diesel engine takes less fuel to give the same power. Less fuel, less CO_2. Nevertheless, the stratified charge and the flame evolution are cause of intense particulate production. Moreover, the higher temperatures achieved in the compression stroke by Diesel engine are enough to keep the nitrogen in the air away from its inert zone, producing nitrogen oxides. The last two issues have been successfully overcome with the introduction of DPF and SCR, respectively, as mandatory equipment for modern vehicles (DPF from Euro4, 2008; SCR with Euro6, 2014).

Gasoline and CNG/methane engines, during the same years of development, only relied on basic improvement of their TWC systems (3-ways catalyst, oxidative), ignoring NOx and PM generation.

PM forms in that area of the flame which is more likely to be quenched, interrupting the combustion and leaving carbonaceous products unburned. It's a characteristic of sprayed charges. As many gasoline engines have been equipped with Direct Injection, they started suffering quite the same issues of Diesel. That's why there is a discussion about the effectiveness of installing GPF (gasoline particulate filter) as mandatory equipment, like they do with Diesel units (86).

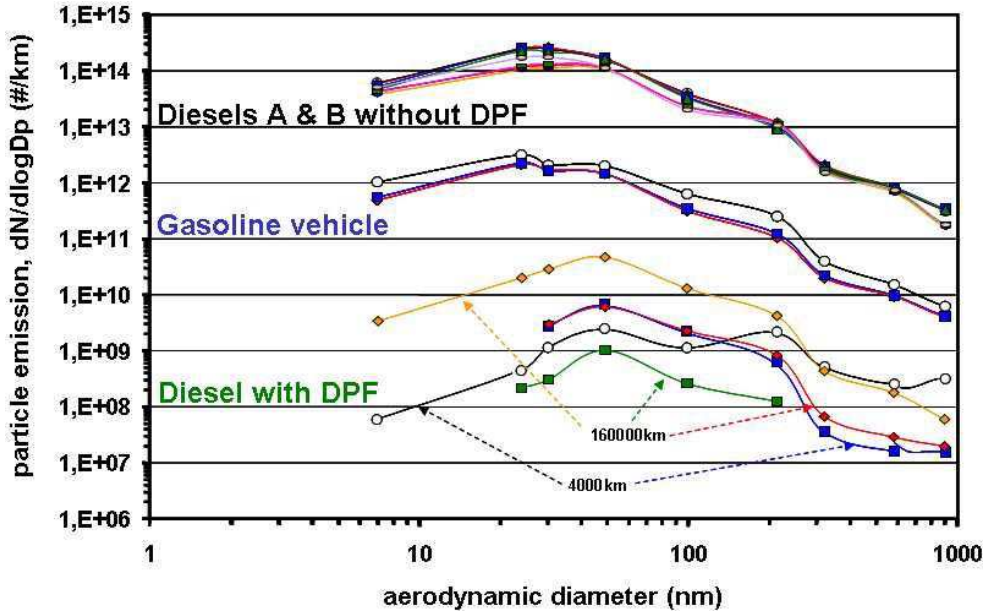

Figure 67 PM emissions of bare Diesel engine, DPF equipped Diesel engine and Gasoline engine (87)

Talking about witch hunts, CAA and EuroX regulations have brought a lot of benefits to the quality of air of our cities but, incredibly, sometimes it appears to be not enough. More Majors, at least in Italy, choose to control vehicles traffic with special ban, no traffic areas and no traffic days. With scarce success.

In order to improve, for real, the quality of the air, people should change their way of life. And driving less polluting vehicles is only a tiny step towards this goal (Figure 68) (88).

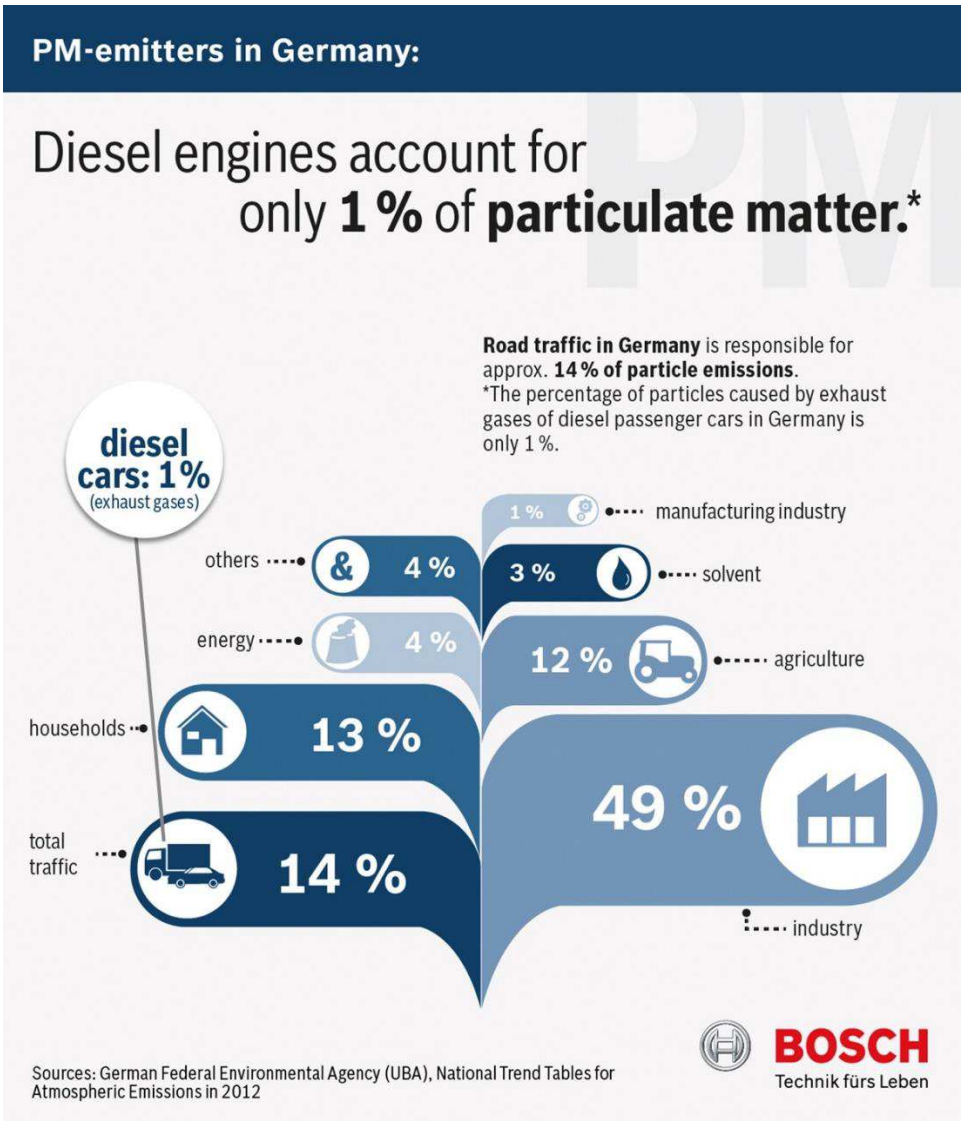

Figure 68 Agents affecting the quality of air [source: in picture]

2.1.1 Soot Abatement

In recent years, some legislations have been introduced in order to limit the emissions from private transportation and the technology of the abatement systems has improved very fast. (89) (90) (91) (92)

To keep these pollutants under control, along with design strategies, complex exhaust after-treatment systems (ATS) are widely adopted, consisting in catalytic converters of oxidative kind (3-way Catalyst, DOC – Diesel Oxidative Catalyst), reductive (on board $DeNO_x$ devices) and filters (DPF/GPF, Diesel or Gasoline Particulate Filter, see Figure 69).

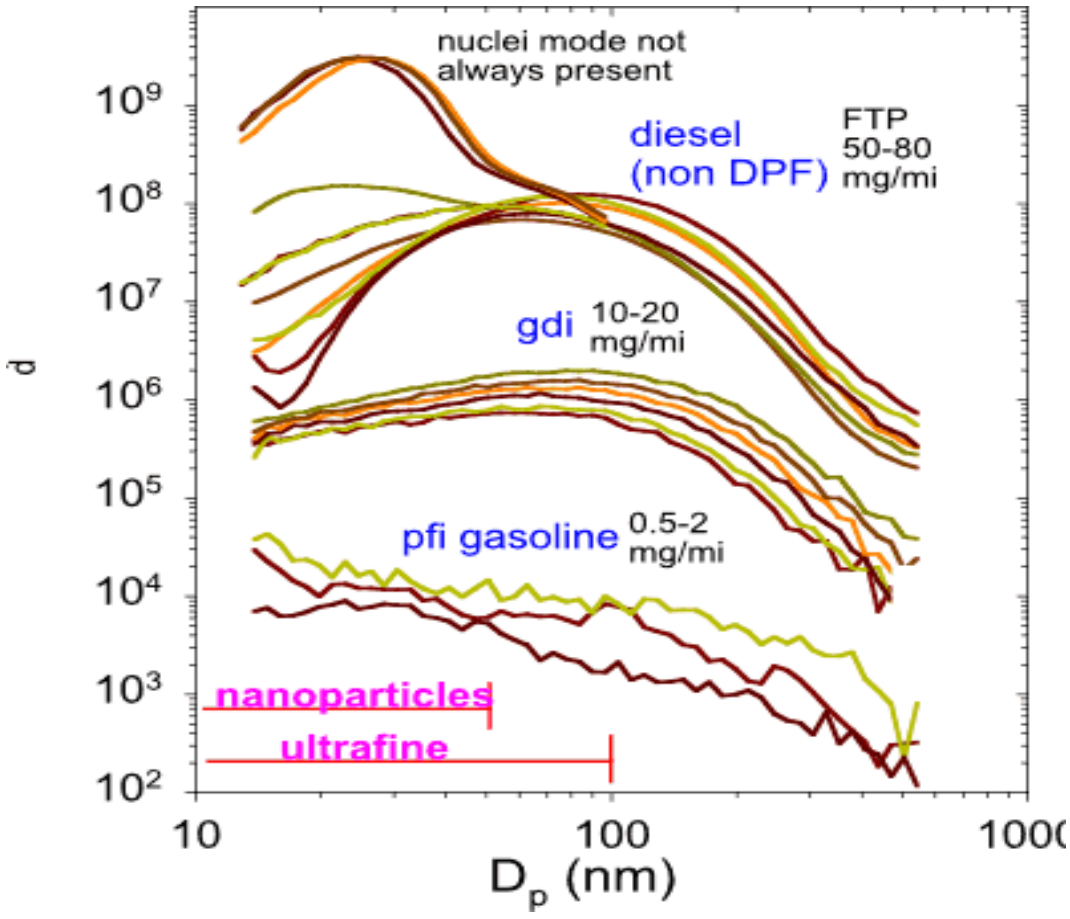

Figure 69 PM emissions from gasoline and Diesel engines in steady state. PFI: Port Fuel Injection; GDI: Gasoline Direct Injection. Sometimes bimodal, nuclei mode is highly variable, depending on fuel type, exhaust dilution conditions and numerous other factors (93)

A clean engine should be able to provide the same or higher performances burning less fuel, and consequently emitting less pollutants (see Chapter 3). If less fuel is burned, less CO_2 and VOC are produced. But PM and NO_x remain an issue.

Despite the different nature of these two compounds, there is a thin line connecting them and making it possible to use the same ATS for their combined abatement (94). These mechanisms of assisted soot combustion are under investigation and their development should reach breaking technologies like SCRoF (Selective Catalyst Reduction on Filter) which do reduce, in a singles device, the emissions of both NO_x and soot.

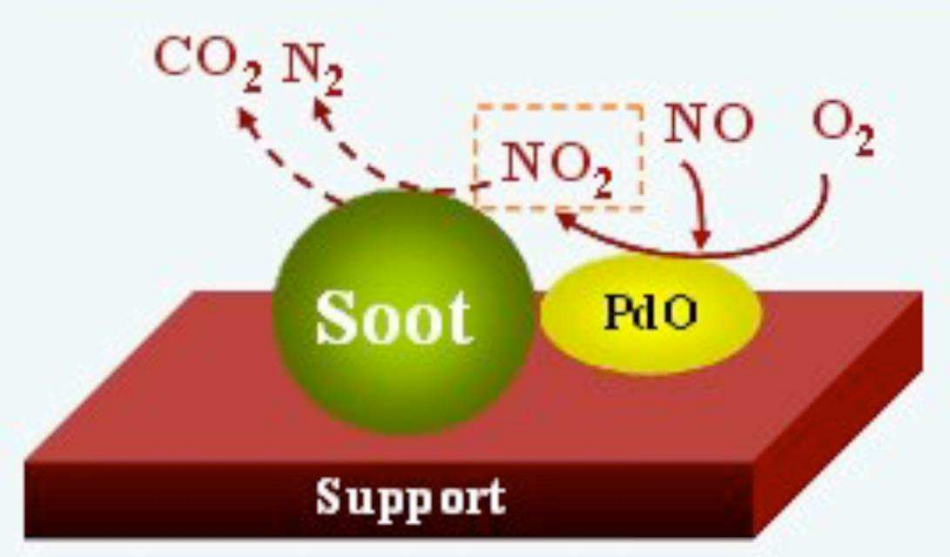

Figure 70 NOx-assisted soot combustion schematic (94)

The first step towards the development of these new ATS could be to improve the efficiency of current DPF (95).

Literally from Miceli et al., 2014 (96):

The DPF is a ceramic filter with alternate-plugged channels, in which the flue gases enter the open channels at the inlet, cross the porous ceramic wall of the channel, where soot particles are retained, and finally exit the filter from the neighbouring channels. The soot particles deposit in the pores of the ceramic walls and progressively form a soot layer on top of the wall, which is called cake (96). *The latter generates a drop in pressure across the filter, which becomes unsustainable for the engine; therefore, the cake periodically needs to be burned off, in order for*

the filter to regenerate. Regeneration is currently achieved through the post-injection of fuel from the engine (97) (98)*, which causes a relevant fuel penalty for modern engines.*

Initially, these filters were made of bare Silicon Carbide but, driven by impelling regulations, the abatement of soot from I.C.E. emission is getting harder and harder and catalytic coatings onto the filter channels have been introduced.

A catalyzed DPF would require less post-injections for its regeneration or even provide less back-pressure to the engine. However, noble metals catalyst are expensive and such systems would be hard to sell on the market (Figure 71).

For these reason, the coating on these DPF is mainly made of an oxidative layer based not on noble metals but on redox-capable rare earth oxides, such as CeO_2 (cerium oxide IV, or simply *ceria* in this work).

Literally from Miceli et al., 2015 (99):

Particulate matter (PM) is a complex compound and it is made of carbonaceous particles (called soot) along with adsorbed gases, ashes, sulfates and condensed vapors (soluble organic fraction, SOF). This system has diameters in the range of few nanometers up to hundreds of nanometers, and even beyond (100) (101)*, and it is associated to several problems in terms of human respiratory diseases and environmental issues* (81) (82)*.*

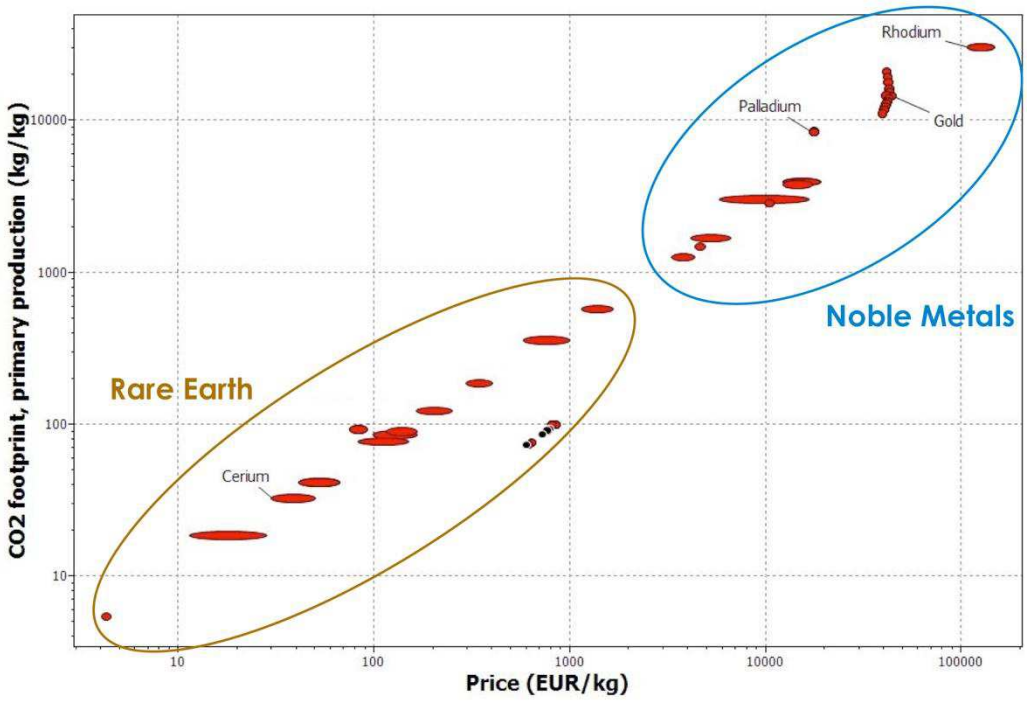

Figure 71 Ashby plot to compare sustainability and costs of noble metals catalysts and rare earths The lower, the better. The final goal to reduce CO_2 emission of I.C.E. should not be considered just as when the engine is running, but also as the overall impact of that technology.

Ceria is considered to be a redox oxide, able to undergo to redox cycles as it can range from Ce^{4+} to Ce^{3+} from lean to rich conditions, respectively, and so storing oxygen and giving it back to promote the combustion of soot. This characteristic is due to the intrinsic activity of the catalyst (shape, specific surface area (102)) and to its particular surface reactivity. More in detail, this enhanced surface reactivity may be caused by oxygen vacancies, which promote the oxygen mobility, improving the *oxygen pump* mechanism (103).

Interesting starting points for further development are: increasing surface area, engineering a better shape and increasing oxygen mobility.

There have been some attempts to introduce ceria directly through the fuel (so called FBC, fuel borne catalysts (104)) with interesting results as far as the abatement of soot is concerned. Despite the encouraging results, this system turned up to be generating solid nanoparticles which were, however and again, dangerous for human health. Finally FBC solution has been abandoned, consecrating the DPF as unique ATS for soot abatement. Since its first introduction in 2000, DPF quota

has been increasing year after year and finally became a standard equipment of Diesel cars since 2008 (Euro4). From 2014, with Euro6 regulation, some gasoline cars with Direct Injection engines are supplied with particulate filters as well (GPF). (105) (106) (107) (108) (109) (110)

Intuitively, the more oxidative is the coating, the more efficient is the filter. Indeed, this is partly true. Being the combustion of soot a homogeneous catalysis process (solid-solid), the contact between soot particles and catalyst has been proved to play an important role (111). There is room to improve the performances of CeO_2 by enhancing its capability to embrace the particulate particles.

Another important advantage of using ceria as catalytic coating in DPF is the ease of coating. Solution Combustion Synthesis (SCS) is a rough but effective technique for obtaining, in few minutes and even *in situ* on a substrate, an oxide from a salt, heating up an aqueous solution containing fuel (usually glycine or urea) (112). This means that, in order to produce a coated DPF, the ceramic monolith can be dipped into the ceria's precursor solution and then heated to start the exothermic reaction.

This step can be repeated till obtaining the level of coating needed from the specific application. The morphology of the resulting oxide is utterly uncontrollable, but the performances are surprisingly constant; for this reason, SCS ceria is considered to be a perfect reference for every other ceria-based catalyst, included the ones presented in this work.

2.1.2 Lab-scale setup

It is worth noting that, when testing a soot-oxidative catalyst, there are few methods for screening: lab-scale, mid-scale and full-scale.

Full-scale is a test with a real engine, mounted on a proofstand, with a real size ATS. The mid-scale involves a smaller DPF, mounted in an ad hoc test rig with tailored cannings, furnaces, cylinders and soot generator. Finally, in lab-scale, soot and catalyst are mixed as powder, charged in a quartz reactor and tested in a furnace (a so called TPC, Temperature Programmed Combustion), which schematic is depicted in Figure 72.

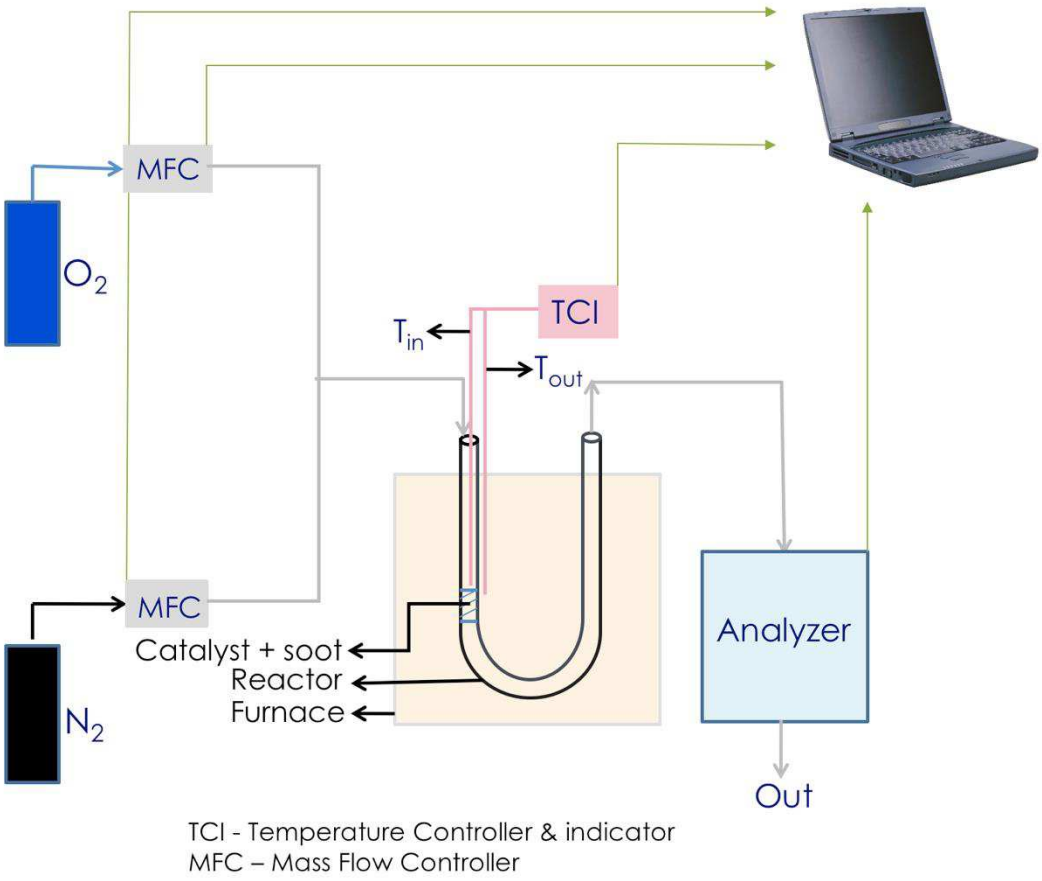

Figure 72 TPC lab-scale test rig configuration used during the investigation described in this work

This last methodology is indeed perfect for ranking the intrinsic activity of a catalyst, but it requires accurate preparation to be adapted for solid-solid catalytic reactions. In mid and real-scale in fact, the catalyst is not provided as powder, but as a thick and solid layer, coating the channel of the filter.

The contact is not just between the catalyst particles and the soot particles (as in a TPC test) but between the soot layer (so called, soot cake) and the catalytic layer (Figure 73).

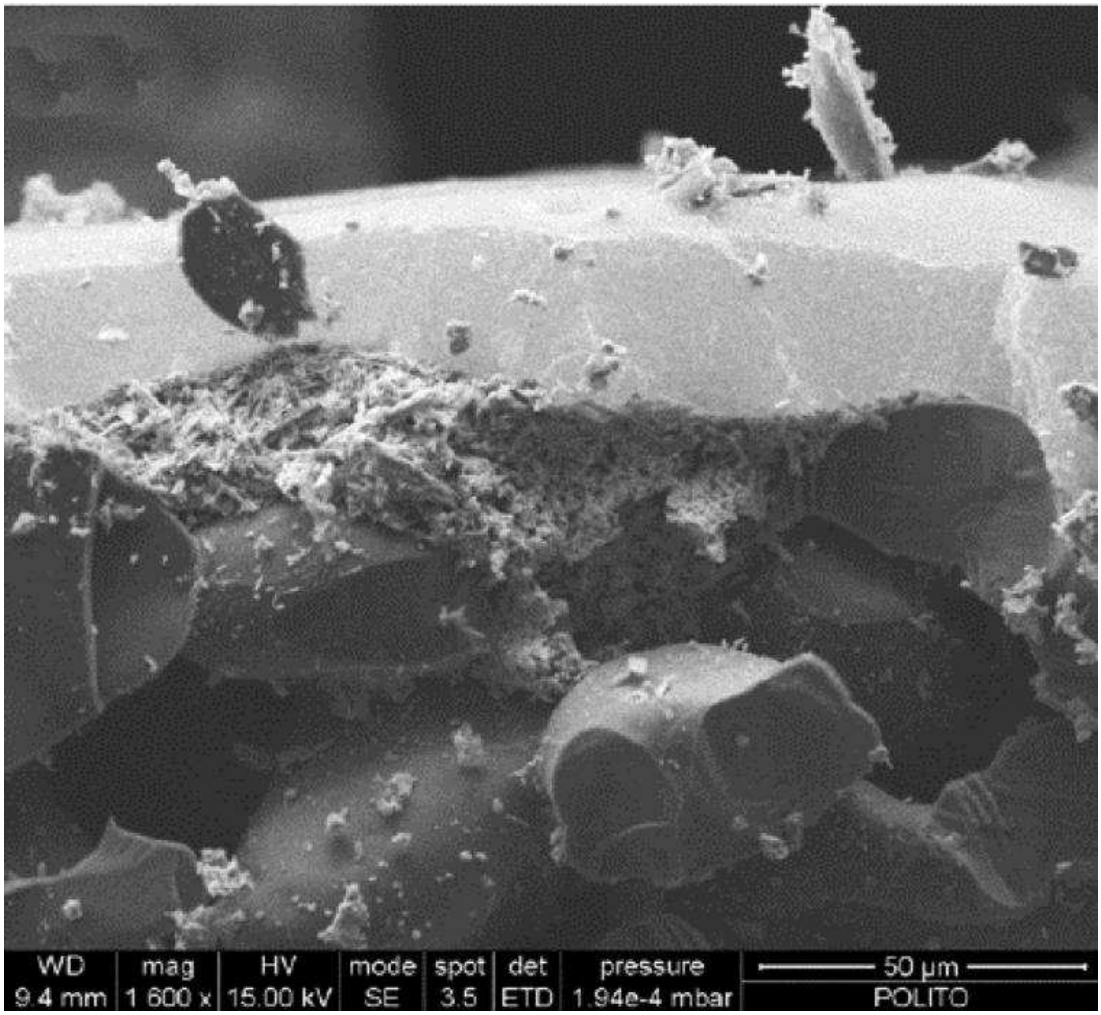

Figure 73 FESEM of a soot cake upon a fiber shaped ceria catalyst bed. Both catalytic and soot cake layers measure about 20 um (with a corresponding back pressure of 600 mbar, absolutely unrealistic). (102)

From here the need to distinguish at least two different configurations of soot/catalyst contact and, consequently, of TPC types:

- **Tight contact**: obtained by mixing 45 mg of catalyst with 5 mg of soot and 100 mg of inert silica inside a ball mill for 15 minutes at 50 rpm. It measures the intrinsic oxidative power of the catalyst.
- **Loose contact**: the same mixture but gently mixed by hand with a spatula for 1 minute. It simulated the real conditions of a DPF and gives information about the real performances of the catalyst. Neeft et al. proved that the soot-catalyst contact in a DPF is as loose as that of powder mixed by hand with spatula (113).

So, the ratio catalyst/soot is 9:1, the heating temperature program is from room to 750 °C at 5°/min and the feed is a mixture of oxygen at 10% in nitrogen at 100 Nml/h.

All the mixtures have been made using Printex-U, by Degussa, as reference synthetic soot.

2.2 Designed morphologies

2.2.1 Nanofibers

A first proposal of improved morphology for ceria-based catalyst has been the fibrous shape (102). The aim of this designed morphology was to create a web able to embrace the soot particles so tightly to increase the number of contact points, that are the points from where the combustion ignites (Figure 76).

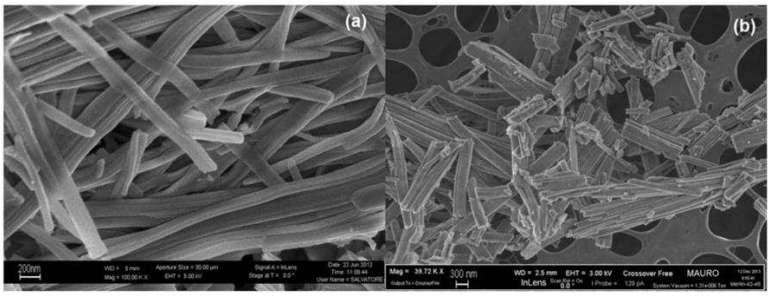

Figure 74 FESEM images of the CeO2 nanofibers at × 100,000 (a) × 40,000 (b) level of magnifications (114)

This approach should be way more efficient than classic SCS ceria, which uncontrolled morphology (see Figure 75) and coarse sizes do not allow so many contact points. The prolonged process of synthesis of ceria nanofibers does not allow to achieve high specific surface areas but the performances of nanofibers versus SCS ceria, measured in TPC analysis, showed that nanofibers do actually decrease the peak temperature of CO_2 conversion in comparison to SCS catalyst. This was a first proof that enhancing the number and quality of contact points is more effective and significant than surface area in solid/solid catalysis.

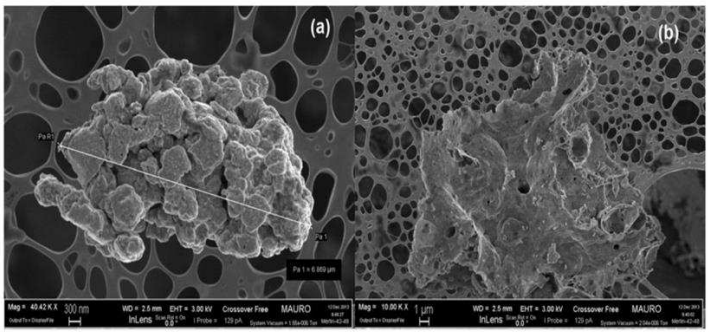

Figure 75 FESEM images of SCS ceria nanopowders at 40000x (a) and 10000x (b) level of magnification (114)

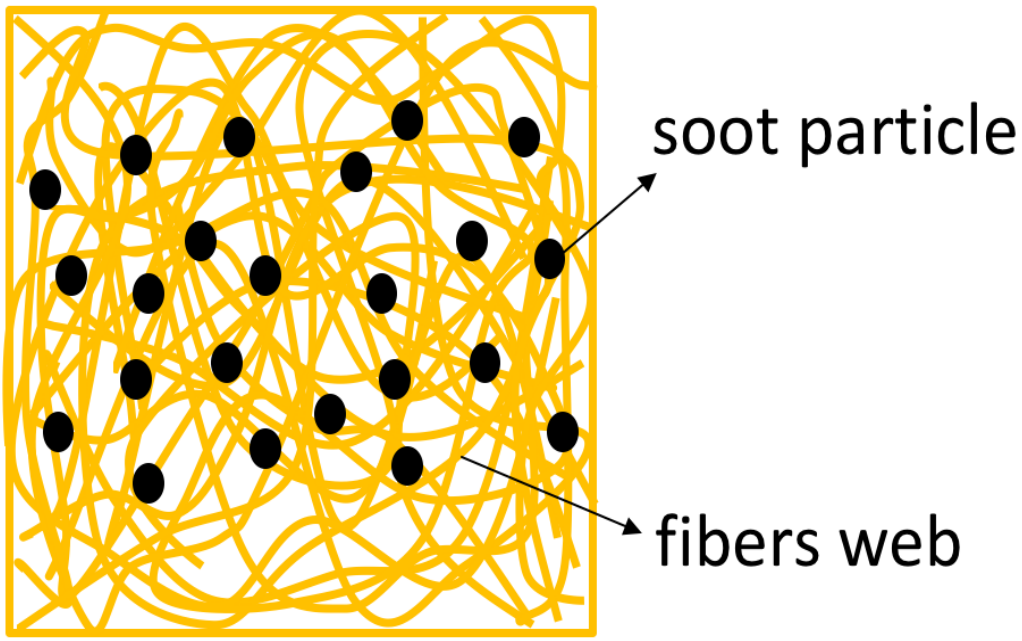

Figure 76 Schematic representation of how ceria nanofibers should work

Just as comparison, the method of synthesis of these two first morphologies, literally from Miceli et al., 2014 (114):

The CeO_2 nanofibers were synthesized by means of the precipitation/ripening method (115)*: starting from a 1 M aqueous solution of cerium (III) nitrate hexahydrate precursor (Sigma-Aldrich, St. Louis, MO, USA, 99%), the fibers were synthesized using a rotary evaporator and varying the NaOH/citric acid molar ratio. The residence time and conditions inside the evaporator led to different morphologies. A clear fibrous structure was obtained for a ratio of 0.8 at a constant temperature of 60°C for 6 h. One-hour drying at 110°C and calcination for 5 h in air at 600°C were performed. These processes did not cause the fibrous structure to collapse after the thermal treatment.*

The SCS was also used for the ceria catalyst preparation (112) *in order to compare the foamy catalyst obtained with this technique with the above- mentioned alternative morphologies. In the SCS technique, a homogeneous aqueous solution of metal nitrates and urea is placed in an oven set at a constant temperature of 650°C. The solution quickly begins to boil and froth, and ignition then takes place.*

The exothermic reaction, due to urea combustion, provides the heat necessary for the endothermic transformation of nitrates into the desired oxide. The whole process is over in a few minutes, and the result is a foam that crumbles easily. In this case, the size and shape of the CeO_2 structures were not tunable as in the other two cases, although a foamy structure and a moderate SSA were easily reached.

2.2.2 Self-assembled stars

Thinking at the real application, the loose contact conditions in a real-scale DPF and the sizes of catalytic layer and soot cake layer, it comes in mind that probably beside developing the catalyst powders it could have been a good idea to improve the performances of the entire catalytic layer as well.

From here the idea of designing a new catalyst with the following characteristics:

- Ceria-based: cheap and with redox capabilities
- Nano-structured: enhanced surface reactivity
- Micrometric size: comparable to soot cake size
- Medium-high specific surface area: improves the oxygen pump
- 3D shape: Good grip, tiling or coating capabilities

When the morphology is flat-like or the size of the catalyst is very small, such as nanofibers, the resulting catalytic layer is a two-dimensional flat bed (Figure 77), on which the soot oxidation undergoes to a slow FIFO procedure (first in, first out): the very first soot layer deposited on the catalytic bed will be *oxidized catalytically*, leaving space to the upper soot stratum and so on.

Figure 77 Tiling capabilities of a 3D shape (left) and a 2D shape (right). For nanoscaled elements, the resulting layer will be 2D however.

But about to invert these characteristics? What happens when the catalyst has bigger sizes? Or when it has a three-dimensional shape? Would the resulting coating get some benefits or gain better performances?

To find an answer to each of these doubts, a new ceria-based catalyst has been used for soot-abatement applications: the self-assembled star (116).

The particular morphology does fulfil all the characteristics desired in the previous paragraphs. Ceria Self-assembled Stars (SAS) are cheaply obtained via hydrothermal synthesis in particular reactors, which allow to control their structure at a nanoscale level; their final size can be tuned from hundreds of nanometers up to micrometers; their shape is a three-dimensional star, improving the grip with the SiC substrate and the tortuosity of the coating itself; BET area (specific surface area) is way higher than ceria SCS and nanofibers, promising a better oxygen pump and maybe good performances even in heterogeneous catalysis.

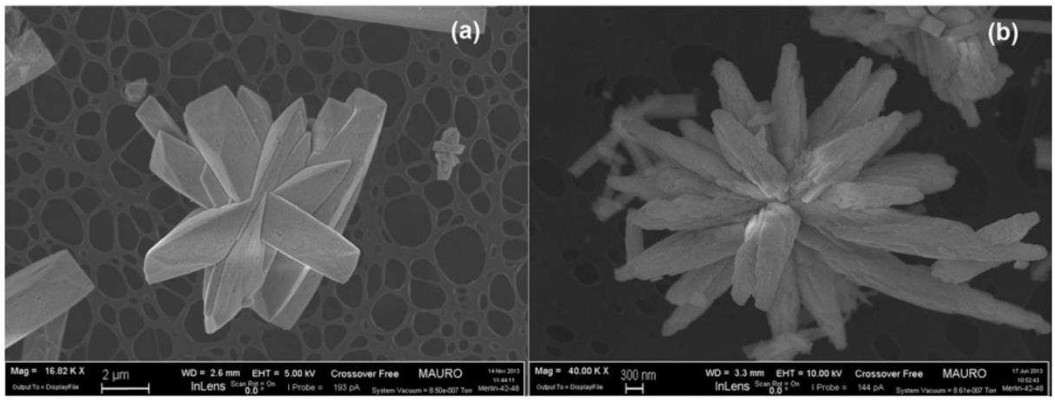

Figure 78 FESEM images of the CeO2 SA-stars at 12 h (b) and 24 h (a) different residence times (114)

The method of synthesis of these self-assembled stars is, literally from Miceli et al., 2015 (114):

The CeO_2 self-assembled stars were prepared by mixing 0.2 M of cerium (III) chloride heptahydrate, 0.01 M of CTAB (both from Sigma-Aldrich) aqueous solutions and 80 mmol of solid urea. A hydrothermal treatment at 120°C for 12 to 24 h led to a precipitate, which was centrifuged, rinsed, filtered, dried at 60°C for 24 h and finally calcined at 600°C for 4 h (116). *The residence time inside the reactor in hydrothermal conditions affects the size and shape of these systems, […].*

They are denominated *self-assembled* because the particular starred shape is obtained spontaneously during the hydrothermal synthesis, with the help of CTAB dispersant. The tendency of ceria rods to agglomerate in parallel rows is visible also

for nanofibers but the 3D morphology is achieved only for bigger rods sizes and with the presence of a specific amount of dispersant.

The controlled speed of dropping of the two precursor solutions, the use of a dispersant and the ramped thermal treatment, which is milder with respect to the thermal treatments of SCS and nanofibers, allow to obtain a very thin crystallite, a crucial aspect that will be later discussed in this chapter (Table 8).

However, ageing thermal treatment consisted in 5 hours in air in a furnace at 600 °C and it is a standard method for all the catalysts of this study.

2.2.3 Comparisons between coarse and engineered morphologies

XRD: X-Ray Diffractometry

Well, the very first move after synthetizing a catalyst is to check the phase of the resulting powder; XRD is the perfect instrument and as the goal is, independently from the morphology, aiming to a cubic fluorite structure for these ceria-based materials, since this configuration indicates the correct type of oxide (CeO_2, *Fm-3m* spatial group). Not just the phases can be detected via XRD, but also accurate investigations about the grains size, somehow related to the quality of the method of synthesis in case of nanostructured materials.

Table 8 Crystallite sizes of catalysts calculated with Debye-Scherrer method via XRD. Crystallites are the smallest coherent crystallographic domain and cannot be evaluated with microscopy techniques.

Crystallite size	SCS	Nanofibers	SAS	Aged SAS
min	24	10	2	4
max	55	100	10	23
avg	45	72	9	15

Crystallites size has been calculated using the Debye-Scherrer formula after XRD analysis. Because the number of coherent crystallographic domains (crystallites) influences the response to X-rays Diffraction (XRD signal), a higher number of crystallites would start appearing on the spectra before and after the characteristic peak, that is that the so called FWHM (Full Width Half Maximum) of a XRD peak is higher for finer structures (finer, not smaller). The more it goes in nanometric scale, the larger the XRD peaks. XRD diffractograms depicted in Figure 79 clearly confirm the conclusions of the crystallites size analysis, in fact the SAS spectrum has wider peaks than the other two. The slightly fuzzy curve is only due to a combination of noise and instrument resolution.

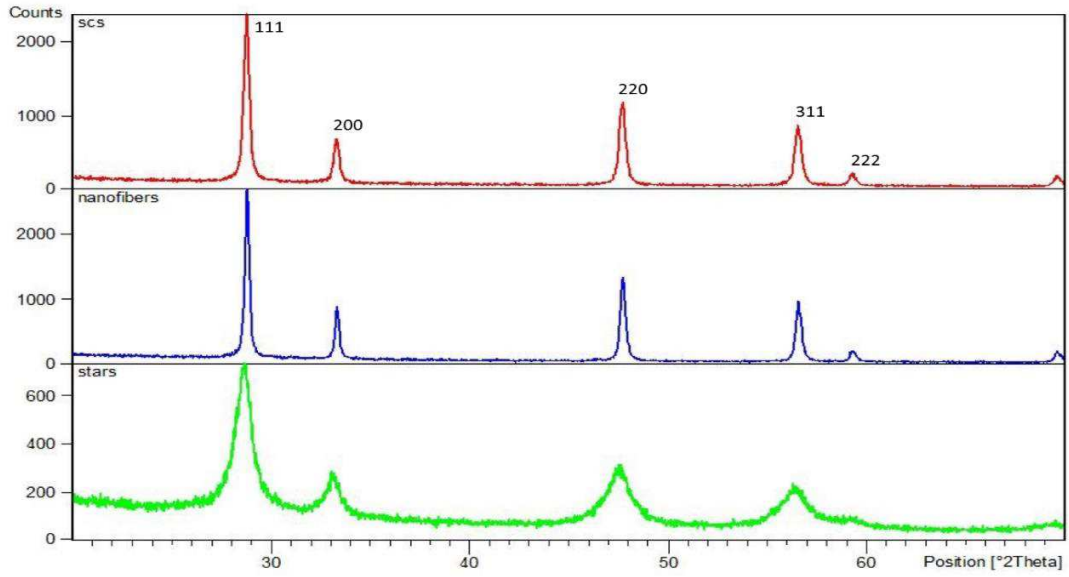

Figure 79 XRD diffractograms of SCS, Nanofibers and Self-assembled Stars. Diffractograms are comparable to standard CAS 34-0394, space group $Fm\bar{3}m$ (fluorite).

As already reported, in solid/solid catalysis the quality and number of contact points is more important than what specific surface area is in heterogenous catalysis. Nevertheless, for a redox capable catalysts like the ceria-based ones, a good surface area could allow a better oxygen mobility, with fast and effective give and recharge. SAS have a surface area orders of magnitude higher than SCS and nanofibers (Table 9)[10].

Table 9 Specific surface area list of ceria-based catalysts (m^2/g), obtained via BET analysis (99) (114)

Catalyst	fresh	aged
SCS	29	13
Nanofibers	4	1
SAS	124	64

[10] This characteristic opens a chance for a better NOx-assisted soot combustion, since this approach merges homogeneous and heterogeneous catalysis and requires both good contact and good surface area.

BET: Specific Surface Area

Together with the measurement of the specific surface area, with the same BET machine also a porosimetry has been conducted, to add information to the morphology characterization of these catalysts (Figure 80). For each hysteresis, the lower curve is referred to the adsorption phase, the upper to the desorption. The particular shape for which, at a certain step, the discharging has a sort of delay, resulting in a step, indicated that the pores of those materials are bottleneck shaped. A deep explanation below, literally from Miceli et al., 2015 (99):

In particular, a type IV classification of the adsorption isotherms (according to the IUPAC (117)*) can be assigned: the predominance of slit shaped pores can be inferred from the hysteresis of the adsorption–desorption curves, the SCS belonging to the H3 type while the SA stars of the H4 one. H3 looping type of SCS powders is characterized by no microporosity, but just mesoporosity (the average pore size being 80.9 Å). Conversely, H4 type attributed to the SA stars is ascribed to the presence of a certain microporous volume, distributed in narrow slit pores. This is confirmed by the pores' size estimation, the average value being 28.5 Å for the SA stars. Finally, the aged SA stars have lost 1/4th of their microporous volume, as can be seen from the lower amount gas adsorbed at low p/p0 (see also Table 10); however, it maintained its mesoporous volume, due to the same shape of the hysteresis curves with respect to the fresh sample. This microporous loss is greatly responsible for the SSA drop, given the high contribution that micropores give in the total specific surface of the catalyst.*

The average pore size for the aged SA stars was 29.2 Å; therefore, most of microporosity was lost as inner porosity, while the average pore opening size was retained.

An higher SSA entails a higher oxygen adsorption and availability for the soot oxidation reaction: in particular, the porosimetry of SA stars shows that this porosity was available at low partial pressures of N_2 (Figure 80), in contrast to the behavior of the SCS catalyst, which is an indication of a better surface exploitation of SA stars.

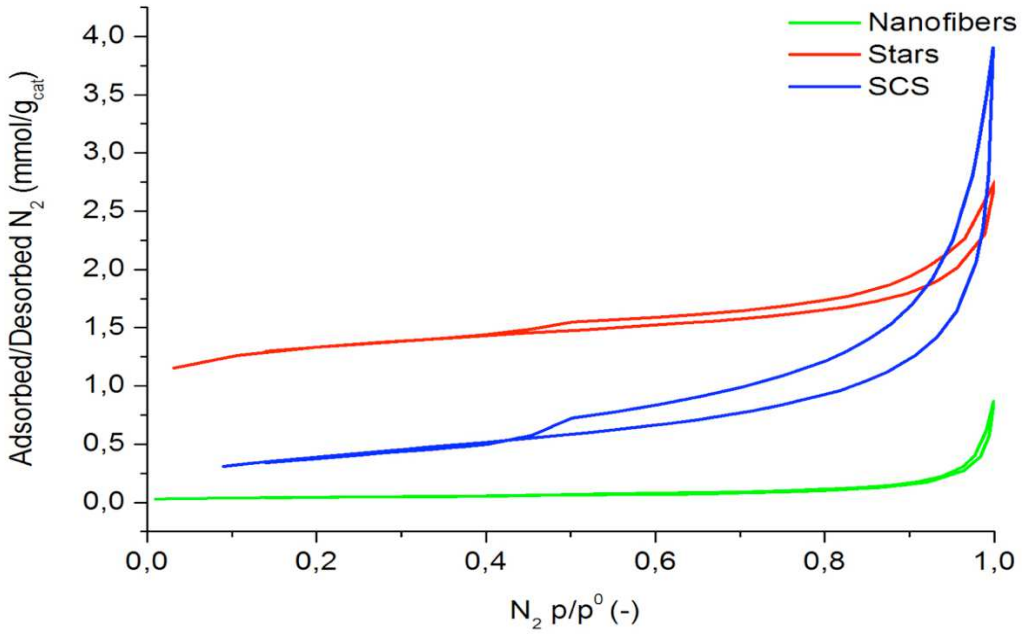

Figure 80 Porosimetry of SCS, nanofibers and SAS fresh catalysts. Hysteresis indicates bottleneck shaped macropores for these materials. For automotive application, the most relevant area of the plot is at low partial pressures (left).

Table 10 Comparison of porous and microporous volume of SCS and SAS plus average porous sizes (fresh and aged)

Catalyst	Porous Volume (cm^3/g)	Microporous Volume (cm^3/g)	Average Size (Å)
SCS	0,052	0	80,9
Aged SCS	0,033	0	82,3
SAS	0,079	0,040	28,5
Aged SAS	0,048	0,029	29,2

FESEM: Scanning Microscopy

Usually, the basic characterization of a catalyst consists of BET measurements (for Specific Surface Area) and TPE (Temperature Programmed Experiments). In this case, prior of the basic set of analysis, microscopy is essential in order to be sure of having achieved the desired morphology. SEM/FESEM instruments have been used to check the powder resulting from each synthesis as far as shape, size, atomic composition and coating capabilities are concerned.

Following a collection of pictures of the aforementioned SCS, nanofibers and SAS ceria-based catalysts.

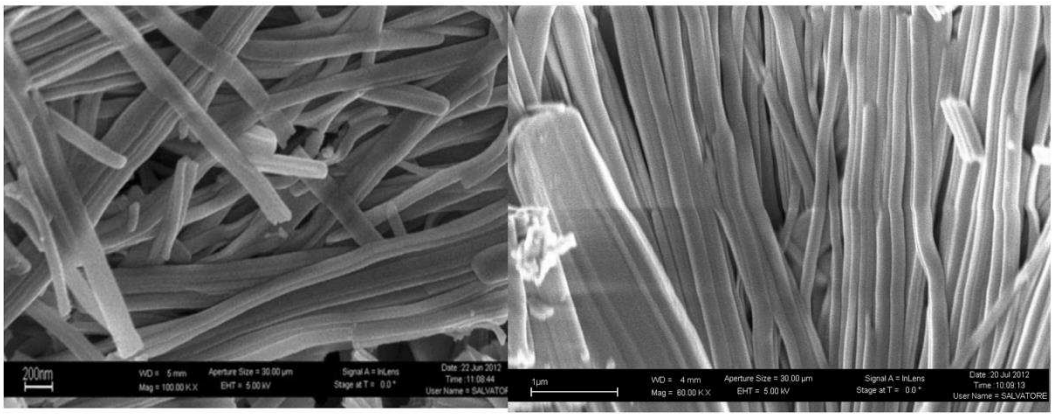

Figure 81 Ceria nanofibers at FESEM. The diameter of the single fiber is nanometrical and the desired web does appear in the pictures, nevertheless nanofibers tend to agglomerate in bunches (102)

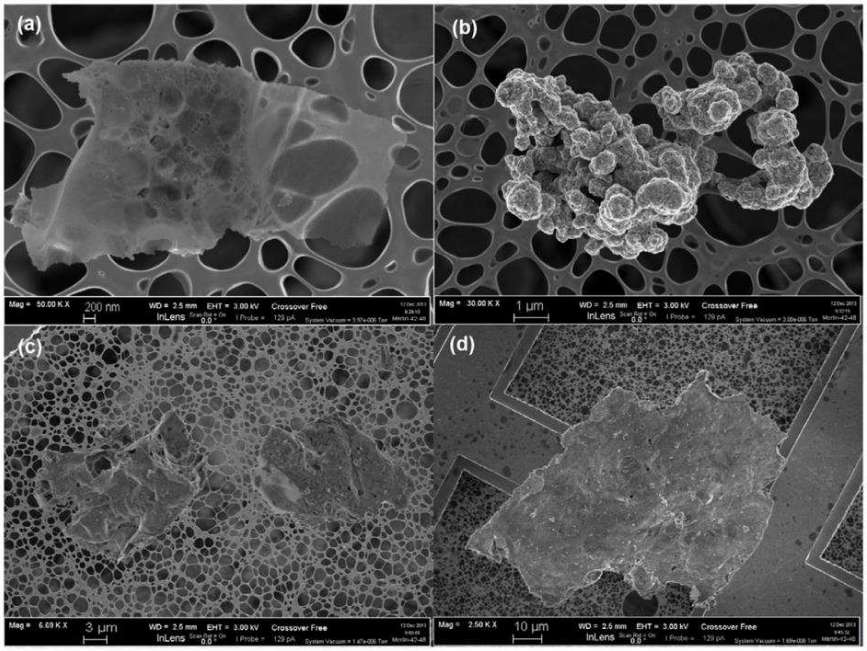

Figure 82 SEM images SCS powders. Morphologies obtainable with SCS technique are uncontrollable and unpredictable. Size distribution: (a) sub-micrometric to (b–d) micrometric (b–d) particles; shape distribution: flat (a, c, d) and aggregate-wise (b) particles. (99)

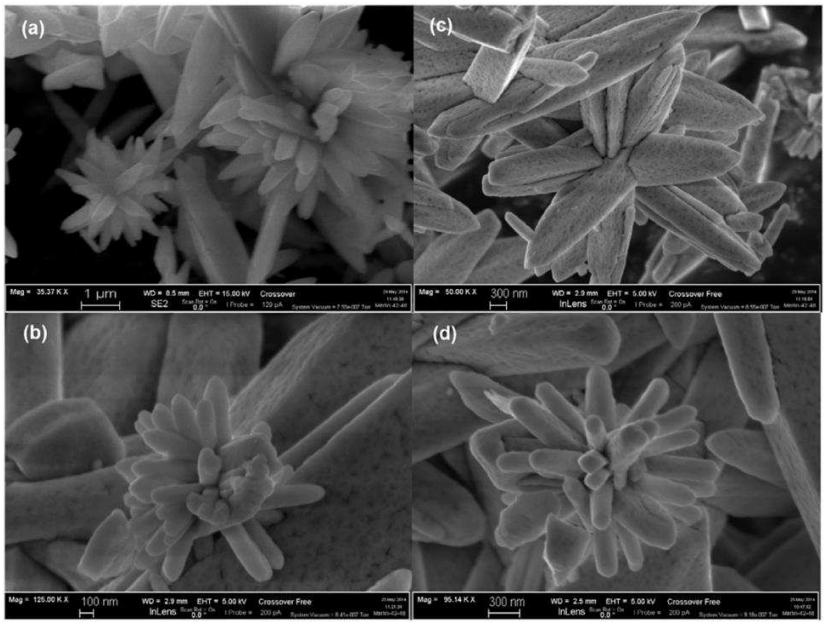

Figure 83 SEM images of SA stars. Size distribution: (a–b) micrometric and (c-d) sub-micrometric particles (99). Sizes depends on synthesis condition like time, temperature and CTAB concentrations.

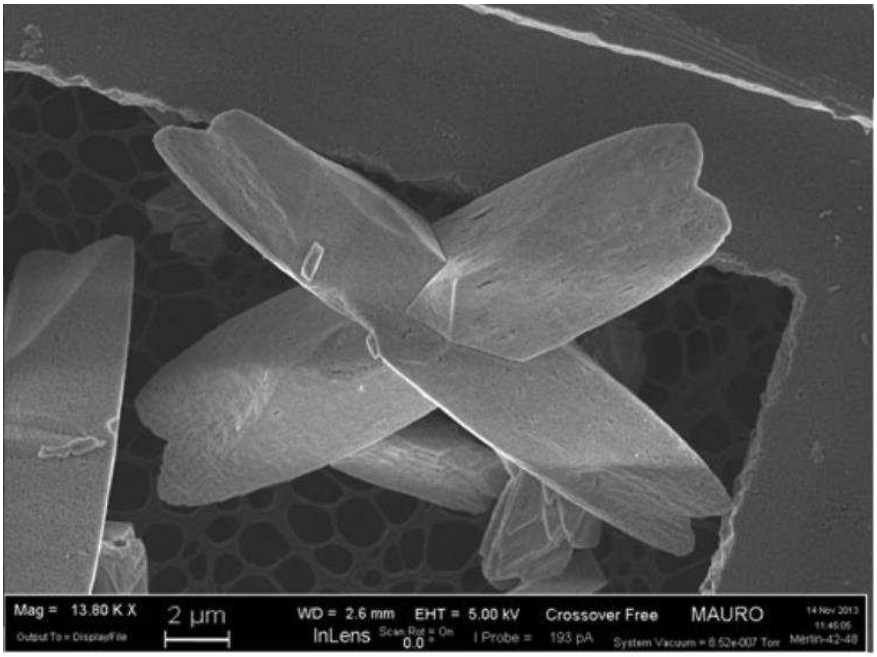

Figure 84 SAS at FESEM. Sometimes, the 3D stars break down into 2D shapes but the wrecked structure is somehow still able to stand up and get stuck with the others, so forming a 3D catalytic layer anyway.

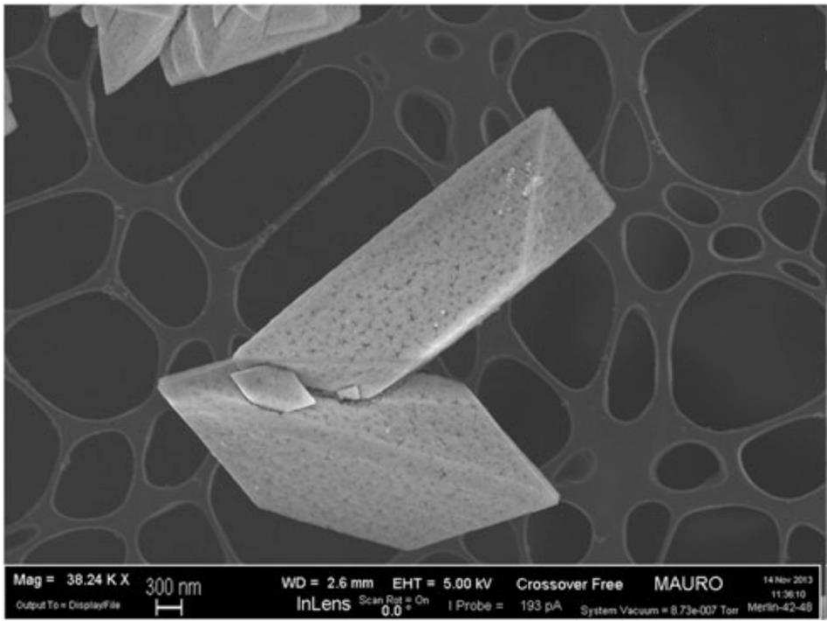

Figure 85 SAS at FESEM. Precise geometries from the hydrothermal synthesis. The crack come up after the particular ageing treatment and maybe responsible of the higher surface area of these catalysts (114)

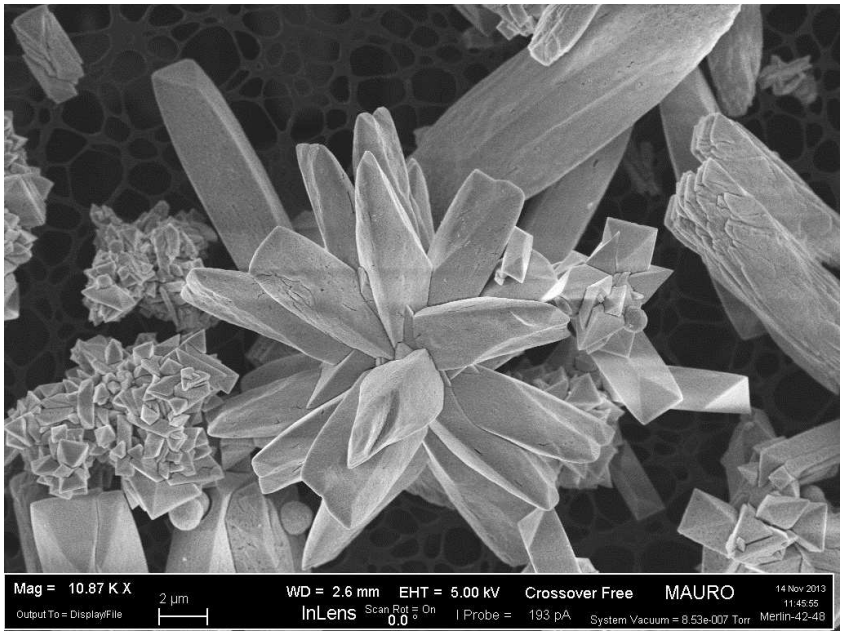

Figure 86 SAS at FESEM. In the picture are ensemble: stars, building rods and small nuclei. Not all the nuclei are able to grow and display the starred micrometrical shape.

TPC: Soot Combustion Capability

When the basic characterization of the powder is completed and all the desired morphologies have been achieved, it is possible to rank their performances via TPC (Temperature Programmed Combustion).

The samples are prepared according to the contact types descripted in the previous paragraphs, tight and loose, and the test is led in a furnace heated at 5°/min up to 750 °C using a 100Nml/min flow of 10% oxygen in nitrogen.

A blank run with just soot into the U-tube quartz reactor is run at the very beginning to set a reference. This kind of test and test rig are extremely sensitive to the operating conditions and, generally, a soot-only blank run is done at every modification of the setup (including the operator).

From Miceli et al., 2014 (114), literally:

The peak temperature, Tp, in the TPC plot of the outlet CO_2 concentration was taken as an index of the catalytic activity. The onset ($T_{10\%}$) combustion temperature, defined as the temperature at which 10% of the initial soot is converted, was also

considered in order to better discriminate between the intrinsic catalytic activities of the prepared catalysts. The half conversion temperature ($T_{50\%}$) was also taken into account. The onset temperature is important to rank the catalysts, according to the catalytic reaction; other phenomena (such as mass transfer or diffusion limitations) may in fact influence the performances of catalysts at higher conversion stages.

All the tests have been repeated three times and the entire test rig is depicted in Figure 72.

The very first thing that comes up from the TPC plots (Figure 88, Figure 89) is the CO_2 emission peak at low temperature of the SAS curves. Low temperature CO2 peak isn't «soot-related» but only a desorption from the high nanoporosity of the SAS. To prove that, we did consecutive TPD/TPO runs (Figure 87):

TPD1: fresh catalyst, heated till 200°C in N_2. We have the CO_2 desorption peak.

TPD2: same catalyst after cooling in N_2. We heated it again in N_2 to 200°C and nothing happened.

TPO3: after cooling in N_2 we let air flow in the reactor and the CO_2 signal started to grow to reach the normal CO_2 concentration in air. At 140°C we can see a higher level of CO_2 and that's because SAS are supplying their adsorpted CO_2, causing a boost in CO_2 emissions.

Again: the SAS low-temperature peak is not catalytic; it is just desorption of CO_2 physisorbed onto ceria surface. Probably, high surface area and nanostructured ceria structures do accommodate their surfaces with CO_2.

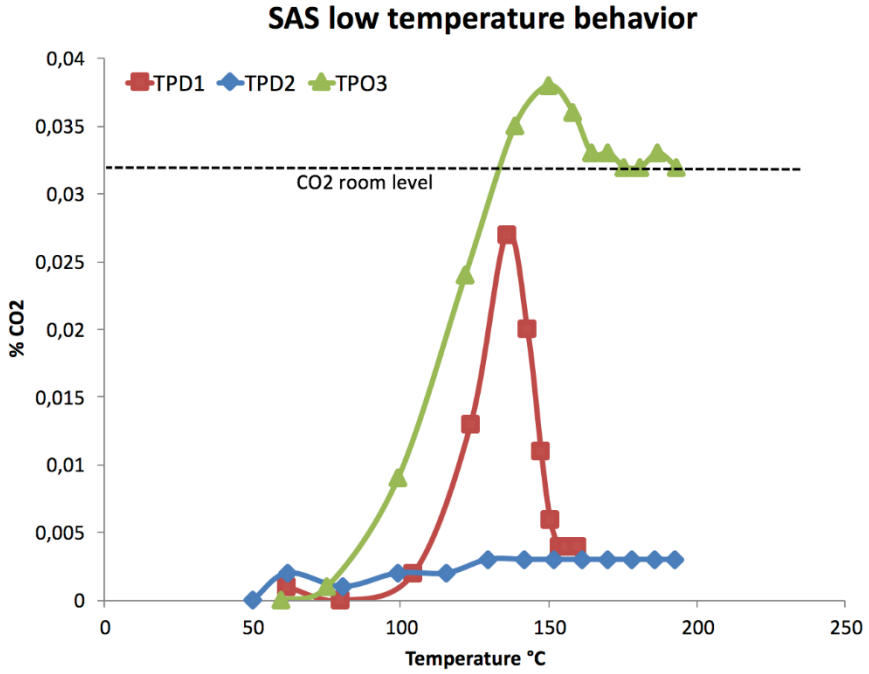

Figure 87 A combo test to check if the low temperature CO2 emission by SAS is catalytic or not

In these combustion experiments SAS showed superior performances, compared to ceria nanofibers and traditional SCS ceria powders, in lowering the soot combustion characteristic peaks' temperatures.

In tight contact conditions (Figure 88), aged SAS are even better than fresh nanofibers, somehow proving that going into nanotechnology is not always a matter of sizes. However, T10% and T50% of SAS and SCS are comparable despite the T10% of SAS in tight contact are visibly lower and promising. Nanofibers try to perform better in loose contact mode (Figure 89) where they show similar behavior of SCS, with SAS still going better in fresh conditions.

What can be said about SAS is, however, that the performances could be better with a higher thermal resistance. At very high temperatures, and in aged conditions, SAS are not outstanding in lowering combustion temperatures. A further step in their development should be to stabilize the structure towards high temperatures, probably with a doping with Zr or combining SAS with two or more oxides, like Gd_2O_3, PrO_2, CuO and ZrO.

In Table 11 the results from TPC of the three catalysts can be found, listed by combining data from CO_2 emissions and CO_2 conversion plots.

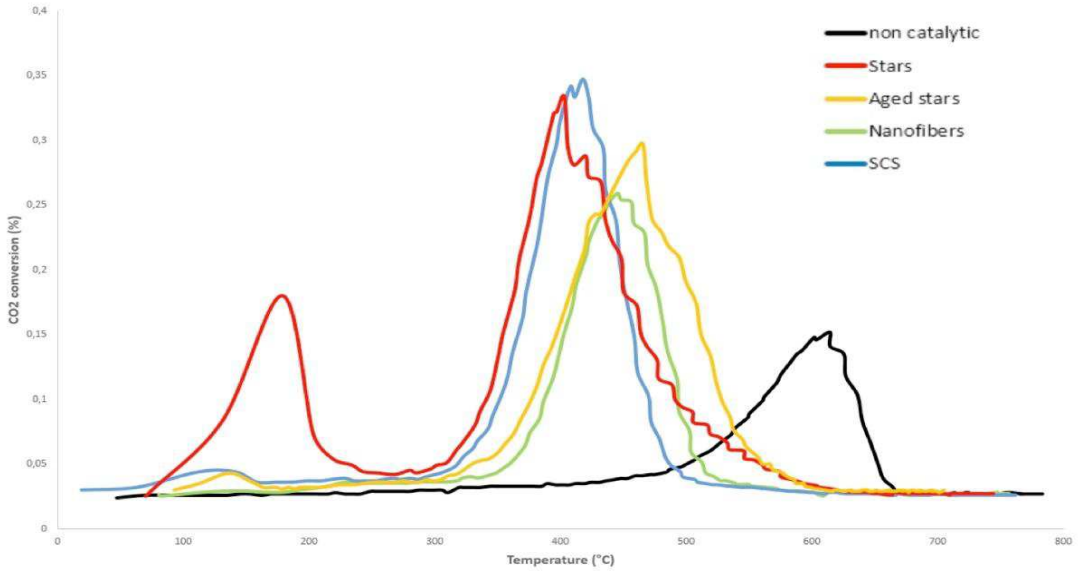

Figure 88 TPC curves in Tight Contact mode (114). Low-T peak is just desorption. Tight contact mode displays intrinsic catalytic capabilities of materials as the particles are intimately closed each other. However, it's unrealistic.

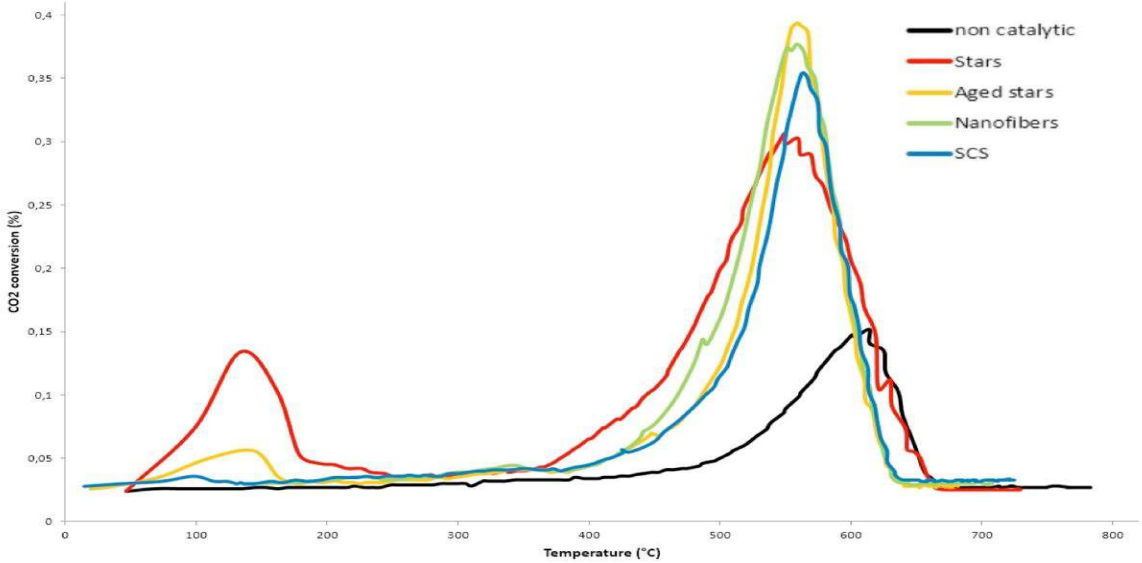

Figure 89 TPC curves in Loose contact mode (114). Low-T peak is just desorption. Loose contact reproduces the real-scale DPF conditions and it's useful to rank ultimate catalysts' performances.

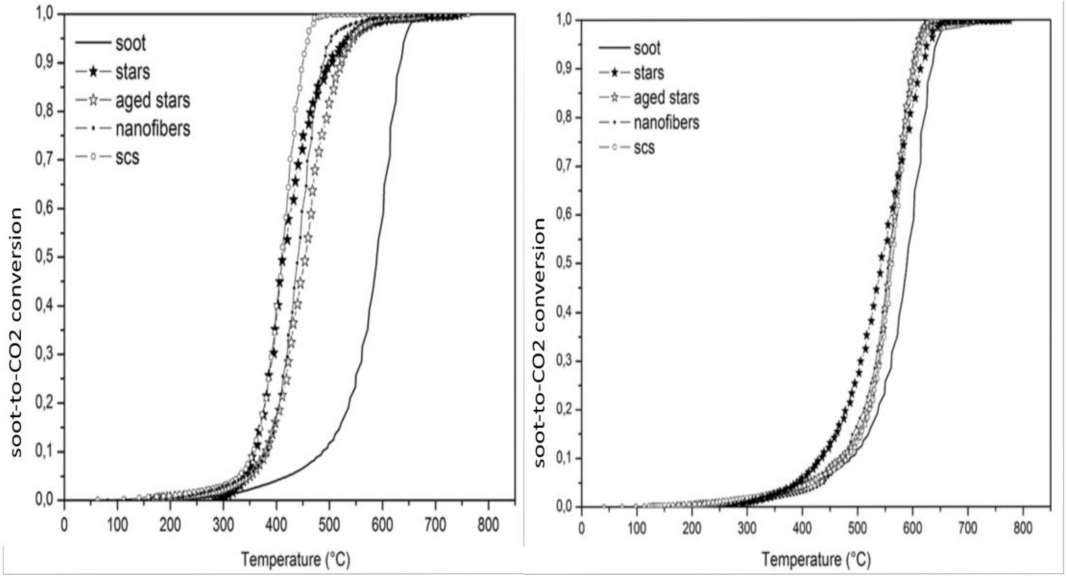

Figure 90 Soot-to-CO2 conversion curves from TPC tests. SAS show the best on-set at T10% and T50% but then thermal effects start degrading those structures and performances get down to standard SCS ceria. Left, tight mode. Right, loose mode (114).

Table 11 TPC performances of SCS, nanofibers and SAS ceria-based catalysts (114)

		$T_{10\%}$ (°C)	$T_{50\%}$ (°C)	T_p (°C)
Soot		487	588	614
Nanofibers	Tight	383	439	445
	Loose	480	555	560
SCS	Tight	358	411	417
	Loose	483	562	562
SA stars	Tight	354	410	403
	Loose	435	543	552
Aged SA stars	Tight	381	453	465
	Loose	473	559	559

After this first run of experiments and characterization, it followed the abandon of the development of ceria nanofibers, due to their tricky synthesis and poor performances compared to the arising self-assembled stars.

HRTEM: Transmission Microscopy

In order to investigate the particular surface reactivity of these catalysts, HRTEM (High Resolution Transmission Electron Microscopy) has been involved as instrumental analysis. Beside the suggestive and useful images, TEM analysis allows to undergo very small portion of material to a sort of XRD analysis, studying directly the planes of diffraction.

Massively, catalyst powder showed to be CeO_2, with cubic fluorite structures, $Fm\bar{3}m$ space group and CAS #340394 but, for very first nanometers of matter (on the surface) there could be different phases, maybe the reason of the different behavior of these morphologies.

It has been proved that some hydrothermal synthesis are able to spot out unstable lattice planes and, in particular for ceria, also to turn the cube into an octahedron (118). For SAS, this tendency can be noticed from Figure 85. HRTEM investigations are needed to understand whether the obtained SAS catalysts do expose more active ceria plains to soot oxidation, generally {310}, {100} and {110} for a cubic lattice, or even completely different structures (118) (119). These surfaces may be oxygen-defective and accommodated by adsorbed charge compensating species (like CO_2 itself), and oxygen vacancies bring more oxygen mobility and availability for soot oxidation (120).

Literally, from Miceli et al., 2015 (99):

HRTEM magnifications evidenced that, on the very surface of the catalysts, structures have a different nature from bulk. In particular, the TEM analysis of the surface grains and crystallites of SA stars (Figure 91) revealed that are oxygen defective, such as rhombohedral Ce_7O_{12}, monoclinic Ce_6O_{11} and cubic CeO_{2-x} (JCPDS Nos. 710567, 320196 and 491415, respectively) and this peculiarity may explain the high activity of SA stars towards soot combustion, later reported. Oxygen defects in fact, promote mobility by lattice vacancies from the bulk to surface and vice versa, enhancing redox cycles and oxidative power. During the TEM analysis of SCS powders (Figure 93), such peculiarity was not found; infact

SCS ceria fringes of diffraction indicate the occurrence of CeO_2 cubic structure planes, essentially in all the spots checked (JCPDS No. 340394).

Pictures about aged SA stars show that the intense thermal treatment promoted atomic diffusion and grain sintering: in particular, crystallites' boundaries move from an incoherent surface in fresh conditions (Figure 91 and Figure 94) to a semi-coherent surface condition (Figure 94) when the catalyst has undergone aging.

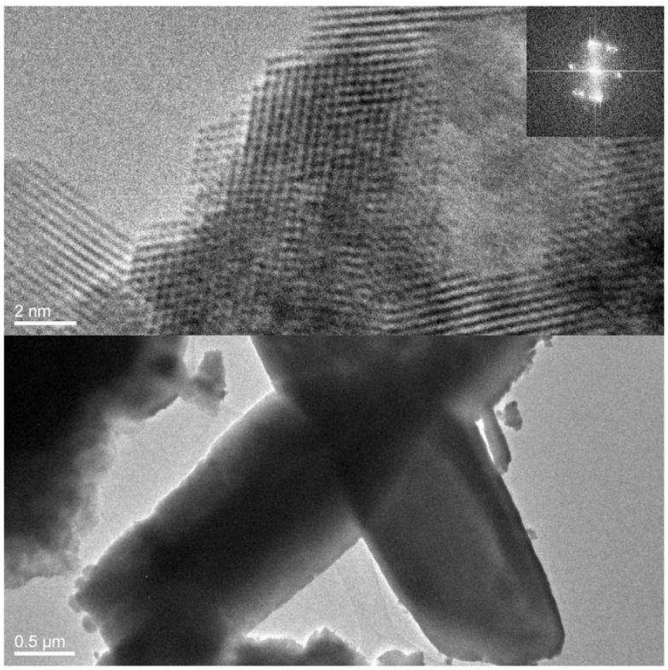

Figure 91 SAS at HRTEM. Low magnification below, high magnification above and diffraction pattern in top-right. In the upper section of this image (1000000x), it can be seen an example of mesoporous, reason for the high surface areas of these materials. (99)

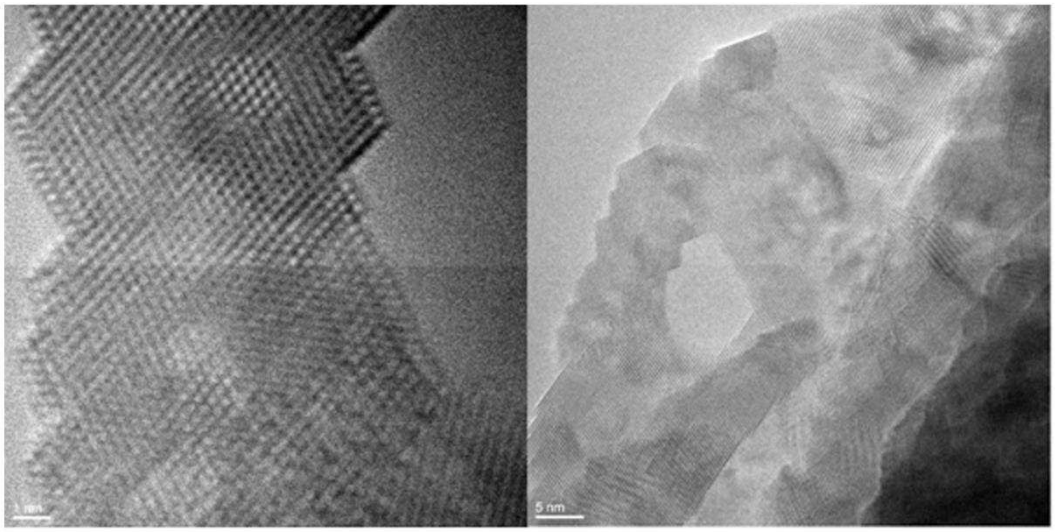

Figure 92 SAS at HRTEM. Again, other examples of mesopori at different magnifications. Left, 1.500.000x; Right, 800.000x. (99)

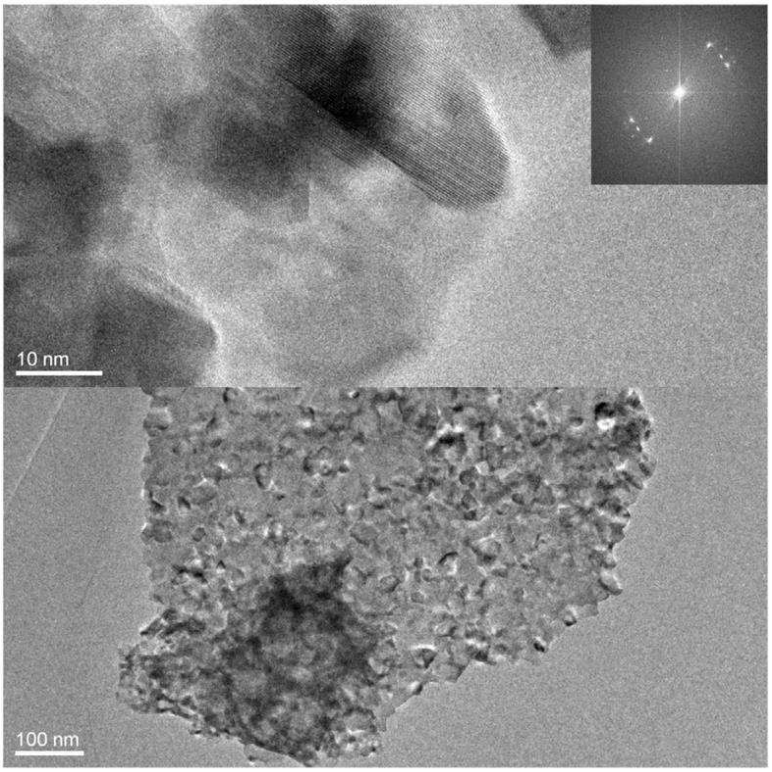

Figure 93 SCS at HRTEM. At low magnification, the fuzzy morphology of SCS materials is displayed also by ceria. In TEM mode, the irregular thickness makes it hard to see diffraction fringes (99)

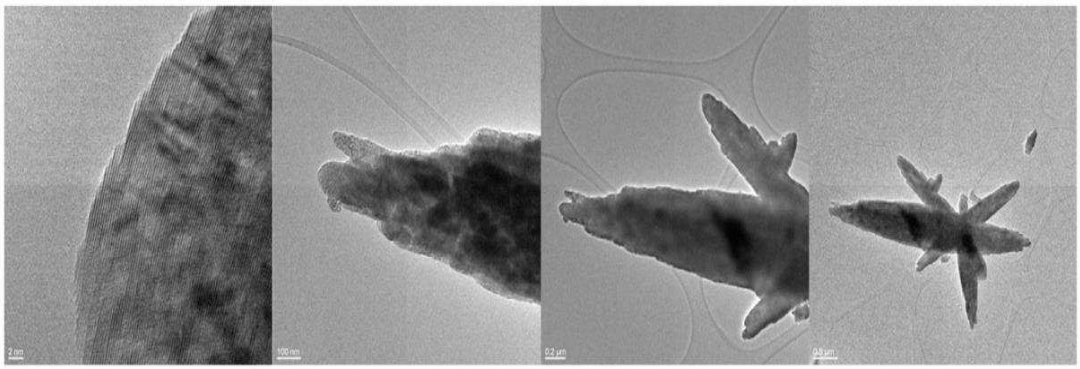

Figure 94 Aged SAS at HRTEM. In the highest magnification image, it can be seen the crystallographic planes somehow melted and smooth, as a sort of sintering occurring. Incremental zoom; right to left: 4000x , 8000x , 20,000x and 600,000x (99)

So, it seems that SAS do have oxygen defective structures on their surfaces, which can promote oxygen mobility (improving the so called "oxygen pump") or that it need a different surface accommodation (increasing C/CO/CO_2 affinity). Both these options could explain the better TPC performances of SAS compared to ceria nanofibers and SCS powder and they are probably also the reason of the SAS bad performances at high temperatures. Thermal ageing means sintering, and so modifying, these tiny and particular lattice planes, which are maybe responsible of a higher soot-combustion activity.

XPS

Cerium Oxide (IV) is a redox capable material and with XPS surface analysis the ratio between Ce^{3+} (Ce3d5/2) and Ce^{4+} (Ce3d3/2) can be revealed, as a quantitative analysis of oxygen states available on the surface of the catalysts (121). Ce^{3+} is the oxidation state of Ce_2O_3 while Ce^{4+} is the one as in CeO_2.

High Resolution spectra have been harvested for O1s and C3d (in the range 870– 930 eV) and of course for C1s, used as shifting reference for calibration (122). Lately, the spectra have been deconvoluted to distinguish between the two different cerium oxidation states.

Literally, from Miceli et al., 2015 (99):

A comparison of the three spectra reveals that all peaks essentially overlap, and for this reason was not worth being reported here. Table 3 reports the related quantitative analysis, and it can be noticed that cerium states and availability for all samples has no difference at all; in fact, the Ce4+/Ce3+ ratio was 1.85, 1.77 and 1.79 for fresh SA stars, aged stars and SCS powder respectively. The main difference was actually unveiled by O1s quantitative analysis: O1s, in this case, presents two peaks (as showed in Fig. 10): the first at lower binding energy relative to bulk oxygen, and the second corresponding to surface oxygen (122). *Fresh stars on the other side, seem to have a greater oxygen presence on its surface, actually about 30% more than the other two catalysts. This allows stars to manifest a higher catalytic activity, […]. The XPS investigation on surface oxygen conditions also indicates that aged stars and fresh SCS powder two materials have almost the same surface oxygen availability.*

Summarizing, the amount of CeO_2 on the surface is higher in SAS than SCS and nanofibers which reflects of course a higher quota of surface oxygen. Quite obvious comparing Ce_2O_3 versus Ce_2O_4 structures. Not so obvious when remembering that all the three catalysts were namely CeO_2 (Ce_2O_4). However, the oxygen content of SAS is generally greater and may enhance the oxidative power of this catalyst.

All the results from the deconvolution of the curves and the recognition of each oxidation states are summed up in Table 12.

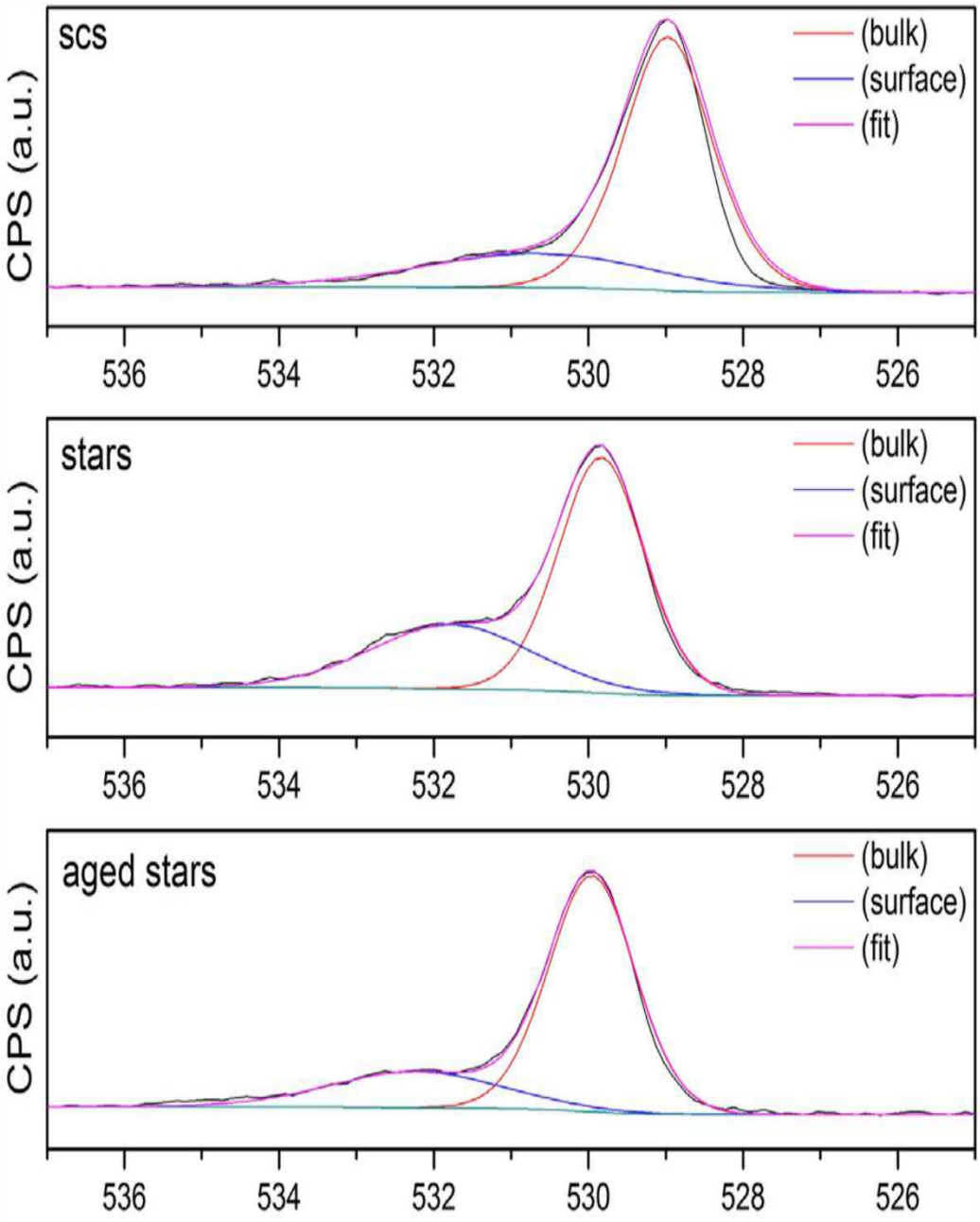

Figure 95 XPS spectra of O1s, with fitting curve and deconvoluted peaks (99)

Table 12 Quantitative analysis of XPS spectra after curves deconvolution (99)

O1s			Ce3d		
eV	%at		eV	% at	
SA stars					
529,83	66,12	Bulk	881,53	29,22	4+
531,77	33,88	Surface	897,63	17	4+
			900,13	11,7	3+
			915,93	11,95	3+
			884,88	13,27	4+
			902,74	7,11	4+
			888,1	5,23	3+
			906,6	4,52	3+
Aged SA stars					
529,96	76,71	Bulk	881,68	23,62	4+
532,22	23,29	Surface	897,68	21,27	4+
			900,19	7,78	3+
			915,94	14,26	3+
			887,97	10,78	4+
			884,27	8,17	4+
			906,65	8,35	3+
			902,08	5,78	3+
SCS powders					
528,97	74,7	Bulk	881,67	28,22	4+
530,67	25,7	Surface	897,67	17,67	4+
			900,17	10,73	3+
			916,06	11,63	3+
			884,81	8,64	4+
			888,27	9,71	4+
			902,54	7,97	3+
			906,76	5,43	3+

2.2.4 Nanocubes and further designs

With the ceria nanofibers out of this contest and the proposal of nanostructured ceria stars, the development of new and better ceria-based however continued, but with more awareness about those aspects which really improve the performances of these catalysts towards soot combustion: surface reactivity hence quality of contact points.

With this in mind, another designed morphology has been proposed, in place of nanofibers in the catalysts study: ceria nanocubes.

Literally, from Piumetti et al., 2016 (123):

[…] ceria nanocubes (denoted as "Ce-NC") were prepared via the hydrothermal method: proper amounts of NaOH (24g) and Ce(NO3)3·6H2O (2.2g) were dissolved in 35mL and 5mL of bi-distilled water, respectively. The two solutions were then mixed together and stirred for 1 h to obtain a milky slurry. The final mixture was transferred to an autoclave (150 mL) and then aged at 165 ◦C for 24 h. The fresh precipitate was washed and dried at 60 ◦C overnight. Finally, the powder was calcined at 550 ◦C for 4 h.

The prolonged and still hydrothermal synthesis push towards the most stable solid configuration for ceria, which having a cubic lattice tends to build up as a cube. As one can see in Figure 96, the resulting cubes'size is only few nanometers and since they agglomerate in thick hard grains, resulting micrometrical as the other two morphologies. NC agglomerates were so hard and compact that 10min at 20 rad/s in a ball-mill with three agate balls was needed to obtain powders as fine as the other catalysts.

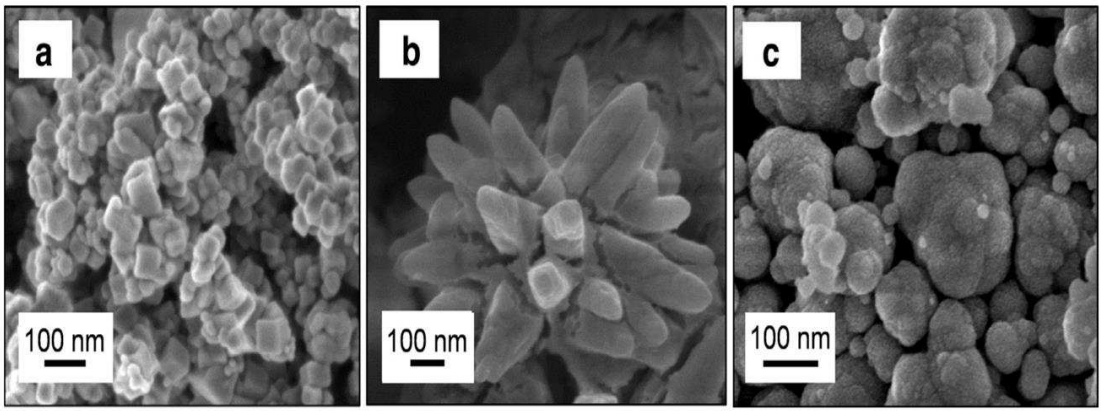

Figure 96 Direct shapes comparison: (a) nanocubes (b) self-assembled stars and (c) scs ceria catalysts at FESEM (123)

At HRTEM (Figure 97), ceria nanocubes showed to have an abundance of highly reactive (100) and (110) surfaces.

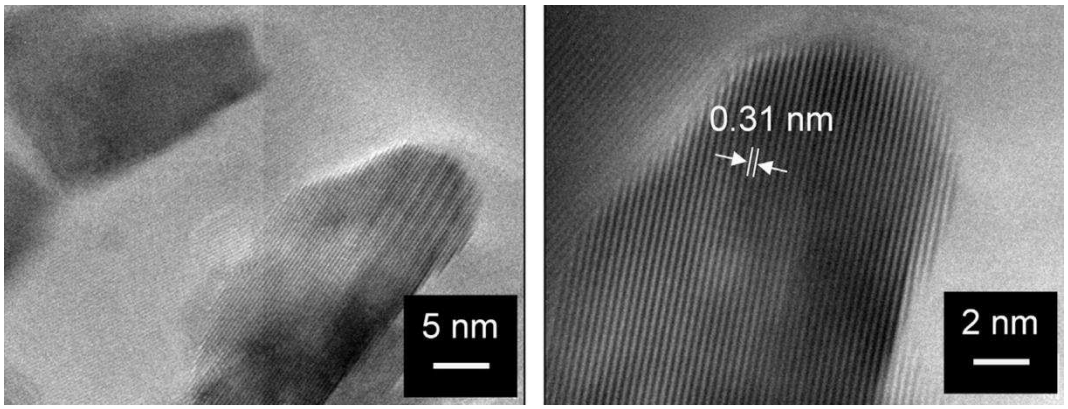

Figure 97 Ceria-NC (nanocubes) at HRTEM. At higher magnification (800000x) distance between planes can be evaluated. (123)

The results from BET and XRD (Table 13) confirm that the properties of ceria nanocubes are intermediate between SCS ceria and SAS.

Table 13 Comparison of basic characteristics of SCS, SAS and NC ceria-based catalyst

Catalyst	Porous Volume (cm^3/g)	S_{BET} (m^2/g)	Crystallite Size (nm)
SCS	0,052	72	30
NC	0,01	4	54
SAS	0,079	124	10

A new way of investigating catalytic soot-combustion is offered by the introduction of a thermal stage for optical microscopes (Figure 98). It is essentially a sealed chamber with a quartz view on top, platinum heaters under the stage holder and ports for gas circulation and it can be installed under a traditional optical microscope with ease. By programming the heaters with proper ramps and regulating the gas flow in order to reproduce the conditions as in the TPC tests, it is possible to capture in time-lapse the catalytic combustion of soot, if the sample is a solid mixture of catalyst and particulate matter, as example.

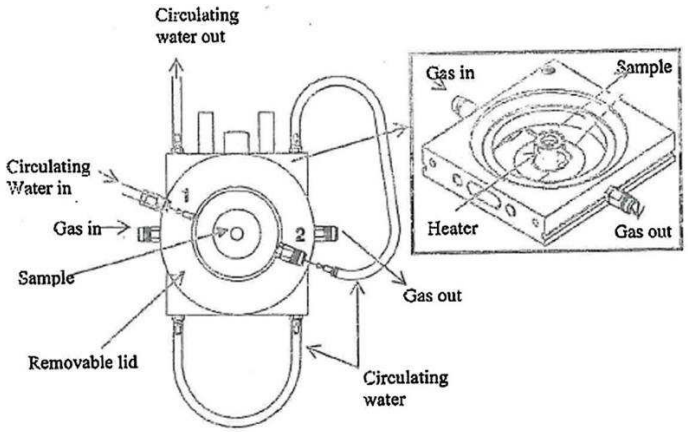

Figure 98 Linkam Stage TS1500 has been used to capture time-lapse pictures of soot and catalyst in live action (123)

In this paragraph, *SCS ceria* catalyst may also be called *Ceria-ND*, where *ND* stands for “nitrate decomposition”.

In Figure 99 the output of this particular investigation shows in a very suggestive way the disappearing of soot agglomerates loosely placed on the catalysts. The

specimen of this picture are 1:9 soot:catalyst loose mixtures but the control on the spot at the microscope was not as accurate as desired due to instruments limitations.

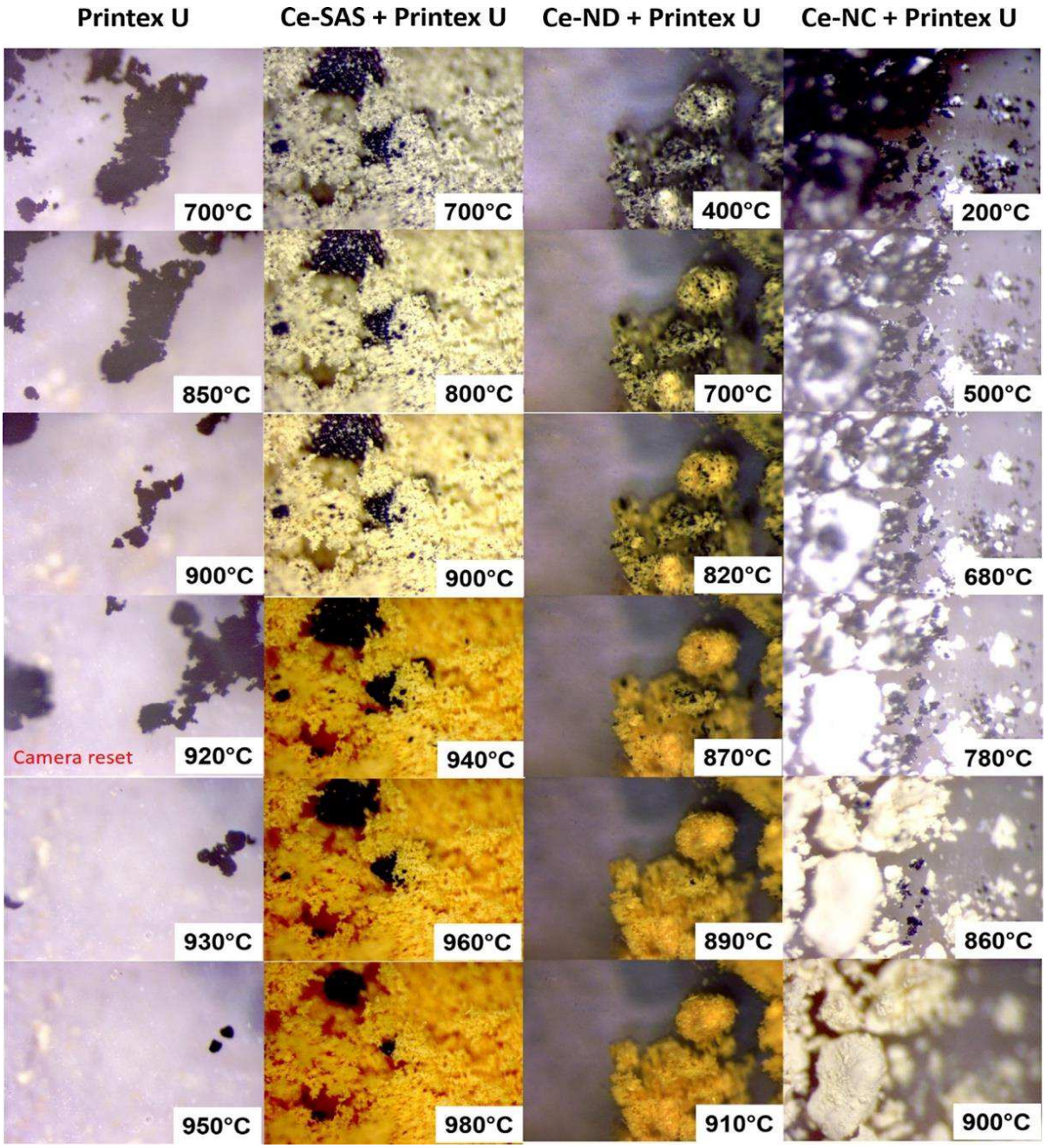

Figure 99 A comparison of time-lapse pictures captured with optical microscope and thermal stage holder. Ceria-ND stands for "nitrate decomposition", another way for referring to SCS ceria; Printex-U, by Degussa, is a commercial soot available for research purposes. (123)

Looking at the plots resulting from both in loose and tight mode TPC tests (Figure 102), depicting activity towards CO and CO_2 and overall soot conversion, a first comment goes to the worst performances of SAS. If in the previous studies SAS always overcome ND ceria, this time peak temperatures and conversion integrals of stars results always to be worst compared to traditional ND catalyst. The explanation to this unpredictable behavior is that while the simplicity of the synthesis of ND ceria, the Solution Combustion Synthesis, leads these materials to have *on average* always the same characteristics and properties in spite of all the possible variables (operator, reactor type, pollutants…), the complexity of the method to obtain self-assembled stars keeps quality inconstant. Unsealed reactors, pollutants in the vessels, odd thermal gradients in the furnace or even diverse amount of urea may keep the reaction far from the desired goal, producing unpredictable morphologies (sometimes, also nanocubes!) or, mostly, starred morphology with worst or better performances. For this reason, the results showed in the previous sections have to be considered as average for SAS catalysts. For the test campaign with nanocubes and SAS, the quality must have been really poor. However, the very high surface area, allowed SAS to reach the best performance in oxidating soot at low temperatures and towards CO oxidation.

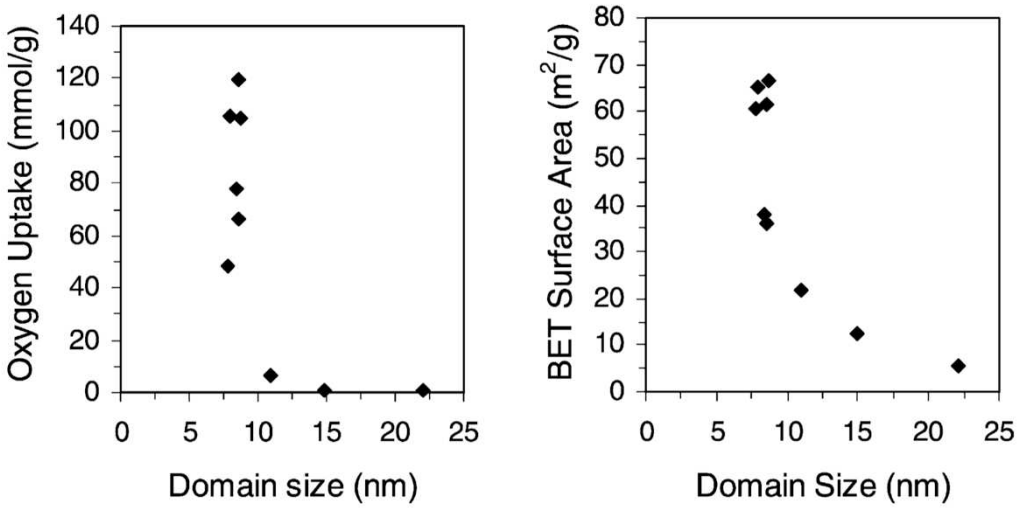

Figure 100 (Left) Oxygen uptake measurements as a function of ceria domain size for 1% loaded Pt ceria catalysts and (right) BET surface area vs. ceria domain size (124)

A must in further development of SAS is to improve the overall quality of the production methods.

In this campaign, the catalysts with higher surface area have been the worst in abating soot. This is another confirmation that in solid-solid catalysis the contact mode is more important than specific surface area. And it is also a confirmation of the important role of specific highly-reactive planes exposed in this kind of materials, as already proved in different studies. (125) (126) (127)

However, in a real application (i.e. a DPF installed on a running vehicle), those catalysts work alternatively in oxidizing and reducing conditions - indeed they have been selected because of their redox capabilities - and a higher surface area should allow faster or better "oxygen refill". This have to be proved directly and, however, it is subject of other types of tests; Jacobs et al., already showed a relationship between the crystallites size, the surface area and overall oxygen uptake of ceria-based catalysts (Figure 100), indicating that finer structures manage more oxygen just thanks to high surface areas. (124)

Another relevant information from TPC results is the multimodal behavior of nanocubes and their very low CO_2 peak temperatures (Figure 101). The deconvolution of the CO_2 emission loose tests curve of the three catalysts shows that nanocubes has three peaks instead of two, as the other materials (Table 14 for numerical results). However, soot oxidation at high temperatures can hardly be named as catalytic, since there may be radical mechanisms involved as well.

Table 14 Results of the CO_2 peaks deconvolution for the Ce-NC, Ce-SAS and Ce-ND catalysts under "loose" contact conditions (5/45 soot-to-catalyst weight ratio). The areas corresponding to the peaks are expressed in terms of peak temperature and% of the total area below the CO_2 curve (123). Temperatures are in °C, Areas in m^2/g.

Catalyst	T peakI	A peakI	T peakII	A peakII	T peakIII	A peakIII
SCS	431	31,3	493	60,2	582	8,5
NC	-	-	522	52,5	582	47,5
SAS	-	-	529	72,2	587	27,8

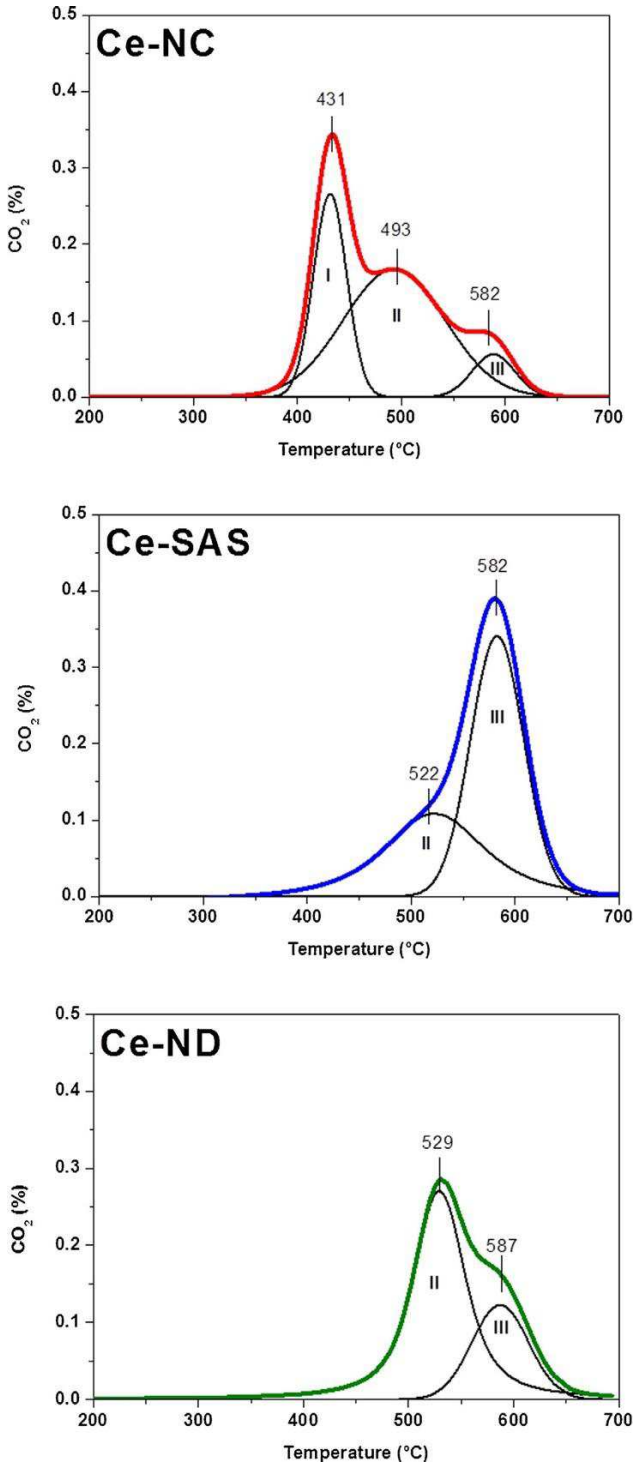

Figure 101 CO_2 peaks deconvolution for the Ce-NC, Ce-SAS, and Ce-ND catalysts (5/45 soot-to-catalyst weight ratio) under "loose" contact conditions (123)

Generally speaking, ceria nanocubes exhibited the best overall performance of the whole set of catalysts, with the lowest CO_2 peak temperatures and this may be due to the specific families of planes exposed, result of the hydrothermal synthesis, as already explained.

At this point, an investigation on the ratio soot:catalyst have been done, to assess again the relevance and the role of contact in particulate abatement (Figure 103). Mixtures of soot and ceria have been prepared with ratios of 5:45 (the standard used in the rest of this work), 9:41, 15:35 and 20:30; they have been all tested in TPC in loose contact mode. The aim of this task is to determine the contribution of the catalytic activity (with a specific kinetic) and the radical (non catalytic, variable) activity for these catalysts. As expected, higher ratio of soot-to-catalyst led to higher peak temperature as well as a diminished CO_2 sensitivity, probably related to different equilibria with CO. From the lower (5:45) to the higher (20:30), the *delta* in CO_2 peak temperatures was 124 °C for nanocubes, 14 °C for SAS and 4 °C for ND ceria. As all the work of SAS and ND ceria occurs at high temperatures, distinguish between catalytic and non-catalytic behavior is quite tricky. SAS showed a low sensitivity to T10% temps while the lowest T10% temp comes up from nanocubes, proving their better intrinsic activity.

Literally, from Piumetti et al., 2016 (123):

[…] high-surface area catalysts (Ce-ND, Ce-SAS) result to be less effective, thus confirming the surface-sensitivity for this reaction. Furthermore, the accessible (real) surface area plays a key role for this solid–solid reaction mediated by gas-phase oxygen. Therefore, a higher dependence of the oxidation activity on the soot-to-catalyst ratios appears for the nanostructured catalyst (Ce-NC), thus confirming its higher accessible surface area (i.e. more interactions between soot and catalyst) despite its very low specific surface area measured by the BET method.

So now there is a third definition of surface area: the *traditional*, of the catalyst itself, the *grouping*, of the catalytic layer, and the *accessible*, related to the area really in contact with soot particles. Only the first is measurable with BET analysis however. It still remains the concept that, for NOx-assisted soot combustion, traditional surface area is expected to be the highest possible, as these reactions mix solid-solid and gas-solid catalysis.

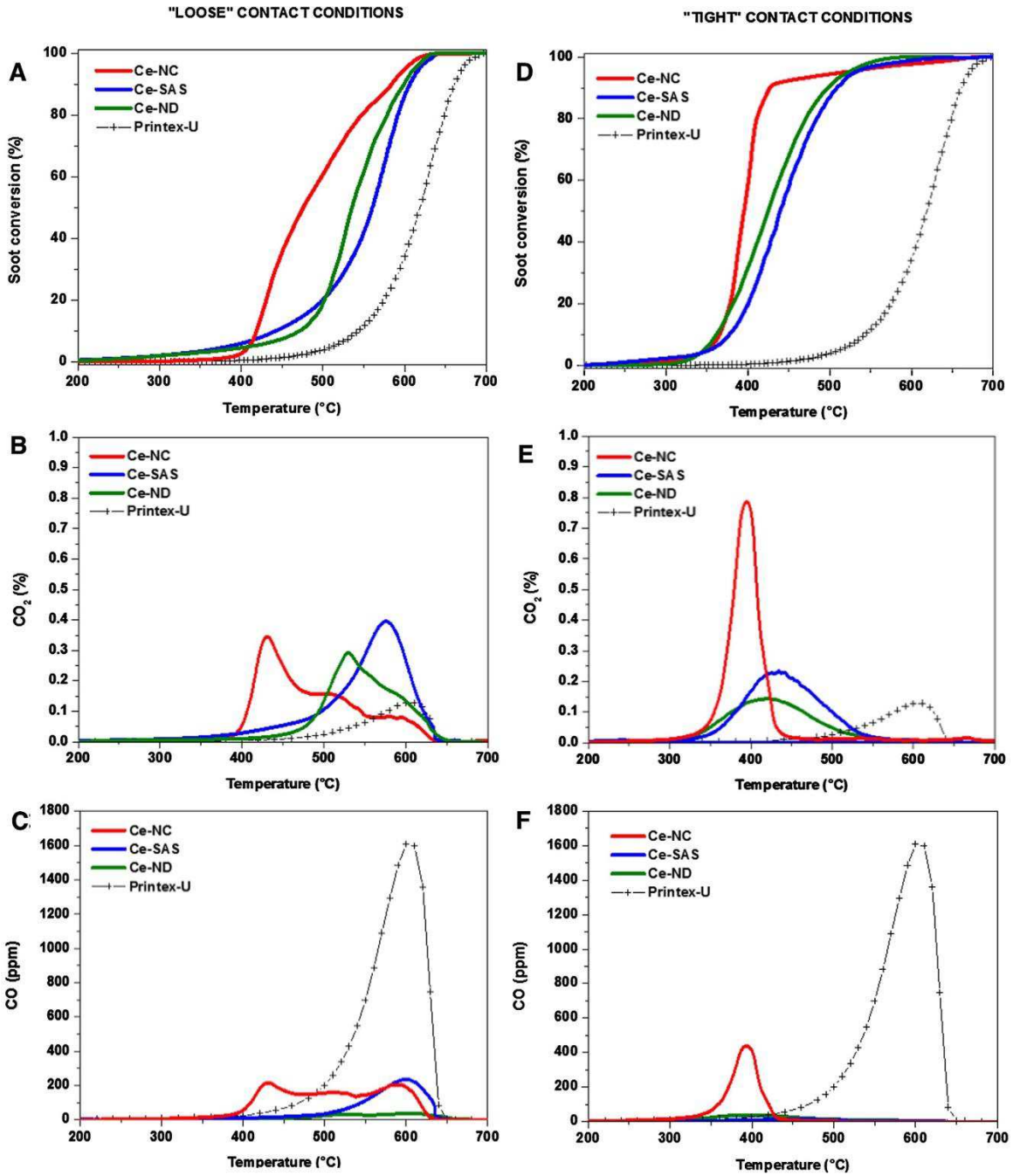

Figure 102 Soot conversions (%) (A and D), CO2 concentrations (B and E), and CO concentrations (C and F) over the prepared catalysts (1:9 soot-to-catalyst weight ratio) under "loose" (left column) and "tight" (right column) contacts (123)

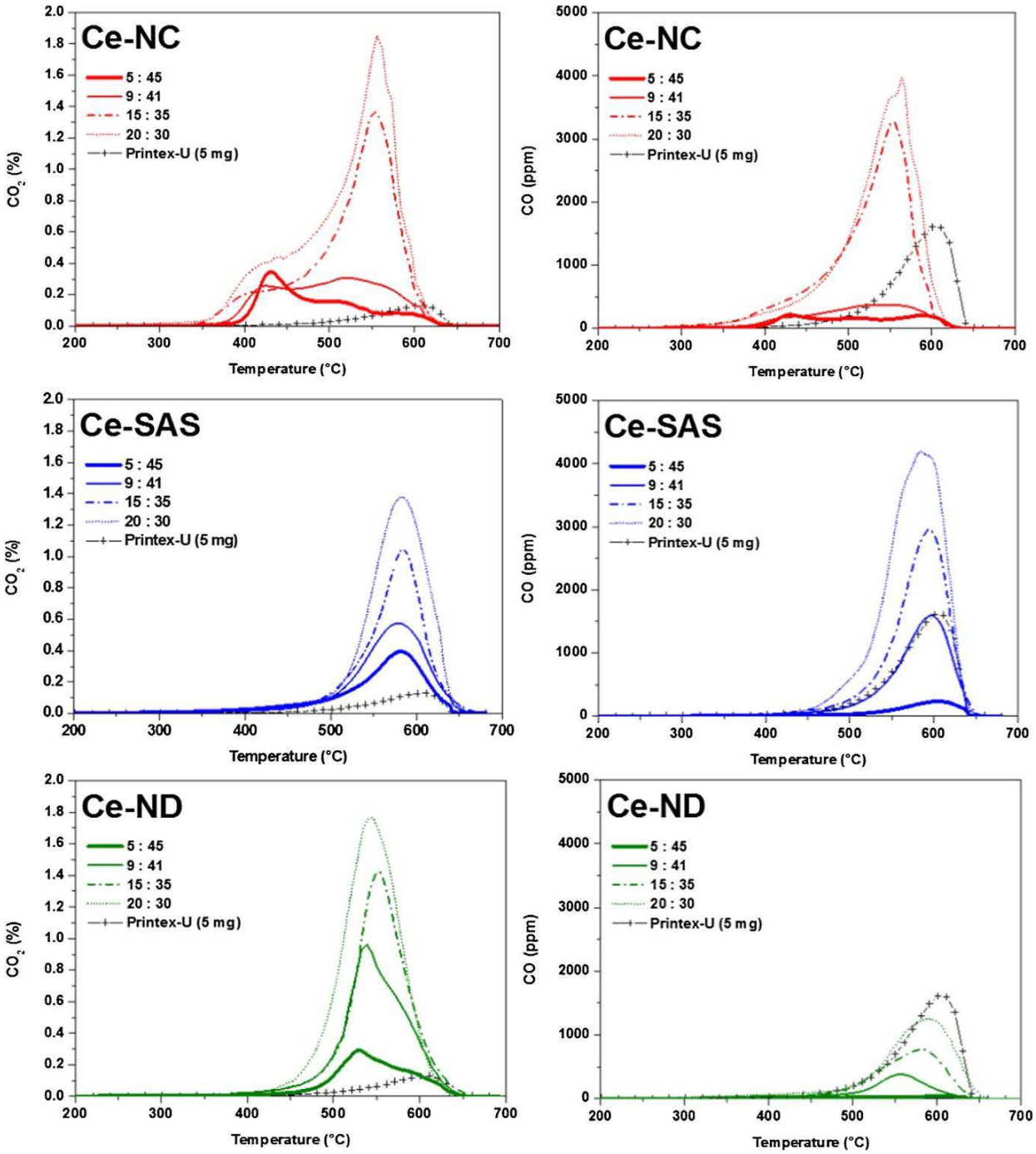

Figure 103 CO2 and CO concentrations over the Ce-NC, Ce-SAS, and Ce-ND catalysts at different soot-to-catalyst weight ratios (namely, 5/45, 9/41, 15/35 and 20/30) under "loose" contact conditions (123)

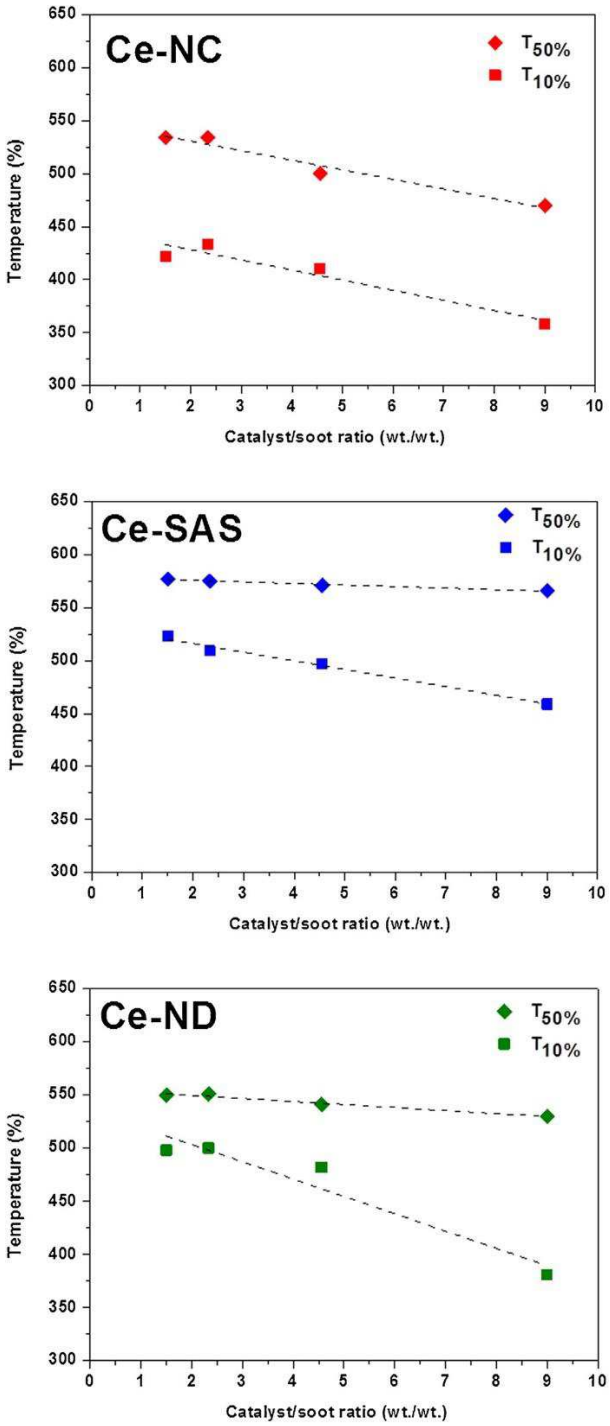

Figure 104 Temperatures at which10% and 50% soot conversions (T10%andT50%, respectively) are reached as a function of the catalyst-to-soot ratios (wt./wt.) (123)

2.3 Mid-scale setup

The final application of these catalyst is to coat a real-size particulate filter (DPF or GPF). The production of powder in laboratory is limited to few grams per batch while a real-scale filter would require hundreds of grams, keeping the time spent for synthesis unsustainable with high costs for a prototypal stage. Not to mention the case where the coating is meant to support noble metal catalysts, in which costs tend to rise even more.

Furthermore, in real-scale test with real engine installed on a proofstand, the independent factors that can influence the test become too many for a basic and full understanding of the phenomena surrounding soot abatement (actually, it's the same for every application): the weather, the fuel, the lubricant can cause uncontrollable working conditions and unpredictable results at each test.

Usually, the procedure for the development of a catalyst has to start with basic characterization, followed by TPC tests in artificial condition with just powders.

As already discussed in the previous paragraphs, lab-scale powder-only TPC tests are useful for screening and for basic research about intrinsic activity of catalysts but, since those tests are run with just powders and artificial mixtures, they are not fully significant for real-scale applications, with ceramic substrates and catalytic coatings and a soot cake growing upon them.

How to manage the need to scale up with the need of fast and sustainable campaigns? With mid-scale testing.

In the DISAT laboratories there was a first attempt of mid-scale test rig but hardly reliable so, through years, it has been improved and upgraded till obtaining a reliable instrument to play with (Figure 107).

The improvements are listed below:

- C-free refractory gaskets
- AISI316L conic flanges and cylindrical reactor
- Improved bypass
- Single Differential Pressure Controller
- Flat slabs filtration stage
- Mass Flow Controller station
- Coaxial long thermocouples with cordierite stand

Basically, a soot generator PALAS GFG 1000 produces size-settable graphite particles which flow, in a mixture of Ar and air, through a canning hosting the DPF

sample, which is in turn placed into a furnace. A differential pressure sensor calculates the delta-P between inlet and outlet of the canning. Two thermocouples are mounted coaxially, placed on a cordierite stand inside the canning to prevent bad sensoring, and they are in contact with the front and the rear of the DPF for delta-T measurements. The outlet is connected to a split linked to various gas analyzers and a SMPS/CPC (Small Mobility Particle Sizer/Condensation Particle Counter)

The aerosol can be eventually mixed with other gaseous species and it can flow directly into the canning or bypass it, a useful trick to characterize SG particles prior filtration with SMPS.

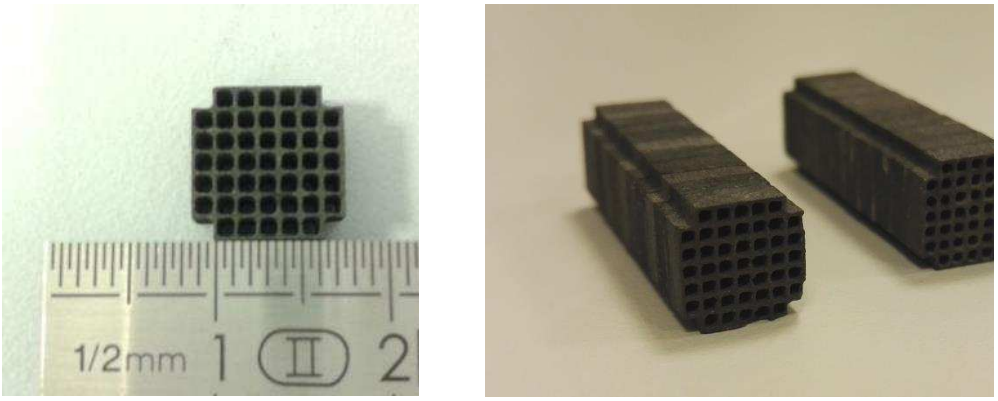

Figure 105 SiC monolithes are hand-carved to mid-scale size (128)

Figure 106 Small DPF are manually plugged and inserted into cordierite adaptors, to fit the mid-scale canning (128)

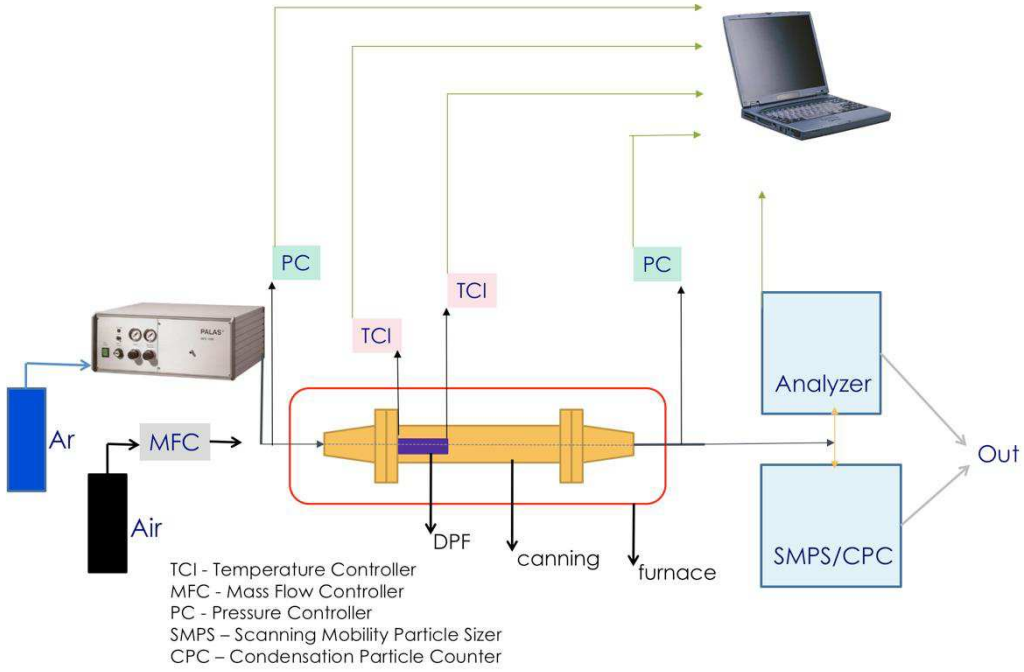

Figure 107 Mid-scale test rig schematic

The size of the graphite particles from the SG can be regulated by setting the frequency of the electric arc, and the instrument range can cover almost the same range of a real Diesel engine (Figure 108). There is an advantage in using a synthetic soot generator instead of a real engine or a flame-based soot generator: the quality of the particle is high and reliable. It is not afflicted by humidity, fuel type, engine map point, etc… It is eventually possible to change the quality of the graphite electrode in case.

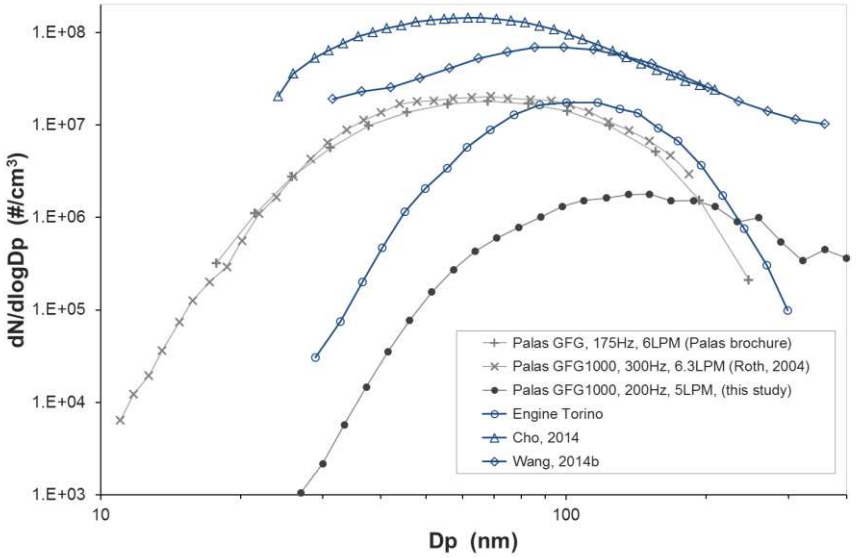

Figure 108 Normalized particle size distribution of the soot generator Palas GFG 1000 and comparison with the distribution in the exhaust of different engines (128) (129) (130)

Unfortunately, the development of a better mid-scale plant has been conclused too late for a comprehensive study of catalysts with designed morphologies, like the one proposed in this work as lab-scale. The laboratory activities stopped at the bare filter (without catalytic coating).

In collaboration with the University of Seville, some innovative DPF made by bioSiC have been prepared and tested with the aforementioned test rig (128).

The *greenifying* of vehicles is not just a matter of clean fuels, engine efficiency and exhausts treatment. The entire life of a car, from design to demolishing, can be redesigned in order to have the lowest CO_2 footprint possible (or whatever other equivalent indicator) and the chance of producing particulate filters from renewable sources, with lower environmental impact, is indeed extremely interesting (131). Nevertheless, the part of this partnership of interest for this thesis is mainly the one related to the capabilities of mid-scale testing apparatus, its reliability and its potential, aimed to further works and investigations. So deep discussions about the bioSiC filters properties and characteristics won't be found reading this section.

The main characteristic of a bare particulate filter are the filtration efficiency and pressure drop.

2.3.1 Mid-scale rig potential

The filtration efficiency of a filter can be calculated as the ratio between the number concentration of soot particles deposited inside the filter and the number concentration that it has to face at the inlet (Eq. 2):

$$\eta = \frac{N_{in} - N_{out}}{N_{in}} \quad (2)$$

This formula can be used both for calculating the transient efficiency and the filtration efficiency as function of the particles size. Indeed, as the particles diameter increases, the filtration efficiency increases as well, because the soot nuclei tile easier on smaller porosities and the soot cake itself, the real filtrating agent, grows faster (128).

The filtration tests have been conducted with a flow of 5 LPM of Argon and a spark frequency of 200Hz, a duration of 5 hours and repeated 3 times. The following regeneration tests have conducted with a mixture of 2,5 LPM of air and 2,5 LPM of pure nitrogen (to achieve a level of oxygen of 10% (114)),in a furnace heated up to 650 °C at 5°/min with a 3 hours dwell. The resulting spatial velocity is 120000 h^{-1} in both the kind of tests.

In Figure 109 the characteristic of two twins DPF and the average behavior[11], in filtrating 50nm sized particles generated by the SG and scanned by the SMPS, are reported. After 3600s, the average filtration efficiency is about 95% and after 7200s can be defined as 100% already.

Despite the SMPS does detect particles with a diameter around 2nm (PM2), the PALAS SG cannot produce enough particles with size under 50nm in order to be counted by the SMPS, the sensitivity of the particle sizer is too low to work with such few numbers of particles. For smaller particles, a real engine can be used for

[11] *The differences between the two identical samples may be partly caused by a variation in the permeability of the material, but more probably by a different porosity distribution, or they may simply derive from the randomness of a hand-made manufacturing process, despite both of them are supposed to come from the same precursor and to be equally manufactured.* (127) [pilar]

the filtration stage at the cost of more unpredictability, due to the uncontrollable nature of real soot compared to the standard and precise behavior of synthetic one.

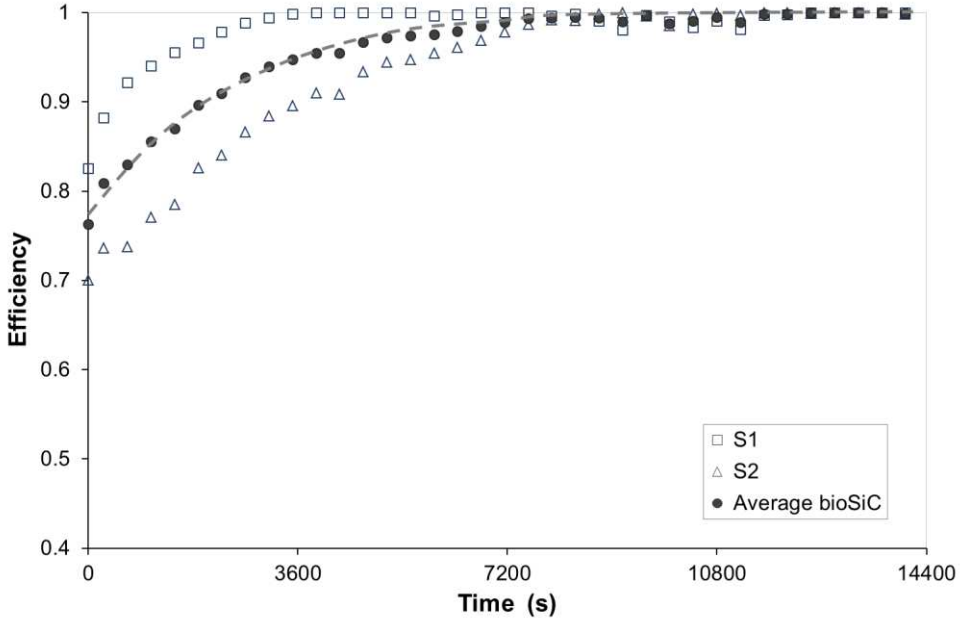

Figure 109 Filtration efficiency of the wall-flow bioSiC filters (128)

The transient evolution of the pressure drop is depicted in Figure 110, as usual with the average curve. In the very first stage, the rise of pressure drop is faster, because the system moves from a condition of low backpressure (the bare filter offers about 20 mbar of backpressure) towards an early condition of clogging. The accumulating of particles upon the SiC substrate, in this case with pores smaller than the particulate, starts creating a tiny layer: a primitive form of soot cake.

The soot cake is the real responsible of the filtration efficiency, as it can be noticed by overlapping the plots in Figure 109 and Figure 110; only when the cake is fully formed the efficiency reaches 100%. But, at this point, also the backpressure starts rising, and when it becomes unbearable for the engine (with values that may range depending on the OEM calibration of the engine itself), it needs a regeneration, nowadays controlled via post-injections of fuels during the scavenging phases, capable of supply additional chemical energy directly into the ATS, now able to reach the complete combustion of the cake.

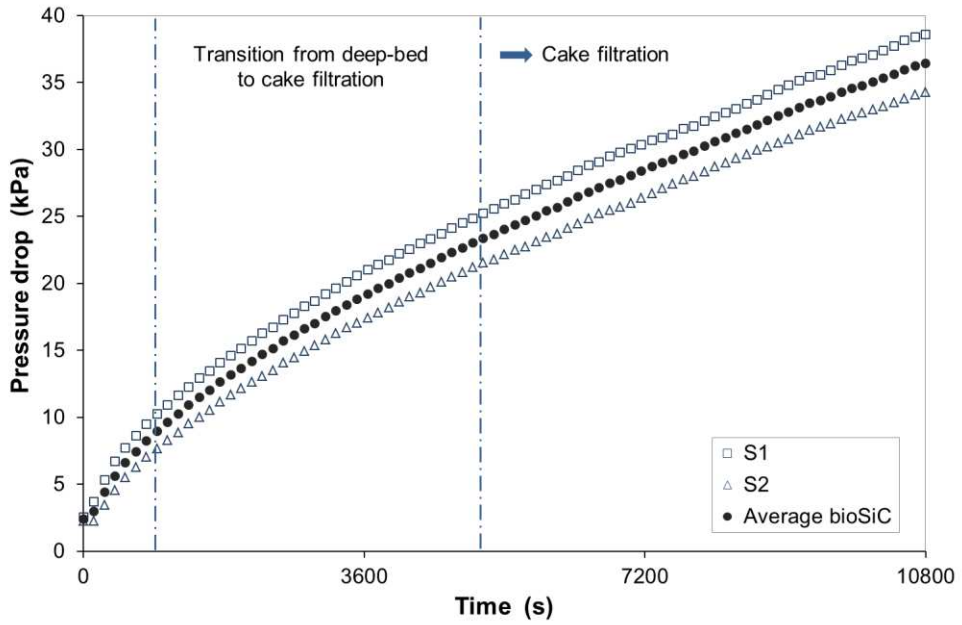

Figure 110 Pressure drop of the wall-flow bioSiC filters (128)

An example of regeneration with the mid-scale rig is depicted in Figure 111.

The pressure drop start rising from the initial value, due to the bare filter alone, up to a value which is calibrated by OEMs. In these cases, the tests prosecuted right prior that the maximum of the sensor's range has been touched (600 mbar), arbitrarily. Way before that, the pressure drop may reach the set limit, the temperature starts rising due to the heat supplied by the furnace (furnace switched on at 400 mbar of backpressure). It takes time to heat the system and the pressure drop continues its rise when, after 1h of heating, the regeneration begins. The pressure curve drops at the same rhythm as the temperature curve rises, indicating that the exothermal reaction of combustion plus the supplemental heat are cleaning the DPF. For a complete and consistent regeneration, the furnace keeps heating for a 3h dwell. At the end, furnace is set off, the temperature decreases and a last decrease of backpressure is observed, due to the cooling of the flowing gases and their change in viscosity.

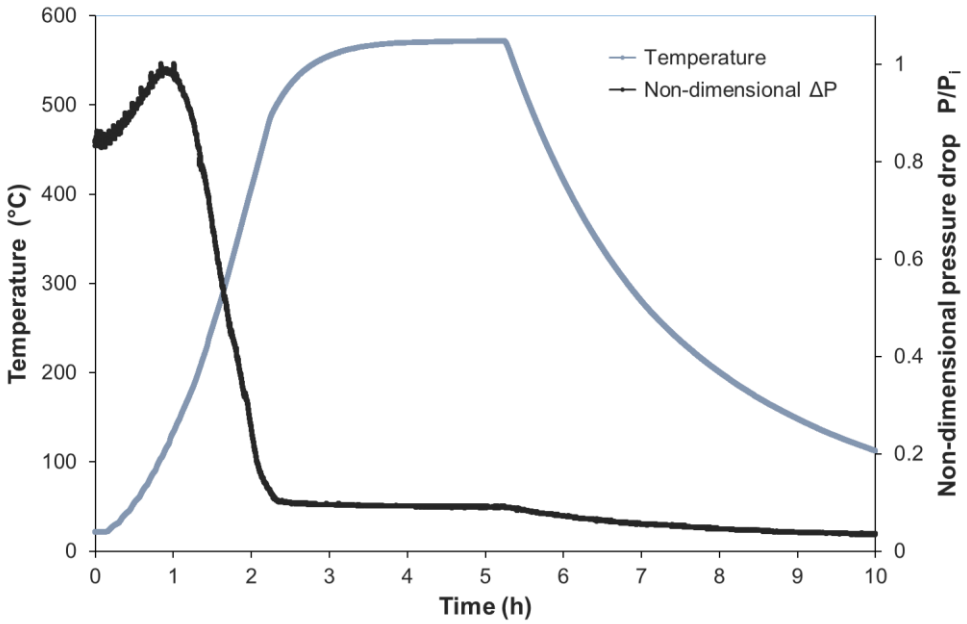

Figure 111 Evolution in the temperature and the non-dimensional pressure drop during the regeneration process (128)

2.3.2 Further works

In lab-scale testing the effectiveness of controlled morphology of ceria-based catalyst towards soot combustion has been proved, confirming that specific shapes bring highly reactive planes, enhancing the oxidative power of the catalyst.

The final stage of these investigations is with real DPF. The effectiveness of particular shapes also to form catalytic layers able to embrace better the sook cake, allowing to start the catalytic reaction from multiple layers of cake and not just from that one in touch with the flat coating, has still to be proved. Is a catalytic coating with a fuzzy topology able to burn a soot cake faster than a flat coating?

A micrometrical starred shape like SAS, may be able to form this kind of coating. Eventually, there could be the opportunity to create a multifunctional coating with separated levels for each pollutant (i.e. a first level with SAS/ceria for soot and a lower SCS/baria layer beneath for NOx) Figure 112.

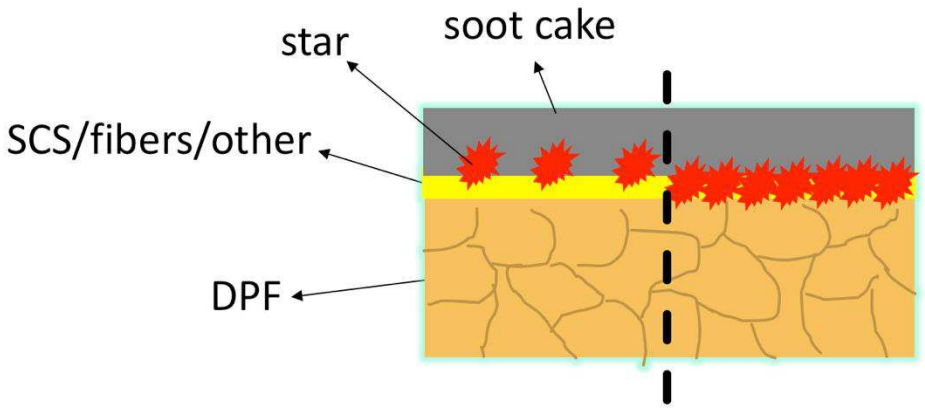

Figure 112 Possible coating applications of SAS. Right: as unique coating. Left: in a multifunctional coating, coupled with underlying 2D catalysts.

SAS seems to offer comfortable spots to soot particles to agglomerate in (Figure 113), and sizes that can be comparable to the thickness of a real soot cake (few microns). The covering effect (the "grip" on the SiC substrate) seems to be high (Figure 115) but without the clogging effect of *in situ* SCS (Figure 114), suggesting that with same amount of ceria (usually 10%w), the pressure drop of the clean filter would be lower with SAS coating, a nice-to-have for these applications, since the needs of regenerations would be generally lower.

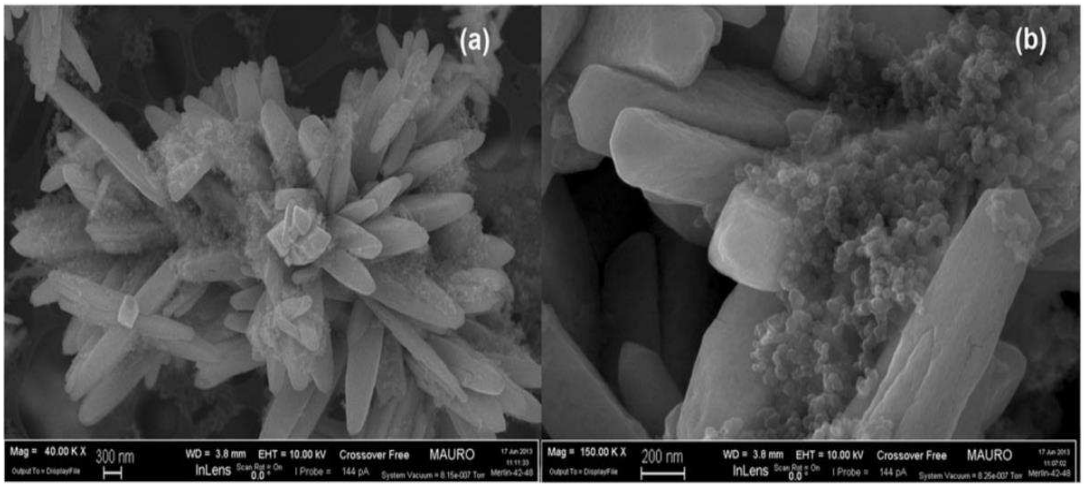

Figure 113 SAS with soot particles (loose contact, powders). (a) 40000x (b) 150000x. (114)

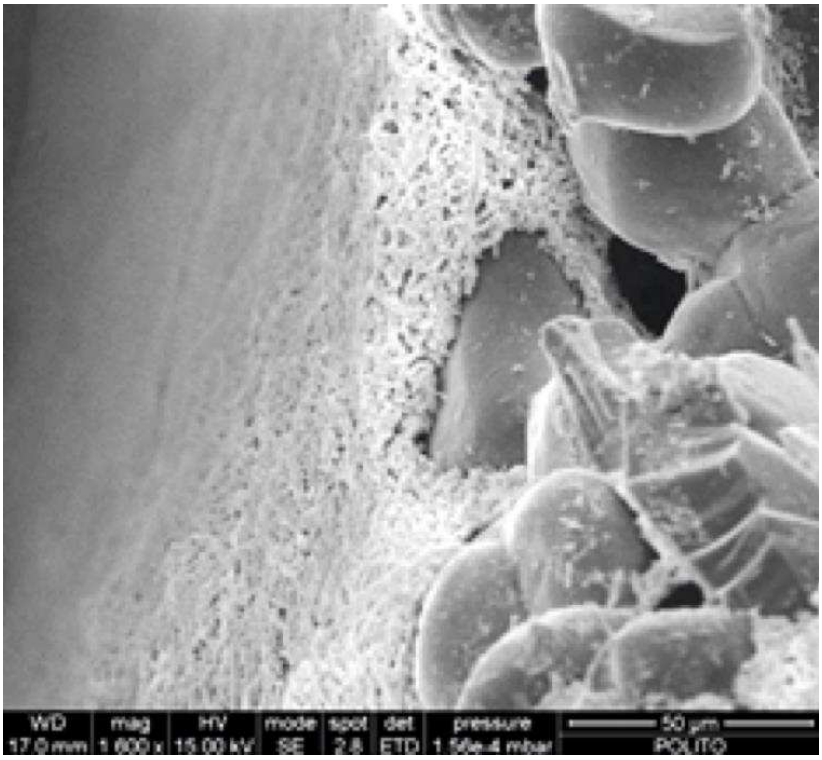

Figure 114 Ceria nanofibers coating the wall of a SiC DPF, 10%w. The topology of the coating is perfectly planar and regular. The coverage is uniform. (102)

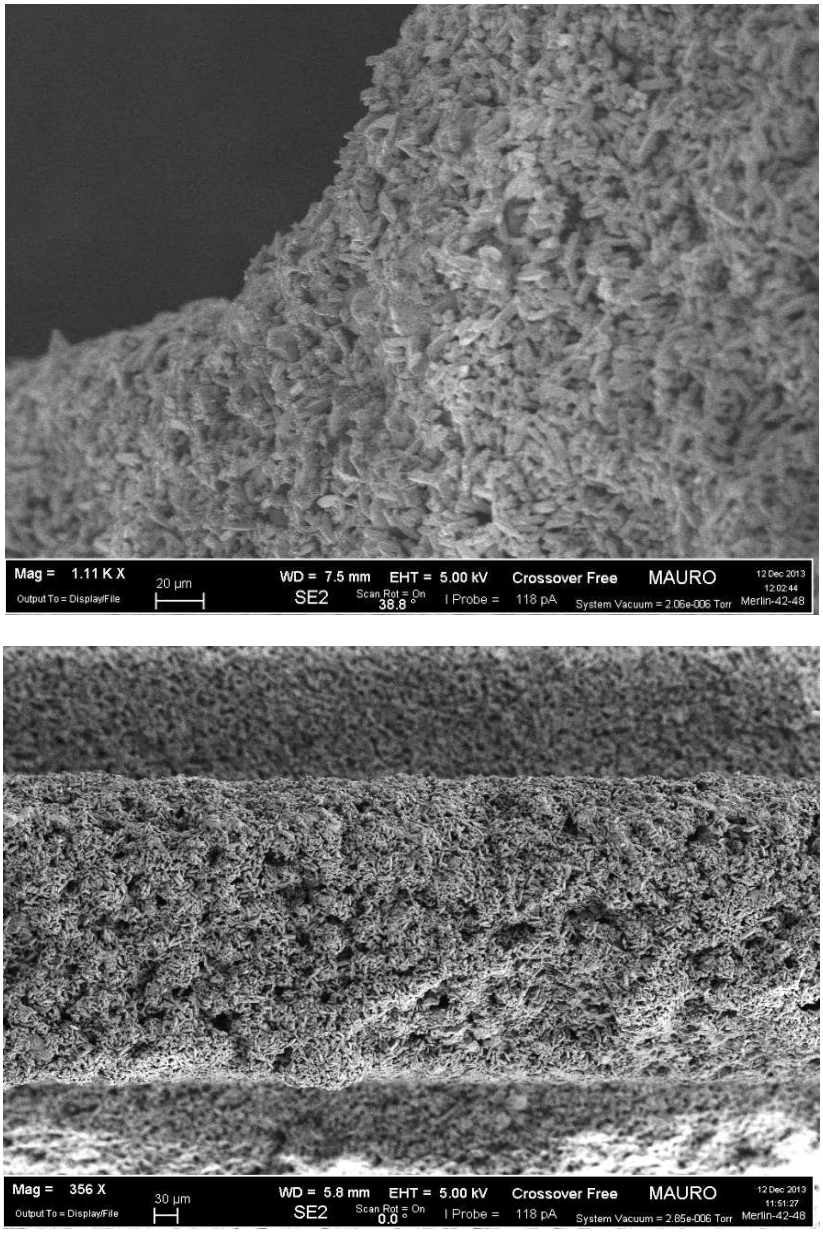

Figure 115 SAS coating on SiC DPF, 10%w. The coverage is complete and uniform, and the topology of the coating is tridimensional like the catalyst itself.

Further investigations are needed to test these new catalysts close to real conditions, like as coatings and not as powders anymore. The test rig for this kind of works has been prepared and checked and it's fully working.

Chapter 3

Fuels for HCCI-like engines

3.1 HCCI: background

Equipping the engine with better ATS or coating its components with DLC are likely to be retrofitting techniques, eventually adoptable in most engines worldwide. What these solutions can do is to improve by some percentage points the cleanliness of engines they have been coupled with.

Of course, throughout more than a century of history, the combustion engine has been constantly developed in order to gain more power and torque, to squeeze out every bit of energy from each drop of fuel only for the sake of performances. This means however, that the overall efficiency of I.C.E. has increased over time.

Time changes and today, increasing the efficiency of an engine means to lower its fuel consumption (that is its polluting emissions). In addition to constraining regulations by modern Governments, customers - at least in the most developed economies - show a new sensitiveness towards greener vehicles and not only to great performances.

This added value, with its increasing of the market share of the greener OEM, is a great slice of the driving force about developing greener vehicles.

Generally, the overall efficiency of a I.C.E. is a sum of several efficiencies

$$\eta_{tot} = \eta_{vol} \cdot \eta_{therm} \cdot \eta_{mech} \qquad (3)$$

where η_{vol} is the volumetric efficiency, the pumping one, η_{therm} is the thermal efficiency and η_{mech} is the mechanical efficiency, friction and vibrations related.

However, it can be explained in several ways, depending on the point of view of the analysis (thermal, mechanical, etc…), as example, this way:

$$\eta_{ideal} = \frac{1}{r_c^{\gamma-1}} \qquad (4)$$

where r_c is the compression ratio and γ is the heats specific ratio of the fluid (for I.C.E., γ is considered as the one of air - as N_2 - 1.4), or even this way (Carnot cycle):

$$\eta_{therm} = 1 - \frac{Q_{out}}{Q_{in}} \qquad (5)$$

where η_{therm} is the thermal efficiency and Q is the heat, which indicates how much energy from the combustion is lost in the exhaust with still lots of enthalpy. (132)

As example, using the aforementioned formulas to compare the most spread engine types, Diesel and Otto, one could easily notice that a Diesel engine, having no throttle, has a higher volumetric efficiency and the same cycle, with its higher compression ratio (18:1 for a common Diesel car versus 9:1 for a common gasoline car), brings higher overall efficiency.

That said, it is intuitive that strategies aimed to improve the efficiency of an engine would automatically lower its pollutant emissions. These strategies can involve the friction and the vibrations reduction, like less moving components, better lubrication or better equilibrium and/or the pumping capabilities, like better fluids-flows or higher compression ratios.

There are indeed also other methodologies, like faster combustions, particular scavenging timings, different thermal managements and so on, but right like the first mentioned, their development is but a business for a chemical/materials engineer. Historically, the development of the design of I.C.E. has been a prerogative of automotive engineers.

It is worth noticing that an engine is a very complex kind of chemical reactor, which transforms the energy stored in fuel into mechanical power, through fuel combustion (oxidative reactions). There is indeed room for chemical engineers…

With a better comprehension of the oxidative reactions inside the reactor and providing enhanced fuels, the improvement of the combustion processes is possible and all the equations above have in common the characteristic of the fuel. Indeed, the main difference between Diesel and Otto engine is not the fuel itself, but how the fuel burns: what makes a Diesel engine is not the Diesel fuel; Rudolf Diesel, in 1892, firstly developed its thermal machine and then started searching for the best fuel fitting the machine prerequisites. It happened that a particular blend of C16 hydrocarbons had those characteristics which worked perfectly within a Diesel cycle based engine.

This would only be a nice anecdote to explain how fuels and combustion are the core of these applications.

In a Diesel engine, a fresh charge made of pure air is pumped inside the cylinder and strongly compressed to achieve really high temperatures; only after that the fuel is injected into the chamber and auto-ignites (Compression Ignition) generating a complex flame (Stratified Charge). In an Otto engine, the fresh charge made of a mixture of air and fuel (Homogenous Charge) is pumped into the cylinder and compressed, hopefully without auto-ignition, while the combustion is ignited by a sparkplug (Spark Ignition) (132), SCCI and HCSI, respectively.

There is actually a third kind of thermal machine, which is indeed the fusion of SCCI and HCSI, the so-called HCCI engine (Homogenous Charge Compression Ignition) and it is considered as a chimaera by every automotive engineer, since its development is incredibly hard to pursue.

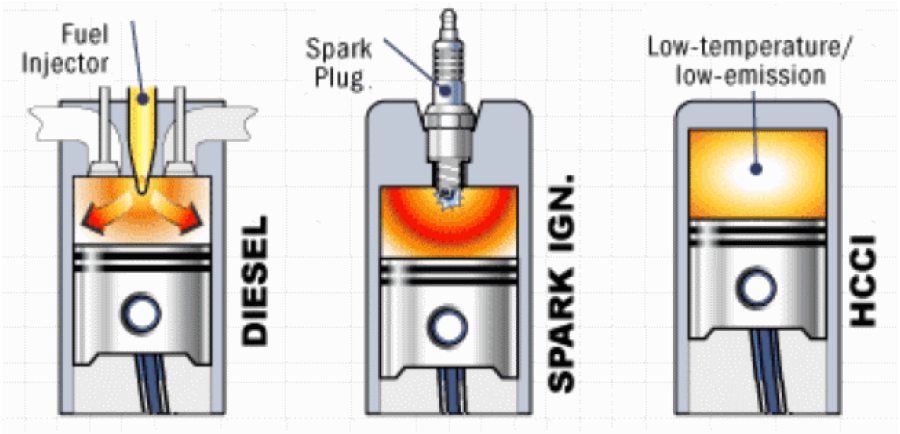

Figure 116 Schematic of SCCI (left), HCSI (middle) and HCCI (right) combustions. (133)

HCCI is a concept for which a homogenous charge of fuel and air is pumped in the cylinder, like a gasoline engine, and the high compression is enough to let the charge auto-ignite around the top dead center, like a Diesel engine (Figure 116). What is totally new in this cycle is that the combustion starts from a thousand points homogenously distributed in the chamber, with no knocking nor stratified charge. Of course, to avoid knocking or uneven mixture, the charge should be the leanest possible (134). The problem with lean mixtures is that the flame does not propagate unless the combustion is homogeneous[12]. Furthermore, because the thousand flames have less volume to expand, the combustion is quicker and cooler. All these characteristic of HCCI cycle lead to a field of working conditions in which nor soot neither NO_x can be formed (Figure 117). And working in lean conditions with efficiency above 50%, also HC and CO_2 emissions are dramatically reduced, maintaining - if not improving - the engine performances. (132)

In the past years, there have been some prototype cars equipped with HCCI-like engines, like Daimler DiesOtto (135) and Volkswagen GCI (136); nowadays, Mazda claims to start selling its Sky-Active X engine, an HCCI-like gasoline engine, with its cars in 2019, thanks to its study about low compression ratio - compression ignition engines (137).

These HCCI engine examples have some key technologies in common (of course, they are stiffer than traditional gasoline engines!), as for the auto-ignition of gasoline, which is actually assisted by a sparkplug in those cycles in which the energy of compression is not enough. All of them create (with multiple injections or with pre-chambered sparkplugs (138)) tiny environment with very rich mixtures (lambda = 0,85) that is more likely to ignite excited by a spark, near the head of the chamber; the piston coming from below is applying its pressure to a lean main charge, which sums up with the pressure coming from the head. This double pressure can create a fake high compression ignition, making the engine a *variable compression ignition engine.* On the other side, controlling cold EGR can help to quench the mixture when the HCCI range of load is achieved. Finally, the homogeneity of the charge can be obtained with intelligent multiple injections strategies, variable valves timings and proper designs of tumble and swirl moves of

[12] Yet to understand if a pure HCCI combustion has few initial flamelets propagating or it is a real all volume reaction (flameless).

the mixture. Real variable compression ratio engines do exist and are, actually, able to run HCCI (139) (140) (141). Their applications will be further discussed.

However, a control cycle-to-cycle is essential for smooth transition from traditional to HCCI range because, as said, engines cannot work in HCCI-like mode all ranges. Gasoline engines, in particular, cannot be HCCI in low loads and in high loads with very high compression ratios. This type of control can be assisted by precise pressure sensors in the chambers, linked to fast ECUs able to manage the spark advance, injectors, valvetrain and so on. The mathematical models described into the ECUs code are extremely hard to develop and are, indeed, the real secret of HCCI technology.

To build these models, combustion of fuels must be fully understood and its description developed with virtual tools, like CAE and CFD.

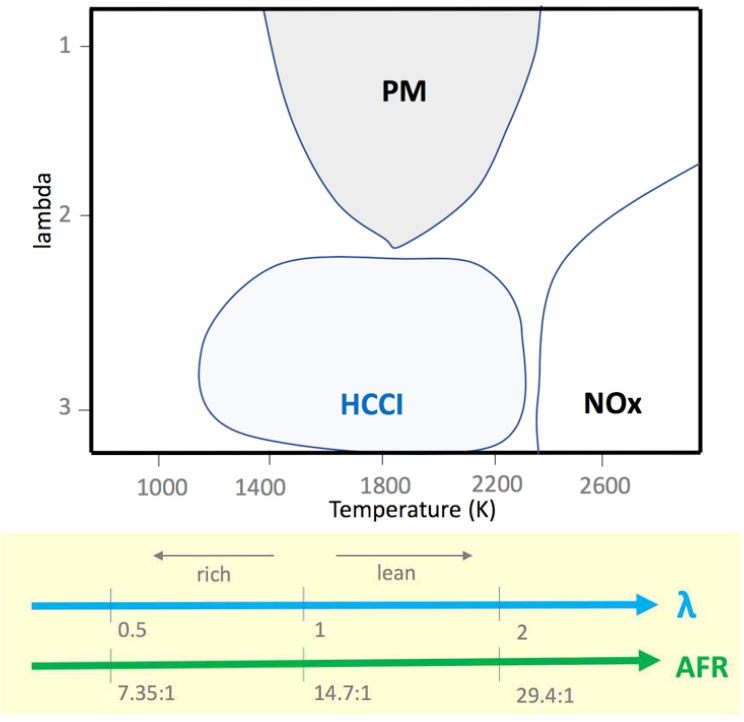

Figure 117 HCCI engines work in lean conditions and in a field in which PM and NOx cannot be formed. Lean combustion is essential for CO and soot abatement but, without flame temperature reduction, NO_x will stay a problem.

3.2 HCCI fuels

What does it take to build a HCCI engine? Trivially, one could just take a Diesel engine, mount a port injection or multiple direct injection system and let it run with gasoline. Unfortunately, gasoline has a limited resistance to auto-ignition and would easily burn uncontrolled in a high compression ratio engine, such as a Diesel one. Then let's try to run a gasoline engine with Diesel fuel: due to the low compression ratio of these engines, Diesel fuel won't burn at all.

The hardware has clear requisites, such as high compression ratio and tough design, the combustion has to be fast, homogeneous and cool, the mixture has to be lean but… the right fuel is still unknown. This is the HCCI paradox: combustion phasing is so crucial and delicate that HCCI is all about fuel chemistry but, since the good control of all the parameters needed for a HCCI combustion (T_{inlet}, Compression Ratio) can only be achieved with accurate, real-time sensoring of traditional fuels (gasoline, diesel…). Unless an ideal HCCI fuel turns up…

And yet it is possible to list the characteristics of this hypothetical HCCI fuel:

- Good volatility
- High Auto-ignition point

And a last, but not least, characteristic of this fuel should be its *sustainability*: it should be made from renewable sources.

Good volatility, because the charge has to become a homogenous gaseous mixture in the time of the aspiration and compression strokes, yet helped by injection strategies, and chamber tumble and swirl movements. Low volatility would require even higher compression ratio to provide the energy for fuel evaporation, possibly reaching the ignition point in the wrong piston position, resulting in knocking or misfire. Finally, volatility is not really an issue since the homogeneity of the mixture in the chamber can be achieved with opportune injection strategies or components geometry. Hot EGR has been proved to help HCCI combustion by enhancing fuel evaporation and promoting combustion with hot radicals. Effects of cold EGR are not been evaluated in these terms yet. This requirement however, could be more effective on Port-Injection engines rather than Direct-Injection, where the high pressures allow the formation of a fine, homogenous spray; homogeneity in DI engines can be achieved with multiple injections strategies.

High auto-ignition point, because the fuel must stand the high compression until the top dead center is reached by the piston without auto-ignition. Possibly, because the start of the combustion in these engines is self-regulated by the fuel itself (not by spark, as in gasoline engines, or by injection, as in Diesel engines), there should be strategies to help the fuel to get to its auto-ignition point always when it is expected to happen, not in advance and not too late.

The high compression ratio is the key for which HCCI engines have that high overall efficiency. Moreover, high compression ratios allow to burn leaner mixtures, with improved fuel reduction. The higher the compression ratio, the higher the efficiency and the lower the emissions. Eventually, water addition to the mixture could steal heat from the compression and cool down the conditions of the charge during the compression stroke.

Literally from Mittal et al.,2009 (142): *The propensity of a fuel to auto-ignite corresponds to its auto-ignition chemistry at the local end gas temperature and pressure.*

The ideal HCCI combustion is now supposed to be made not by a single flame, for which the flame speed coincides with the combustion speed (so-called, *propagation speed*), rather thousands of little flamelets that have less space to expand before touching the neighbor flamelets. The combustion speed is very high as resulting effect of the sum of thousands of low speed flames occurring in the same volume.

A fuel able to provide very high flame speed, without proper control, would generate pressures unbearable for the engine, uneven combustions or even severe knocking, able to destroy the engine itself in few crankshaft revolutions. Also, in this case water addition or cold EGR could quench the flamelets, reducing both flame speed and temperature (and pressure peaks). (143)

It is considered an advantage to have high flame speeds, because the lean limit flame propagation would be improved (143). The lean limit flame propagation explains how a flame can be extinguished by controlling its stretching.

Literally from Yuriy et al., 2008 (144): […] i*n positively stretched flames, this effect tends to increase flame temperature and extend flammability limits for mixtures with Le < 1 (Le, Lewis number).*

There are a few of other characteristics that could be nice to have:

- The ideal HCCI fuel should have a single or few components recipe, which is easier to manage as far as combustion timings may concern. Eventually, a dual component recipe should be made with an easy to ignite part, which starts the combustion and acts like a sparkplug, and a more resistant part, which mitigates the first component.
- Short-chain hydrocarbons improve the knock resistance because molecules are harder to become radicals and they even have a simpler auto-ignition chemistry, which helps a lot during the development of this kind of technologies. Branched chains are also effective for their particular combustion reaction paths.

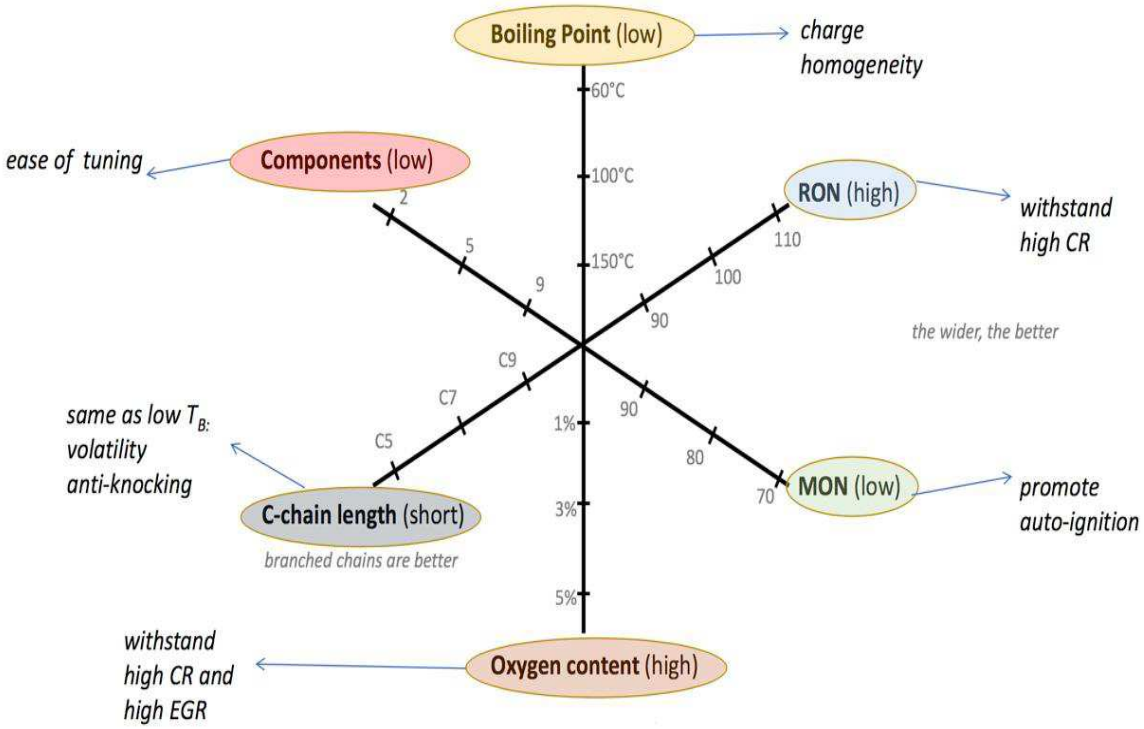

Figure 118 A plot to easily rank HCCI fuels ideal candidates. The larger the area of the hexagon is, the better. EGR could be an important factor both for achieving the lean combustion and controlling temperature in the chamber.

Auto-Ignition

Technically speaking, fuels can be ranked using characteristic values like RON and MON for gasoline, CN for Diesel fuels and DVPE. DVPE[13] (Dry Vapor Pressure Equivalent) is used to indicate the vapor tension of the fuel; the higher the value is, the higher the fraction of fuel evaporates at a given temperature. This data is not just useful for HCCI applications but, more practically, to indicate "winter fuels" as a higher volatility helps in cold starts where the environmental temperatures are particularly low.

RON and MON (Research Octane Number and Motor Octane Number) are gasoline-only numbers, determined experimentally by using a reference engine and reference fuels, made only by iso-octane and n-heptane.

For these two components, a value of RON100-MON100 is assigned to iso-octane and RON0-MON0 to n-heptane. The test with the engine is aimed to verify the presence or not of knocking (advanced uncontrolled auto-ignition) when precise operating conditions are applied (Table 15).

Table 15 RON and MON tests compared. Oil and Coolant temperature are the same for both tests. Air-Fuel ratio, Compression Ratio and Inlet Pressure can be adjusted to successfully end the test (145)

	RON	**MON**
Engine Speed (rpm)	600	900
Inlet Air Temperature (°C)	52	149
Ignition Timing	13° bTDC	19-26° bTDC

[13] Some countries use the equivalent RVP, Reid Vapor Pressure, to indicate the vapor tension of fuels.

CN (Cetane Number) is a Diesel-only fuel number and is a sort of inverse RON. Since Diesel fuels are meant to ignite as soon as they are injected into the hot chamber with precise delay, the accuracy of ignition timing is desired, and it can be quantified with cetane number, considering the cetane a compound with the highest ignitability (CN100) and alpha-methyl naphtalene the one with the lowest (CN0). Commercial Diesel fuels range above CN50.

The main difference between RON and MON tests is that the MON test is more severe towards fuel: since engine speed is higher, air is hotter. The ignition timings are advanced as consequences. They are however, equally considered in fuel description, as they are representative of low loads (RON) and high loads (MON) engine conditions.

The reference fuel in these tests is a mixture of iso-octane and n-heptane (PRF, Primary Reference Fuel) and the amount of each compound depends on the examined fuel.

The reference fuel has to perform the same as the incognito fuel: if it takes a blend of 90% iso-octane and 10% n-heptane to couple with the unknown fuel, then this last one will be classified as RON90.

Commercial gasoline, all around the World, may vary in RON/MON according to local regulation. In average, gasoline for private transportation can be considered as RON90/MON80 yet it is possible, especially in motorsport and for high-end vehicles, gasolines with RON above 100. How can it be?

Well, first of all, it is worth remembering that gasolines are blends. It is possible to go beyond the limit of RON100 considering other compounds with anti-knocking power even higher than iso-octane that can be added to the main recipe. When such chemicals are additivated to gasoline, they increase its resistance to auto-ignition. Eventually, such compounds could become one of the main ingredients of the fuel recipe, making possible to use a poor refinery product, adjusted with such kind of improvers. Examples of these compounds are: tetraethyl-lead, benzene, toluene, alcohols and MTBE/ETBE (Methyl / Ethyl tert-butyl ether).

Throughout years of experience, gasoline has been boosted in octane for the sake of engines performances and it was found that many of these substances were not compatible with human health and environment so, currently, the most used *octane booster* are ethanol and ETBE. Moreover, oxygenated compounds help to achieve a complete, faster and cleaner combustion.

Comparing two fuels, one with RON95 and another with RON90, the one with the higher number will better bear the compression with no risk of unwanted auto-ignition (knocking), so RON is a practical way to measure the potential of a gasoline in terms of performances, given that higher boost pressures and high compression ratios are needed to squeeze more horsepower out from an engine. In some countries, at the pump station, fuels can be labelled by RON only (trusting that the average MON is about 10 points lower than RON), by both RON/MON or by AKI (Anti-Knock Index), which is the straight average value between RON and MON.

Literally, from Johansson, 2016 (146):

[…] the condition in the cylinder after compression is different from the RON and especially MON cases. With high boost and effective intercooling (as in modern engines), the pressure level is high, whereas the temperature is moderate, and hence the T/p ratio is low. This is in stark contrast to the MON case where the inlet temperature is high and compression ratio moderate, yielding moderate pressure after compression. For the MON case, the T/p ratio will be very high. The RON condition will be something in between with a moderate T/p ratio. It is thus argued that for a given RON number, a fuel with a lower MON will ignite easily at high temperature and low pressure (high T/p ratio) and, as a consequence, ignite less easily at low temperature and high pressure (low T /p-ratio). In other words, for a given RON, a fuel with a low MON will be less prone to autoignition at high pressure and low temperature. This is how modern engines are operated.

Recently, a more accurate measure of anti-knocking is given by the Octane Index OI (147):

$$OI = RON - K \cdot S \qquad (6)$$

where S is the sensitivity (RON-MON) and K a factor depending on temperature and pressure of each engine load conditions. K ranges during engine running; then,

OI decreases as load increases, because K has negative sign[14] (142). If S is not zero, then RON is different from MON and OI ranges as well as K and load (inversely). One of the first issues when characterizing fuels is that PRF fuels have no sensitivity at all, plus the limit of RON100 constraining special high performances applications.

In special applications, like motorsport or HCCI engines, PRF are not enough to characterize the anti-knocking power of gasolines. For all these reasons, a new reference fuel has been proposed: the TRF (Toluene Reference Fuel, a toluene, n-heptane, iso-octane mixture), which can finally describe gasolines with RON higher than 100 and with evaluable sensitivity (Figure 120).

The sensitivity of a gasoline indicates how the anti-knocking power of that fuel can change moving from light loads to high loads. Hence the importance of this parameter is to scout out a proper fuel for HCCI-like engines, since the control of the combustion is self-regulated by the fuel itself.

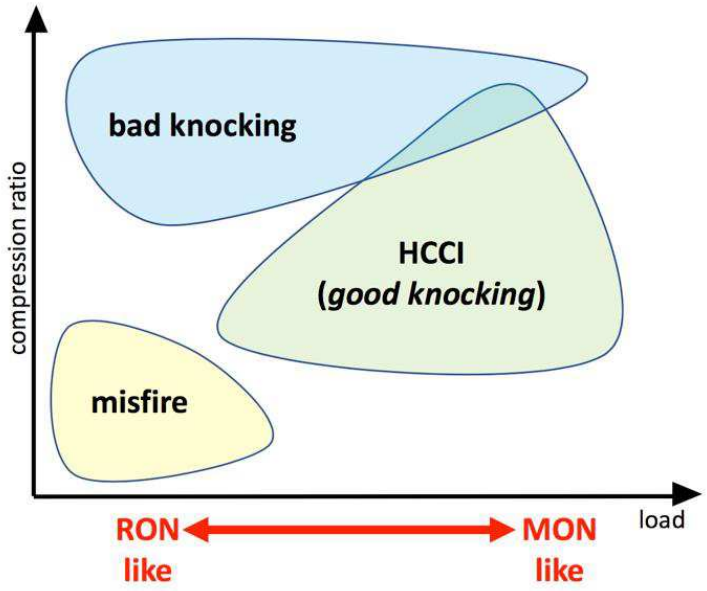

Figure 119 HCCI range of a gasoline engine.

[14] From (141): *[...] for domestic engines, K is now negative, having decreased from a value of 1 in 1930. This decrease in K is primarily due to better engine cooling, better engine breathing, and the usage of fuel injectors.*

When a fuel shows high sensitivity, it demonstrates great knock resistance in RON mode (low load) but less knock resistance in MON mode (part and high loads) like it was a sort of dual fuel recipe. I.C.E. cannot be running pure HCCI all across their map, but likely in part and high loads (Figure 119). Fuels ability to withstand compression at low loads is still needed, but in part and high loads they are expected to auto-ignite, so their knock resistance is desired as lower *only* in those conditions. So, a good fuel for HCCI-like engines should have great sensitivity.

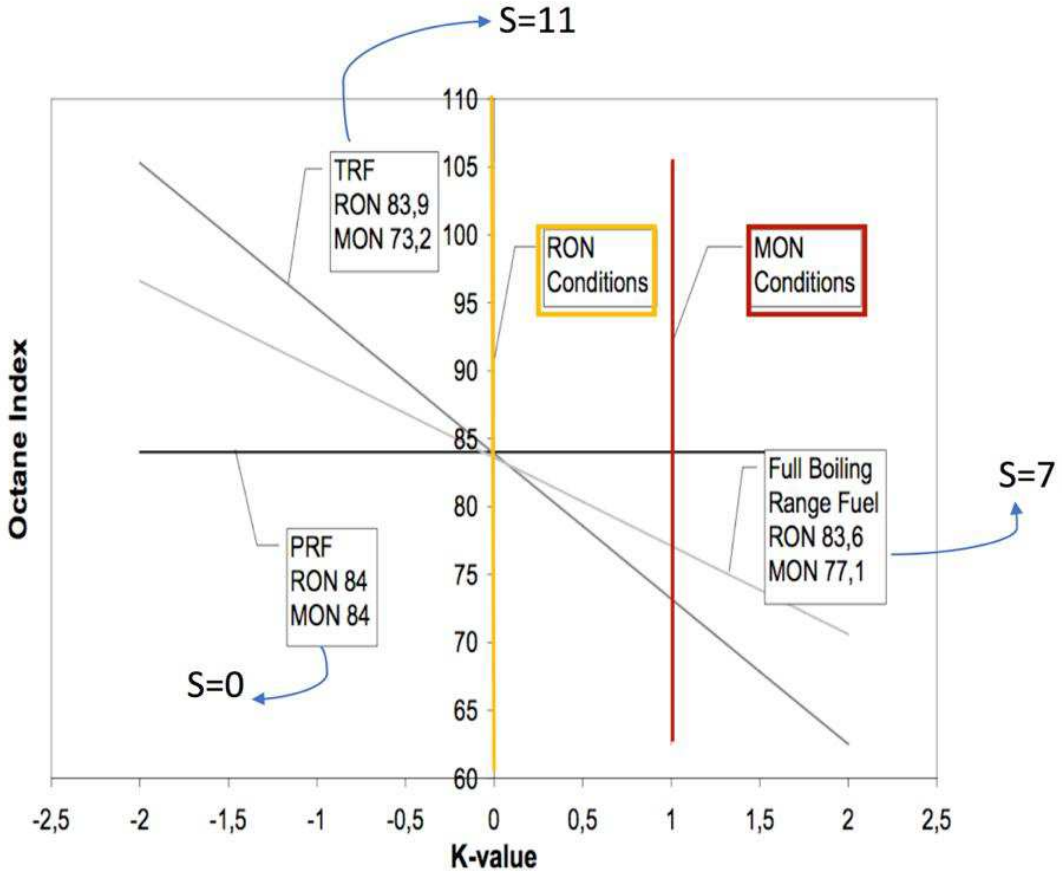

Figure 120 How the sensitivity of fuels influences performances in light and high loads. (147)

3.2.1 Traditional fuels vs New fuels

There are indeed chemical compounds which have all that particular characteristics previously descripted, some of them can be also made from renewable resources and they are also considered to be cleaner than gasoline and Diesel fuels: alcohols. Ethanol, butanol and methanol have been investigated as HCCI fuels with encouraging results from the proofstands, but without the approval of accurate test campaigns, due to the expensiveness of these tests. Despite their effectiveness, some fuels cannot however be used as universal HCCI fuel because of incompatibility with health and environment. Others simply cost too much to be considered in large scales. The alcohol with the higher chance to be used in series applications is ethanol, however. Moreover, ethanol can be easily obtained from green and renewable resources and its availability could be eventually increased with proper incentivizing policies.

However, only considering the most common private or light commercial vehicles, the most spread fuels are gasoline and Diesel (148). One of the biggest success of I.C.E. equipped vehicles is their reliability: all across the World, the same engine can rely on a spread grid of pump stations and, even if the qualities of fuels may vary from a country to another, that engine will run with almost the same performances everywhere.

Literally, from Bohacz, 2003 (149):

A higher compression ratio leads to a better thermodynamic cycle and hence higher efficiency. Hence, it is only with high-octane fuels HCCI can be expected to achieve high efficiency. Diesel-like fuels need very low compression ratio and therefore less efficiency.

This leads to an interesting observation. Most SI engines today are operated with a compression ratio around 9:1 – 12:1. If we should operate such engines in HCCI mode, the most suitable fuel would be Diesel. Diesel engines, on the other hand, use a compression ratio of around 16:1–18:1. If such engines would be operated in HCCI mode, the most suitable fuel would be gasoline with a high octane number. So, in short, the most suitable fuel for an SI engine is Diesel and the most suitable fuel for a Diesel engine is gasoline if they are run in HCCI mode.

Easy to say that, both for the will of a greener approach and the need of high octane gasolines, the traditional commercial fuels are not so adequate. That said, it is easy to indicate ethanol as the correct fuel for HCCI applications but then, as far as fuels may concern, the reality is that a conversion of all the World's mindset *all of a sudden* is impossible and an eventual fuel transition would be tricky and challenging, even for the sake of health and environment.

But speaking of challenges, what about developing HCCI engines using only gasoline and Diesel fuels, eventually with just few little adjustments in their recipes?

Up to date, the largest part of gasoline engines on the market run flawlessly with RON95 and can eventually self-adapt with slightly poorer fuels, while the average compression ratio ranges from 9:1 to 12:1 (Diesel engine are about 20:1) (148) (132). HCCI-like applications run with compression ratios between conventional gasoline and Diesel engines and, in the lightest scenario – 12:1 – gasoline is meant to stand a relatively strong compression, maybe beyond the edge of its capabilities.

Trying to develop HCCI-like combustions with current gasolines available at the pump station would result in spectacular (and dangerous) engine failures at the proofstand. The gasoline simply would auto-ignite during the compression stroke, because the HCCI compression ratio is higher, with noticeable knocking.

Ethanol

An interesting alternative fuel for HCCI engines (both Otto and Diesel based) seems to be ethanol, in wet form or anhydrous, blended with gasoline/Diesel (150).

Ethanol, or better *bioethanol* (since the main source of this chemical is biomass, currently), is a high-octane fuel, with high flame speed, perfectly water-mixable and oxygenate. High octane number helps standing high compression ratios and pressure boost, a primary requisite for un-throttled HCCI engines, then the high flame speed allows faster and more complete combustions, increasing both performances and cleanliness; ethanol moreover, is perfectly mixable with water, which can be a problem, if blended with HC fuels, because the consequent phase separation could result in dangerous water injections directly into the engine, or an advantage, because wet ethanol could embed the water cooling effect directly in the fuel, without complex water injections strategies and technologies. Being an alcohol, that is an oxygenate compound, ethanol can better withstand extremely rich and extremely lean mixtures, where the conditions of the charge may compromise the stability of the flame; furthermore, oxygenate species help HC and soot burning gaining a cleaner combustion.

Of course, there are some drawbacks which could make complicated a straight introduction as fuel for traditional engines. As examples, ethanol is an aggressive solvent that can seriously damage some plastic components of the vehicle; its low vapor pressure, compared to gasoline can be an issue in cold starts, where the mixture wouldn't form because of bad fuel vaporization; finally, ethanol has a high affinity and miscibility with water and a low cetane number: the first can be a problem for both Diesel and gasoline engines, the last only for Diesel engines. (151) (152) (153) (154)

These issues however, can be easily solved with some cheap modifications on the vehicles, like ethanol-resistant polymers, intake pre-heating and EGR management, cetane improvers and absolute ethanol based fuels. So cheap modifications that could even be retrofitted on the existing fleet.

Over the years, the interest of ethanol as alternative fuel for vehicles has increased, driven by oil crisis and *greenification* of the global economy. All these critical aspects about its spread usage has been investigated and interesting management strategies has been developed to control ethanol combustion, even in HCCI mode:

- Trapping of internal residual gas (155)
- Forced induction (156)
- Variable valve timing (157)
- Wet ethanol (158)
- Chamber geometry (159)
- Heat recovery (160)

Some innovations were totally essential to ethanol as fuel, like all the thermal management, needed to overcome the low volatility, and chamber geometry/variable valves timings to adapt the compression ratio and swirl/tumble movements for the particular mixture (161). Among all of them, one is even more interesting because of positive implications in CO_2 global reduction and in fuel life cycle assessment pollution indicators: the usage of wet ethanol.

Despite ethanol is largely used, in variable amount, in the formulation of modern engine fuels, its great limitation, in terms of costs and fuel quality, is the affinity with water. For this reason, huge efforts are made to produce absolute ethanol (above the azeotrope[15]) to prevent fuel water contamination. The resulting dry ethanol, however, can slowly absorb humidity from environment, slowly polluting the fuel in the tank, making ethanol blends like disposable fuels (162).

Nobody wants an expensive and disposable fuel.

Wet ethanol allows to be used as produced with simple distillation, with water, and a proper engine would be designed to bear and manage water flushings and water in the combustion. It has been proved that ethanol can withstand HCCI combustion if blended up to 40% of water, with opportune expedients. (163) (164)

Introducing water in the mixture, however, can be positive also for traditional engines. The most important effect of water is, of course, the cooling effect on the charge, due to vaporization during the compression stroke that is able to steal heat, mitigating the effects on the mixture (water is an anti-knocking agent).

[15] Plain ethanol/water distillation can achieve up to about 95% ethanol. Above this threshold, vapor phase has the same composition of liquid (azeotrope). In order to achieve higher concentration of ethanol (99%), expensive – and polluting - chemical processes must be used, increasing the final price of the product and, curiously, decreasing its green footprint.

Water addition has the effect of slightly modify the thermodynamics of the engine, because compressing a polyatomic species (like water) costs less work than a biatomic species (like nitrogen, air); the overall work of the thermal machine is due to the differences between the expansion work and the compression work: if the compression work is lowered by water, then the expansion work would result higher. Water addition increase efficiency.

Water injection in traditional engines is one of the current automotive challenges, and one of the stumbling block is right the immiscibility between gasoline/Diesel fuel and water itself. Could ethanol be a sort of interfacial compound between the two phases? (165) (166) (167)

Also, a flame quenching effect is appreciable during the power stroke, lowering flame temperatures with resulting low NO_x production, although a higher production of HC and CO is inevitable. In HCCI engines however, the particular stoichiometric ratio of the mixture and the low temperature of combustion, should allow even lower NOx and soot emissions. So, an opportune ATS made at least of oxidative catalysts and particulate filters with DeNOx should be sufficient to guarantee a cleaner drive. (168)

Nowadays, bioethanol is produced with a dedicated agriculture in amount per year which is not suitable for a massive fuel conversion of the fleet. Moreover, the contingent food war - which may start if soil is used more for fuel harvesting instead of food production - could lead to sad consequences. To be really competitive as fuel, a new and more sustainable way of production of bioethanol should be developed and wet-ethanol-ready engines should appear on the transportation market.

HCCI combustion

Again, from the hardware point of view, there are few improvements to be implemented in current gasoline engines, right enough to achieve a stiffer design; this time, there is nothing about the components: the core of this application is the control of the combustion.

And, in particular, there are two aspects that are critical:

- The point of ignition
- The speed of combustion

Thanks to the high compression ratio (reason of high efficiency), the charge is able to ignite without the help of the sparkplug, right because the temperatures and pressures in the chamber are, *at a certain crank angle*, correct for the ignition of the fuel. Because the point of ignition ranges depends on engine rev speed, it takes some expedient to inflame or to quench the charge.

Boosting intake pressure helps to increase the temperature during the compression stroke, when the combustion has to be encouraged; cold EGR dilutes the charge with inert gas and can calm it down, while hot EGR, both for thermal and radicals effect, triggers immediately the combustion. Start-Of-Injection can be used to control the charge homogeneity, i.e. anticipating the SOI, while multiple injections can keep the power stroke more gradual and bearable for the engine components.

Lately, also water injections have started to be studied, to quench both the charge and the flame. All these gimmicks are however surrounding conditions since they all are not enough to achieve a reliable HCCI-like combustion with consistency: the main factor is the fuel.

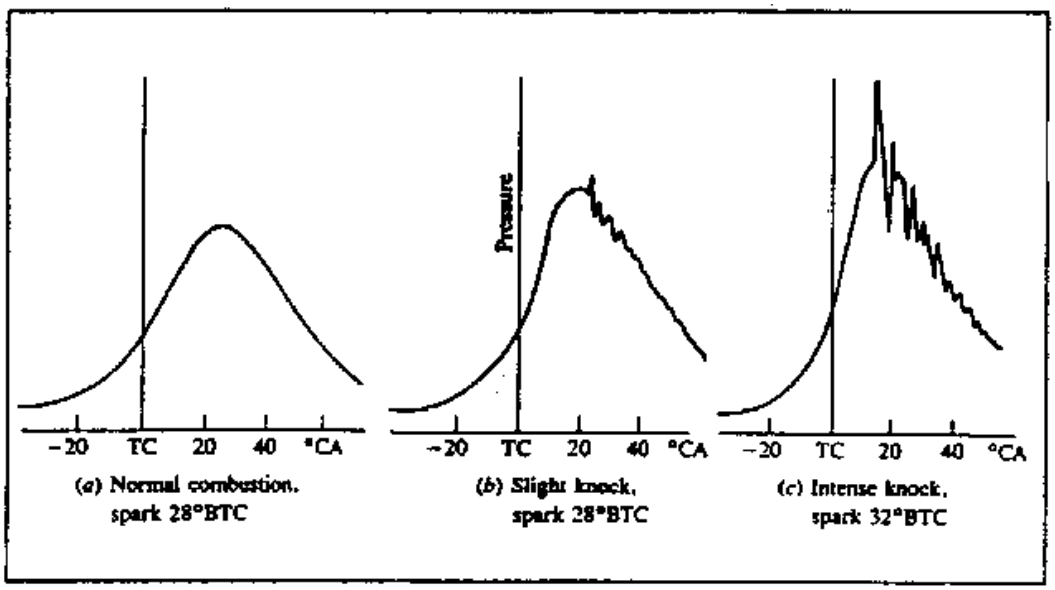

Figure 121 Spark advancing provokes bad knocking (169)

The HCCI combustion is meant to be homogenous so, instead of a single point of Start-Of-Combustion (SOC), like in the gasoline engine, or of a single burning surface, like in the Diesel engine, here there are thousands of ignitions point equally distributed in the chamber. This means that the burning of all the chamber is faster, because each flamelet has a small path before encountering its neighborhood instead of running alone all across the chamber, and that the instant pressure is higher than a traditional combustion, because all the charge is burning simultaneously. This last aspect is extremely critical because the pressure peaks can be twice or three times higher than a traditional combustion and it can be the cause of severe damage or even instant failure for the engine components.

Just to say that a bit of knocking is not an issue for an engine, if it is limited to few cycles, but HCCI combustion is meant to have always high pressures and, especially during the transient cycles from traditional to HCCI mode, these can be really dangerous (Figure 122). So, it is important to keep these pressures as low as possible, and this means that the fuel has to ignite with precise timings.

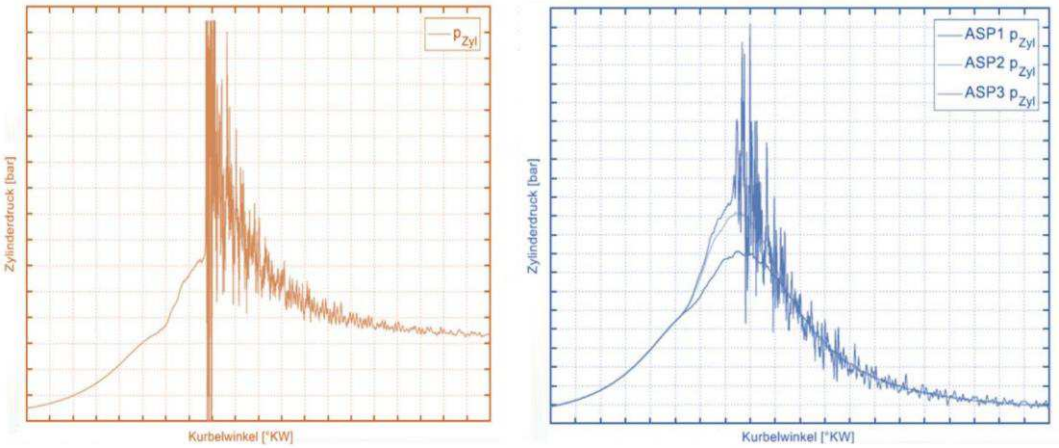

Figure 122 Instant bad knocking, due to uncontrolled mode-switching (red). Uncontrolled cycle-by-cycle mode-switch (blue). Axis units removed for restricted permissions.

As said at the beginning of this paragraph, it should be easier to convert all the World to ethanol, but this option is far from reality: if a new HCCI-like engine is going to be developed, it will use current gasoline as fuel.

Of course, commercial gasoline has been the first fuel to be tested but with scarce success; nevertheless, with accurate tuning of the recipe, it may even be achieved the correct formulation of HCCI-compliant gasolines, with lower flame speed and tunable ignition point.

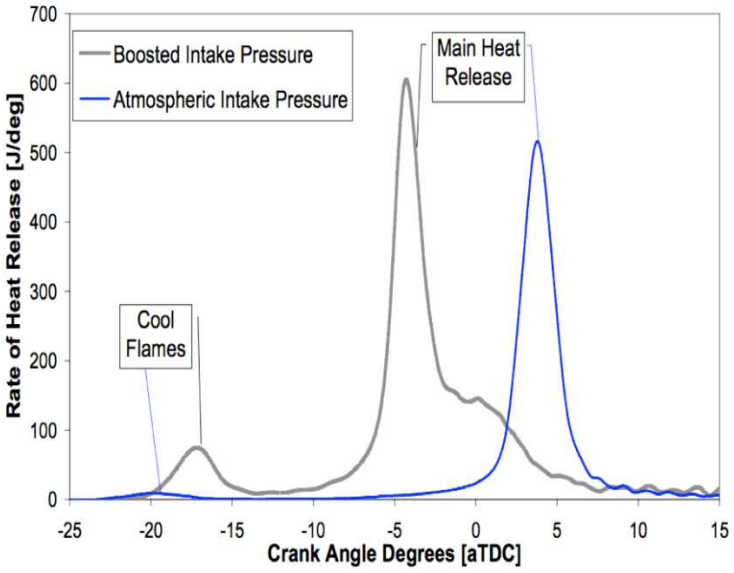

Figure 123 Normal combustion heat release (blue) and the completely different profile of an advanced combustion kindled by cool flames (grey). (170)

In particular, the ignition point is the most crucial factor of the two; the tunability of this fuel characteristic may derive from a full comprehension of the low temperature reactions. A funny fact is that, historically, gasoline has been developed to resist as much as possible to auto-ignition, mostly inhibiting low-temperature reactions which may lead to little exothermic phenomena called *cool flames* (Figure 123). These cool flames should be able to provoke an advanced ignition of gasoline, leading to engine knock. Current gasoline recipes try to provide a blend which acts like a *single-stage ignition* fuel; probably, a good HCCI gasoline should work like a *two-stage ignition* fuel.

A reasonable way to develop a good HCCI fuel gasoline without fancy chemicals and without shaking up the fuels market, the feedstocks, the economies and so on, would be adding ethanol to a proper base gasoline. This simple solution would have several positive effects:

- RON and sensitivity increase; this could allow to design engines with even higher compression ratio and, consequently, higher efficiency
- flame speed reduces, reducing the risk of engine damages
- cleaner combustion
- dual fuel blend: one component acts as a spark and the other quenches the flame

- ethanol is a renewable and sustainable resource
- ethanol can be the interface compound with water (i.e. for water injection); this could be eventually a drawback, since ethanol absorbs humidity and separates from gasoline, resulting in too much water in the tank bottom that can be risky for the engine next start.

The exact amount of ethanol in a HCCI fuel (from 10 to 85% as example) or, at last, the feasibility of a pure ethanol HCCI engine has to be investigated.

3.2.3 Virtual engines

At this point, all that is left to do is to work at the engine proofstand and execute a precise DoE with several types of fuels coupled with the above-mentioned strategies. Unfortunately, there is no one among the carmakers which can afford such a risky test campaign on the benchtest: each mistake can cost an engine and the hardware modifications needed to go along with the development can take months to be accomplished. Definitely, benchtest is not anymore the field of a development campaign for automotive rather than a mere validation test.

Nowadays, the development of a new engine goes with a deep work on virtual benches. Components design, assembly geometries, fluids dynamics, thermal management and even pollutant emissions can be developed or benchmarked with virtual engines. Only after encouraging results from simulations engines can be assembled and tested on real benches; this way, development costs have been dramatically decreased while the accuracy of the investigations and the engines quality has increased. All the carmakers, and other proactive actors in automotive, have developed - or used in license - software for the virtual development of their engines and surroundings (i.e.: FEV, Magneti-Marelli, GT-Power, Star CD but also Porsche, Daimler, VW, GM…).

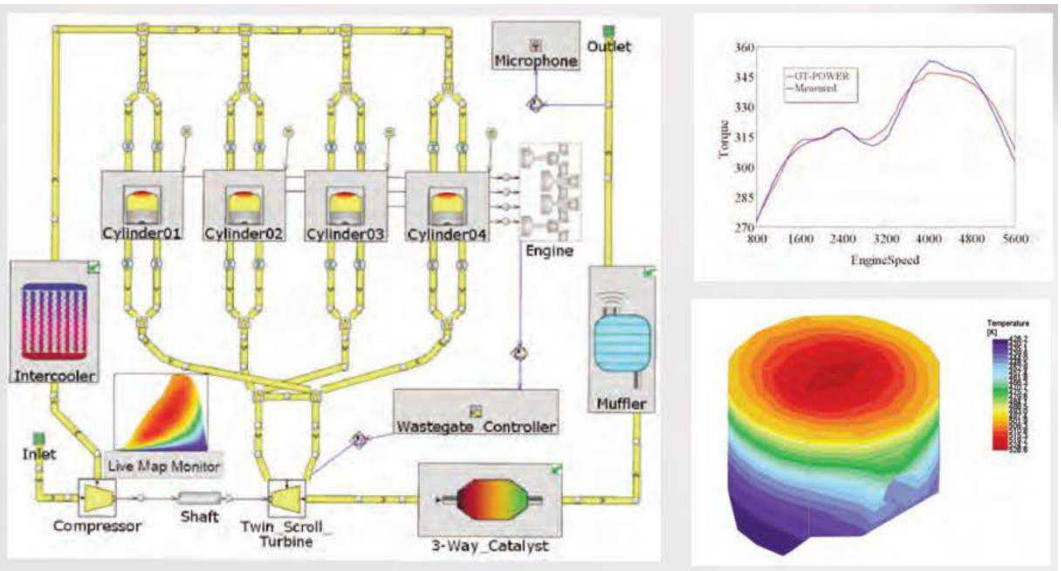

Figure 124 GUI and some 0D (up right), 1D (left) and 3D (down right) outputs from GT-Power suite, one of the most used virtual engine (from GTsoft website).

This approach was born with the introduction, from the '80s, of the Engine Central Unit, the on-board computer programmed to manage the engine during its uncountable operating conditions, without efforts from the driver. Only from 2000s these software gained enough reliability for these delicate tasks (171). Currently, there are several central units on-board, with specific tasks, running complex codes in real-time and this up-scaling allowed OEMs to differentiate models not anymore because of the engine but only for the instructions included in the code of the ECUs. These codes, compared to vehicles, engines and components, are unexploitable for the other competitors and actually are under severe intellectual properties regulations.

These ECUs run 0D/1D models[16], studied within 1D software environment and validated on real benches, to manage engines developed with CFD-3D!

	0D	1D	3D
Behavior	System dynamics as a function of time	System dynamics as a function of time and one dimension	System dynamics as a function of time and space
Type of model	Lumped parameter ordinary differential equations or differential-algebraic equations	Ordinary differential equations or differential-algebraic equations	Partial differential equations
Inputs	Component-connectivity model; component behavior models; context	Component-connectivity model; component behavior models; context	3D CAD configuration; material properties; context
Critical expertise	Model abstraction	Model abstraction	Grid generation
Typical use	Component sizing; design space exploration; preliminary verification of performance and function	Component sizing; design space exploration; preliminary verification of performance and function	Detailed analysis and verification of performance, risks, and failure modes
Common tools	MATLAB/Simulink, Modelica, C, Java, Excel	MATLAB/Simulink, Modelica, C, Java, Excel	Various open and proprietary CFD and FEA solvers

Figure 125 Characteristics and differences between 0D, 1D and 3D modeling approaches (172)

[16] 0D and 1D models could be based on ordinary differential equations (ODEs) or differential-algebraic equations (DAEs) that are easier to solve. By contrast, 2D and 3D models are based on PDEs, which are difficult to solve. The easier the calculus, the cheaper and faster the ECU, the better the engine control.

Developing a new kind of combustion for an engine which may be modified in some component or mechanism to go with the combustion itself is a complex task and would use 0D, 1D and CFD-3D modeling plus requiring a certain degree of freedom for the simulations developers. Such level of freedom is not always possible with commercial closed-source software, so the best scenario would be *to have your own software.*

QuickSim

Thanks to a partnership with FKFS[17] (Stuttgart, Germany), it has been possible to conduct these investigations with a special software, called *QuickSim*, for which the code was available to modifications. QuickSim is a 3D-CFD software (tridimensional Computational Fluid Dynamics) like many others available but with some interesting advantages; the first, for policy QuickSim is not available in licensing and its usage and development is strictly controlled by the original authors and the engineering students at the institute, and the last is that, unlike its competitors, it uses a coarse mesh and very few boundary conditions for its calculations, reducing simulations duration from days down to hours, with no issue for the accuracy of the results (171). The strict control over the software allows quick modifications and improvements with practically no delay from the request while the particular meshing technique allows to increase the precision only when needed and maintain the grid coarse elsewhere. The grid contains not only the combustion chambers but also the air-box and the exhaust system, so the boundary conditions are but unknown and therefore easy to manage in the equations. In about 20 years of activity, QuickSim (coupled with software like Star CD and/or GT-Power, for the graphical side) has been successfully employed to develop gasoline/Diesel/CNG engines, from series to motorsport, two and four strokes; adapting itself to each case study and with its intrinsic high speed of simulating, QuickSim is often able to follow the proofstand activities in real time, with even the capability of forecasting engines behavior. For all these reasons, this unique software has been lately chosen by some OEMs to develop HCCI-like engines. Further discussions about this topic will be found in this chapter.

[17] *FKFS - Forschungsinstitut für Kraftfahrwesen und Fahrzeugmotoren Stuttgart - (in English: Research Institute of Automotive Engineering and Vehicle Engines Stuttgart), is a private, nonprofit research and development institute for the automobile and supplier industry, focusing on vehicle technology, engine technology, and vehicle mechatronics, founded in 1930.* [Wikipedia]. FKFS is closely linked with IVK-University of Stuttgart.

3.2.4 Virtual fuels

Back to the topic, despite the diffusion and the success of these solutions, all the parameters regarding the combustion of gasoline (but this is true also for other fuels) are usually supplied as a *black box*, therefore the developer has no degrees of freedom when trying to swap fuels or to use exotic blends, which is right what is needed in HCCI development. There are of course some models describing auto-ignition and flame speed, but usually these are simple fittings of experimental data, so without new data (for new fuels), these equations cannot be modified on purpose. Furthermore, these models have been created based on generic gasolines which are representing a sort of average of all the recipes available on the market. Yet it is possible to develop traditional combustion engines, right thanks to the generic behavior of these gasoline models.

From a modeling point of view, a fuel is but a set of thermal, transport and physical data, an auto-ignition model and a flame speed model. However, there have been initially argues about the presence or not of a proper flame in HCCI engines, meant as a front, separating burned from unburned, advancing through the unburned. Finally, in HCCI combustion, it has been observed with chemi-luminescence based techniques that the combustion starts from the walls and propagates towards the center, right the opposite behavior of a standard SI combustion. So, the interpretation of the ideal HCCI combustion changed a bit. (143) For this reason, look-up tables (LUT) of flame speed for given fuels will be supplied as well as the essential auto-ignition LUT.

HCCI development needs to use slightly or utterly different fuels, so the first obstacle to stumble upon is: is it possible to find out there proper gasoline and other fuels flexible models to play with?

Actually, QuickSim uses – of course – a lot of models for its simulations (energy balance, working process, heat transfer, etc.) and of course there are some models of fuels, but these are not very suitable for HCCI investigations. As far as gasoline engines may concern, the flame speed of gasoline is described by Gülder's model and the ignition point is a setting from a look-up table.

Gülder's model (from 1984) allows to calculate the flame speed S_L of a generic RON90 gasoline as function of air/fuel ratio λ, pressure p, temperature of unburned gas T_{unb} and internal gas recirculation amount x_{exh}. It is, however, a mathematical fitting and not all the variables have physical meaning and are specific for each given fuel (Z, W, F_{exh}, ς) .

$$S_L(\lambda, p, T_{unb}, x_{exh}) = Z \cdot W \cdot \left(\frac{1}{\lambda}\right)^{\eta} \cdot exp\left[-\varsigma \cdot \left(\frac{1}{\lambda} - \Phi_m\right)^2\right] \cdot \left(\frac{T_{unb}}{T_{ref}}\right)^{\alpha} \cdot \left(\frac{p}{p_{ref}}\right)^{\beta} \cdot (1 - F_{exh} \cdot x_{exh})$$

Figure 126 Gülder's equation of gasoline flame speed. It is function of AFR, pressure, temperature and EGR (171). It is simply a fitting from laboratory tests data and some coefficients have no more than a mathematical meaning; for this reason, this equation is not very flexible when changing fuel. (173)

Up to now, this set of data has been successfully used for traditional combustion gasoline engineand so it will be in the future (as far a RON90 gasoline, the Gülder modeled fuel will be considered a standard). But if one would move from generic gasoline to something more sophisticated, it takes new experimental campaign in a laboratory (with that exact sophisticated recipe) to collect data for Gülder's flame speed and ignition point table (Figure 126). There is, for this particular study, the need of more flexible models about fuels.

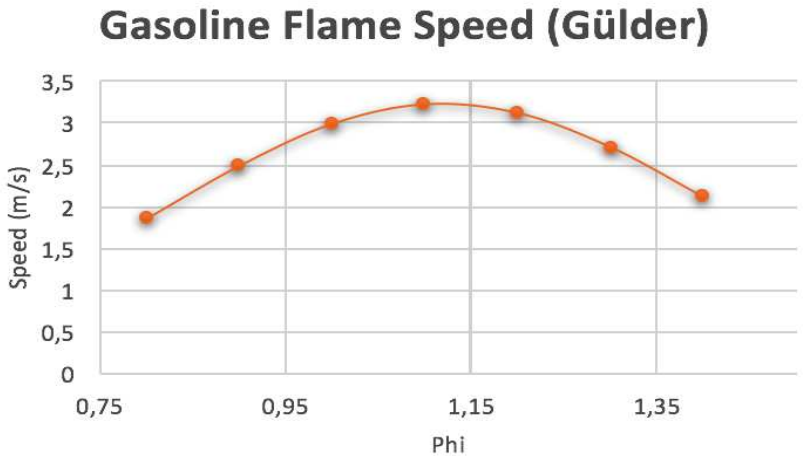

Figure 127 The generic flame speed curve obtained with Gülder equation and its data.

Up to date, QuickSim has no models for describing the auto-ignition of its gasoline, which is set directly by the operator, according to literature or experimental data.

An alternative approach to laboratory is to use thermokinetics and energy balance to describe how a bunch of hydrocarbons burns or ignites. This method, away from human errors, should be more reliable, quicker and cheaper than a real test campaign. The ideal reaction of hydrocarbon combustion follows this *generic reaction*:

$$H_xC_y + O_2 \rightarrow {}_yCO_2 + {}_{x/2}H_2O$$

which could be immediately re-written to go with real conditions, taking into account incomplete combustion and NO_x formation (it follows a *generic reaction* which cannot be balanced of course):

$$H_xC_y + {}_aO_2 + {}_bN_2 \rightarrow {}_cCO_2 + {}_dH_2O + {}_eN_2 + {}_fCO + {}_hHC + {}_iNO_x$$

It is intuitive that a generic hydrocarbon, and in particular long chain hydrocarbons like gasolines, do not turn into CO_2 immediately, but follow specific paths, which depend on the external conditions (pressure, temperature, reactants). Moreover, not all the possible paths are available for a given conditions and not all the conditions lead to the final state of CO_2.

A reaction path (so-called *mechanism*) is just the chain of intermediate reactions, from the start to the end of the combustion, that can be grouped at least in these generic steps:

- Initiation: reactants start becoming radicals
- Propagating: radicals and reactants are comparable in number
- Branching: radicals outnumber reactants
- Termination: finals products are formed consuming radicals

The initiation step is caused by the first decomposition of the reactants; propagation step involves a radical/molecule reaction with the generation of another radical; branching reactions produce more radicals per each radical in the reactions; and, finally, termination step reactions lead to the final products combining all the remaining radicals. Termination is not meant to happen every time. As example, the generation of a flame is due to branching reactions predominating over termination, with a large generation of radicals resulting in a fast decomposition of the fuel. (174)

The longer the chain, the longer the path. Thermokinetics mechanisms may get even more complicated when hydrocarbons are mixed together or when other kinds of species are involved in those reactions. Fuels, which are usually complex mixtures of hydrocarbons, can exploit different mechanisms according to the presence or not of a particular compound, and to its exact amount in the mixture.

Combustion kinetics mechanisms can be used inside engineering software like Ansys ChemKin, OpenFoam or Cantera, within which one can design proper reactors and set specific boundary conditions where the reactions can take place. Each mechanism must be followed by thermal data and transport data of each species considered in all the reactions; considering the energy of the system at its final state and the conditions of the reactor, these software can scan the mechanism, searching for the most stable state, that is the right direction thorough the reactions path leading to termination. The complexity of the reactor can be a reason for dead slow calculation, so this is a crucial factor to keep in mind.

Because of this complexity, the first approach was done using gasoline surrogates such as PRF and, later, TRF. Detailed and simplified mechanisms for these generic gasolines are largely available and are actually successfully used to describe combustion phenomena which are not strictly focused on the fuel composition (heat transfer, reactors design, etc.).

Of course, these basic mechanisms cannot describe even closely the complexity of fuels auto-ignition neither the complexity of a real gasoline recipe and its blends. It takes different mechanisms, still simplified - for the sake of speed - but with more components than PRF and TRF surrogates (two and three, respectively).

3.3 Cantera

Before focusing more into fuels related topics, it is worth mentioning the environment which hosted all these simulations: Cantera.

Literally, from Godwin et al., 2017 (175):

Cantera is a suite of object-oriented software tools for problems involving chemical kinetics, thermodynamics, and/or transport processes.

Cantera provides types (or classes) of objects representing phases of matter, interfaces between these phases, reaction managers, time-dependent reactor networks, and steady one-dimensional reacting flows. Cantera is currently used for applications including combustion, detonations, electrochemical energy conversion and storage, fuel cells, batteries, aqueous electrolyte solutions, plasmas, and thin film deposition.

Cantera is a 0D-1D CFD software kit, made of C++ codes, aimed to build reactors, and even networks of reactors, to investigate on thermodynamics, transport properties and thermokinetics of reacting systems. It is supplied as an open source module for Python and for MatLab but the majority of features are only available via the Python shell.

It has been chosen instead of OpenFoam and Ansys ChemKin for its being open source (that is, open to modifications), well supported by the community, flexible in reactor design, *less* hardware demanding than the competitor and reliable in results. Graphical output can be obtained adding proper packages to the Python/Cantera setup after the installation.

The reaction mechanisms useful for these investigations can be the same as for Ansys ChemKin, which are the most spread, although converted from .ck to .cti format with the supplied converter. Conversion however, is but flawless and every line of the mechanism has to be checked manually after each run, until all the errors are corrected.

For the flame speed script, the reactor has a constant volume design with a 1D grid set to count speed. The system considers the H_2O generated from the combustion and can evaluate the influence of a simple EGR made of N_2/CO_2. A steady,

laminar[18], 1D pre-mixed[19] flame is kindled at precise reactor conditions (temperature, pressure, EGR, lambda) and runs across a grid which describes the reactor length. The resolution of the grid is also settable. The time it takes to cover the points of the grid sets the speed. From a standard example reactor, in bundle with Cantera's package, Hann et al. developed a better one, aimed to evaluate the ignition point of methane for automotive applications (176) (177); the current auto-ignition script used within this thesis, which is capable now to work with gasoline surrogates, has been derived from that version.

The auto-ignition script uses a zero-dimensional, constant volume reactor; it is considered homogeneous both in composition (no other species can be added to the system) and, of course, conditions. An EGR fraction made of N_2/CO_2 can be considered, as the effect of combustion H_2O in the mixture, but it has the same temperature and pressure of the other reactants. The reactor conditions are set and the time it takes for the fuel to auto-ignite, depending on its low and high temperatures reactions, sets the auto-ignition timings. The ignition is defined as the point at which the system has a temperature 400 K higher than the previous state. As for the other script, starting from the basic reactor provided as sample in Cantera, Urban et al. developed a more complex script to study the flame speed of CNG fuel; from this script, a new version for gasoline surrogate fuels has been developed and finally used for this work.

In the last script, Cantera evaluates the energies of the intermediate reactions with the energies of reactants and final product (equilibrium state problem). If these are compatible with the boundary conditions of the reactor, a specific path of reaction is selected instead of another.

[18] not influenced by air streams
[19] mixed before ignition

3.3.1 Kinetic Mechanisms

A kinetic mechanism is a collection of data related to a certain number of chemical species, usually about their reactions and their thermal and transport information. (178)

To solve a combined flow-diffusion-reaction problem it takes a comprehensive collection of data about reaction stoichiometry and rate constants, reaction thermo-chemistry (ΔH, ΔG, ΔS), thermodynamic properties (heat capacity ratios, enthalpy, density) and transport properties (diffusion, viscosity and thermal conductivity).

In literature, different types of kinetic mechanism can be found: PRF, TRF, ethanol, bio-Diesel, gasoline surrogated and blends mechanisms can be downloaded or purchased from academic groups websites or from private laboratories repositories. The first characteristic is about the number of species and the number of reactions included. The higher these two numbers, the more accurate the modeling, but the hardware demanding increases too! For this reason, some mechanisms can be provided as *detailed* or *reduced*, depending on the numbers of reactants and reactions.

Moreover, in these applications, there are two main conditions:

- Auto-ignition, regarding low temperatures reactions
- Flame speed, involving high temperatures reactions

Usually, mechanisms are developed with specific purposes and it is hard to find one which is enough detailed to rise accuracy but reduced, not to be a burden for the hardware and, most of all, to find one which combines the sets of low-temp reactions with the high-temp reactions right for the application object of this study. Unless developing a brand new, tailored, kinetic mechanism, of course[20], which would be utterly off topic.

A kinetic mechanism needs of course to be validated with laboratory data, using particular rig like Rapid Compression Machines or fast camera equipped burners. Once it is validated, the works involving those mechanisms are generally considered validated as well. One of the ending goals of this work is to complete

[20] This would be a really tricky task…

the set of models of virtual engine tools (like QuickSim) in order to use directly the engine as validating instrument for the models.

So, the very first step, before letting the Cantera session begin, is to scout out a proper kinetic mechanism. One of the most influential institute worldwide, which usually provides these particular mechanisms, is the Lawrence Livermore National Laboratory (LLNL), while in Italy there is the CRECK group at Politecnico di Milano, which also provides some interesting fuel kinetic mechanisms.

Among basic gasolines like PRF and TRF, there are more complex reactive sets about gasoline surrogates; in particular, the LLNL reduced mechanism has 323 species, the detailed one has 679 species (with 5627 reactions) (179). CRECK has 153 species in reduced version and 1389 in detailed version (with 3465 reactions) (180). Furthermore, the same mechanism can be supplied with the same species number but a lower number of reactions.

It is worth noting that, at the time of the simulations test campaign, the scripts were running on an Intel i7-6700k/32GB-RAM/500GB-SSD machine (high-end hardware, ~100GFlops) and it was not even capable of charging the detailed mechanisms on RAM before starting the code. Both LLNL and CRECK mechanisms could have been used in the reduced edition but the number of species/reactions has not been considered adequate, because they missed some of the ingredients considered as crucial for a good gasoline surrogate, as further discussed.

Finally, a third kinetic mechanism has been used to investigate on gasoline surrogates; it is indeed a more detailed edition of the Lamoureux mechanism (181), particularly recommended for NOx formation studies, improved for first by Pitsch et al. (182) and finally by Fandakov et al. (183), who also validated the results.

This mechanism resulted to be lighter for the PC hardware since it has 483 species and 2155 reactions and, most important, it allows to reproduce the designed gasoline surrogate recipe.

3.4 Gasoline surrogate

If PRF and TRF, two real gasoline surrogates, barely describe their reference fuels, how can PRF/TRF mechanisms be expected to work with accuracy?

From the reactants list of the Lamoureux mechanism, only few should be sorted to create the "virtual fuel recipe", just for hardware management, and those few have to be relevant in describing low and high temperatures reactions behavior, negative temperature coefficient (NTC)[21], etc.

To improve the describing capability of the Python scripts, a new virtual gasoline recipe has been developed and then implemented in them. The generic formulation of a commercial gasoline has been dissected into its main compounds groups and the most representative of each group (in gasoline applications) would have been chosen, among those available in the kinetic mechanism. Actually, in the revisited Lamoureux list, all the designed compounds were present with no embarrassment, like looking for inadequate alternatives.

This collection of compounds should allow to generate gasoline surrogate formulations way more detailed than basic PRF and with the same advantages of TRF in terms of RON and sensitivity evaluation. Addition of napthenes and olefins improves the accuracy of the models and keeps the surrogates closer to real fuels formulations. Ethanol blends are also possible, opening opportunities for evaluations and studies of dual fuels and greener fuels (and, not least, even to motorsport oxygenated gasolines).

Beside the final goal of the detailed surrogated fuels' LUT for QuickSim, some investigations about the properties of ethanol blends have been carried out, modeling ethanol additivated TRF fuels, from 15% to 85%, and pure ethanol itself.

[21] NTC (further focused) is a mechanism for which, in a typical timing/temperature auto-ignition plot, there is a central region where the decreasing timings invert the trend and start rising again, like the fuel were more resistant as temperatures rise. If this happens, that fuel has a formulation that expresses differently in low and high temperatures and the inverted trend is the mark of the switch from a behavior to another. Typically, paraffines and alkanes show evident NTC regions and these are considered to be relevant in the formation of cool flames, a hot topic in HCCI applications, but above all an essential feature of a fuel.

Table 16 Components of a new gasoline surrogate virtual fuel

Name	Type	Mech. ID
iso-Octane	isoparaffine	IXC8H18
n-Heptane	paraffine	NXC7H16
Cycle-Hexane	napthene	C6H12X1
2,4,4-trimethyl 1-pentene	olefine	IXC8H16
Toluene	aromatic	A1CH3
Ethanol	oxygenated	C2H5OH

3.5 Auto-ignition

As said, because QuickSim is not provided with a flexible but accurate auto-ignition model (but just a simple trigger), the first move of this activity has been to use the Python script, the Fandakov's mechanism and the six-components surrogate recipe to build some look-up tables (LUT) about auto-ignition timings of selected fuels.

Generally, the LUT have four dimensions; following, the four arrays:

- Temperature (500: 20 :1200 K)
- Pressure (50, 100 and 150 bar)
- Lambda (0.8: 0.1 :1.8)
- EGR (0 and 50%)

Actually, to check the accuracy and reliability of the script, a characterization of its outputs has been done with simpler, quicker, PRF and TRF surrogates. This approach allowed to understand more about virtual fuels characterization and, in general, fuels characteristics step by step, from the basic surrogate to the detailed one.

Negative Temperature Coefficient

At first glance, the auto-ignition plots of most of these virtual fuels show an evident change in behavior, with a sort of bell in the middle range. This is called Negative Temperature Coefficient region.

When the temperature increases, the auto-ignition delay of a mixture fuel-oxydizer usually decreases. For some compounds, leading ahead from low to high temperatures ranges, there is an intermediate state where the ignition delays invert their trend and start increasing, like as temperatures were falling (but they are augmenting). This negative interval can last about 200-300 K then the decreasing delays reappear, restoring the normal trend. As said, that region is called Negative Temperature Coefficient (NTC) and it signs the switch from a low temperature ignition kinetic to a high temperature ignition kinetic and it is a characteristic of high alkanes.

Literally, from Prince et al., 2011 (184):

The development of an NTC zone arises from the reversible addition of an oxygen molecule to the alkyl radical, not just once, but twice. To see how this may be possible in the simplest terms, let R denote the alkyl, I the intermediate produced by the first addition of oxygen to R, and J the radical resulting from the further addition of oxygen to I. Unlike I, the intermediate J is sufficiently active that it always obeys a good steady-state approximation, and besides its dissociation to I and O_2, it also decomposes to a third intermediate K (an alkyl-keto-hydro-peroxide), which leads to chain branching. With this scheme, it is possible to explain the NTC and two-stage ignition phenomena.

When two alkanes exhibit their ignition kinetics, the initial trends at low temperatures can be associated to low loads, RON conditions and they can be ranked as the more "ignition resistant" according to their ignition delay. What is remarkable with NTC-showing fuels is that, at high temperatures - that can be related to high loads (MON conditions) - the less RON performant fuel can close the gap with the other one, thanks to a wider NTC. This behavior indicates that the recovered fuel can stand more the switch from RON to MON modes. As explained in the previous paragraphs, sensitivity has an important role in fuels combustion (and, in particular, in HCCI combustion) and, from the virtual model point of view, the description of the NTC region should be the most accurate. In this sense, Fandakov mechanism gives back interesting results (Figure 128).

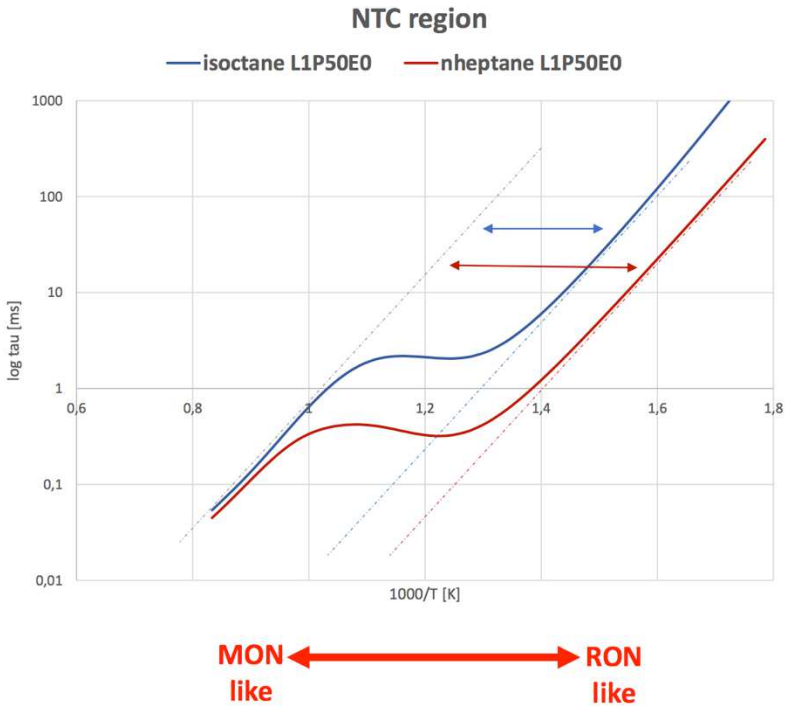

Figure 128 Negative Temperature Coefficient of iso-octane and n-heptane. The plot is overlapped with RON/MON conditions graph with sensitivity indicated by the arrows.

Pressure, EGR and Lambda influences

Considering the idea of not changing fuel at all, of designing an HCCI-like engine able to run with traditional RON95 gasoline, what parameters the engine technology should be able to control in order to control the auto-ignition triggered combustion? Intake pressure and temperatures, charge mixture, injection timings and strategies, spark advance (for Spark Assisted Compression Ignition engines), cooling strategies, charge dilution and Valves timings are the active ways with which a modern engine can be tuned during its operations[22]. Some of these are based on thermal effects and their influence on fuels cannot be investigated directly in CANTERA, it takes a CFD tool (like QuickSim) instead. The non-thermal effects which can influence ignition kinetics of fuels are pressure, dilution and mixture.

[22] Intake pressure and Valve Timings are a smart way to vary the compression ratio from the designed one, without implementing expensive mechanical solutions. A *fake* compression ratio can be achieved by decreasing the power of the compression stroke opening the valves or by increasing the amount of air into the cylinder with an air boost.

Mixture stoichiometric ratio is an effective and immediate way to control the auto-ignition timings of gasoline (Figure 129). As lambda increases, timings increase too, as the fuel were more and more knock resistant. The NTC region keep its temperatures range, as the lambda effect only influences the reactions speed and the flame stretching, not the fuel kinetics.

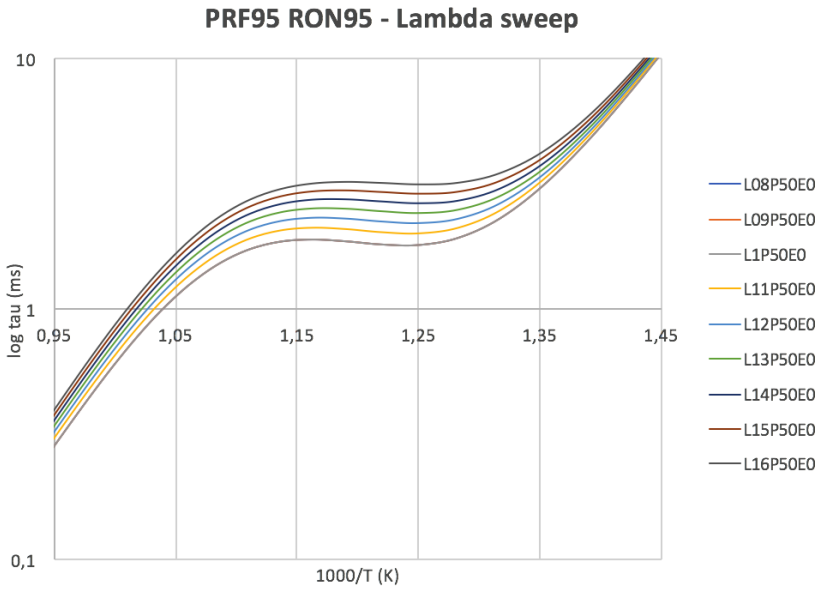

Figure 129 Influence of lambda to auto-ignition and NTC of a PRF95, from L 0-8 to L 1.6

The other simple way to regulate the auto-ignition of gasoline is to control the intake pressure. Nowadays, a very large quota of vehicles is equipped with turbochargers, from city cars (as consequence of downsizing), to Common Rail Diesel (where turbochargers made a revolution) to high-end sporting vehicles (for performances and torque sustain) so, control over intake pressure is but an issue at all. In particular, high pressures let the auto-ignition delays decrease, resulting in a more reactive fuel (Figure 130). Of course, the fuel cannot distinguish if the pressure is raised because of the piston or of another agent (somehow the same principle of SACI engines, where the pressure of the first kindle helps the auto-ignition of the remaining unburned charge). NTC regions still untouched.

Finally, in Figure 130 and Figure 131, it is possible to see how the effect of a cold EGR calms gasoline, with lower auto-ignition timings. One should clarify the differences between hot and cold EGR: cold EGR is an exhaust recirculation from

outside the cylinder, through a heat exchanger (intercooler), its ingredients are also unburned radicals, but its temperature cannot trigger any reaction; hot EGR is a quota of burned gas entrapped (for purpose) into the cylinder thanks to opportune scavenging strategies, like variable valve timings. The hot EGR contains the same radicals as cold EGR, but these do have the power of ignite the fresh charge. Actually, it is considered feasible to run an engine up to 50% of cold EGR, while it is considered risky, because of uncontrolled fuel auto-ignition, to go above 1% of hot EGR[23].

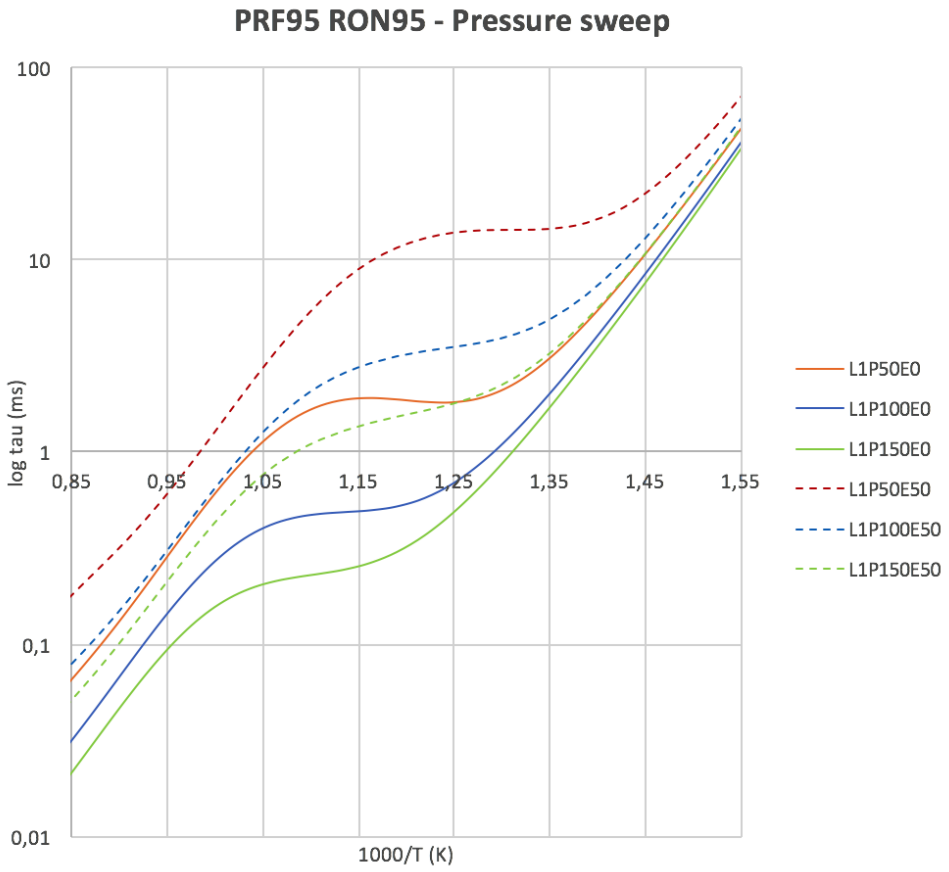

Figure 130 Influence of pressure to auto-ignition and NTC of a PRF9

[23] There are, actually, engine designs which use the reactivity of hot EGR to trigger the combustion: these engines are called Reactivity Controlled Compression Ignition (RCCI). (189)

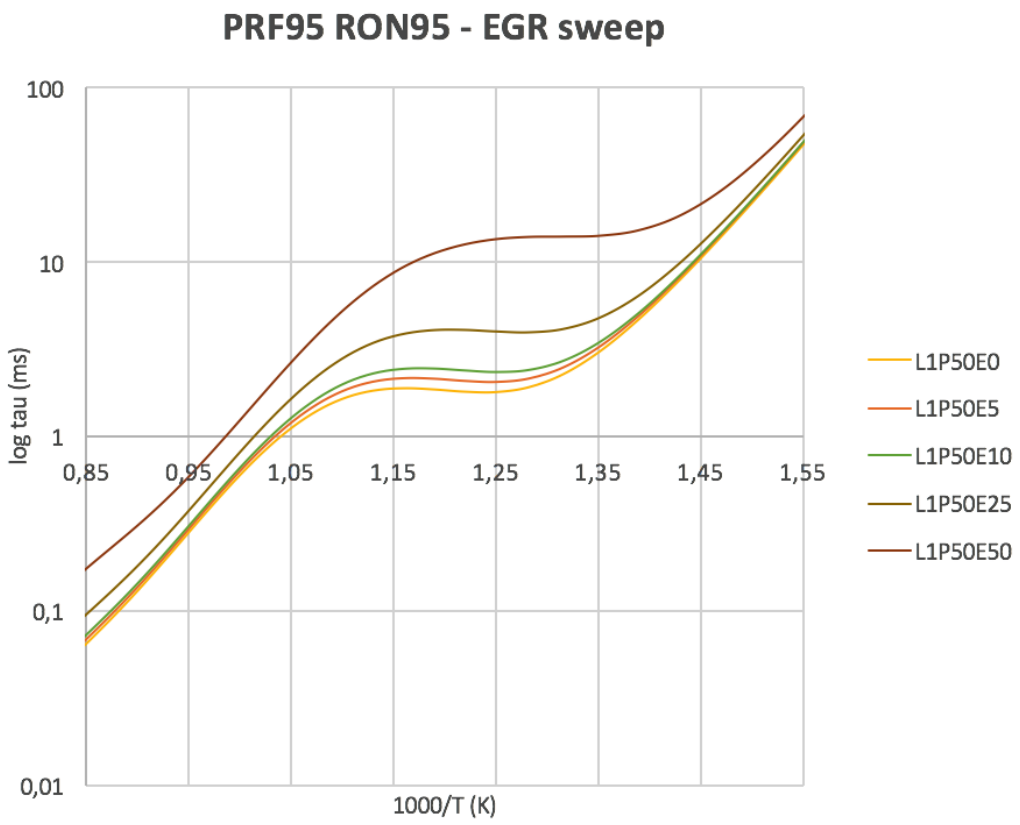

Figure 131 Influence of cool EGR to auto-ignition and NTC of a PRF95

Ethanol blends

If ethanol, as said in the previous paragraphs, is meant to be one of the best alternative fuel for HCCI-like engines, it is worth trying to understand more about its auto-ignition characteristics. Ethanol is known as an oxygenated, high knock resistance fuel and, comparing its ignition plot with the other component of a traditional high RON surrogate like TRF, it seems that this property is well confirmed. Moreover, in Figure 132, the fact that toluene is considered to have a higher RON/MON even than ethanol is confirmed as well; these plots, of course, have been gained with no prejudice about fuels RON/MON, but just on their chemistry and kinetics. A last important characteristic of toluene and ethanol is that they have no NTC region, that means that their combustion kinetics is not different from low to high temperatures.

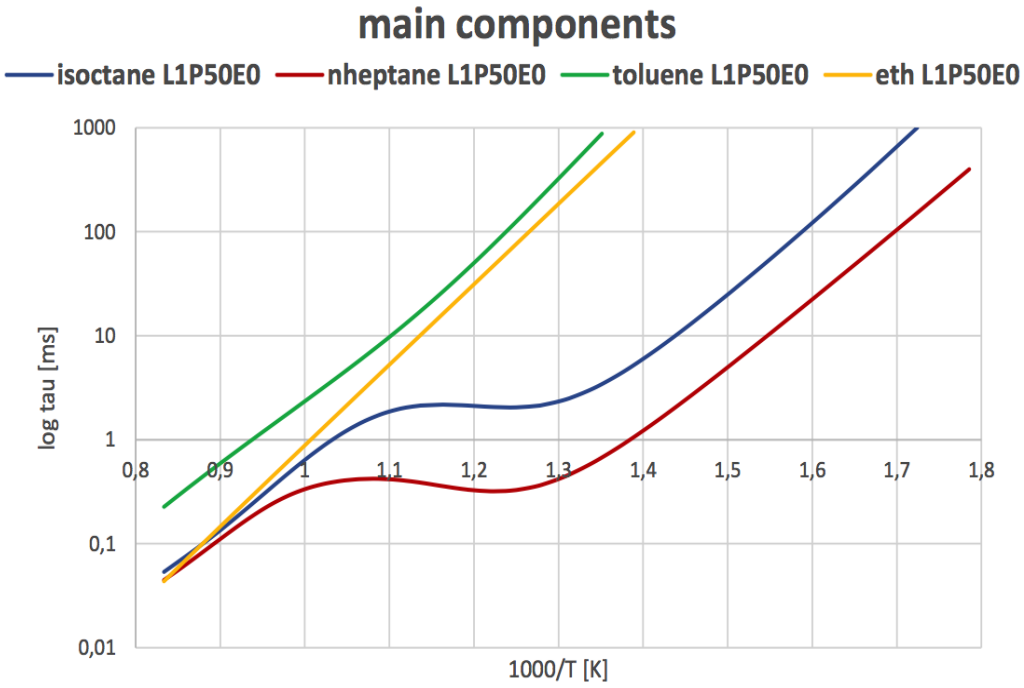

Figure 132 Auto-ignition profiles of the main components of TRF-Ethanol virtual fuels

Currently, some ethanol blends are already commercially available at the pump station, with comparable RON/MON numbers than pure gasolines, despite adding ethanol to gasoline does increase its numbers. The reason for this is that the base gasoline has a poor quality and ethanol is added not to increase final RON/MON, but to let them arise to levels that could be acceptable for modern engines.

However, ethanol-added gasolines are an interesting opportunity and a series of blends made of TRF40 and absolute ethanol have been simulated with CANTERA (Figure 133).

Firstly, absolute ethanol is for real, as ethanol is mixable with gasoline but also with water, while gasoline and water are not. This discrepancy may lead to huge practical problems: an ethanol blend, stored in a tank for enough time to let it absorb humidity, may reach the separation point from where the heavy water settles on the tank bottom, where the spill of the pump is installed. Injections of water into a *not water-ready* engine is extremely dangerous for its integrity. Of course, this problem does not exist for pure ethanol used as fuel, but it could even be an advantage since the water does act as octane booster in the compression stroke and as a flame quencher in the power stroke.

Finally, the addition of ethanol to TRF40 leads to increased auto-ignition timings, because alcohol is an octane booster. When ethanol reaches about 85% of the blend, NTC region seems like disappeared but there still is a valuable dual-mode behavior. E85 could be an interesting fuel in HCCI development since it has ethanol as main ingredient, which is knock resistant, oxygenated and water proof, and a small but still countable share of less knock resistant gasoline. This gasoline quota would ignite easier than ethanol and could act as a homogenous kindle in the chamber.

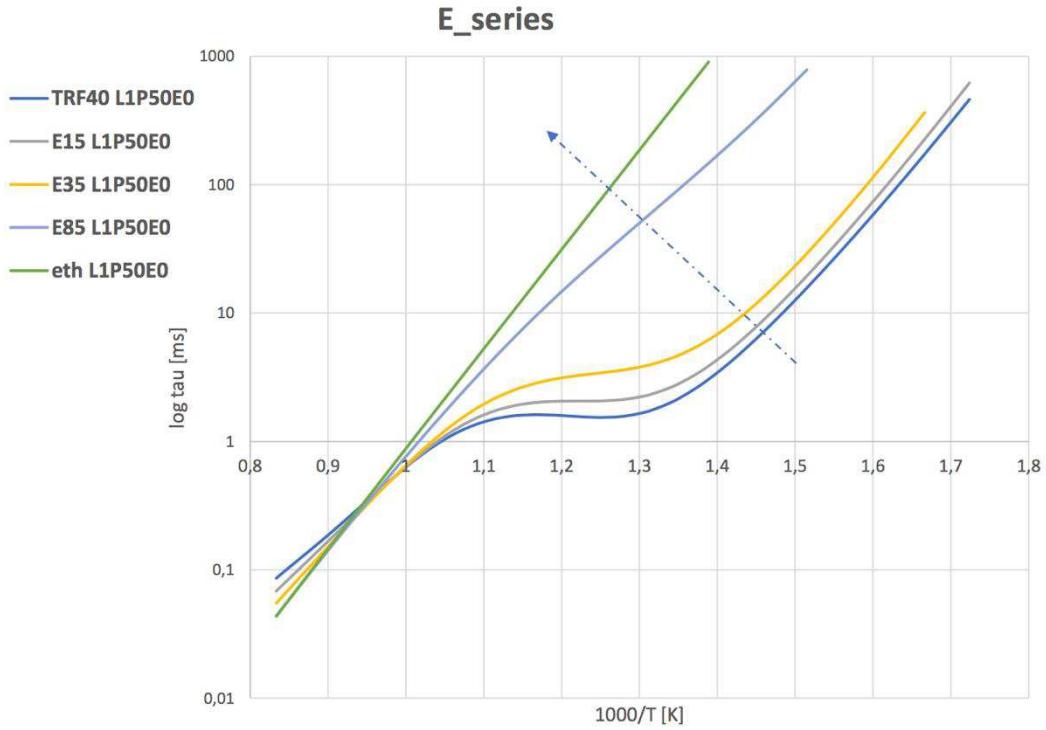

Figure 133 Auto-ignition profiles of Exx ethanol blends, from 0% to 85% and pure ethanol

Finally, in Figure 134, auto-ignition behavior of the proposed six-components gasoline surrogate is showed and compared to the traditional PRF and TRF surrogates. The difference is pretty clear, since the addition of iso-octene and cyclohexane, on purpose to retrace a real gasoline specification, leads to a completely different curve shape, where the NTC region is less evident and smaller.

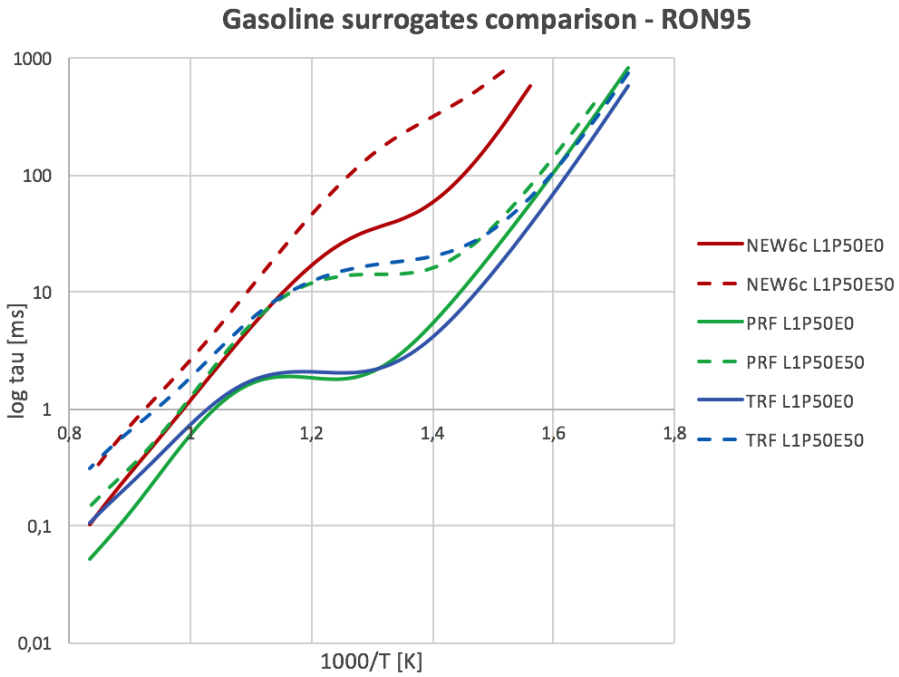

Figure 134 Comparison between auto-ignition profile of PRF, TRF and the new six-components gasoline surrogate New6c (all RON95) with and without cold EGR effect.

Cold EGR and Water injection

Two last investigations have been done about fuels auto-ignition in Cantera. A first about water injection and its capability to keep the charge calmer during compression stroke, like increasing the octane number, by absorbing part of the compression heat. Within Cantera, which only care about chemistry and kinetics, such thermal effects are not evaluable and those incredible small differences, noticed from data analysis, have to be explained with some kind of participation of water to intermediate reactions, slowing down some reactive steps of the reactants or radicals.

Absolutely in topic with Cantera is the investigation about cold EGR, here featured by CO (Figure 136). Despite CO radicals are considered to be enough reactive, the EGR temperature is the same of the rest of the mix, so the final triggering effect is way lower. Nevertheless, tiny amount of CO is able to reduce the auto-ignition delays compared to inert EGR, proving that exhaust external recirculation can act as an intermediate agent to control the combustion.

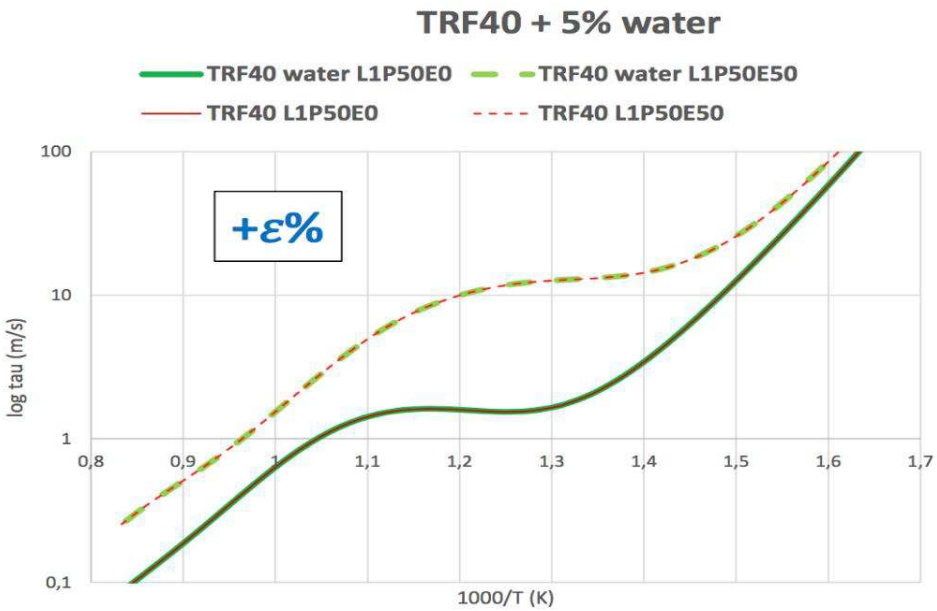

Figure 135 Effects of water injection on auto-ignition of a TRF40 fuel (RON90) in Cantera. Since the reactor is homogeneously mixed, there are only slightly quenching effects from water addition. These heat transfer investigations can be made in QuickSim instead (CFD)

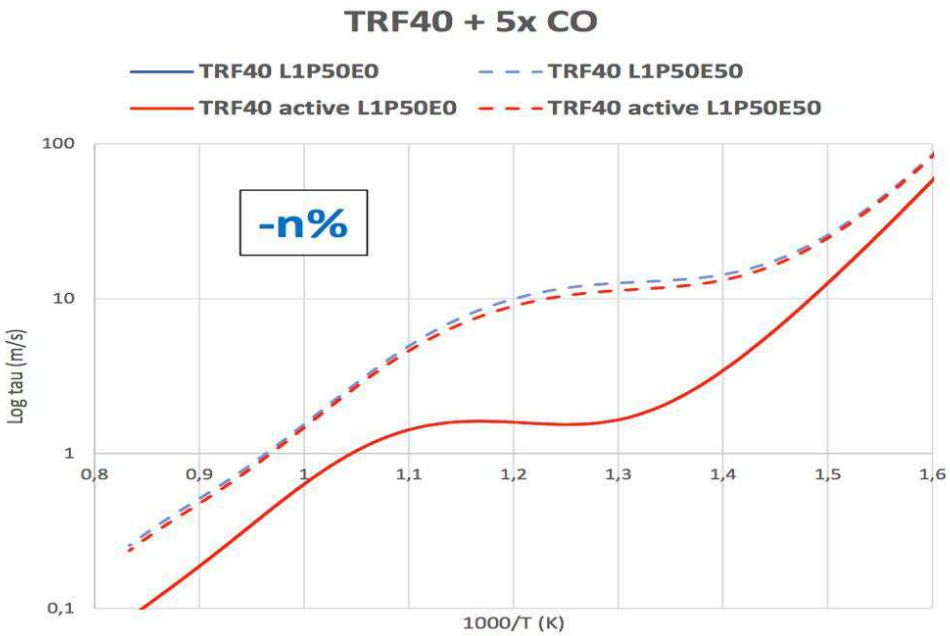

Figure 136 Effects of active EGR (CO addition) on auto-ignition of a TRF40 fuel (RON90) in Cantera. CO in the inert cool EGR changes the reactants ratio and can move the kinetics path considerably. Effect of hot CO radicals (hot EGR) cannot be simulated in this reactor: it takes a reactors network in Cantera.

Auto-ignition model validation

Of course, Fandakov mechanism has been validated by its author with experimental data, using a Rapid Compression Machine; one of the final goal of this task is to let QuickSim validate its fuels model using directly the engine testbench: if the bench data are the same as in the virtual engine, the fuel model must be effective and valid.

Figure 137 depicts the differences between Fandakov and CRECK gasoline mechanism. Both derive from Lamoureux and LLNL respectively, so these last two have not been added to the comparison, since they would result almost overlapped.

The most relevant differences are to be found in how the mechanisms describe the NTC region and how different fuels behaviors are represented. A PRF fuel, with CRECK mechanism, seems to have lower timings than Fandakov's; a TRF CRECK surrogate seems to have lower timings than Fandakov's.

NTC regions of the two mechanisms are slightly different but still comparable and with the same range. Keeping in mind that a six-components gasoline surrogate would be extremely hard to get with a high-end PC hardware if based on LLNL-CRECK mechanism, the value of Fandakov's is finally clear and contingent discrepancies can be accepted for the sake of speed (not to mention that Fandakov's can be used, for some extent, also for flame speed investigations, which would keep the data set more congruent).

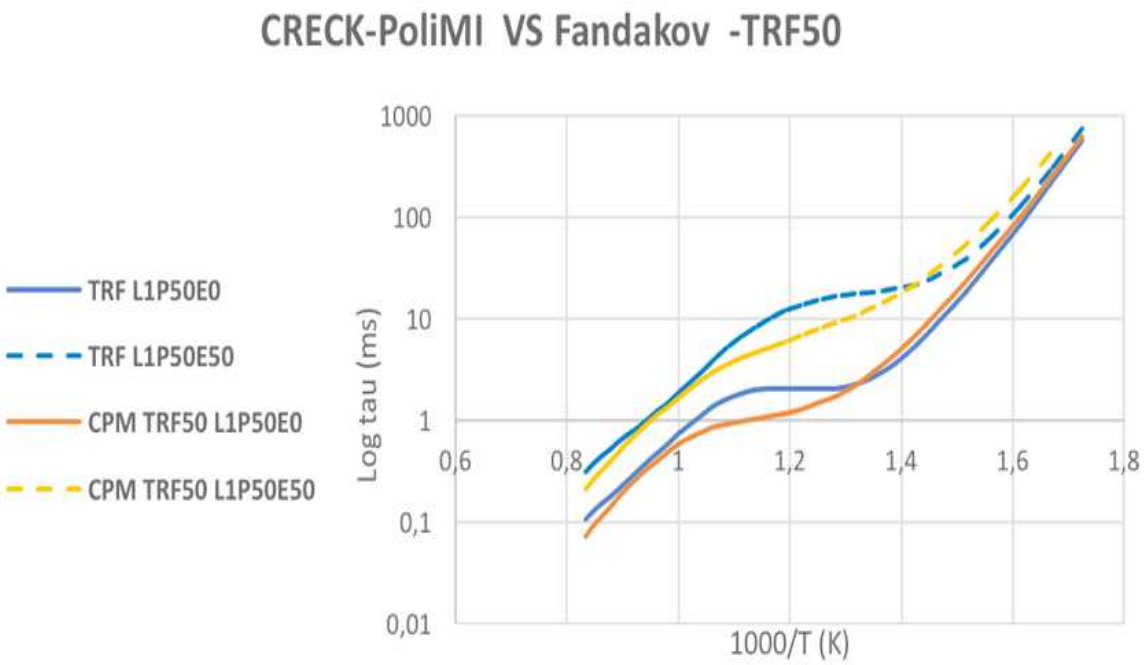

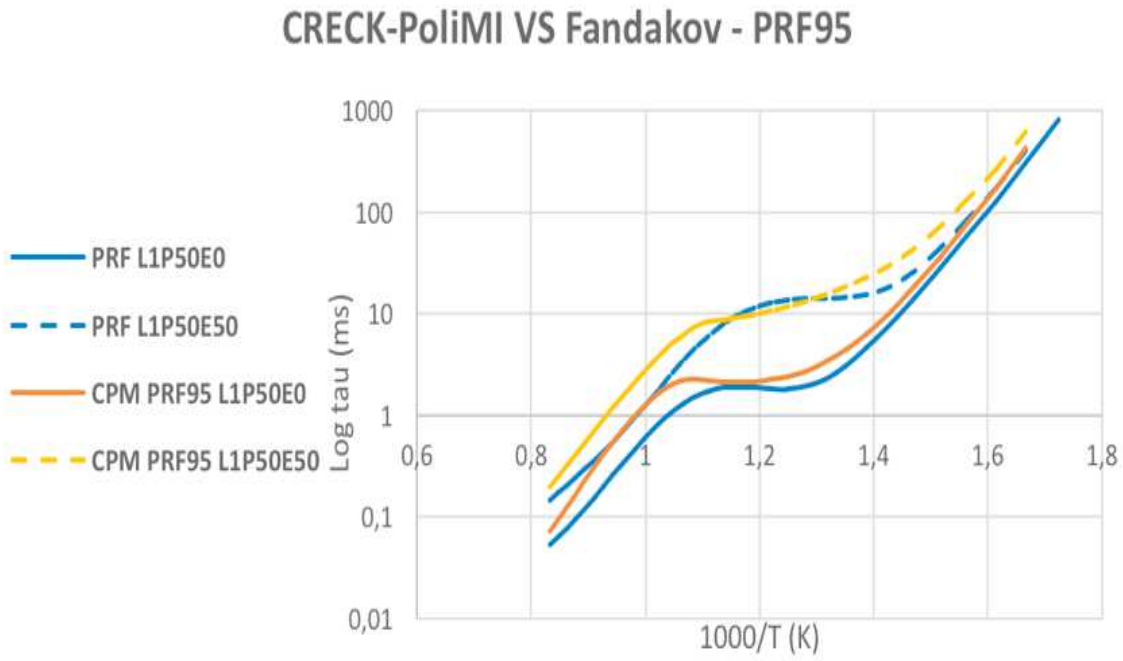

Figure 137 Comparison between auto-ignition output of two different reference fuels from CRECK (modified LLNL) and Fandakov mechanisms (fuel components are the same)

3.6 Flame speed

To complete the new fuel data set of QuickSim, also flame speed has been investigated, with the same approach as auto-ignition: a more reliable and real recipe, a reliable mechanism and a smart Python script for Cantera.

As already said, QuickSim already has a flame speed model, based on Gülder work, which is representative only of a RON90 pure gasoline. This model has been used successfully for years and it would be even used for other decades, but it is not suitable for investigations regarding other types of fuel, like HCCI just to give ax example.

Comparing Cantera and Gülder flame speeds, it seems that Gülder offers higher values (Figure 138); this is not acceptable in HCCI investigations since high flame speeds could be source of misinterpretations in QuickSim and lead to inexistent knocking and detonation phenomena.

Moreover, Gülder model always asks the operator where the maximum on the lambda axis is so, if the operator does not know this information, the calculation is impossible or unreliable; eventually, Gülder is not able to calculate the flame speed when EGR is over about 40%, limiting the opportunities of investigation.

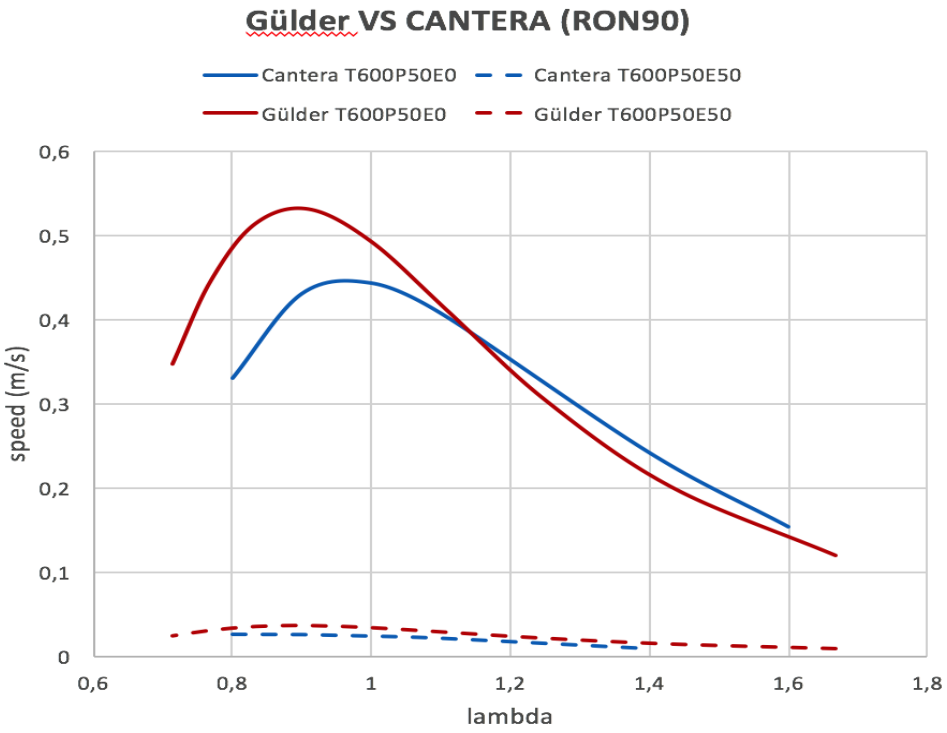

Figure 138 Flame speeds from Cantera and Gülder model compared, with and without EGR.

In Figure 139, a partial result of the four arrays scan in the Python script are depicted for a TRF40 surrogate fuel (temperature, pressure, lambda, EGR). A TRF40, with 40% of toluene, has about RON90 and can be directly compared with Gülder's fuel. As expected, flame speed increases as temperature increases while it decreases as pressure rises and squashes the flame itself. Cold EGR simply slows down the flame. These behaviors were expected.

What is unpleasant and awkward to notice is that, after weeks of calculation time[24], some outputs are not complete; not all the arrays length has been scanned or even skipped totally. This is actually a feature of the Python script, for which if the scan of a grid is not successfully fulfilled, instead of stopping everything or maybe crashing, the code simply skips to the next step until it finds stability.

[24] For the six-components fuel, Auto-ignition script scans the four arrays in two days while the flame speed script takes three weeks for the same recipe, mechanism and arrays.

It seems that the main cause of this inconvenient is poor hardware. Since the computer where the scripts are run is a i7-6700k/16GB-RAM/500GB-SSD (~100GFlops), it is clear that these flame speed calculations need a really powerful hardware, much more like a cluster than a simple workstation. In the preliminary steps of this task, many points of the arrays and even many entire arrays have been skipped by the script for the sake of stability.

Flame speed of ethanol blends, when calculated with Cantera, are more convincing. Finally, ethanol has the right flame speed (universally considered as higher than gasoline) and the blends' characteristics can be described with all their peculiarities (Figure 140). Kinetics seems absolutely more reliable.

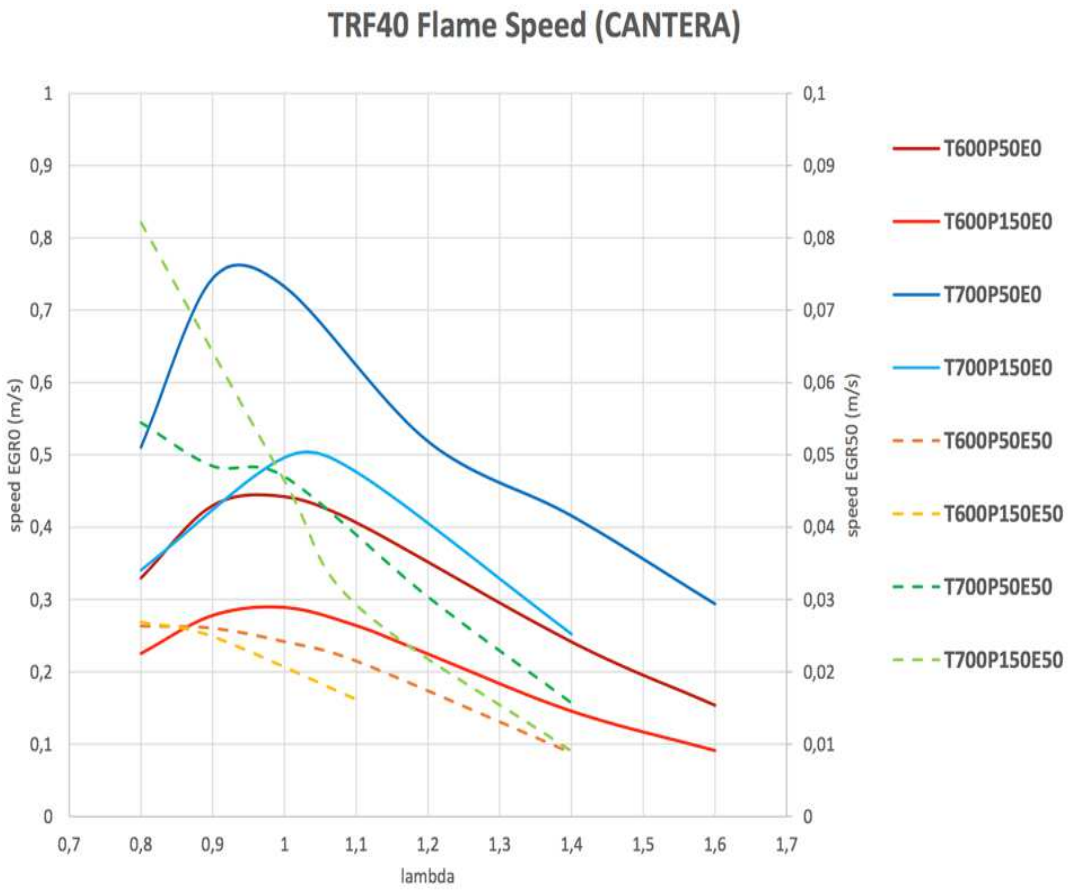

Figure 139 Flame speed on Cantera of a TRF fuel as pressure, temperature and cold EGR change

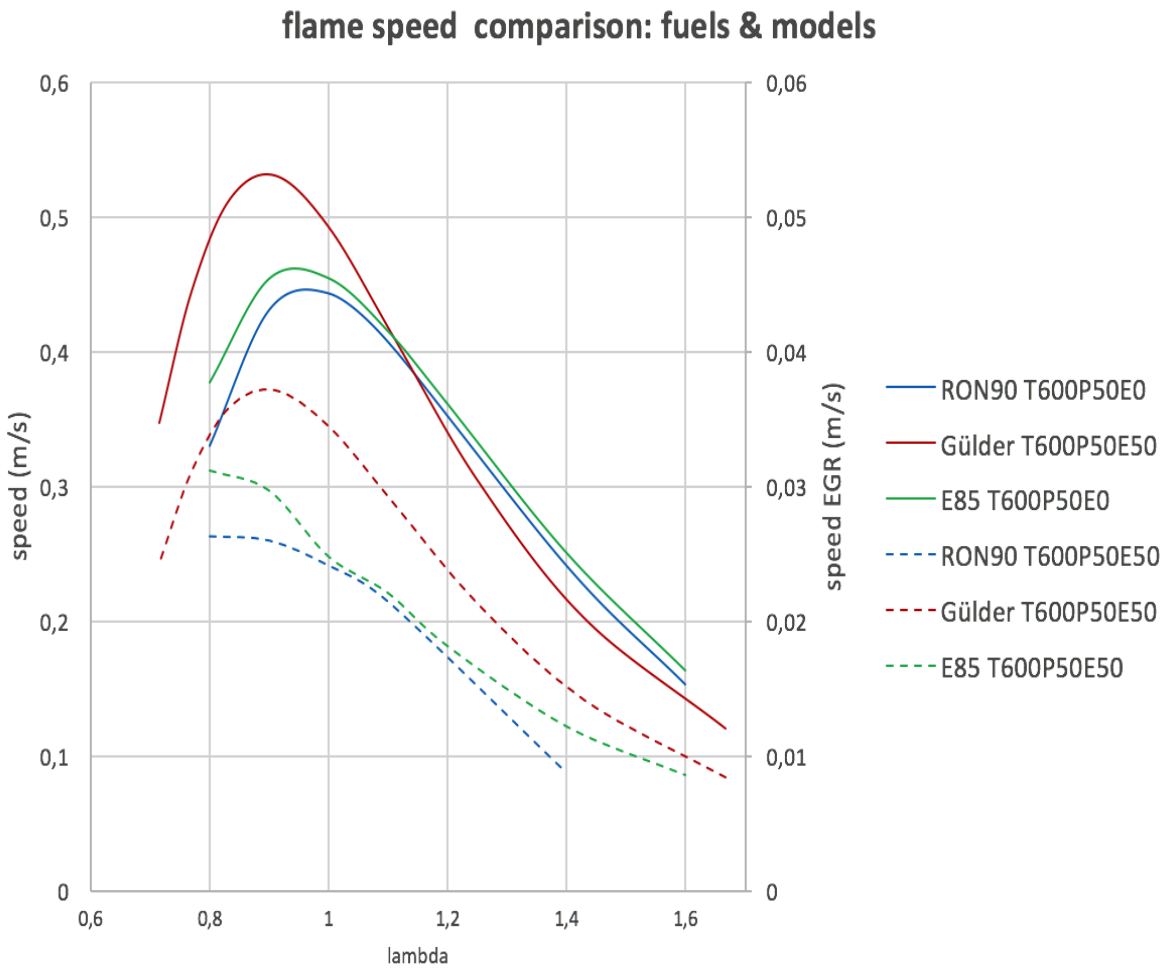

Figure 140 Differences of flame speed between TRF40, E85-TRF40 and Gülder RON90 gasoline

Of course, flame speed of the proposed six-component gasoline surrogate is being calculated, scanning the aforementioned four arrays. In Figure 141, a shot at high temperature of the New6c fuel, with a comparison between aspirated and boosted intake pressure.

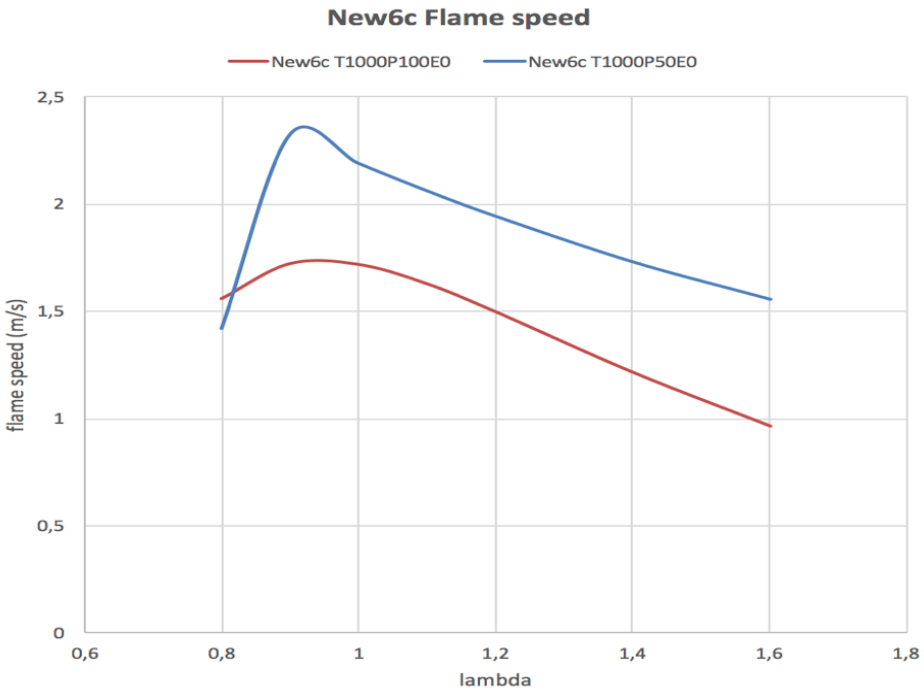

Figure 141 Flame speed of New6c gasoline surrogate at very high temperature with and without the effects of pressure boost

Comparing the LLNL family (LLNL and CRECK) and Fandakov mechanisms, one can notice how CRECK and LLNL are close to each other, in contrast with Fandakov mechanism, which is focused more on low temperature reactions (Figure 142). This approach is considered to be correct, in fact HCCI is a low temperature combustion and that set of kinetics paths are worth of deeper description. Moreover, for this reason the Fandakov mechanism is able to describe very well both the low temperature auto-ignition world and the high temperature flame speed one.

Gülder curve, despite being referred to a different fuel (it's a RON90 generic gasoline, not a PRF), shows higher flame speed for the same operative conditions. As said, this may lead to issues in interpreting HCCI combustions and its related phenomena; on the contrary, at high lambdas, where HCCI is meant to work, the speed is lower than all the mechanism, which seems to grant more consistency because they do not oscillate between knocking and misfire like the 0D Gülder equation does. Not to forget the fact that Gülder is not editable.

The peak of speed is the same for all the mechanisms and Gülder equation.

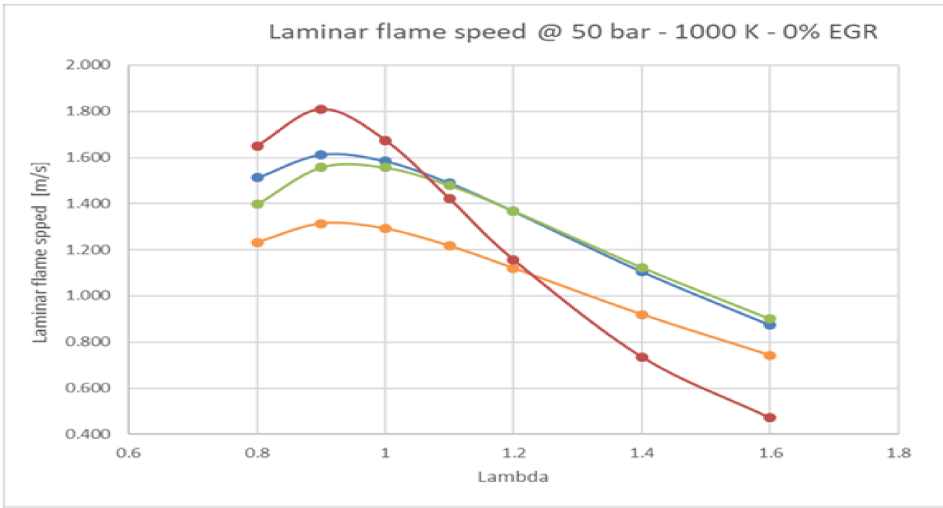

Figure 142 Comparison between CRECK (blue), LLNL (green), Fandakov (orange) mechanisms with PRF95 and Gülder model (red), related to a generic RON90 gasoline

More about Gülder's fuel model

Although ethanol coefficients for the Gülder gasoline model exist (173), combining gasoline and ethanol values would result in a fake fuel, a pure math exercise (Figure 143). The results are not very convincing: ethanol flame speed should be higher than gasoline and the combo has no adherence to reality (model's data are the same for all the fuels). In general, flame speeds are higher than Cantera's.

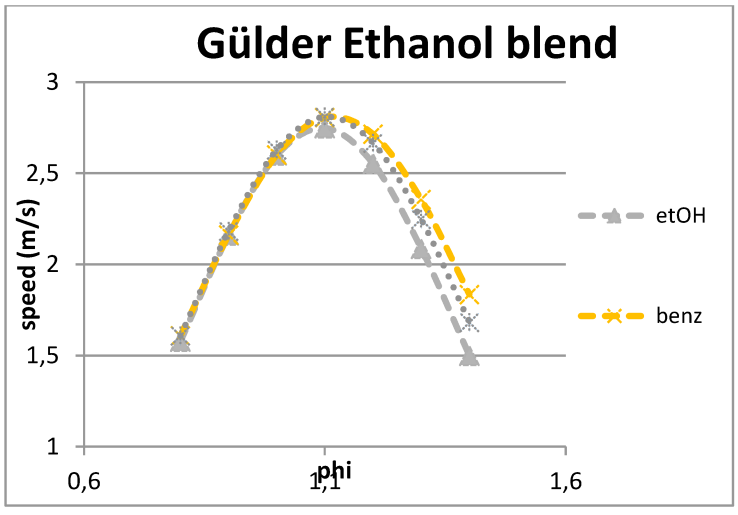

Figure 143 Modeling ethanol blends with Gülder has awkward effects.

Despite these weird outcomes, Gülder model is being working successfully as gasoline surrogate since 1984 and with this function the interpretations of its results are indeed helpful.

Trying to investigate on engine parameters (temperature, boost, phi[25], EGR),influencing gasoline combustion by using Gülder's, some nice achievements came out from a real test bench in Munich.

This out-of-agenda task has been useful to understand how to achieve a calmer compression stroke and to handle the combustion. Generally, intake temperature and pressure boost increase the flame speed of gasoline, while very rich/very lean mixtures slow it down.

In addition, EGR has a freezing effect on flame, at least within Gülder's simulation. With these indications, some experiments have been done at Munich Technical University (by Prof. Wachtmeister).

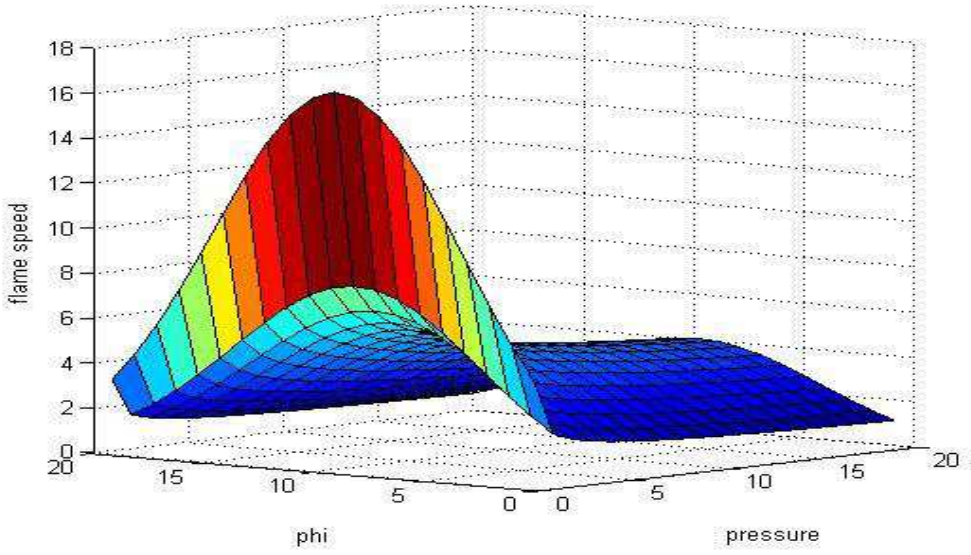

Figure 144 Flame speed as function of phi and pressure, with Gülder model (MatLab)

[25] $\phi = \frac{1}{\lambda}$

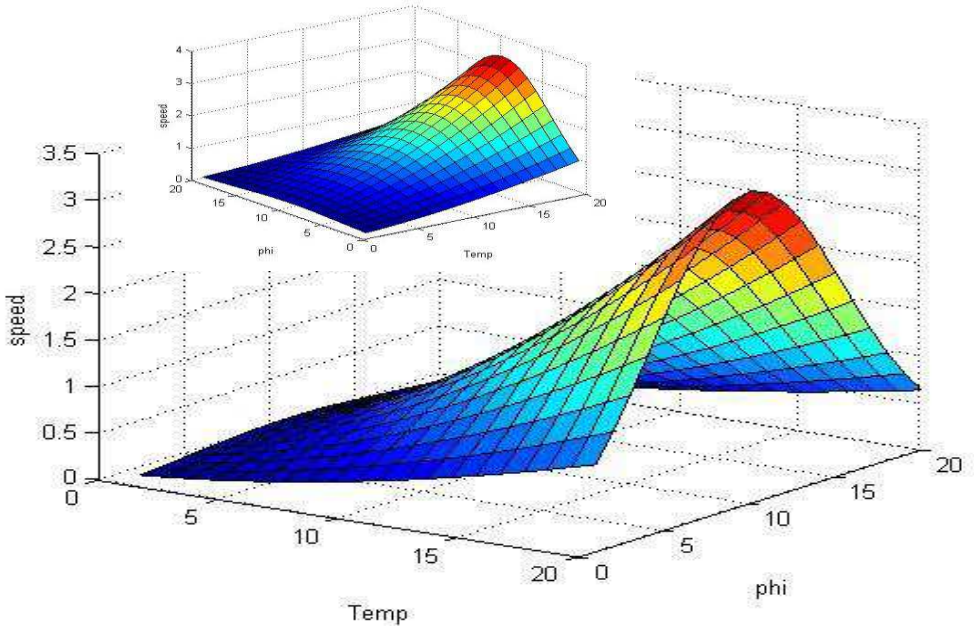

Figure 145 Flame speed as function of phi and temperature, with Gülder model (MatLab)

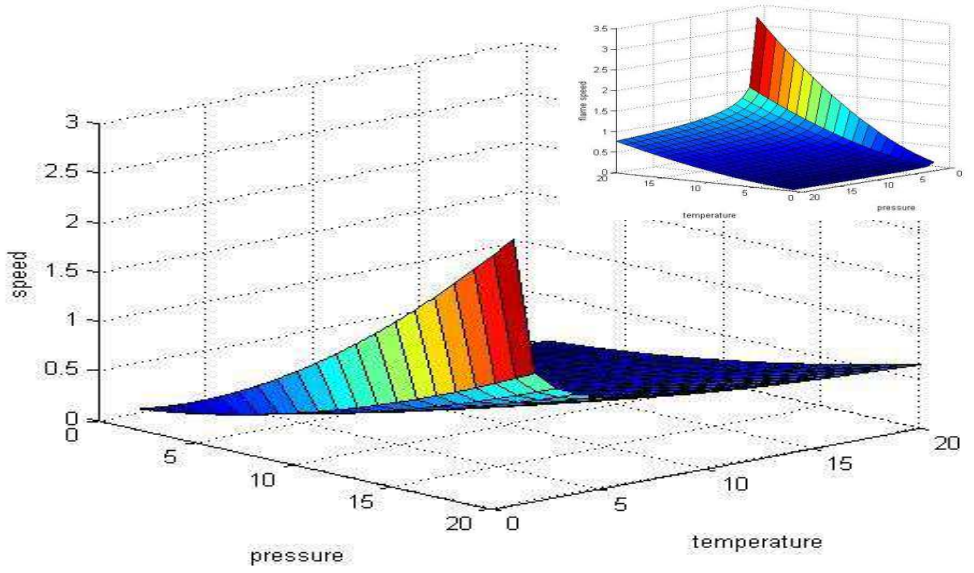

Figure 146 Flame speed as function of temperature and pressure, with Gülder model (MatLab)

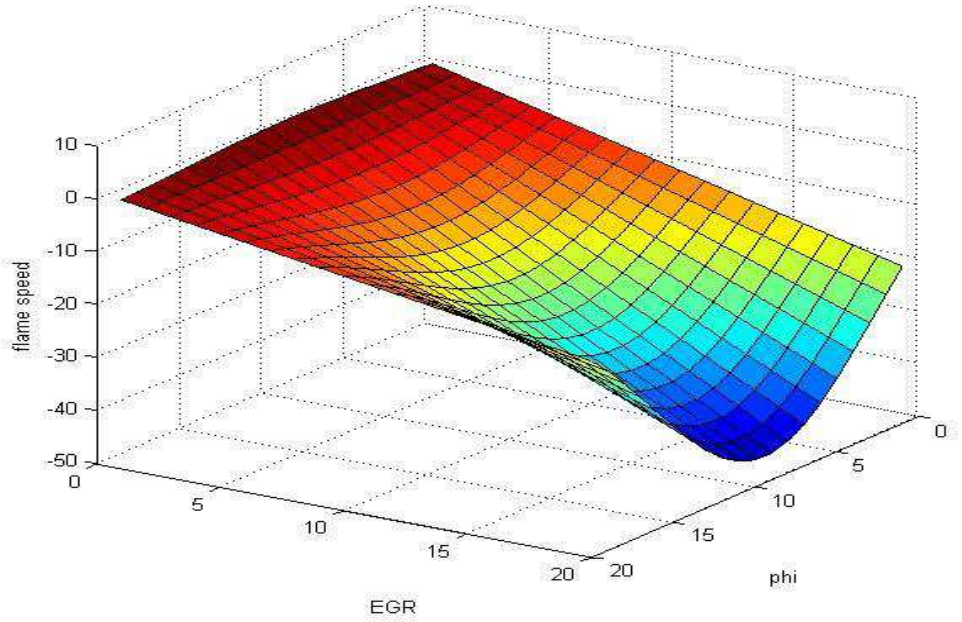

Figure 147 Flame speed as function of phi and EGR, with Gülder model (MatLab)

With a single cylinder high performance engine, equipped of pre-chambered sparkplug and exhaust throttle (a sort of fake EGR valve), some experiments have been carried out, searching for a smooth transition from traditional SI combustion to SACI combustion.

Without dispatching non-disclosable data about the engine and the test campaign, the HCCI range (SACI, indeed) was achieved by moving towards leaner mixtures, regulating the spark advance, tuning the intake and exhaust (fake EGR) pressure and backpressure, and controlling the inlet and outlet temperatures.

Of course, several commercial fuels have been used, but only a few had the characteristics for working in those conditions. The results from the proofstand are depicted in the following pictures.

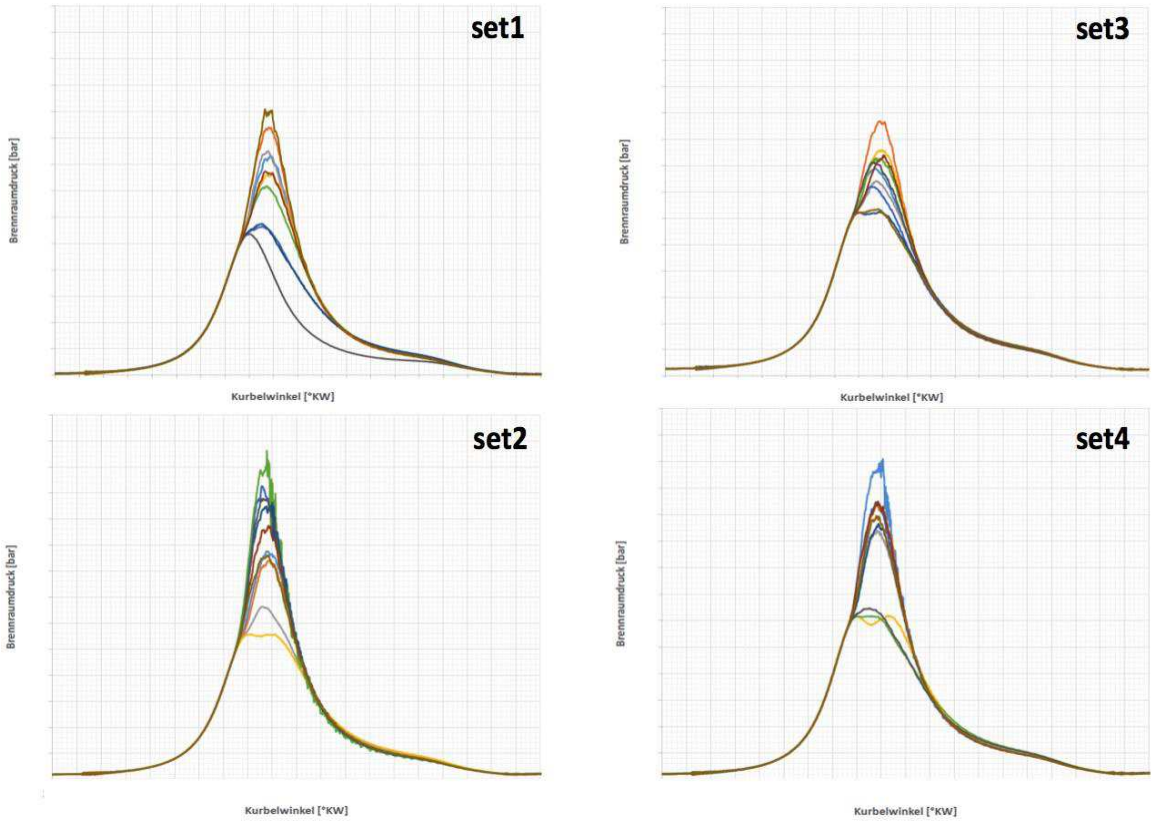

Figure 148 Trying to go into SACI mode with a real engine. Here, several HCCI combustions achieved with four different fuels. (Munich TU, 2017). Axis units removed for restricted permissions.

If the fuel has not the right characteristics (RON/MON, volatility, components quota, etc.) the SACI combustions are not regular and they will easily evolve in bad knocking. Unfortunately, with QuickSim and Gülder models, it is only possible to use RON90 generic gasoline in the virtual engine. But, with that kind of fuel, QuickSim has been able to determine the right conditions for a reliable SACI combustion (Figure 149), with an overlapping description of reality, that have been successfully reproduced at the proofstand, achieving a smooth and regular series of HCCI-like combustions pressure peaks.

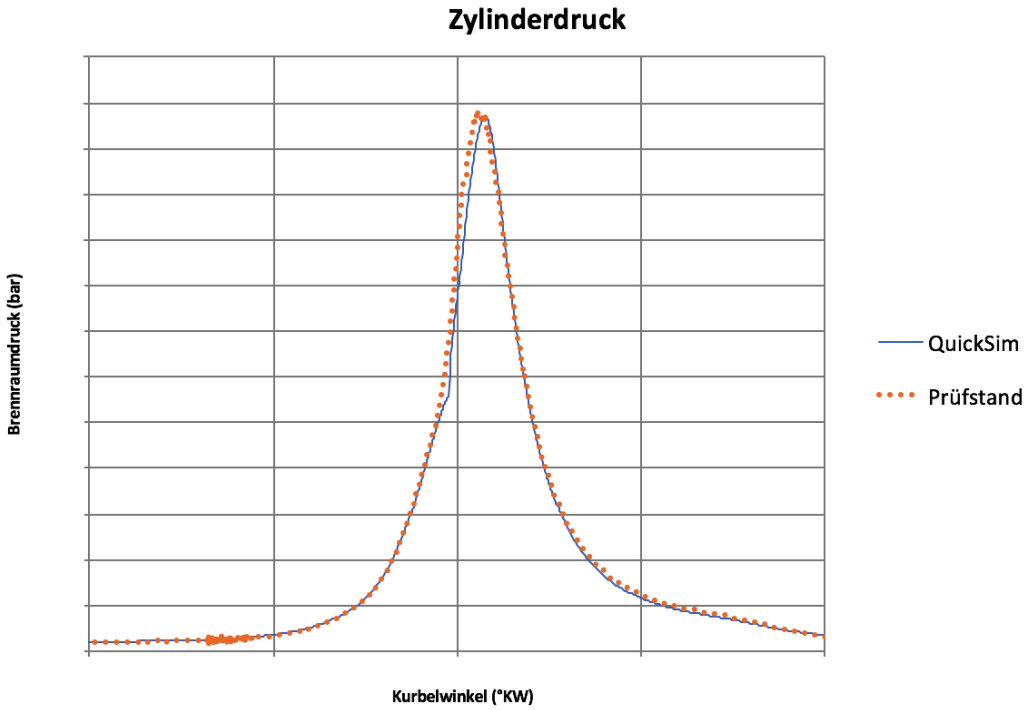

Figure 149 QuickSim simulation of SACI combustion pressure peak is totally overlapping the real profile (FKFS/Munich TU, 2017). Axis units removed for restricted permissions.

When all the LUT about auto-ignition and flame speed of the requested fuels will be ready and their presence implemented into QuickSim source code, a powerful virtual engine will have been developed, with the capability of investigating new engine cycles and combustions and alternative fuels.

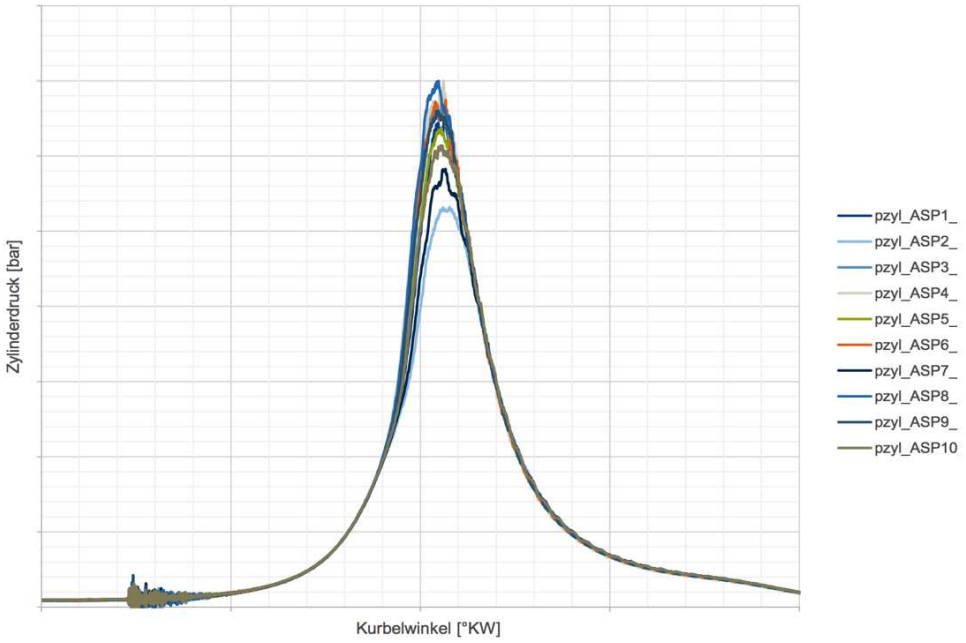

Figure 150 Several, constant, HCCI combustions. Achieved with proper settings AND the right fuel (Munich TU, 2017). Axis units removed for restricted permissions.

Until then, the description is reliable (because transposing virtual engine settings on the real engine has been successfully done) but not very accurate, since some characteristic of the combustion are not completely defined (Figure 151). Probably, Gülder model is not effective for HCCI combustion, where the flame has a completely different behavior on comparison to traditional SI engines.

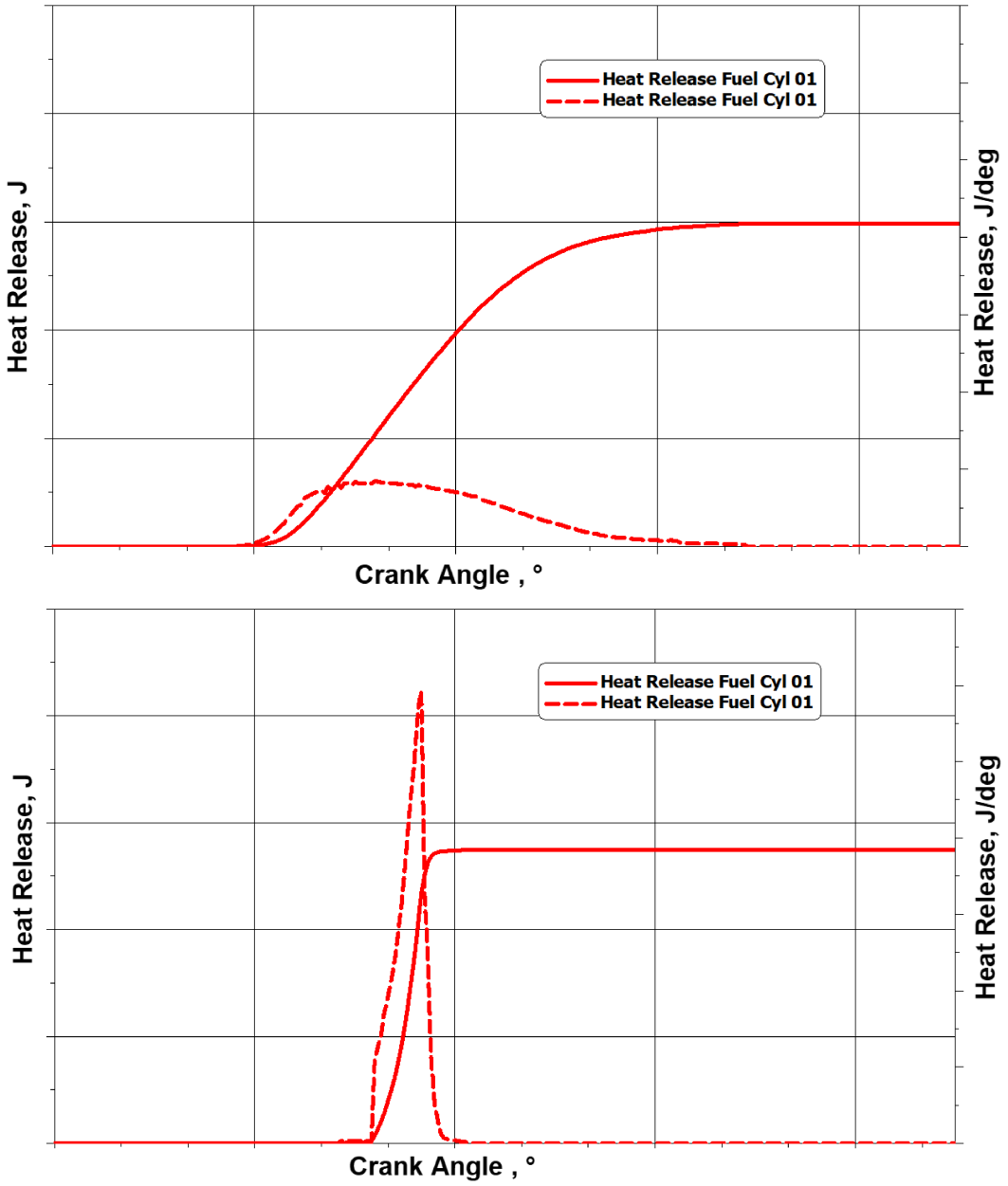

Figure 151 Heat release / Crank Angle plot of SI (upper image) and HCCI (lower image) combustions simulation on QuickSim (FKFS, 2017). Axis units removed for restricted permissions.

Conclusions

Lubricants

By seeking thermodynamic and mechanical efficiency, the downsizing approach has led to engines built with lighter alloys, thin lubricants and low-friction components. Since iron components are generally covered with special coatings and, in general, iron is day by day less used in engines construction, swapped with lighter but softer aluminum (for this reason, always coated), there is no more certainty about the effectiveness of traditional oil recipes, tailored on chemistry of ferrous surfaces.

To investigate the validity of traditional oil recipes, several experiments have been run, involving two types of surfaces (bare steel and DLC coated steel) and two oil additives, symbolizing the group of friction modifiers (by MoS_2) and the group of anti-wear agents (by ZDDP). After a preliminary screening, a PAO base oil has been chosen for all the formulations, with a 4 cSt kinematic viscosity, in order to keep the results reliable and useful for current and future applications.

All the friction and wear tests have been executed on a Mini Traction Machine with a program able to follow the formation and evolution of the tribofilms' friction properties and, in the end, the surfaces and tribofilms characterization has been fulfilled with Electron microscopy, profilometry, Raman spectroscopy, Atomic Force microscopy and XPS spectroscopy.

ZDDP anti-wear agent and MoS_2 friction modifier are two extreme pressure oil additives, which activate themselves when the right conditions of temperature and pressure are achieved by the tribosystem. Their particular chemistry, rich of S and P, keep them able to be a good interface between iron and the oil film, resulting in high performance tribofilms. At least, with bare steel surfaces.

Coupled with DLC coatings, these two essential compounds still form the same tribofilm as on bare steel (because they are triggered by temperature and pressure, not by the surface type), but the effectiveness of this tribofilm is not able to enhance the already good performances of DLC.

DLC is able to be wear resistant, thanks to its diamond domains, and also to show low friction, thanks to its graphite domains. Furthermore, the transfer of graphite layers from a surface to another is the secret of this coating material. ZDDP is designed to form a glassy layer on iron surfaces, and so it does even on DLC but the morphology of this last tribofilm is fuzzy and it does not allow the graphite layer transferring anymore. MoS_2 still works as expected.

Finally, both ZDDP and MoS_2 contain S and P, which are responsible of catalysts poisoning and health issues. In this work, an alternative lubricant formulation has been proposed. Based not on expensive graphene or exotic esters, but on micrometric cheap h-BN particles. The friction and wear results achieved with this simple and inexpensive recipe are promising and seem to be worth of more investigation, particularly on how to design the proper lubrication system on the engine, that should be capable to work with particles willfully microsized.

Catalysts

As particulate matter and NO_x emissions are addressed as *public enemies* by USA, UE and China governments, their abatement is a steady trend topic, more than ever.

Soot particles emissions have been significantly reduced with the introduction of the particle filter, firstly on Diesel vehicles (DPF); this device has been recently improved with catalytic coatings aimed to lower the soot combustion temperature and so reducing the need of expensive – and polluting – post-injections, used to kindle the regeneration of the filter.

Studies proved the efficacy of contact, over surface area, in solid/solid catalysis so, in this work, some ceria-based catalysts have been studied as a function of their morphologies: nanofibers, self-assembled 3D microstars and nanocubes.

Nanofibers carry out the idea to create a sort of web, instead of a thick solid layer, able to entrap every soot particle (avg diameter 50 nm); the tricky method of synthesis and the thick layer that nanofibers however form keep this solution very far from a forthcoming application: the soot cake is way thicker than the fibers web so, when the cake is formed, only a little quota of it really stays in touch with the catalysts.

Self-assembled 3D nanostars have been used to overcome this problem. Their micrometrical size and their particular starred shape allow to achieve the same

channel coverage with less coating (good to limit filter backpressure) and to pierce the soot cake, being the sizes of the two layers finally comparable. Moreover, it allows to engage a catalytic combustion with more than one layer of soot cake per time, a sort or multilevel approach.

How can it be, *in these times*, that micro could be better than nano? Well, size does not matter in this application. The nanotechnology stays in the synthesis procedure, which allows an extremely fine crystallites structure, highly reactive planes exposed and high surface area (good for NO_x abatement) while the catalyst single particle has to be comparable in size to its objective: the whole soot cake. High temperatures, however, tend to sinter this material, discouraging its usage as it is at this stage of development.

Nanocubes, finally, came to merge all the key characteristics of the predecessors: nanometrical size and nanometrical structure. Finally, a catalyst with ageing resistance, good contact properties and highly reactive planes exposed. Nanocubes show a low surface area however, so they are not very suitable to entangle the abatement of soot and NO_x as self-assembled stars. Moreover, they tend to agglomerate and this would be a reason for thick coating formations, same as for nanofibers.

Finally, soot-abatement oriented catalysts should have the aforementioned features of high reactivity, multilevel approach, high surface area, high ageing resistance and grant lower filter backpressures. Within this work, the answer would be a more evolved self-assembled star, maybe reinforced by using Zr, Gd, Pr or Cu doping or by co-oxide depositions. Up to now, self-assembled stars are the lone to show high surface area, a promising factor for combined NO_x/soot abatement, and great coverage efficiency, for lowering the filter pressure drop.

Fuels

On the way towards a low emission vehicle, the upstream solution is to design more efficient engines. Downsizing itself was a way to achieve a more efficient engine, with the addition of turbochargers, variable valve timings, multiple high-pressure injections directly in the cylinders and complex ECU managements. The thermal cycle however, the thermodynamic aspect of the engine, is still based on Otto and Diesel descriptions, and their variants.

There is, however, a third thermodynamic cycle, a mix between Otto and Diesel, which is proved to have higher efficiency. In this cycle, the mixture is homogenous in the chamber (like in Otto engines) and it is self-ignited after compression (like in Diesel engines): it's the HCCI cycle. Unfortunately, such an engine resulted, in the past, extremely hard to develop because of the poor control of the combustion, often occurring out of timing, with dangerous knocking effects.

Nowadays engines are not developed right on the test benches, rather on software tools (the so-called, *virtual engines*), able to simulate every aspect of the device thanks to mathematical descriptions, that can be more or less accurate. These models can be derived by mathematical concepts (i.e. the heat transfer) or experimental fittings (i.e. the fuel flame speed).

Of course, the most important aspect of an HCCI engine is the combustion and the models about fuels characteristic should be as flexible as possible, since there could be the need of modifying the fuels recipes in accordance with the engine responses. This degree of freedom is not possible with experimental fittings, but it can be with thermokinetics based models.

The third task of this work has been to focus more on the hypothetical characteristics of an ideal HCCI fuel and then to develop a flexible and reliable way to determine auto-ignition and flame speed LUT for a generic virtual engine. It appeared that high RON, high sensitivity fuels should be more suitable for HCCI applications and, with this opportunity, it arises the chance to propose ethanol blended gasoline, or pure ethanol, as greener and more sustainable fuel.

The development of Cantera reactors for auto-ignition (0D) and flame speed (1D), driven by a smart kinetics mechanism, allow accurate description of both low and high temperatures reactions kinetics and the delivery of the promised LUT for a new six-components gasoline surrogate, able in turn to retrace real fuels more precisely than traditional three components surrogates, like PRF and TRF, with the advantage of being also able to describe ethanol blends.

The collection of these LUT and their implementation into the virtual engine tool source code is still on going, but the study about the ideal HCCI fuel has already led to encouraging results, achieving engine settings for a regular and controlled HCCI combustion at the test bench, yet using a commercial gasoline with just a slightly different recipe.

Ethanol blends and pure ethanol are the next in line to be tested as soon as the virtual engine will be finally ready to use its new fuels descriptions.

Final considerations

People and many governments around the World are calling for a quick transition from traditional polluting transportation to a new, more sustainable and zero emissions mobility. That's because private, public and commercial transportation do have a huge impact on human health and environment. It is not just about the smog in the cities, but also for the evident consequences of the current approach on the soils consumption, seas inking, materials waste, coal needed for energy demand of production and so on.

Few decades ago, people were concerned about the end of the oil era and what would have happened after. Curiously, nowadays people are aware that way before the oil crisis, there will be an even worst environmental crisis.

The need of a greener transportation is urgent, more than ever. Mobility is a very transversal topic and there are a lot of subtopics deserving attention and promising of improving the cleanliness of transportation concepts, from IT to fuels, from tires to paintings and brakes, from fuel stations to charging strategies, from lubricants to hybrid engine units. Last, but not least, from manual to autonomous drive.

However, what Research and Technology can do to prevent the worst scenario is somehow limited by social and logistic stumbling blocks.

In the high-populated metropolitan areas, public transportation could be improved and *greenified* with trains, bike lanes and car sharing, but not all the people live in there. There will be a quota of population which always needs "autonomy of distance" and "autonomy of recharge" with its vehicle, or special applications where the electric engine is not the most suitable solution (fireguards trucks, ambulances, war vehicles, isolated areas…).

The awaited *electric revolution* seems to have started in these very last years, along with nice initiatives like car-sharing, car-pooling, floating fleets and better public

and bikes mobilities, even if all these initiatives are not very spread among people yet.

Indeed, electric cars and bikes are already available on the market, from the city car to the high-end sport vehicle, but their autonomy is perceived as lower than traditional cars and, currently, recharge durations are not very encouraging for such an expensive purchase. It will take time for Society to be ready to manage fast battery recharging of cars without crashing of the electric grid (it takes, at least, a higher quota of renewable sourced energy into the grid). And then what happens however, when the focus on the energetic sources scheme will move from oil to lithium?

In Europe, some governments are discussing, and some already stated, about the ban of selling I.C.E. equipped vehicles starting from 2040. It may seem a future far from now but actually the European mainframe does need all those years of development to be able to bear such a revolution. Does Europe have to focus only on a far electric future or on a greener I.C.E.? If we opt to go for electric, what should we do in the meanwhile?

These were the questions at the source of this work.

Some people are working on electric vehicles technology, in order to overcome the thermal engines issues, while some other people are obstinately trying to squeeze out the most from current vehicles (I.C.E. equipped), as pollution may concern, to get to that greener future but with limited damages to health and planet Earth. The idea is that a better usage of greener I.C.E. vehicles could result in a lower pollution compared to converting the entire fleet to electric if, like today, the source of energy still rely on fossil fuels.

Chemical engineering do have a main role in this I.C.E.'s rescue plan, because of the relevance of after-treatment systems, of tribology and lubricant technology and because of fuels and combustion development. These topics, in turn, can be divided into thousands of subtopics so this work cannot be comprehensive of all the possible solutions towards a greener internal combustion engine, but rather it is just a small step in that direction.

I.C.E. has been being a reason for pleasure and pain of mankind since more than one century and, despite all, it won't fade away so easily: rather, it is still worthy of development, now more than ever.

References

1. ***Leduc et al., Downsizing of Gasoline Engine: an Efficient Way to Reduce CO2 Emissions, Oil & Gas Science and Technology - Rev. IFP, Vol. 58, No.1, pp. 115-127, 2003.***

2. ***Knecht, Diesel engine development in view of reduced emission standards, Energy, Volume 33, Issue 2, Pages 264-271, 2008.***

3. ***Holmberga et al., Global energy consumption due to friction in passenger cars, Tribology International, Volume 47, March 2012, Pages 221-234, 2012.***

4. ***Taylor, Automobile engine tribology—design considerations for efficiency and durability, Wear, Volume 221, Issue 1, Pages 1-8, 1998.***

5. ***Bhushan, Handbook of Micro/Nanotribology, Boca Raton: CRC Press LLC, 1999.***

6. ***Kondo et al., Tribological Properties of Ionic Liquids, Ionic Liquids - New Aspects for the Future, Dr. Jun-ichi Kadokawa (Ed.), InTech, 2013.***

7. ***Stachowiak, «Ch.2 Physical Properties of Lubricants,» in Engineering Tribology, Elsevier, pp. 11-35, 2014.***

8. ***Lubricants and Lubrication. 2nd Ed. Edited by Th. Mang and W. Dresel, WILEY-VCH Verlag GmbH & Co. KGaA, Weinheim, 2007.***

9. ***Spikes, H.A. The History and Mechanism of ZDDP. Trib. Lett. 17, 469-489, 2004.***

10. ***Burn, The Mechanism of the Antioxidant Action of Zinc Dialkyl Dithiophosphates, Tetrahedron, 22 (7), 2153-2161, 1966.***

11. ***Johnson, The Tribology and Chemistry of Phosphorus-Containing Lubricant Additives, Advances in Tribology, Prof. P. H. Darji (Ed.), InTech, 2016.***

12. ***Parsaeian et al., A New Insight into the Interfacial Mechanisms Involved in the Formation of Tribofilm by Zinc Dialkyl Dithiophosphate. Applied Surface Science, 403. pp. 472-486, 2017.***

13. ***Grossiord et al., MoS2 single sheet lubrication by molybdenum dithiocarbamate. Tribol. Int. 31(12): 737-743, 1998.***

14. ***Yamamoto et al., Friction and Wear Characteristics of Molybdenum Dithiocarbamate and Molybdenum Dithiophosphate, Tribology Transactions Volume 32 - Issue 2, 1989.***

15. ***Girotti et al., The Contribution of Lube Additives to the Life Cycle Impacts of Fully Formulated Petroleum-Based Lubricants, American Journal of Applied Sciences, Volume 8, Issue 11, Pages 1232-1240, 2011.***

16. ***Xianguo, Tribology of composite materials, Tribology of Nanocomposites, pp.41-60, 2012.***

17. ***Holmberg et al., Tribology International 47 pag. 221–234, 2012.***

18. ***de Vincente et al., Rolling and sliding friction in compliant, lubricated contact. Journal of Engineering Tribology, Proceeding of the Institution of Mechanical Engineers, 220:J55–63, 2006.***

19. ***Friedrich et al., PVD CrxN coatings for tribological application on piston rings 8, pp:661 – 668, 1997.***

20. ***Kostylev et al., Advanced Chromium Carbide Coatings on Piston Rings by CVD: A Highly Adaptable 5, pp:22 – 26, 2012.***

21. ***Picaset al., HVOF coatings as an alternative to hard chrome for pistons and valves 8, pp:477 – 484, 2006.***

22. ***Holmberg et al., Coatings tribology - properties, mechanisms, techniques and applications in surface engineering, Elsevier Tribology and Interface Engineering Series, No.56. Amsterdam, Netherlands: Elsevier e 2009.***

23. ***Kunkun et al., Toughness Assessment and Fracture Mechanism of Brittle Thin Films Under Nano-Indentation, Fracture Mechanics - Properties, Patterns and Behaviours, Dr. Lucas Alves (Ed.), InTech, 2016.***

24. ***Horiuchi et al., "Method of Applying DLC Coating on Aluminum Alloys, " Tribology Online 5, Vol. 3, 136-143, 2010.***

25. ***Ryk et al., Testing piston rings with partial laser surface texturing for friction reduction. Wear 261:792–6, 2006.***

26. ***Mourier et al., Action of a femtosecond laser generated micro-cavity passing through a circular EHL contact, Wear 264(5-6):450–6, 2008.***

27. ***Tomanik, Friction and wear bench tests of different engine liner surface finishes, Tribology International 41(11):1032–8, 2008.***

28. ***Tonder, Inlet roughness tribodevices: dynamic coefficients and leakage, Tribology International 34(12):847–52, 2001.***

29. ***Xu et al., Study on the structure and tribological properties of anodic oxide films of aluminum, submitted to Thin Solid Films, 1996.***

30. ***Tao et al., Wear 196 pag. 214, 1996.***

31. ***Gili et al., Laboratory screening of novel coating grades applied to key powertrain components, CRF Workshop AIT 22022012, 2012.***

32. ***Neville et al., Compatibility between tribological surfaces and lubricant additives—How friction and wear reduction can be controlled by surface/lube synergies, Tribology International 40 1680–1695, 2007.***

33. ***Robertson, «Diamond-like Amorphous carbon» Materials Science and Engineering, vol. 37, pp. 129-281, 2002.***

34. ***Götze et al., Tetrahedral Amorphous Carbon Coatings for Friction Reduction of the Valve Train in Internal Combustion Engines, Advanced Engineering Materials, 2014.***

35. ***Podgornik et al., DLC coating of boundary lubricated components—advantages of coating one of the contact surfaces rather than both or none. Tribology International 36: 843-9, 2003.***

36. ***Cui et al., Quantitative measurements of sp3 content in DLC films with Raman spectroscopy. Surface and Coatings Technology, 205: 1995-9, 2010.***

37. ***Podgornik et al., Tribology International e 36 843, 2003.***

38. ***Liu et al., Influence of environmental parameters on the frictional behavior of DLC coatings, Surf Coat Technol. 94–5 [463–8], 1997.***

39. ***Enke et al., Frictional properties of diamondlike carbon layers. Appl Phys Lett 36(4):291–2, 1980.***

40. ***Hogmark et al., Design and evaluation of tribological coatings. Wear 246(1–2):20–33, 2000.***

41. ***Voevodin et al., Nanocomposite and nanostructured tribological materials for spacet. Compos Sci Technol 65(5): 741–8, 2005.***

42. ***Liu et al., An investigation of the relationship between graphitization and frictional behavior of DLC coatings. Surf Coat Technol 86–87(1–3 Part 2):564–8, 1996.***

43. ***Bremond et al., Test temperature effect on the tribological behavior of DLC-coated 100C6-steel couples in dry friction. Wear 254(7–8):774–83, 2003.***

44. ***Vanhulsel et al., Study of the wear behaviour of diamond-like coatings at elevated temperatures. Surf Coat Technol 98(1–3):1047–52, 1998.***

45. ***Erdemir et al., Tribological performance of diamond and diamond-like carbon films at evaluated temperatures., Tribol. Trans. 39(4):787–94, 1996.***

46. ***Neville et al., Compatibility between Tribological Surfaces and Lubricant Additives--How Friction and Wear Reduction can be Controlled by Surface/lube Synergies, Tribology International 40, 10-12, 1680-1695, 2007.***

47. ***Vengudusamy et al., Tribological Properties of Tribofilms Formed from ZDDP in DLC/DLC and DLC/Steel Contacts, Tribology International, 44, 2, 165-174, 2011.***

48. ***Bobzin et al., Lubricated PVD CrAlN and WC/C coatings for automotive applications. Surface and Coatings Technology 204(6– 7):1097–101, 2009.***

49. ***Haque et al., Effect of friction modifiers and antiwear additives on the tribological performance of a hydrogenated DLC coating. Journal of Tribology e 132(3), 2010.***

50. ***Haque et al., Non-ferrous coating/ lubricant interactions in tribological contacts: assessment of tribofilms, Tribology International e 40(10–12):1603–12, 2007.***

51. ***Shinyoshi et al., Wear analysis of DLC coating in oil containing Mo-DTC, SAEInternational e 2007.***

52. ***Kano et al., "Ultralow Friction of DLC in Presence of Glycerol Mono-Oleate (GMO)," Tribology Letters, 18, 2, 245-251, 2005.***

53. ***Topolovec-Miklozic et al., Behaviour of boundary lubricating additives on DLC coatings. Wear 265(11–12):1893–901, 2008.***

54. ***Vengudusamy et al., Tribological properties of tribofilms formed from ZDDP in DLC/DLC and DLC/steel contacts. Tribology International 44(2):165–74, 2011.***

55. ***Mufti et al., Friction properties of DLC/DLC contacts in baseoil. TribologyInternational 44(7–8):922–32, 2011.***

56. ***Gangopadhyay et al., Friction, wear, and surface film formation characteristics of diamond-like carbon thin coating in valvetrain application. TribologyTransactions 54 (1):104–14, 2010.***

57. ***Tung et al., Tribological characteristics and surface interaction between piston ring coatings and a blend of energy-conserving oils and ethanol fuels, Wear 255(7–12):1276–85, 2003.***

58. ***Kano et al., "Ultra-Low Friction Properties of DLC Lubricated with Ester-Containing Oil-Part1:Pin-on-Disc & SRV Friction Tests," Transient Processes in Tribology, Tribology Series, 43, 689-692, 2003.***

59. ***Kano, Diamond-Like Carbon Coating Applied to Automotive Engine Components, Tribology Online, 9, 3 135-142, 2014.***

60. ***Kano, "DLC Coating Technology Applied to Sliding Parts of Automotive Engine," New Diamond and Frontier Carbon Technology, 16, 4, 2006.***

61. ***Simic et al., Comparison of alcohol and fatty acid adsorption on hydrogenated DLC coatings studied by AFM and tribological tests, Journal of Mechanical Engineering, vol. 59, no. 12, p. 707, 2013.***

62. ***Yang et al., Friction reduction mechanisms in boundary lubricated W-doped DLC coatings, Tribology International 70 26–33, 2014.***

63. ***Komori et al., Effect of surface morphology of diamond-like carbon coating on friction, wear behavior and tribo-chemical reactions under engine-oil lubricated condition, TribologyInternational 84 100–109, 2015.***

64. ***Castillo et al., Nanolubricants for Diesel engines: Related emissions and compatibility with the after-treatment catalysts, Tribology International, vol. 72, pp. 198-207, 2014.***

65. ***Eisentraeger et al, Biodegradability testing of synthetic ester lubricants––effects of additives and usage, Chemosphere 48 89–96, 2002.***

66. ***Spikes et al., New Bench Test to Study Mild Lubricated Wear, Proceedings of WTC2005 World Tribology Congress III, Washington D.C., USA, 2005.***

67. ***Ciulli et al., The influence of the slide-to-roll ratio on the friction coefficient and film thickness of EHD point contacts under steady state and transient conditions. Tribology International, 42/200 (4). pp. 526-534, 2008.***

68. ***Meheux et al., Influence of slide-to-roll ratio on tribofilm generation, Proceedings of the Institution of Mechanical Engineers, Part J: Journal of Engineering Tribology, Vol 222, Issue 3, pp. 325 – 334, 2008.***

69. ***Dementjev, «X-Ray photoelectron spectroscopy reference data for identification of the C3N4 phase in carbon-nitrogen film,» Diamond and Related Materials, n. 9, pp. 1904-1907, 2000.***

70. ***de Jong, «Sulfidation Mechanism of Molybdenum Catalysts Supported on a SiOa/Si(100) Model Support Studied by Surface Spectroscopy,» J. Phys. Chem. , vol. 97, pp. 6477-6483, 1993.***

71. ***Brown, «An XPS study of the surface modification of natural MoS2 following treatment in an RF-oxygen plasma,» Applied Surface Science , n. 134 , pp. 11-21, 1998.***

72. ***de Barros'Bouchet, «Boundary lubrication mechanisms of carbon coatings by MoDTC and ZDDP additives,» Tribology International, vol. 38, pp. 257-264, 2005.***

73. ***Ferrari, Determination of bonding in diamond-like carbon by Raman spectroscopy, Diamond and Related Materials, Volume 11, Issues 3–6, Pages 1053-1061, 2002.***

74. ***Cho et al., Evaluation of ring surfaces with several coatings for friction, wear and scuffing life, Transactions of Nonferrous Metals Society of China 19(4):992-996 , 2009.***

75. ***Pawlak et al., A comparative study on the tribological behaviour of hexagonal boron nitride (h-BN) as lubricating micro-particles—An additive in porous sliding bearings for a car clutch, Wear 267 1198–1202, 2009.***

76. ***Yao et al., Borate Esters Used as Lubricant Additives, Lubrication Science 14-4, 415, 2002.***

77. ***Kimura et al., Boron nitride as a lubricant additive, Wear 232 199–206, 1999.***

78. ***Shen et al., Synergistic lubricating effects of borate ester with heterocyclic compound, Wear 246 55–58, 2000.***

79. ***Wang et al., Tribological study of a novel borate ester containing dialkylthiophosphate group as multifunctional additive, Industrial Lubrication and Tribology 61/1 33–39, 2009.***

80. ***Gupta et al., Gasoline, Diesel and Ethanol biofuels from grasses and plants, Cambridge Press, 2010.***

81. ***Englert, Fine particles and human health – a review of epidemiological studies, Toxicol. Lett. 149 235–242, 2004.***

82. ***Neumann, Health risk of combustion products: toxicological considerations, Chemosphere 42 473–479, 2002.***

83. ***Künzli, Ultrafine Particles and Health: Reviewing the Evidence in the Current Policy Context, 21th ETH Conference on Combustion Generated Nanoparticles, Zürich, June 21th 2017.***

84. ***EPA, California Notify Volkswagen of Clean Air Act Violations / Carmaker allegedly used software that circumvents emissions testing for certain air pollutants, US: EPA. 18 September 2015. Retrieved 1 July 2016.***

85. ***https://www.Dieselnet.com/tech/fuel_cng.php.***

86. ***Muñoz, Are GDI vehicle exhaust genotoxic like non-treated Diesel exhaust?, 21th ETH Conference on Combustion Generated Nanoparticles, Zürich, June 21th 2017.***

87. ***Ecotraffic Report, "Particle and NOx emissions from automotive Diesel and petrol engines - A 2009 update." (Figure 10 on page 33), 2009.***

88. ***Vojtíšek, On-road measurement of emissions of reactive nitrogen compounds and greenhouse gases from Euro 6 Diesel and natural gas vans using an on-board FTIR, 21th ETH Conference on Combustion Generated Nanoparticles, Zürich, June 21th 2017.***

89. ***Aneggi et al., Catalysis by Ceria and Related Materials, 2nd ed., Imperial College Press, London, pp. 565–621, 2013.***

90. ***Heck et al., Catalytic Air Pollution Control: Commercial Technology, 3rd ed., Wiley-VCH, Hoboken, New Jersey, pp. 518, 2006.***

91. ***Lox et al., Handbook of Heterogeneous Catalysis, 2nd ed., Wiley-VCH, Weinheim, pp. 2274–2344, 2008.***

92. ***Fino et al., Powder Technol. 180 74–78, 2008.***

93. ***Maricq, Particle Emissions from Motor Vehicles: Current and Future Technologies, Air Pollution as a Climate Forcing: A Workshop, NASA, 2002.***

94. ***Guo et al., NOx-assisted soot combustion over dually substituted perovskite catalysts La1−xKxCo1−yPdyO3− , Applied Catalysis B, Environmental, 2013.***

95. ***http://www.Dieselnet.com/papers/9804mayer/.***

96. ***Bensaid et al., Modeling of Diesel particulate filtration in wall-flow traps. Chem Eng J, 154(1–3):211–218, 2009.***

97. ***Pontikakis et al., Dynamic filtration modeling in foam filters for Diesel exhaust. Chem Eng Comm, 188:21–46, 2001.***

98. ***Bensaid et al., Numerical simulation of soot filtration and combustion within Diesel particulate filters. Chem Eng Sci, 65:357–363, 2010.***

99. ***Miceli et al., Effect of the morphological and surface properties of CeO2-based catalysts on the soot oxidation activity, Chemical Engineering Journal 278 190–198, 2015.***

100. ***Marchisio et al., Modeling of Diesel particulate filtration in wall-flow traps, Chem. Eng. J. 154 (1–3) 211– 218, 2009.***

101. ***Caroca et al., Detailed investigation on soot particle size distribution during DPF regeneration, using standard and bio-Diesel fuels, Ind. Eng. Chem. Res. 50 (5) 2650–2658, 2011.***

102. ***Bensaid et al., CeO2 catalysts with fibrous morphology for soot oxidation: the importance of the soot–catalyst contact conditions. Catal Today, 216:57–63, 2013.***

103. ***Aneggi et al., On the role of lattice/surface oxygen in ceria–zirconia catalysts for Diesel soot combustion. Catal Today, 181:108–115, 2012.***

104. ***Song et al., The role of fuel-borne catalyst in Diesel particulate oxidation behavior, Combustion and Flame, Volume 146, Issues 1–2, Pages 73-84, 2006.***

105. ***Bueno-Lopez, Appl.Catal.B146 (2014)1–11, 2014.***

106. ***Burch, Catal. Rev. 46 (2004) 271–334, 2004.***

107. ***Russell et al., Catal. Rev. Sci. Eng. 53 (2011) 337–423, 2011.***

108. ***Eastwood, Critical Topics in Exhaust Gas Aftertreatment, Research Studies Press Ltd., Baldock, pp. 400, 2000.***

109. ***Bensaid et al., Can. J. Chem. Eng. 89 (2011) 401–407, 2011.***

110. ***Russo et al., Catal. Today 176 (2011) 417–423, 2011.***

111. ***Van Setten et al., Realistic contact for soot with an oxidation catalyst for laboratory studies. Appl Catal Environ 2000, 28:253–257, 2000.***

112. ***Palmisano et al., High catalytic activity of SCS synthesized ceria towards Diesel soot combustion, Appl Catal Environ, 69(1–2):85–92, 2006.***

113. ***Neeft et al., Appl. Catal. B 8 (1996) 57–78.***

114. ***Miceli et al.: CeO2-based catalysts with engineered morphologies for soot oxidation to enhance soot-catalyst contact. Nanoscale Research Letters 9:254, 2014.***

115. ***Yu et al., Synthesis and characterization of cerium dioxide fibers, Mater Chem Phys, 118(2–3):410–416, 2009.***

116. ***Rao et al., Tuning, via counter anions, the morphology and catalytic activity of CeO2 prepared under mild conditions. J Colloid Interface Sci, 373:46–56, 2012.***

117. ***Kaneko, Determination of pore size and pore distribution: 1. Adsobernts and catalysts, J. Membr. Sci. 96, 59–89, 1994.***

118. ***Aneggi et al., Shape-dependent activity of ceria in soot combustion, ACS Catal, 4:172–181, 2014.***

119. ***Sayle et al., The role of oxygen vacancies on ceria surfaces in the oxidation of carbon monoxide, Surf Sci, 316:329–336, 1994.***

120. ***Kullgren et al., Supercharged low-temperature oxygen storage capacity of ceria at the nanoscale. J Phys Chem Lett, 4:604–608, 2013.***

121. ***Zhang et al., Cerium oxidation state in ceria nanoparticles studied with X-ray photoelectron spectroscopy and absorption near edge spectroscopy, Surf. Sci. 563 74–82, 2004.***

122. ***Radotoiu et al., Satellites in Ce 3D X-ray photoelectron spectroscopy of ceria, Dig. J. Nanomater. Biostruct. 8 (4) 1535–1549, 2013.***

123. ***Piumetti et al., Contact dynamics for a solid–solid reaction mediated by gas-phase oxygen: Study on the soot oxidation over ceria-based catalysts, Applied Catalysis B: Environmental 199 96–107, 2016.***

124. ***Jacobs et al., Applied Catalysis A: General 252 (2003) 107–118, 2003.***

125. ***Piumetti et al., Appl. Catal. B 180 (2016) 271–282, 2016.***

126. ***Piumetti et al., Appl. Catal. B 165 (2015) 742–751, 2015.***

127. ***Aneggi et al., Catal. Today 197 (2012) 119–126, 2012.***

128. ***Orihuela et al, Experimental measurement of the filtration efficiency and pressure drop of wall-flow Diesel Particulate Filters (DPF) made of biomorphic Silicon Carbide using laboratory generated particles, Applied Thermal Engineering, Applied Thermal Engineering 131, 41-53, 2018***

129. ***Cho et al., The effects of filter porosity and flow conditions on soot deposition/oxidation and pressure drop in particulate filters. Energy, 77, 327–337, 2014.***

130. ***Wang et al., Modeling Study of Metal Fiber Diesel Particulate Filter Performance. SAE Tech. Pap., 2015-01–10, 1–9, 2015.***

131. ***Bauer, The environmental performance of current & future passenger vehicles, 21th ETH Conference on Combustion Generated Nanoparticles ETH Zurich, June 19th – 22nd 2017.***

132. ***Heywood, Internal Combustion Engine Fundamentals, McGraw-Hill Education, 1988.***

133. ***Bisetti et al., Probability density function treatment of turbulence/chemistry interactions during the ignition of a temperature stratified mixture for application to HCCI engines modeling, Combust. Flame 64:571-584, 2008.***

134. ***Bontorin et al., Investigation of the Impact of Lean Mixtures on the Performance of GDI Engines, SAE Technical Paper 2016-36-0326, 2016.***

135. ***Zaidi, Development of a Direct Injection-Homogeneous Charge Compression Ignition (DI-HCCI) Heavy Duty DiesOtto Engine by using Effervescent Atomization, SAE Technical Paper 2009-01-2701, 2009.***

136. ***Willand et al., The GCI combustion process from Volkswagen - Influence of combustion chamber wall and fuel, MTZ worldwide - Springer, Volume 69, Issue 4, pp 56–61, 2008.***

137. ***Bridjesh, A Survey On Low Compression Ratio Diesel Engine, ARPN Journal of Engineering and Applied Sciences, Vol. 10, 22, 2015.***

138. ***Chiodi et al., "Development of an Innovative Combustion Process: Spark-Assisted Compression Ignition," SAE Int. J. Engines 10(5), 2017.***

139. ***Schneider et al., "Development and Experimental Investigation of a Two-Stroke Opposed-Piston Free-Piston Engine," SAE Technical Paper 2016-32-0046, 2016.***

140. ***De Bortoli Cassiani et al., "Variable Compression Ratio Engines," SAE Technical Paper 2009-36-0245, 2009,.***

141. ***Ryan et al., "HCCI in a Variable Compression Ratio Engine-Effects of Engine Variables," SAE Technical Paper 2004-01-1971.***

142. ***Mittal et al, The Shift in Relevance of Fuel RON and MON to Knock Onset in Modern SI Engines Over the Last 70 Years, 2009-01-2622.***

143. ***Kiat, Advances in Internal Combustion Engines and Fuel Technologies, Chapter 4, Charalambides, Homogenous Charge Compression Ignition (HCCI) Engines, InTech, 2013.***

144. ***Yuriy et al., Experimental and computational study of lean limit methane-air flame propagating upward in a 24 mm diameter tube, Combust. Sci. and Tech., 180: 1812–1828, 2008.***

145. ***Morgan et al., Mapping surrogate gasoline compositions into RON/MON space, Combustion and Flame 157, 1122–1131, 2010.***

146. ***Bengt Johansson, Fuels and Combustion, Biofuels from Lignocellulosic Biomass: Innovations beyond Bioethanol, First Edition. Edited by Michael Boot, Wiley-VCH Verlag GmbH & Co. KGaA, 2016.***

147. ***Kalghatgi, Auto-ignition Quality of Gasoline-like Fuels in HCCI Engines, SAE Powertrain & Fluid Systems Conference & Exhibition, October 2003, in Pittsburgh, PA, USA. SAE 2003-01-3215.***

148. ***Struben et al., Transition Challenges for Alternative Fuel Vehicle and Transportation Systems, Environment and Planning B: Urban Analytics and City Science, Vol 35, Issue 6, pp. 1070 – 1097, 2008.***

149. ***Bengt Johansson, Fuels and Combustion, Biofuels from Lignocellulosic Biomass: Innovations beyond Bioethanol, First Edition. Edited by Michael Boot, Wiley-VCH Verlag GmbH & Co. KGaA, 2016.***

150. ***Ramana et al., Development of Alternative fuels for HCCI Engine Technology, IJEDR, Volume 3, Issue 2, 2015.***

151. ***Lu et al., Fuel design and management for the control of advanced compression-ignition combustion modes, Progress in Energy and Combustion Science, 37, 741-783, 2011.***

152. ***Yao et al., Progress and recent trends in homogeneous charge compression ignition (HCCI) engines, Progress in Energy and Combustion Science, 35(5): 398-437, 2009.***

153. ***Komninos et al., Modeling HCCI combustion of biofuels: A review, Renewable and Sustainable Energy Reviews, 16, 1588- 1610, 2012.***

154. ***Zhao, Homogeneous Charge Compression Ignition (HCCI) and Controlled Auto Ignition (CAI) Engines for the Automotive Industry, Woodhead Publishing Limited 2007 (CRC) Press, Boca Raton, Florida).***

155. ***Yap et al., An investigation into bioethanol homogeneous charge compression ignition (HCCI) engine operation with residual gas trapping, Energy and Fuels, 18(5): 1315-1323, 2004.***

156. ***Yap et al., An investigation into propane homogeneous charge compression ignition (HCCI) engine operation with residual gas trapping, Fuel, 84(18): 2372- 2379, 2005.***

157. ***Zhang et al., The combustion and emission characteristics of ethanol on a port fuel injection HCCI engine, SAE Paper: 2006-01-0631, 2006.***

158. ***Flowers et al., Improving Ethanol Life Cycle Energy Efficiency by Direct Utilization of Wet Ethanol in HCCI Engines, SAE Paper: 2007-01-1867, 2007.***

159. ***Vressner et al., Combustion Chamber Geometry Effects on the Performance of an Ethanol Fueled HCCI Engine. SAE Paper: 2008-01-1656, 2008.***

160. ***Saxena et al., Wet ethanol in HCCI engines with exhaust heat recovery to improve the energy balance of ethanol fuels, Applied Energy, 98(0): 448-457, 2012.***

161. ***Peng et al., Study the ethanol SI/HCCI combustion mode transition by using the fast thermal management system, Chinese Science Bulletin, vol. 52 no. 19 pag. 2731-2736, 2007.***

162. ***Türkan et al., The effects of ethanol-gasoline blends on combustion and performance in a DI-HCCI engine, International Conference on Renewable Energy Research and Applications Madrid, Spain, 20-23 October 2013.***

163. ***Mack et al., Demonstrating direct use of wet ethanol in a homogeneous charge compression ignition (HCCI) engine. Energy, 34(6): 782-787, 2009.***

164. ***Megaritis et al., Effect of water blending on bioethanol HCCI combustion with forced induction and residual gas trapping, Energy 32 2396–2400, 2007.***

165. ***Patel et al., Water Injection Effects On Performance Characteristics Of A Ci Engine, IOSR Journal of Mechanical and Civil Engineering (IOSR-JMCE), Volume 11, Issue 3 Ver. II, 2014.***

166. ***Iyer et al., Experimental Study on the Effect of Water Injection in an Internal Combustion Engine, IOSR Journal of Mechanical and Civil Engineering (IOSR-JMCE), PP. 58-64, 2017.***

167. ***Mingrui et al., Water Injection for Higher Engine Performance and Lower Emissions, Journal- Energy Institute 90(2), 2016.***

168. ***Viggiano et al., A comprehensive investigation on the emissions of ethanol HCCI engines, Applied Energy 93, 277–287, 2012.***

169. ***Bohacz, Tuning ACCEL/DFI 6.0 Programmable Fuel Injection, HPBooks, 2003.***

170. ***Battin-Leclerc. Detailed chemical kinetic models for the low-temperature combus- tion of hydrocarbons with application to gasoline and Diesel fuel surrogates. Progress in Energy and Combustion Science 34, pp.440-498, Elsevier, 2008.***

171. ***Chiodi, An Innovative 3D-CFD-Approach towards Virtual Development of Internal Combustion Engines, Vieweg+Teubner Verlag, Springer Fachmedien Wiesbaden GmbH 2011.***

172. ***Sangiovanni-Vincentelli, "The Tides of EDA," IEEE Design & Test of Computers, pp. 59-75, November-December 2003.***

173. ***Gülder, Correlations of laminar combustion data for alternative S.I. engine fuels, SAE Technical Paper, 841000, 1984.***

174. ***Mishra, Fundamentals of Combustion, pag. 88-96, PHIndia, 2008.***

175. ***Goodwin et al., Cantera: An object- oriented software toolkit for chemical kinetics, thermodynamics, and transport processes, Version 2.3.0, 2017.***

176. ***Hann et al., "Influence of Binary CNG Substitute Composition on the Prediction of Burn Rate, Engine Knock and Cycle-to-Cycle Variations," SAE Int. J. Engines 10(2):501-511, 2017.***

177. ***Urban et al., Simulation of Autoignition, Knock and Combustion for Methane-Based Fuels, SAE Technical Paper 2017-01-2186, 2017.***

178. ***Kee et al., "Chemkin-II: A Fortran Chemical Kinetics Package for the Analysis of Gas-Phase Chemical Kinetics", Sandia National Laboratories, United States, 1989.***

179. ***Mehl et al., "Kinetic Modeling of Gasoline Surrogate Components and Mixtures under Engine Conditions," Proc. Combust. Inst. 33 (1) 193-200, 2011.***

180. ***Ranzi et al., Reduced Kinetic Schemes of Complex Reaction Systems: Fossil and Biomass-Derived Transportation Fuels, International Journal of Chemical Kinetics, Volume 46(9):512542, 2014.***

181. ***Lamoureux et al., Experimental and numerical study of the role of NCN in prompt-NO formation in low-pressure CH4–O2–N2 and C2H2–O2–N2 flames, Combustion and Flame, Volume 157, Issue 10, Pages 1929-1941, 2010.***

182. ***Pitsch et al., Optimized chemical mechanism for combustion of gasoline surrogate fuels, Combustion and Flame, Volume 162, Issue 5, Pages 1623-1637, 2015.***

183. ***Fandakov at al., "Two-Stage Ignition Occurrence in the End Gas and Modeling Its Influence on Engine Knock," SAE Int. J. Engines 10(4), 2017.***

184. ***Prince et al., Short chemical-kinetic mechanisms for low-temperature ignition of propane and ethane, Memorias del XVII Congreso Internacional Anual de la Somim 21 al 23 de Septiembre, 2011 San Luis Potosí, México.***

185. ***Xu et al., Study on the structure and tribological properties of anodic oxide films of aluminum, submitted to Thin Solid Films, 1996.***

186. ***Castillo et al., Nanolubricants for Diesel engines: Related emissions and compatibility with the after-treatment catalysts. In: TRIBOLOGY INTERNATIONAL, vol. 72, pp. 198-207, 2014.***

187. ***Turner, Buoyancy Effects in Fluids, pp. 167, 1973.***

188. ***"Advances in Internal Combustion Engines and Fuel Technologies", Intech - Hoon Kiat Ng, 2013, Chapter 4, Charalambides, Homogenous Charge Compression Ignition (HCCI) Engines.***

189. ***Iyer et al., Experimental Study on the Effect of Water Injection in an Internal Combustion Engine, IOSR Journal of Mechanical and Civil Engineering (IOSR-JMCE), PP. 58-64, 2017.***

190. ***Reitza et al., Review of high efficiency and clean reactivity controlled compression ignition (RCCI) combustion in internal combustion engines, Progress in Energy and Combustion Science, Volume 46, Pages 12–71, 2015.***

Presented in March 2018